

A PARAMETRIC STUDY OF ENERGY ABSORBING FOAMS FOR HEAD INJURY PREVENTION

Svein Kleiven
Royal Institute of Technology
Sweden
Paper Number 07-0385

ABSTRACT

This paper describes a parametric study of foam material properties for interior car surfaces using finite element calculations. Two different head models were used for the impact simulations, a Hybrid III dummy head and a biomechanical head model. The objective was to study the head injury criterion (dummy) (HIC(d)), the angular velocity, the resultant acceleration and, for the human head models, the strain in the brain tissue and the stress in the skull for a variation in foam material properties such as stiffness, plateau stress and energy absorption. The analysis gave at hand that the best choice of material properties with respect to impact using the Hybrid III head model reached different results compared to an impact with the biomechanical head model. For a purely perpendicular impact, the HIC(d) for the head model managed to predict the strain level in the brain quite well. Even though the HIC reached acceptable levels for both a perpendicular and oblique impact towards a 31 kg/m³ EPP padding, the maximum strain in the human head model for an oblique impact was almost twice suggested allowable levels. The difference in the strain in the brain between an oblique and perpendicular impact when impacted with same initial velocity towards the same padding was not predicted by the HIC(d).

INTRODUCTION

Head injuries due to traffic accidents, at work and during leisure, are major diseases in Sweden and worldwide. Globally, the daily incidence rate of transportation injuries is estimated to 30 000 victims and 3 000 deaths [1]. In Sweden, the annual number of cases is more than 20 000 head injuries and the annual rate of head injuries in Sweden over the last 14 years is relatively constant [2]. The main cause of death for people younger than 45 years of age in Sweden is accidents and poisoning. When looking deeper into this cause of death for the younger part of the male population in Sweden, it can be seen that head injuries causes almost 80 percent of the traffic injury deaths [3]. The development of safety systems in cars has exploded over the last 20 years, resulting

in more and more sophisticated methodologies. There are indications that this trend is slowing down. One possible factor is that the crash dummies are not completely human-like and another factor is the roughness of the tolerances and injury criteria that are used to couple output from the dummies with real-life injuries. The interior surfaces of a car compartment are designed to protect the occupants from injury at car accidents through use of energy absorbing materials and clever structural solutions. This is normally done to comply with the extended FMVSS 201 regulation [4]. The primary verification tool in the design process is the Head Injury Criterion (dummy) (HIC(d)) applied in a free motion head-form experimental set-up, where a rigid dummy head is launched towards specific locations. Linear accelerations in three perpendicular directions are measured in the head form during the impact and the performance is evaluated according to the HIC. The test procedure is established internationally and thus used by automotive manufacturers all over the world. HIC was introduced in its present form in crash testing by the National Highway Traffic Society Administration [5] and it has been used for several years in crash injury research and prevention as a measure of the likelihood of serious brain injury. HIC only treats the resultant translational acceleration and the duration of the impulse and no consideration is given to the direction of the impulse or rotational acceleration components [3, 6, 7]. Moreover, studies by Ueno and Melvin [8] and DiMasi *et al.* [9] found that the use of either translation or rotation alone may underestimate the severity of an injury. Zhang *et al.* [10] also concluded that both linear and angular accelerations are significant causes of mild traumatic brain injuries. Recently, it was found that HIC manage to predict the strain level in the brain of a finite element (FE) model for purely translational impulses of short duration, while the peak change in angular velocity showed the best correlation with the strain levels in an FE head model for purely rotational impulses [3]. The HIC(d) together with FE simulations and/or experiments according to the FMVSS 201 regulation has been used in several studies in an effort to improve the interior safety of

vehicles [11, 12, 13, 14]. However, the human head behaves in a more complex way and since the validity of the HIC criterion is intensively debated there is reason to believe that the safety development could be made more efficient through use of more delicate tools in the process, such as biomechanically representative FE models of the human head together with local tissue thresholds. To ensure that a continued high pace is kept when it comes to progress in car safety and primary prevention, it is necessary to find new preventive strategies and methods to complement the safety work practiced today. It is hypothesized in this study that the best choice of parameters for energy absorbing foams of an automotive panel would come out differently if it was made with respect to one or the other criterion. To test this hypothesis, different head models were compared in FE simulations according to the FMVSS 201 regulation using a simplified interior padding. This investigation was performed to illustrate that although the response of a structure may be optimal for a certain impact case when evaluated with a specific set of criteria it might not be favorable for another case, evaluated with respect to another set of criteria.

METHODOLOGY

In order to investigate the potential to improve the safety design, an FE model of the human head has been used. Two different FE head models were used; a model of the featureless Hybrid III dummy head and a biomechanically representative human head model (in the following referred to as human head model). Parametric studies of material properties of energy absorbing foams for idealized impact paddings were performed. Numerical simulations using the dynamic finite element method (FEM) program LS-DYNA [15] was performed.

Human head FE model

The head model used in this study was developed at the Royal Institute of Technology in Stockholm [16]. The head model includes the scalp, the skull, the brain, the meninges, the cerebrospinal fluid (CSF) and eleven pairs of the largest parasagittal bridging veins (Figure 1).

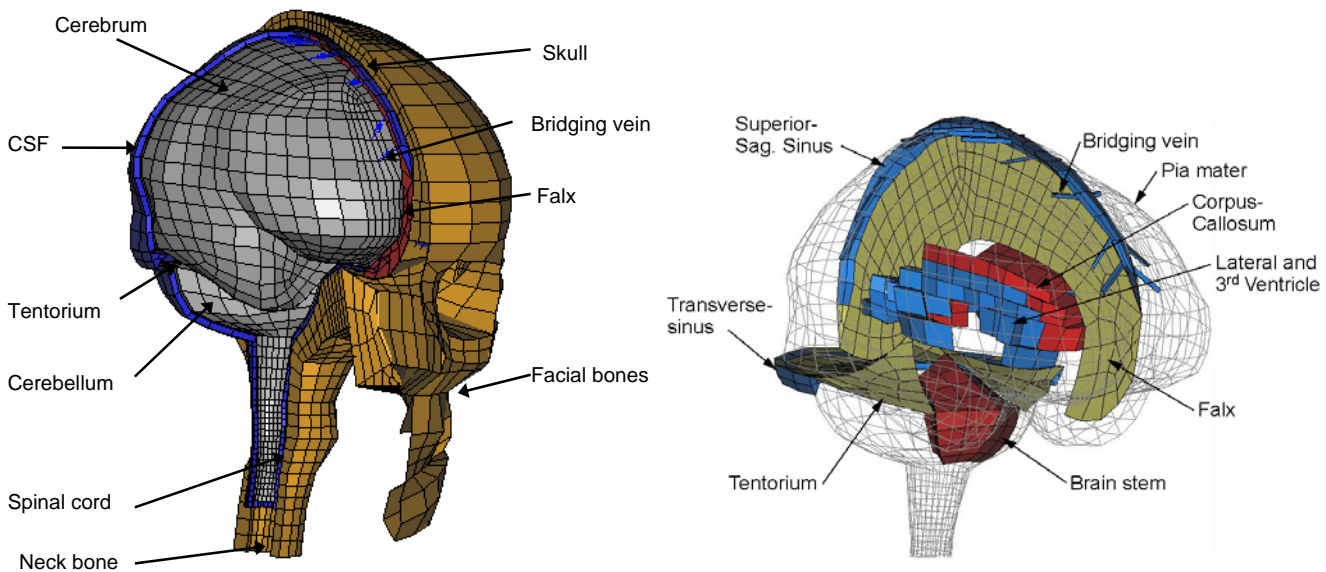


Figure 1. Finite element model of the human head.

In order to better simulate the stress and strain distribution, separate representations of gray and white matter, and inclusion of the ventricles were implemented. The total mass of the head was 4.52 kg and the principal mass moments of inertia were close to the corresponding ones for the hybrid III head. The head model has been validated against several relative motion experiments [17], intra-cerebral

acceleration experiments [3], skull fracture experiments [18], and intra-cranial pressure experiments [19]. The post-mortem human subject (PMHS) experimental data used cover four impact directions (frontal, occipital, lateral and axial), short and long durational impacts (2-150 ms), high and low severity (sub-concussive to lethal), and both penetrating and non-penetrating injuries. To cope

with the large elastic deformations, a third order Ogden hyperelastic constitutive model and corresponding parameters was fitted to include the non-linear elasticity described by Miller and Chinzei [20] as well as the high frequency relaxation moduli determined by Nicolle *et al.* [21]. The stress in the cranial bone, maximum principal strain in the brain tissue, change in rotational velocity of the skull, the HIC(d) and translational acceleration of the skull for

the different foams were determined. To account for the possible loss of load bearing capacity at high contact loading, the stresses in the skull were limited to 90 MPa for the compact bone [22, 23, 24] and 30 MPa for the spongy bone [22, 25] through the use of simple elastic ideally plastic constitutive models. A summary of the properties for the tissues of the human head used in this study is presented in Table 1.

Table 1.
Material properties for the head model used in the numerical study.

<i>Tissue</i>	<i>Young's modulus</i> [MPa]	<i>Density</i> [kg/dm ³]	<i>Poisson's ratio</i>	<i>Yield stress</i> [MPa]
<i>Outer compact bone</i>	15 000	2.00	0.22	90
<i>Inner compact bone</i>	15 000	2.00	0.22	90
<i>Porous bone</i>	1000	1.30	0.24	30
<i>Neck bone</i>	1000	1.30	0.24	
<i>Brain</i>	Hyper-Viscoelastic	1.04	~0.5	
<i>Cerebrospinal Fluid</i>	$K = 2.1$ GPa	1.00	0.5	
<i>Sinuses</i>	$K = 2.1$ GPa	1.00	0.5	
<i>Dura mater</i>	31.5	1.13	0.45	
<i>Falx/Tentorium</i>	31.5	1.13	0.45	
<i>Scalp</i>	Viscoelastic	1.13	0.42	
<i>Bridging veins</i>	$EA = 1.9$ N			

$K =$ Bulk modulus, and $EA =$ Force/unit strain.

FE Hybrid III dummy head

The FE Hybrid III 50th percentile dummy head developed by Fredriksson [26], Figure 2, comprises a rigid skull covered in rubber flesh. The rubber was modeled using material properties according to the calibration tests by Fredriksson [26]. The total weight of the head was 4.52 kg. For stability reasons the head was made featureless by suppression of the nose.

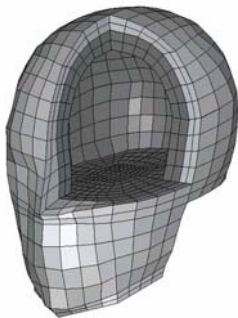


Figure 2. Finite element model of the featureless Hybrid III dummy head.

FE calculations

According to the FMVSS 201 regulation [4], automotive manufacturers have to certify that HIC(d) will not exceed 1000 when impacted with a 4.5 kg free motion head form with a speed of 6.7 m/s. The head form needs to be oriented in a manner so that the impact is nearly perpendicular to the target surface and thereby is likely to give a maximum HIC(d) [4, 14]. HIC is calculated as:

$$HIC = \max_{t_1, t_2} \left[\frac{1}{(t_2 - t_1)} \int_{t_1}^{t_2} a dt \right]^{2.5} (t_2 - t_1) \quad (1)$$

where a is the resultant head acceleration expressed as a multiple of the gravitational acceleration g , and t_1 and t_2 are any two points in time during the impact which are separated by 36 ms or less giving the maximum HIC. HIC(d) is empirically computed

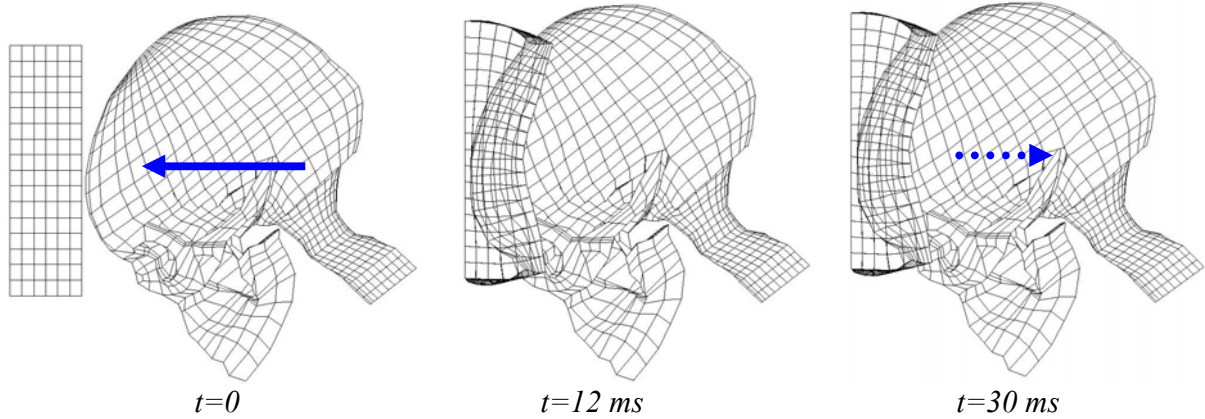
using the free motion HIC to account for the neck restraint [14] in a Hybrid III dummy according to:

$$HIC(d)=0.75446 \cdot HIC+166.4 \quad (2)$$

The head models are henceforth referred to as Hybrid III, and human head, respectively, were impacted towards a 50 mm thick interior padding having a

170*170 mm contact surface with an initial velocity of 6.7 m/s (Figure 3). Perpendicular impacts through the center of gravity of the head models were simulated. Additionally, the padding was tilted 45° to the horizontal plane in an effort to evaluate the influence of an oblique impact. This was done for the choice of padding parameters giving the lowest strain the brain for the perpendicular impact case.

Perpendicular impact through the c.g.:



Oblique impact towards a padding rotated 45°:

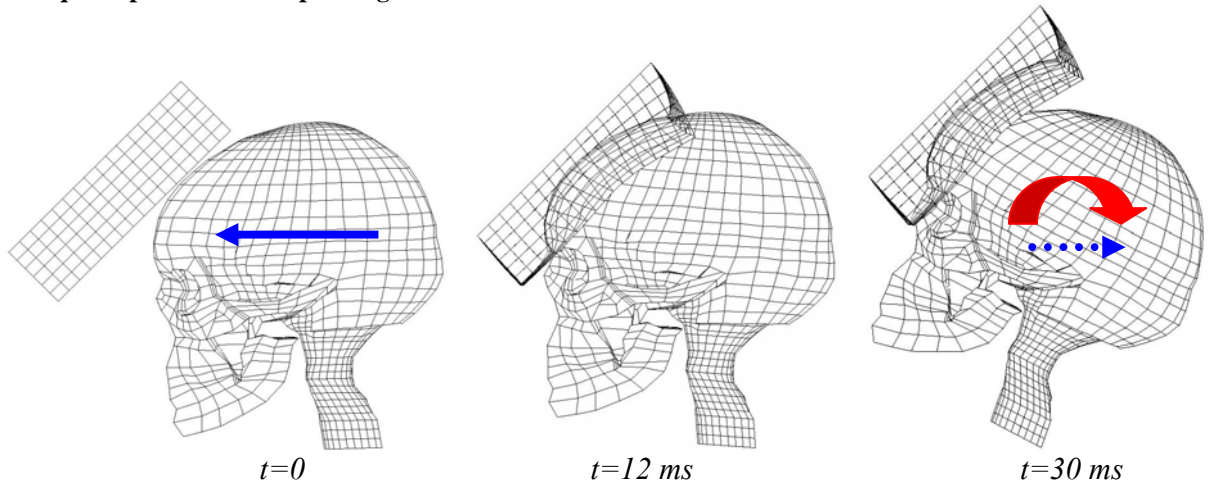


Figure 3. Animation of a perpendicular impact through the center of gravity of the head model (upper) and an oblique towards a 45° tilted padding (lower).

Foam material properties

The material characteristics of expanded polypropylene (EPP) foams have recently been found to be well described (R=0.969-0.999) by a simple empirical relationship which describes the stress-strain as a function of the foam density (Equation 3)

for a wide range of densities (31-145 kg/m³) [27]. The formulation is:

$$\sigma = A(1 - e^{(-E/A)\epsilon(1-\epsilon)^m}) + B\left(\frac{\epsilon}{1-\epsilon}\right)^n \quad (3)$$

where σ and ϵ are engineering stress and engineering strain, respectively, considered positive in compression, and A , B , E , m and n are empirical

constants derived for the particular type of foam. To create an even wider range of material behavior, the material characteristics of a theoretical EPP foam having a density of 14 kg/m^3 was generated and implemented (Figure 4). The EPP foams were modeled using a constitutive model developed for crushable foams in ls-dyna [15].

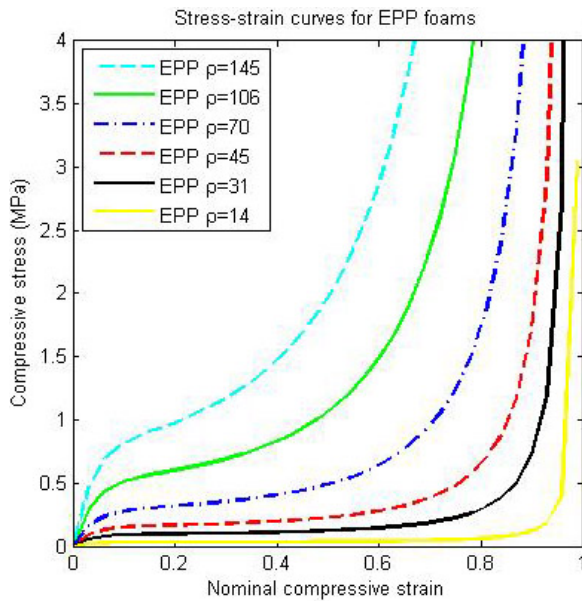


Figure 4. Material characteristics for the EPP foams used in the present study.

Interior contact definition

In order to keep the foam material elements from inverting when compressed under high pressure, an interior contact was defined. *CONTACT_INTERIOR was used in ls-dyna to account for the force transition within the foam, which is especially important when it bottoms out. It was defined so that when one layer of the foam reaches a compression strain of 98%, the internal contact transfers the loading to another layer of foam or to the scalp of the head model (or the rubber skin of the hybrid III model).

RESULTS

The resulting acceleration curves for the lowest and highest densities, as well as for one creating a low

acceleration peak is seen in Figure 5. The load and acceleration curves were filtered using an SAE 1000 low-pass filter. It can be seen that the 14 kg/m^3 foam has the lowest acceleration initially until it bottoms out at a foam compression of 98%. This phenomenon is creating a short duration high spike where the load is transferred to the scalp, skull, dura, CSF and the brain (Table 2).

Different results were obtained from the parameter study with the rigid Hybrid III dummy head when compared to the human head model (Table 2, Figure 6-7). It can be seen that, despite having the same translational mass and initial velocities, the hybrid III model predicts the lowest HIC(d) value for a higher density and stiffer foam than the human head model does; The hybrid III model predicts the lowest HIC(d) value for the 45 kg/m^3 foam while the human head model predict the lowest value for the 31 kg/m^3 foam (Table 2).

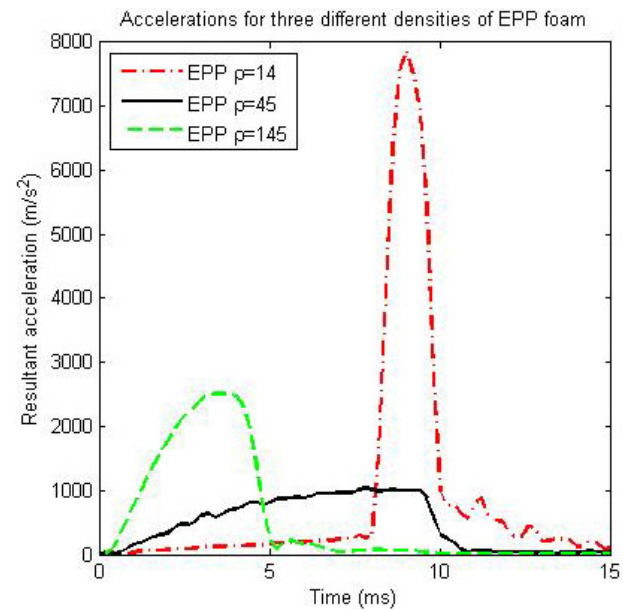


Figure 5. Curves showing the resultant acceleration of the head model using three different densities of EPP foam.

However, the HIC(d) for the head model manage to predict the strain in the brain for a purely perpendicular impact (Table 2).

Table 2.

Summary of the results from the parametric study using the rigid Hybrid III dummy head and the human head model.

		Density (kg/m ³)	14	31	45	70	106	145
Hybrid III	Peak acceleration (m/s ²)		6157	1616	1089	1398	1837	2331
	HIC(d)		6964	578	573	813	1151	1608
Head model	Peak acceleration (m/s ²)		7777	1225	1034	1397	1905	2515
	HIC(d)		11680	488	553	805	1205	1659
	Max princ strain in brain		34.8	8.2	10.0	12.6	14.3	16.3
	Max princ strain in Corp. Call.		19.2	4.0	4.1	4.5	4.7	4.9
	Max princ strain in White M.		34.1	8.2	10.0	12.6	14.3	16.3
	Max princ strain in Gray M.		34.8	6.7	8.1	10.2	11.9	13.6
	Max princ strain in Br.St.		17.4	7.4	8.9	11.2	12.5	14.3
	Max princ strain in Thal./Mid.Br.		14.5	3.7	4.0	4.6	5.1	5.4
	von M. stress in outer compact bone (MPa)		90.0	14.1	7.3	12.5	22.0	34.6
	von M. stress in inner compact bone (MPa)		90.0	13.1	10.1	14.1	20.7	27.8
von M. stress in por. Bone (MPa)		29.3	1.5	0.7	1.1	1.9	3.1	

Also, the lowest stress in the compact and porous cranial bone is found for the 45 kg/m³ foam which correspond to the lowest values of HIC for the hybrid

III head as well as the linear acceleration for the human head model (Table 2). However, the lowest strain in the brain is found for the 31 kg/m³ foam.

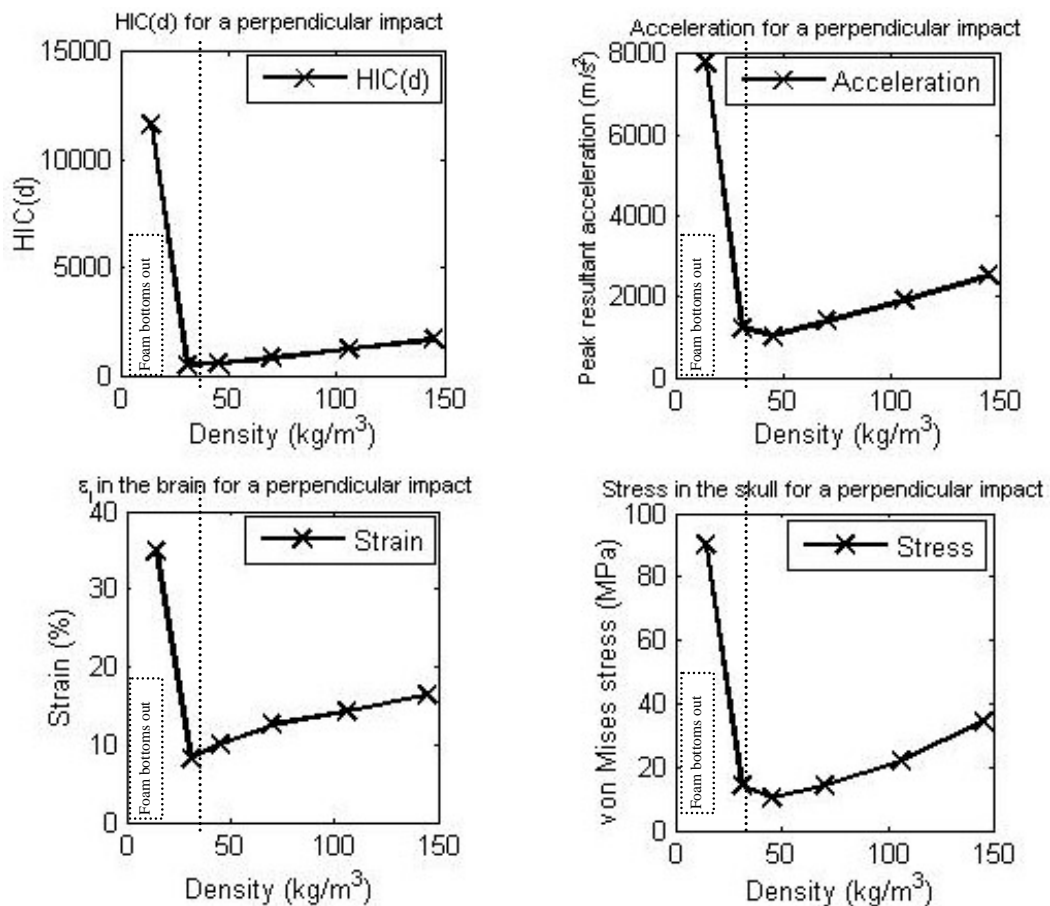


Figure 6. HIC(d) and peak resultant translational acceleration for a perpendicular impact using the biomechanical head model.

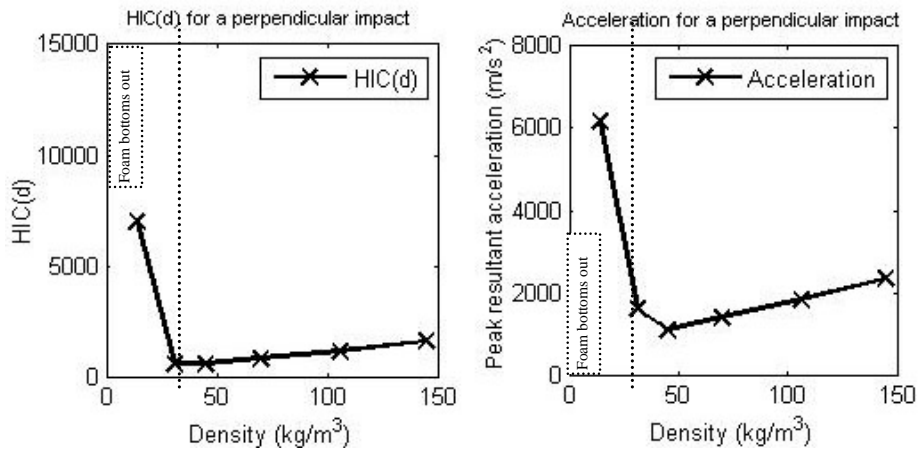


Figure 7. HIC(d) and peak resultant translational acceleration for a perpendicular impact using the HIII dummy model.

When simulating an oblique impact using the foam giving the lowest strain in the brain for the perpendicular impact (31 kg/m³) it was found that the

HIC(d) was reduced by more than 50 percent while the strain in the brain increased more than four times (Figure 8).

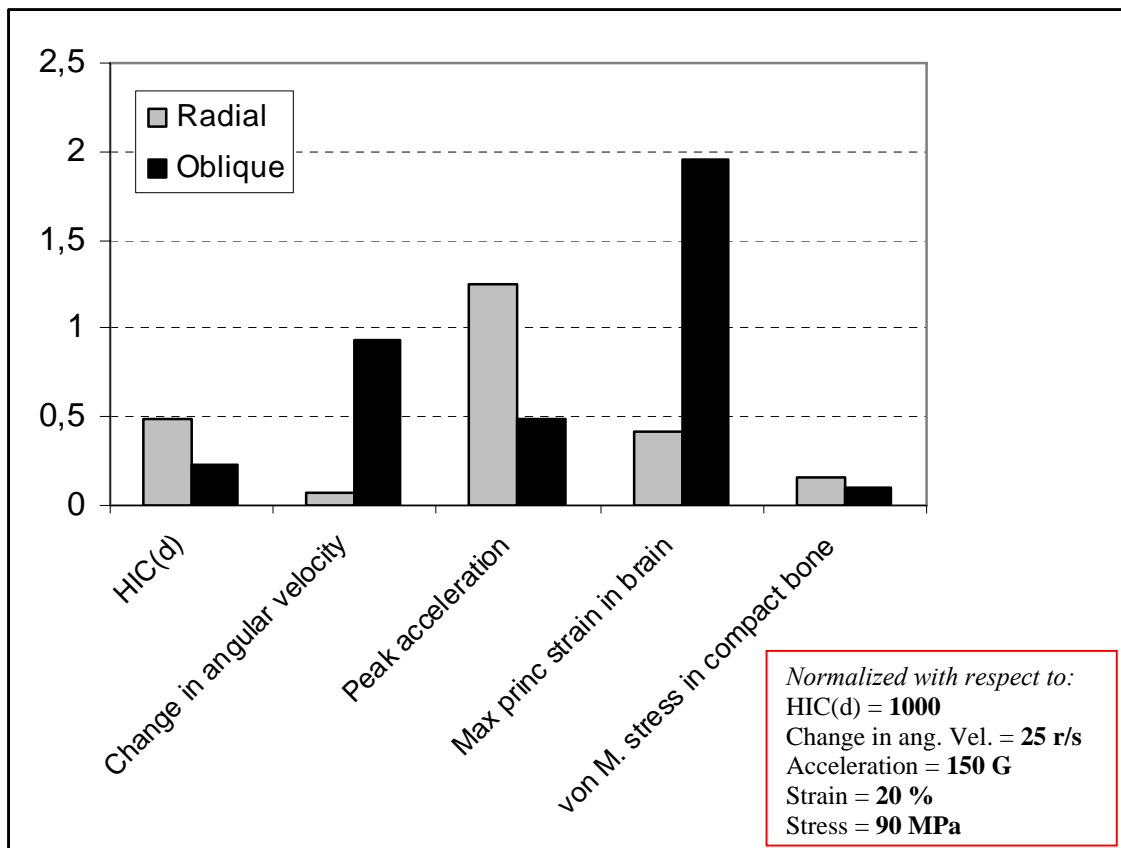


Figure 8. Staple chart summarising the HIC, strain in the brain and stress in the skull for an oblique and perpendicular impact towards the same padded surface.

It is obvious that substantially higher strain levels in the brain are obtained for an oblique impact, compared to a corresponding perpendicular one,

when impacted towards the same padding using an identical initial velocity of 6.7 m/s (Figure 9).

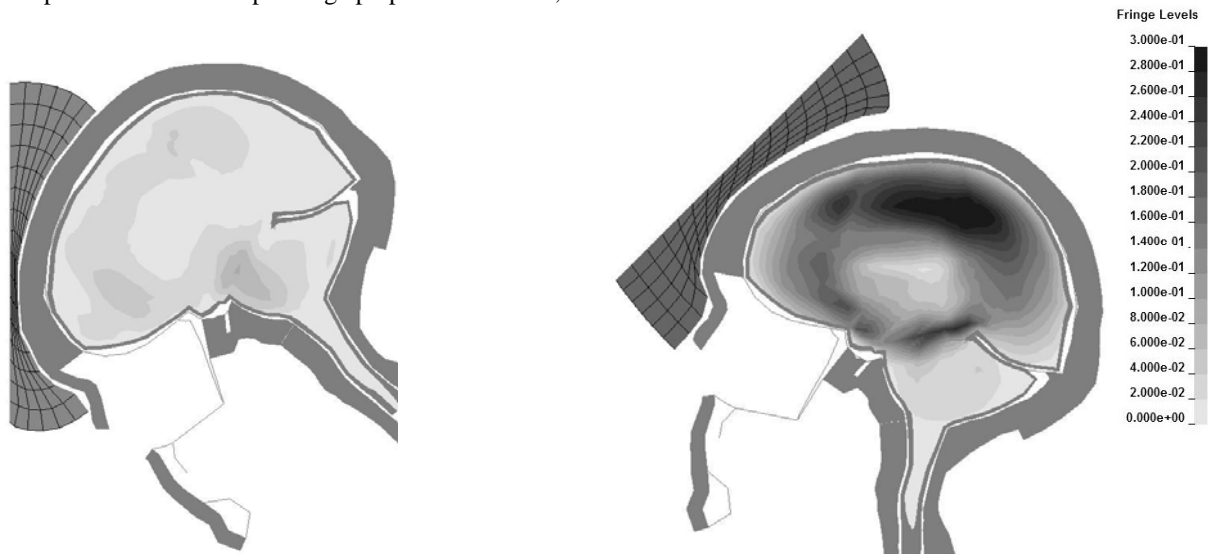


Figure 9. A comparison of the strain distribution (at time for maximum) using the 31 kg/m³ foam for a perpendicular (left) and an oblique impact (right).

DISCUSSION

The best choice of material properties with respect to a perpendicular impact using the Hybrid III head model reached different results compared to an impact with the biomechanical head model. On the other hand, the HIC(d) for the head model manage to predict the strain level in the brain for the purely perpendicular impact. This is supporting the findings of a correlation between the probability of concussion and HIC using predominantly translational concussion data from the NFL [28]. Recently, it was also found that HIC manage to predict the strain level in the brain of an FE model for purely translational impulses of short duration [3], while the peak change in angular velocity showed the best correlation with the strain levels for purely rotational impulses.

The foam giving the lowest strain in the brain was the one with a density of 31 kg/m³. This EPP foam has crush strength at 50 % compression of 125 kPa. The foam giving the lowest HIC(d) in the hybrid III dummy was the one with a density of 45 kg/m³ and a stress at 50 % compression of 230 kPa. This is in correspondence with Chou *et al.* [11] who found that the crush strength for a 50 mm thick B-pillar foam pad should be lower than 345 kPa to keep the HIC below 700.

The difference in the strain in the brain between an oblique and perpendicular impact with same initial

velocity towards the same padding was not predicted by the HIC(d). Even though the HIC reached acceptable levels for both the perpendicular and oblique impact towards the 31 kg/m³ EPP padding, the maximum strain in the human brain model for the oblique impact was almost twice the suggested allowable levels [29, 30]. One of the reasons for this is that rotational effects are transferred to the head when the impact has a tangential component. These induced rotations are known to cause large shear strains in the brain tissue [31, 32]. A low HIC(d) value is predicted for the oblique impact while higher levels strains are found compared to a corresponding perpendicular impact in the same direction. This underlines findings by previous investigators [32] who subjected 25 squirrel monkeys to controlled sagittal plane head motions, and found greater frequency and severity of brain lesions after rotation. This is consistent with the results presented herein, as well as the hypothesis presented by Holbourn [31].

For the pure perpendicular impact an insignificant peak change in angular velocity is found together with relatively low strain levels in the brain. For the oblique impact a large strain level is found in the brain for a large peak change in angular velocity. This corresponds to Holbourn's hypothesis [31] that the strain (and the injury) is proportional to the change in angular velocity for rotational impulses of short durations. Margulies and Thibault [33] presented a criterion for DAI described as tolerance curves of angular accelerations as a function of peak

change in angular velocity. Judging from those curves, angular accelerations exceeding ca. 8 krad/s² combined with an angular velocity of 70 rad/s or higher gives a risk of injury in the adult [33]. For the oblique impact in the present study, an angular acceleration of 3.3 krad/s² and a peak change in angular velocity of 23.5 rad/s was found together with a maximum strain in the brain of 39 percent which is almost twice the suggested tissue level tolerances for DAI [29, 30]. On the other hand, the HIC(d) is not insignificant for the oblique impact. Probably, a combination of the peak change in angular velocity and HIC(d) would predict the difference between perpendicular and oblique impacts of various severities. In this study, impact at only one location of the head is studied and therefore the results might differ depending on what impact location that is chosen. However, an impact to the forehead region was chosen in this study and this region is known to withstand more violence than most other parts of the head both for DAI [32] and for skull fractures [34]. Therefore the presented stress and strain levels for the head would probably be even higher if the impact was from other directions.

Strich [35] found diffuse degeneration of white matter in the cerebral hemispheres, as well as in the brain stem and corpus callosum areas in patients who have endured severe head trauma. This indicates that high strain in the white matter adjacent to the cortex, as seen in Figure 9 of this study, is likely to occur in a real life accident. Correspondingly, low levels of strain can be seen in the vicinity of the ventricles in the model, which supports the hypothesis that a strain relief is present around the ventricles [36].

The bulk modulus of brain tissue [37] is roughly 10⁵ times larger than the shear modulus. Thus, the brain tissue can be considered as a fluid in the sense that its primary mode of deformation is shear. Therefore, distortional strain was used as an indicator of the risk of traumatic brain injury. The maximal principal strain was chosen as a predictor of CNS injuries since it has shown to correlate with diffuse axonal injuries [29, 30, 38, 39, 40, 41], as well as for mechanical injury to the blood-brain barrier [42]. Other local tissue injury measures have also been proposed and evaluated, such as von Mises stress [42, 43, 44], the product of strain and strain rate [45, 46, 47], the strain energy [42], and the accumulative volume of brain tissue enduring a specific level of strain, the Cumulative Strain Damage Measure (CSDM), [9, 48]. However, a correlation has recently been found between the brain injury pattern of a patient being the victim of a motocross accident and the strain pattern in the head model [49]. This strain is very sensitive to the choice of stiffness for the brain tissue [17] and

more work is needed to fully describe the non-linear and viscoelastic response of living brain tissue.

Another possible limitation is the constitutive model used for the foam. However, this model has shown to predict the response in uniaxial compression tests for expanded polystyrene foams of similar densities in a previous study [50]. On the other hand, to model the elastic spring-back of low density foams such as polyurethane foams, probably a different constitutive model should be chosen. Also, the high load and acceleration behavior created when the foam bottoms out is sensitive to the parameters chosen for the foam and the interior contact. In this study, the stress-strain curves were defined up to 99 % compression for all foams, while the interior contact was activated when the strain reached 98 %.

In the extension, protective devices and materials can be optimized to see if the tissue level stresses and strains can be minimized so that the potential consequence in a future accident could be reduced or avoided. Iterative optimization procedures in conjunction with dynamic and non-linear FEA can be used together with detailed FE models to maximize the safety for the humans when impacting towards of interior and exterior surfaces in automotive structures. The existing FE model of the head can be used in optimization of the properties and geometry of energy absorbing materials, so that the stresses and strains on a tissue level are minimized. This methodology has previously been used for optimization of simplified hood structures [51]. The proposed methodology is directly applicable in development of interior and exterior surfaces in heavy vehicles and rail vehicles as well.

CONCLUSIONS

The results emphasize the importance of treating the human brain as a non-rigid body. Although it is obvious it must be kept in mind that in strive for improved safety it is essential to employ physically representative metrics since the applied criteria will drive the development. Hence, local tissue thresholds or more human-like dummies together with injury criteria accounting for both angular and translational kinematics should be used to obtain more physically representative and reliable optima in safety design. This result is conceptually obvious since a global criterion will never cover all the various injury mechanisms characterized by local tissue deformation.

REFERENCES

- [1] Murray, C.J.L. and Lopez, A.D. 1996. "The Global Burden of Disease-Summary." The Harvard School of Public Health, Harvard University Press, ISBN: 0-674-35448-6.
- [2] Kleiven, S., Peloso, P.M. and von Holst, H. 2003. "The Epidemiology of Head Injuries in Sweden from 1987 to 2000." *Journal of Injury Control and Safety Promotion*, 10 (1): 173-180.
- [3] Kleiven, S. 2006. "Evaluation of head injury criteria using an FE model validated against experiments on localized brain motion, intra-cerebral acceleration, and intra-cranial pressure." *International Journal of Crashworthiness*, 11 (1): 65-79.
- [4] U.S. Department of Transportation (DOT), National Highway Traffic Safety Administration (NHTSA). 1995. "Laboratory test procedures for FMVSS 201", TP-201UU-00, Safety Assurance, OVSC, Washington, DC.
- [5] National Highway Traffic Safety Administration, U.S. Department of Transportation (DOT). 1972. "Occupant Crash Protection – Head Injury Criterion." S6.2 of MVSS 571.208, Docket 69-7, Notice 17. NHTSA, Washington, DC.
- [6] Gennarelli, T.A. 1983. "Head injuries in man and experimental animals: Clinical aspects." *Acta Neurochir Suppl.*, 32: 1-13.
- [7] Bellora, A, Krauss, R and Van Poolen, L. 2001. "Meeting Interior Head Impact Requirements: A Basic Scientific Approach." Society of Automotive Engineers, SAE Paper No. 2001-01-0469.
- [8] Ueno, K., Melvin, J.W. 1995. "Finite element model study of head impact based on hybrid III head acceleration: The effects of rotational and translational acceleration." *J. Biomechanical Engineering*, 117(3): 319-328.
- [9] DiMasi, F., Eppinger, R.H., Bandak, F.A. 1995. "Computational analysis of head impact response under car crash loadings." *Proc 39th Stapp Car Crash Conf, Society of Automotive Engineers, SAE Paper No. 952718, Society of Automotive Engineers, Warrendale, PA: 425-438.*
- [10] Zhang, L. Yang, K.H., King, A.I., 2004. "A Proposed Injury Threshold for Mild Traumatic Brain Injury." *J. Biomechanical Engineering*, 126(1): 226-236.
- [11] Chou, C.C., Wu, F., Lim, G.G. and Patel, R. N. 1997. "Optimization design of foam/pillar for head impact protection using design of experiment approach.", *Journal of Passenger Cars*, P-308, X International Conference on Vehicle Structural Mechanics and CAE, Troy, Michigan, USA, Society of Automotive Engineers, SAE Paper No. 971543.
- [12] Barbat, S.D., Jeong, H.-Y. and Prasad, P.P. 1996. "Finite element modeling and development of the deformable featureless headform and its application to vehicle interior head impact testing.", *Journal of Passenger Cars*, SP-1174, SAE International Congress and Exposition, Detroit, Michigan, USA, Society of Automotive Engineers, SAE Paper No. 960104.
- [13] Sounik, D.F., Gansen, P., Clemons, J.L. and Liddle, J.W. 1997. "Head-impact testing of polyurethane energy-absorbing (EA) foams.", *Journal of Materials and Manufacturing*, SAE International Congress and Exposition, Detroit, Michigan, USA, Society of Automotive Engineers, SAE Paper No. 970160.
- [14] Deb, A. and Chou, C.C. 2003. "Headform impact safety design through simulation and testing.", *SAE 2003 World Congress*, Detroit, Michigan, USA, Society of Automotive Engineers, SAE Paper No. 2003-01-1386.
- [15] Livermore Software Technology Corporation. 2003. "LS-DYNA KEYWORD USER'S MANUAL, Version 970"
- [16] Kleiven, S. 2002. "Finite Element Modeling of the Human Head." *Doctoral Thesis. Technical Report 2002-9, Department of Aeronautics, Royal Institute of Technology, Stockholm, Sweden.*
- [17] Kleiven, S., Hardy, W.N. 2002. "Correlation of an FE model of the Human Head with Experiments on localized Motion of the Brain – Consequences for Injury Prediction." *46th Stapp Car Crash Journal*: 123-144.
- [18] Kleiven, S. 2006. "Biomechanics as a forensic science tool - Reconstruction of a traumatic head injury using the finite element method." *Scand J Forens Sci.*, No. 2: 73-78
- [19] Kleiven, S., and von Holst, H. 2002. "Consequences of Head Size following Trauma to the Human Head." *Journal of Biomechanics*, 35 (2): 153-160.

- [20] Miller K, Chinzei K. 2002. "Mechanical properties of brain tissue in tension." *Journal of Biomechanics*, 35(4): 483-90.
- [21] Nicolle, S., Lounis, M., Willinger, R. and Palierne, J.F. 2005. "Shear linear behavior of brain tissue over a large frequency range." *Biorheology*, 42(3): 209-23.
- [22] Robbins, D.H., Wood, J.L. 1969. "Determination of mechanical properties of the bones of the skull." *Exp. Mech.*, 9(5): 236-240.
- [23] McElhaney J.H., Fogle, J.H., Melvin, J.W., Haynes, R.R., Roberts, V.L., Alem, N.B. 1970. "Mechanical properties of cranial bone." *J. Biomechanics*, 3: 495 -511.
- [24] Wood, J.L. 1971. "Dynamic response of human cranial bone." *J. Biomechanics*, 4 (3): 1-12.
- [25] Melvin J.W., McElhaney J.H., Roberts, V.L. 1970. "Development of a Mechanical Model of the Human Head - Determination of Tissue Properties and Synthetic Substitute Materials." 14th Stapp Car Crash Conf, Society of Automotive Engineers, SAE Paper No. 700903.
- [26] Fredriksson, L.A. 1996. "A Finite Element Data Base for Occupant Substitutes." Doctoral Thesis, Dissertation No. 447, Division of Solid Mechanics, Department of Mechanical Engineering, Linköping University, Sweden.
- [27] Avalle, M., Belingardi, G. and Ibba, A. 2007. "Mechanical models of cellular solids: Parameters identification from experimental tests." *International Journal of Impact Engineering*, Volume 34, Issue 1, January: 3-27.
- [28] Newman, J.A. Shewchenko, N., and Welbourne, E. 2000. "A Proposed New Biomechanical Head Injury Assessment Function - The Maximum Power Index." Proc. 44th Stapp Car Crash Conf., SAE Paper No. 2000-01-SC16.
- [29] Bain, B.C., and Meaney, D.F. 2000. "Tissue-Level Thresholds for Axonal Damage in an Experimental Model of Central Nervous System White Matter Injury." *Journal of Biomechanical Engineering*, 16: 615-622.
- [30] Morrison III, B., Cater, H.L., Wang, C.C.B., Thomas, F.C., Hung, C.T., Ateshian, G.A. and Sundström, L.E. 2003. "A tissue level tolerance criterion for living brain developed in an in vitro model of traumatic mechanical loading." 47th Stapp Car Crash Journal, SAE Paper No. 2003-22-0006.
- [31] Holbourn, A. H. S. 1943. "Mechanics of Head Injury." *The Lancet*, 2:438-441.
- [32] Gennarelli, T.A., Thibault, L.E. and Ommaya, A.K. 1972. "Pathophysiological Responses to Rotational and Translational Accelerations of the Head." Proc. Stapp Car Crash Conf., Society of Automotive Engineers, SAE Paper No. 720970, 296-308.
- [33] Margulies, S.S. and Thibault, L.E. 1992. "A Proposed Tolerance Criterion for Diffuse Axonal Injury in Man." *J. Biomech.*, 25 (8): 917-923.
- [34] Schneider, D.C. and Nahum, A.M. 1972. "Impact studies of facial bones and skull." Proceedings 16th STAPP Car Crash Conference, Detroit, USA, , Society of Automotive Engineering, Warrendale, PA, SAE Paper No. 720970.
- [35] Strich, S.J. 1956. "Diffuse degeneration of the cerebral white matter in severe dementia following head injury." *J. Neurol. Neurosurg. Psychiat.*, 19, October 9: 163-185.
- [36] Ivarsson, J., Viano, D.C., Lövsund, P. and Aldman, B. 2000. "Strain relief from the cerebral ventricles during head impact: experimental studies on natural protection of the brain." *J. Biomechanics*, 33 (2): 181 – 189.
- [37] McElhaney, J.H., Roberts, V.L., and Hilyard, J.F. 1976. "Properties of human tissues and components: nervous tissues." *Handbook of human tolerance*, Automobile Research Institute Inc., Tokyo, Japan, 143.
- [38] Bain, B.C., Billiar, K.L., Shreiber, D.I., McIntosh, T.K., and Meaney, D.F. 1997. "In vivo mechanical thresholds for traumatic axonal damage." Proc. of AGARD AMP Specialists' Meeting, Mescalero, New Mexico, USA, 7-9 November 1996, published in CP-597.
- [39] Galbraith, J.A., Thibault, L.E., and Matteson, D.R. 1993. "Mechanical and electrical responses of the squid giant axon to simple elongation." *J. Biomech. Engineering*, 115: 13-22.
- [40] Thibault, L.E., Gennarelli, T.A., Margulies, S.S., Marcus, J., and Eppinger, R. 1990. "The strain dependent pathophysiological consequences of inertial loading on central nervous system tissue." Proc. IRCOBI Conf., Bron, Lyon, France: 191-202.

- [41] Gennarelli, T.A., Thibault, L.E., Tipperman, R., *et al.* 1989. "Axonal Injury in the Optic Nerve: A model of Diffuse Axonal Injury in the brain." *J. Neurosurg.*, 71: 244-253.
- [42] Shreiber, D.I., Bain, A.C. and Meaney D.F. 1997. "In vivo thresholds for mechanical injury to the blood-brain barrier." 41st Stapp Car Crash Conf., Society of Automotive Engineers, SAE Paper No. 973335: 177-190.
- [43] Anderson, R.W.G., Brown, C.J., Blumbergs, P.C., Scott, G., Finney, J.W., Jones, N.R., and McLean, A.J. 1999. "Mechanics of axonal injury: An experimental and numerical study of a sheep model of head impact." *Proc. 1999 IRCOBI Conf.* Sitges, Spain: 107-120.
- [44] Miller, R.T., Margulies, S.S., Leoni, M., *et al.* 1998. "Finite Element Modeling Approaches for Predicting Injury in an Experimental Model of Severe Diffuse Axonal Injury." *Proc. 42nd Stapp Car Crash Conf.*, Society of Automotive Engineers, SAE Paper No. 983154: 155-166.
- [45] Goldstein, D.M., Mazuchowski, E.L., Gdula, W., and Thibault, L.E. 1997. "In vitro and mathematical models of axonal injury in CNS tissue." *Prevention Through Biomechanics, Symposium Proceedings*, Wayne State University: 207-215.
- [46] Viano, D.C. and Lövsund, P. 1999. "Biomechanics of brain and spinal-cord injury: analysis of neuropathologic and neurophysiologic experiments." *J. Crash Prevention and Injury Control*, 1: 35-43.
- [47] King, A.I., Yang, K.H., Zhang, L. and Hardy, W.N. 2003. "Is head injury caused by linear or angular acceleration?" *Proc. IRCOBI Conference*, Lisbon (Portugal): 1-12.
- [48] Bandak, F.A., and Eppinger, R.H. 1994. "A three-dimensional FE analysis of the human brain under combined rotational and translational accelerations." *Proc. 38th Stapp Car Crash Conf.*, Society of Automotive Engineers, Warrendale, PA: 145-163.
- [49] Kleiven, S. 2006. "Biomechanical reconstruction of traumatic brain injuries - Correlation between injury patterns and FE models." *Proc. 5th World Congress of Biomechanics*, München, Germany, *Journal of Biomechanics* 2006; Vol. 39 Suppl. 1, page S154.
- [50] Aare, M. 2003. "Prevention of head injuries: Focusing specifically on oblique impacts." *Doctoral Thesis. Technical Report 2003-26*, School of Technology and Health, Royal Institute of Technology, Stockholm, Sweden.
- [51] Juntikka, R., Kleiven, S. and Hallström, S. 2004. "Optimization of Single Skin Surfaces for Head Injury Prevention – A Comparison of Optima Calculated for Global versus Local Injury Thresholds." *International Journal of Crashworthiness*, 9 (4): 365-379.

REAR SEAT OCCUPANT PROTECTION IN FRONTAL CRASHES AND ITS FEASIBILITY

Richard Kent¹, Jason Forman¹, Daniel P. Parent¹, Shashi Kuppa²

¹University of Virginia

²National Highway Traffic Safety Administration

U.S.A

07-0386

ABSTRACT

As part of NHTSA's Rear Seat Occupant Protection Research Program, the Fatality Analysis Reporting System (FARS) and State Data System (SDS) for Florida, Pennsylvania and Maryland were utilized to estimate relative fatality rates and injury risk ratios between the front and rear seat passengers. In addition, a parametric study of rear-seat restraint parameters was performed to assess chest deflection and head excursion trends for different belt load limits, pretensioner location(s) and stroke, and impact speeds with the Hybrid III (HIII) 50th percentile male and 5th percentile female dummies. Simulation data were validated using 48 km/h frontal impact sled tests with a standard belt system in outboard rear seats of a mid-size passenger car buck.

The real world data suggests that the fatality and serious injury risk in frontal crashes is higher for older occupants in rear seats than for those in front seats. In addition, the relative effectiveness (to mitigate serious injury and death) of rear seats with respect to front seats for restrained adult occupants in newer vehicle models is less than it is in older models, presumably due to the advances in restraint technology that have been incorporated into the front seat position. The simulations demonstrated that adult dummy injury measures in the rear seat can be reduced by incorporating restraint technology (load limiting and pretensioning) used in the front seat, even in the absence of an air bag and knee bolster for load sharing. A force-limiting belt with a pretensioner in the rear seat can maintain or reduce head excursion relative to a standard belt, while significantly reducing chest deformation and thoracic injury risk. In fact, 42 sets of restraint parameters were identified that reduced both head excursion and chest deflection of the 50th percentile male relative to the baseline belt.

INTRODUCTION

Rear seat occupants constitute 14 percent of all vehicle occupants in passenger cars and LTVs. Among these rear seat occupants, 85% are in outboard seating positions and 69% are fourteen years-old or younger and are 5 feet 4 inches or shorter.

Kuppa et al. (2005) reported on NHTSA's initial efforts to examine rear seat occupant protection and presented a double-paired comparison study using the Fatality Analysis Reporting System (FARS) data files to determine the relative effectiveness of the rear seats with respect to the front passenger seat position in frontal crashes. The results indicated that restrained occupants older than 50 years were significantly better off in the front seat than in rear seats. In addition, the presence of a front passenger air bag reduced the relative effectiveness of the rear seat compared to the front seat for all age groups except for children in child safety seats. The most injured body region for adults in the rear seat was the thorax with the source of injury being the shoulder belt. The rear seat position offered improved protection over the front passenger seat for unrestrained occupants of all ages.

Cummings and Smith (2005) conducted a matched cohort analysis of the FARS data files to determine the risk of death of rear seat passengers compared to front seat passengers in motor vehicle crashes. In agreement with the Kuppa et al. (2005) paper, this study indicated that while the fatality risk is lower in the rear seat, the protective effect of the rear seat position decreased with increasing passenger age and with restraint use. The rear seat position offered no additional protection to restrained adults in vehicles with front passenger air bags.

Swanson et al. (2003) found that the average front end stiffness of passenger cars computed from the data collected in the New Car Assessment Program (NCAP) frontal crash test program for model years (MY) 1982 to 2001 shows an increasing trend for newer vehicle models. In particular, there is a significant increase in the stiffness of passenger cars for MY 1998-2001 compared to the previous vehicle models. Concurrently, the NCAP frontal crash test rating program indicates an improvement in vehicle frontal crash test rating with a large percentage of the vehicle fleet for MY 1999 and newer obtaining the highest NCAP scores (NHTSA, Five Star Crash Test Rating, 2007). Vehicles with stiffer front-end structures experience more severe crash pulses, and thus depend more on the occupant restraint system (ie., airbag, seat belts, pretensioners, etc.) to manage the crash energy. In recent years, the front seat occupants have benefited from advanced restraint concepts such as belts with pretensioners and load

limiters, which provide a clear safety benefit in frontal crashes in the field (e.g., Foret-Bruno et al. 1998), and also lead to an improved NCAP frontal crash test rating. For example, Walz (2003) estimated that the combination of pretensioners and load limiters reduced the HIC values by 232, peak chest acceleration by an average of 6.6g, and peak chest deflection by 10.6 mm for HIII dummies in the driver and right front passenger positions. The NCAP frontal crash testing, however, evaluates only the injury risk to front seat passengers, so it has not stimulated the development of similar or other advanced restraint technology in the rear seat.

While previous studies examined the effectiveness of rear seats with respect to front seats, no attempt has been made to examine the effect of changes in vehicle front-end stiffness and the emergence of advanced restraint systems on the performance of rear seats relative to the front seats.

The current paper examines the trends in rear seat occupant protection relative to front seat protection for changing vehicle designs and restraint systems. In addition, the paper examines the feasibility of improvement in rear seat adult occupant protection using advanced restraints similar to those available for the front seat. Sled tests were conducted with a rear seat sled buck of a representative mid-size vehicle with the Hybrid III 50th percentile male (AM50) and 5th percentile female (AF5) dummies. Mathematical simulations of the sled tests using MADYMO were also conducted to determine the effect of pretensioners and load limiters on the kinematics and injury measures of the dummies in the rear seat. This paper presents selected results of sled tests used to benchmark the computational model, as well as the full computational study.

Additional sled tests are ongoing and will include testing with pediatric dummies, additional adult dummies, and adult cadaveric subjects with typical contemporary rear-seat restraints and advanced rear-seat restraints.

REAL WORLD DATA

ANALYSIS OF FARS DATABASES

Kuppa et al. (2005) conducted a double paired comparison study using the FARS data files for the years 1993-2003 to determine the risk of death of outboard rear seat occupants relative to the right front seat passenger. The drivers in those crashes were used as the control group. That analysis examined the fatality risk ratios for front and rear seat occupants by occupant age and restraint status. The effects of advanced restraint systems for the front seat occupants and the increasing vehicle stiffness on

the relative effectiveness of rear seats with respect to front seats were not examined in that study. In addition, no attempt was made to examine the effectiveness of rear seats relative to front seats with respect to non-fatal injury. The current study examines these issues by reanalyzing the FARS datafiles and also examining the State Data System files.

The introduction rate of pretensioners and load limiters into the US vehicle fleet is presented in Figure 1. Before 1999, less than 10% of the vehicle fleet was equipped with a load limiter or a pretensioner. Approximately 40% of the MY 1999 vehicles were equipped with load limiters and 25% were equipped with load limiters and pretensioners. Among MY2002 vehicles, 56% were equipped with pretensioners and 74% equipped with load limiters.

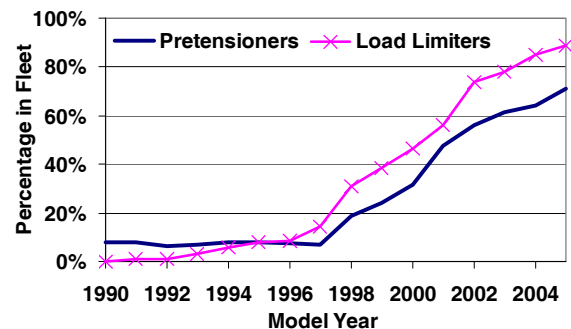


Figure 1. Introduction of advanced belt restraints into the passenger and LTV fleet in the United States.

As shown in Figure 1, there is a bilinear trend in advanced restraint fitment into the passenger car and LTV fleet, with a rapid increase starting at approximately model year 1998. The review by Swanson et al. (2003) of NCAP tests indicated a similar increase in front-end stiffness of passenger cars during this time period. Therefore, in order to examine the effect of advanced restraints and vehicle front-end stiffness on the relative effectiveness of rear seats with respect to front seats, two categories of vehicle model years were considered in this study: 1991-1998 and 1999-2006.

A double paired comparison analysis was conducted using the FARS data files for the years 1993 to 2005 in a similar manner as described by Kuppa et al. (2005). In particular, the relative effectiveness of outboard rear seats compared to the front passenger seat for mitigating fatalities of restrained occupants was examined for the different model year categories and different age groups. Restrained outboard occupants involved in frontal crashes of MY 1991-2005 vehicles with no rollovers were considered. The restrained driver was used as the control group for this analysis.

Two groups of fatal crashes were considered for the double paired comparison study. The first group consisted of fatal crashes where a driver and front outboard right seat passenger were present and at least one of them was killed. The second group consisted of fatal crashes where a driver and a rear outboard seat passenger were present and at least one of them was killed. Each of these groups was further subdivided into different passenger age categories.

If F1 and F2 are the number of driver and front passenger fatalities, respectively, from the first group and F3 and F4 are the number of driver and rear passenger fatalities from the second group, then the relative fatality risk ratio (R) and the effectiveness (E) for the rear seats relative to the front passenger seat is given by Equations 1 and 2

$$R = \frac{F_4 / F_3}{F_2 / F_1} \quad [1]$$

$$E = 100 \times (1 - R) \quad [2]$$

The standard error of the log of the risk ratio (standard error of the log odds = σ) and the error ranges in the effectiveness estimates are given by Equations 3 and 4

$$\sigma = \sqrt{\frac{1}{F_1} + \frac{1}{F_2} + \frac{1}{F_3} + \frac{1}{F_4}} \quad [3]$$

$$E_{lower} = 100 \times [1 - e^{\ln(R) + \sigma}] \quad [4a]$$

$$E_{upper} = 100 \times [1 - e^{\ln(R) - \sigma}] \quad [4b]$$

The results of the analysis are presented in Figures 2 and 3. Note that all the vehicles of model years 1999-2006 are equipped with front passenger air bags, so the rear seat effectiveness for the condition of no passenger air bag could not be computed for this model year category.

When the error bars in the effectiveness estimates presented in Figures 2 and 3 do not pass zero, it implies that the effectiveness estimate is significant ($p < 0.05$). The effectiveness estimates of rear seats relative to front passenger seats for vehicle models 1991-1998 (Figure 2) are similar to that reported earlier by Kuppa et al. (2005). Occupants older than 50 years have a lower risk of death in a frontal crash when sitting in the front passenger seat than in rear seats. The data presented in Figure 3 suggest that the effectiveness of rear seats relative to the front seats is lower for the newer vehicle models than the older models, though the sample size is not yet sufficient to

yield a statistically significant difference. Presumably, advances in front-seat restraint technology are at least a partial explanation for this trend.

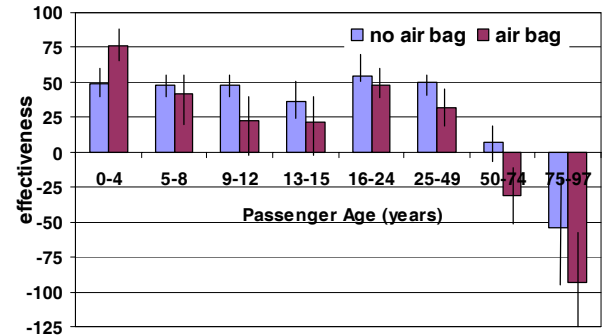


Figure 2. Effectiveness of outboard rear seats compared to front outboard passenger seats with and without front passenger air bag in mitigating fatalities for restrained occupants in MY 1991-1998 vehicles.

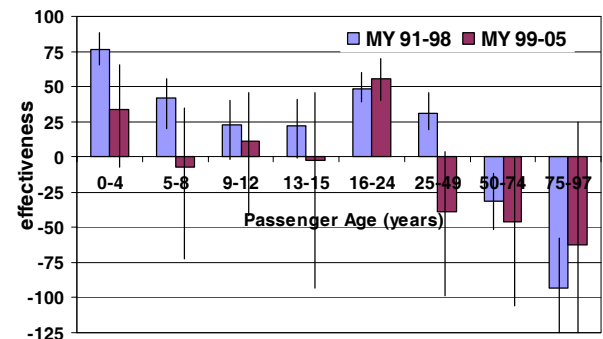


Figure 3. Effectiveness of outboard rear seats compared to front outboard passenger seats in mitigating fatalities for restrained occupants in MY 1991-1998 and MY 1999-2005 vehicles (all vehicles equipped with air bags).

In order to augment the FARS analysis, state data files from the Pennsylvania, Maryland, and Florida were analyzed to determine relative injury risk (including non-fatal injuries) between front and rear seat passengers. The state data files are a compilation of all police accident reports (PARs) of crashes that meet a certain set of criteria. The database contains information describing crash characteristics, and the vehicles and people involved. The data from these three states were selected for analysis because the VIN numbers of the involved vehicles, the crash type, belt status of occupants, the occupant injury severity secondary to the crash, and details of the uninjured occupants were available in the data files. In Florida, the inclusion of a case into the state database is at the discretion of the police officer,

while in Maryland and Pennsylvania at least one vehicle had to be towed for the case to be included in the State Data System.

State data files for the years 1993-2003 were used to extract cases of vehicles (passenger cars and LTVs) of model years 1991 to 2005 involved in frontal crashes. Only frontal crashes with no rollovers were considered in the analysis. The injury severity was grouped into two broad categories. The occupant was classified into the “No Injury” category when he/she sustained no injury, or no evident injury, or evident but non-incapacitating injury. The occupant was classified into the “Injury” category if he/she sustained an incapacitating injury (defined as any injury that is fatal or prevents the injured person from walking, driving, or continuing normal activity that he/she was capable of performing prior to the vehicle crash).

Again, a double paired comparison analysis using the driver as the control group was conducted to estimate the effectiveness (as defined by Equation 2) of the rear seat to mitigate incapacitating injury in frontal crashes compared to the front passenger seat. Restrained drivers and restrained outboard front and rear seat passengers were considered in the assessment of advanced restraints and vehicle stiffness on the injury risk ratio. The analysis was conducted taking into consideration the passenger age, vehicle body type (passenger cars and LTVs), and vehicle model year (MY 1991-1998 and MY 1999-2005).

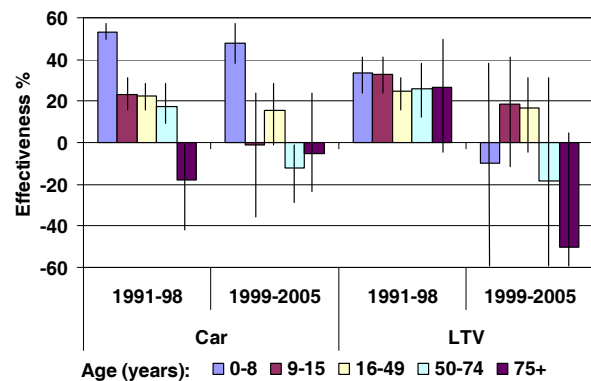


Figure 4. Effectiveness of outboard rear seats compared to front outboard passenger seats in mitigating incapacitating injuries for restrained occupants in MY 1991-1998 and MY 1999-2005 vehicles.

The double paired comparison study of the state data indicates that older occupants (75+ years) are at greater risk of injury in the rear seats than in the front seats (Figure 4). As in the Smith and Cummings (2005) study, the state data indicate that the protective effect of the rear seat position decreases with increasing passenger age. The relative

effectiveness of rear seats compared to the front passenger seat was lower in vehicle models 1999-2005 than in vehicle models 1991-1998 for both cars and LTVs. Due to the small sample size of crashes of LTVs and crashes involving newer vehicle models in the state data files, the relative effectiveness of rear seats for the newer vehicle models and for LTVs are not significant, but both the FARS data and the state data suggest that the introduction of advanced restraints and the greater vehicle front end stiffness may play a role in reducing the relative effectiveness of rear seats compared to front seats.

PARAMETRIC STUDY OF RESTRAINT CHARACTERISTICS – METHODS

The results of the field analyses described above, coupled with the findings from Kuppa et al. (2005) that the most frequently injured body region for restrained adults in the rear seat is the thorax with the source of injury being the shoulder belt, justify further study on the feasibility of incorporating front-seat restraint technology (load limiting and pretensioning) into the rear seat environment. There is an intrinsic tradeoff associated with seat belt load limiting: head excursion increases as chest deformation decreases. This tradeoff is managed in the front seat by load sharing with the air bag and knee bolster, which limits head excursion and mitigates head contacts with the interior vehicle structure. The front seat pan can also be designed to restrict pelvic motion, providing another load-path for restraint and allowing further control of occupant kinematics. In the rear seat there is no air bag to limit head motion, there is less control of knee motion, and the seat pan geometry is dictated largely by the structural requirement of the vehicle chassis. Thus, the belt design alone must address most of the challenge of reducing chest deflection without allowing excessive head excursion. As a preliminary assessment of this tradeoff in the rear seat environment, a computational parametric study was undertaken.

MADYMO version 6.3.1 was used to simulate frontal (12:00 PDOF) impacts with Hybrid III 50th percentile male (AM50) and 5th percentile female (AF5) dummies seated in the outboard rear seating position of a contemporary mid-size sedan (Figure 5). The MADYMO model used in the parametric study was developed using the data collected during a series of rear-seat sled tests of AM50 and AF5 dummies. Three tests were conducted with each dummy at each of two impact velocities, 29 km/h and 48 km/h. Data collected during these tests included head, chest, and pelvis acceleration, chest deflection, neck loads and moments, femur loads, and belt loads.

High-speed video was used to capture the motion of the occupants, as well the shoulder belt retractor payout and belt slip at the buckle. The baseline MADYMO model for each occupant was evaluated against these measurements for the case of no belt load limit and zero pretensioner stroke for the 29 km/h and 48 km/h conditions, placing higher importance on head excursion and chest deflection. Additional benchmarking characteristics included chest acceleration, shoulder belt retractor payout, and belt loads. The initial positions of the head and H-point, as well as the angles of the H-point, torso, femur, and tibia, were adjusted to mimic the initial occupant position from the sled tests. At this position, the face of the 50th percentile male is 540mm from the rear surface of the headrest on the front passenger seat in its rearmost fore-aft track adjustment position. In other words, in the sedan considered here, the head strikes the front seat back, in its rear-most fore-aft adjustment position at a forward excursion of $X_h = 540$ mm (Figure 5). This distance is used as representative of a minimum level of available excursion distance in a typical mid-size passenger car.

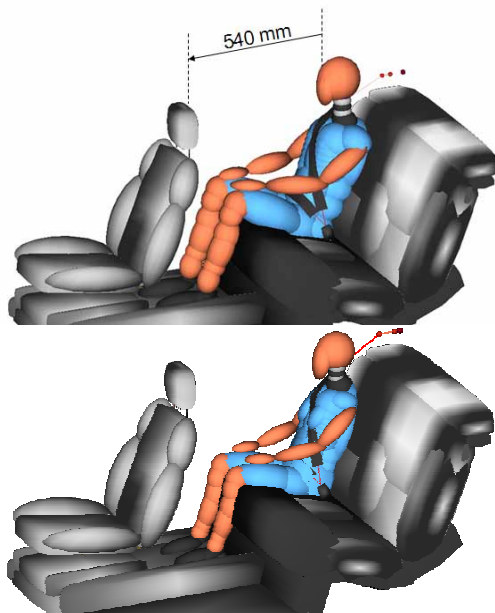


Figure 5. MADYMO rear-seat occupant model with AM50 (top) and AF5 (bottom). Front seat is in the rear-most fore-aft adjustment position.

The model used a hybrid belt system made up of finite element lap and shoulder belts connected with standard MADYMO belt elements. These elements allowed belt slip between the lap and shoulder belts at the buckle and included a force-payout characteristic to capture the film spool effect at the retractor. The force-payout characteristic was

determined from data collected during the rear-seat sled tests. The force was measured by the upper shoulder belt load cell, while the payout was measured by a high-speed camera focused on the shoulder belt, which was marked incrementally at the retractor. Modifications to the retractor, buckle, and lap belt attachment points allowed for pretension at any combination of these locations. When active, the pretensioners triggered at 12ms after the onset of the acceleration pulse (Figure 6).

The parameters considered and the values used in the simulations are listed in Table 2. All possible combinations of values were simulated. Future work will include additional impact speeds and occupant sizes (including children), as well as an assessment of injury tradeoffs with outcomes weighted for field exposure. For this preliminary study, however, the goal was to identify sets of parameters that hold potential for improving the performance of the baseline restraint condition. Two primary outcome metrics were considered in this assessment. First, since the field data indicate an increase in chest injury for older occupants, the maximum chest deflection (C_{max}) was considered. Second, since the clear tradeoff with belt load limiting is an increase in head excursion, the maximum forward (X-axis) displacement of the head center-of-gravity relative to the vehicle (X_h) was considered.

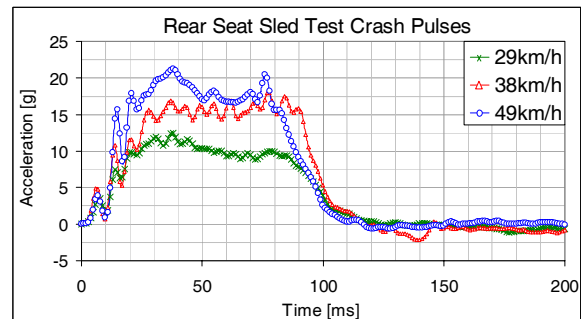


Figure 6. Sled pulses (sled and MADYMO).

A statistical analysis of the simulation data was conducted using general linear models. Regression and MANOVA analyses were performed, and mean injury measures were compared for different levels of the independent variables (load limit, ΔV , pretensioner location(s), and stroke), taking into consideration main and interaction effects. All covariates were considered to be fixed effects. The dependent variables considered in the statistical analysis were X_h , HIC15, maximum chest acceleration, and C_{max} .

Table 2. Parameters and values considered in simulation matrix.

Parameter	Values simulated
Occupant	AM50, AF5
Sled ΔV (km/h)	29, 38, 48
Load limit (kN)	2, 2.5, 3, 3.5, 4, 4.5, 5, 5.5, 6, 8, None
Pretensioner arrangement	1 - Buckle only, 2 - retractor only, 3 - buckle + retractor, 4 - buckle + retractor + lap
Pretensioner stroke (mm)*	0, 25, 50, 75

*In simulations with multiple pretensioners, all pretensioners had the same stroke.

SIMULATION RESULTS

BENCHMARKING OF MODEL

Figure 7 illustrates the general agreement between the MADYMO model and the test data. The chest deflection, shoulder belt tension, and chest acceleration are shown at 29 km/h and 48 km/h with the baseline (no load limiting, no pretensioning) restraint system. Figure 8 shows images throughout the 48 km/h impact sequence, illustrating the kinematic behavior of the model relative to the sled tests.

ANALYSIS OF VARIANCE AND OUTCOMES

The statistical analysis indicated that impact velocity and load limit had significantly greater influence on injury measures for both dummies than did pretension stroke and arrangement. Impact speed had greater influence on X_h , HIC15 and chest acceleration than did load limit, while C_{max} was mainly influenced by load limit. Increase in pretension stroke reduced X_h and HIC15, but had minimal effect on chest acceleration and C_{max} . Buckle pretensioning had higher X_h and HIC15 than other pretension arrangements, with arrangement 4 (lap+retractor+buckle) having significantly lower X_h and HIC15 than the other arrangements. Finally, the sensitivity of injury measures to load limit increased at higher ΔV , but the sensitivity of X_h and HIC15 to pretension stroke and arrangement was not significantly changed for different ΔV .

DESCRIPTIVE ANALYSIS – AM50

The baseline restraint condition resulted in AM50 C_{max} of 22.7 mm, 26.0 mm, and 29.9 mm at 29 km/h, 38 km/h, and 48 km/h, respectively. The maximum AM50 X_h at those three speeds was 138 mm, 178 mm, and 224 mm, respectively. In only two

situations (2 kN limit with a single pretensioner, 0 and 25 mm of stroke, 48 km/h) was X_h sufficient to allow the AM50 head to strike the front seat back in its rearmost position. The head impact velocity relative to the seat back was 6.7 and 7.6 m/s in those cases, but they are not considered to be restraint conditions likely to be used in the fleet. Furthermore, head strike is not a valid criterion for limiting head excursion; variability in vehicle geometry, occupant positioning, collision obliquity, and other factors not

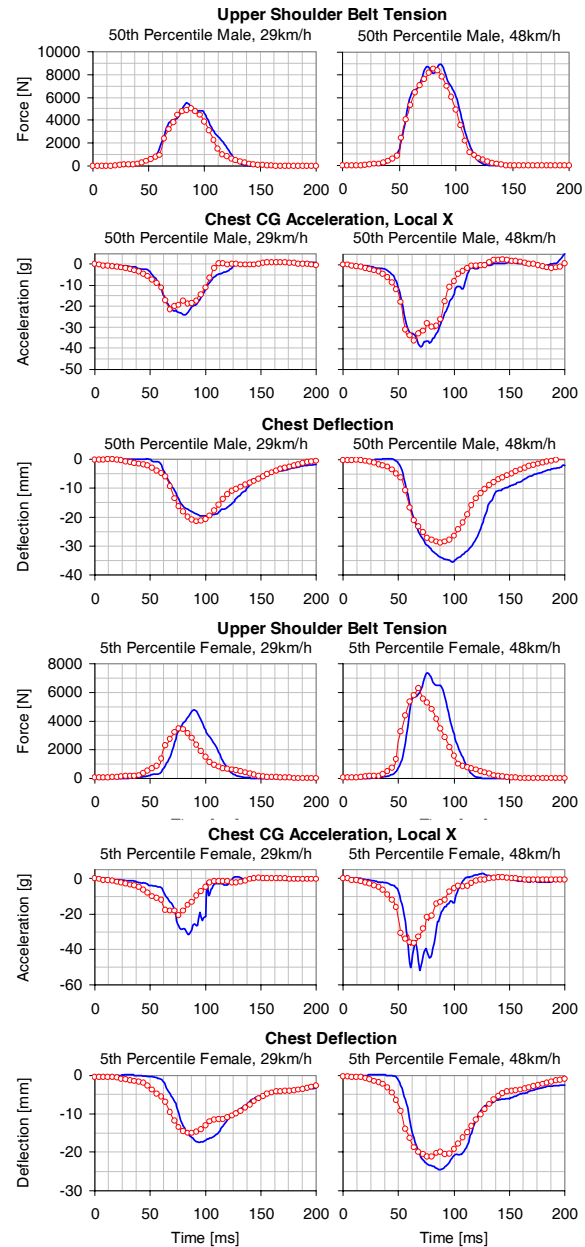


Figure 7. Benchmarking the MADYMO models, with test data in solid blue and MADYMO data in red circles.

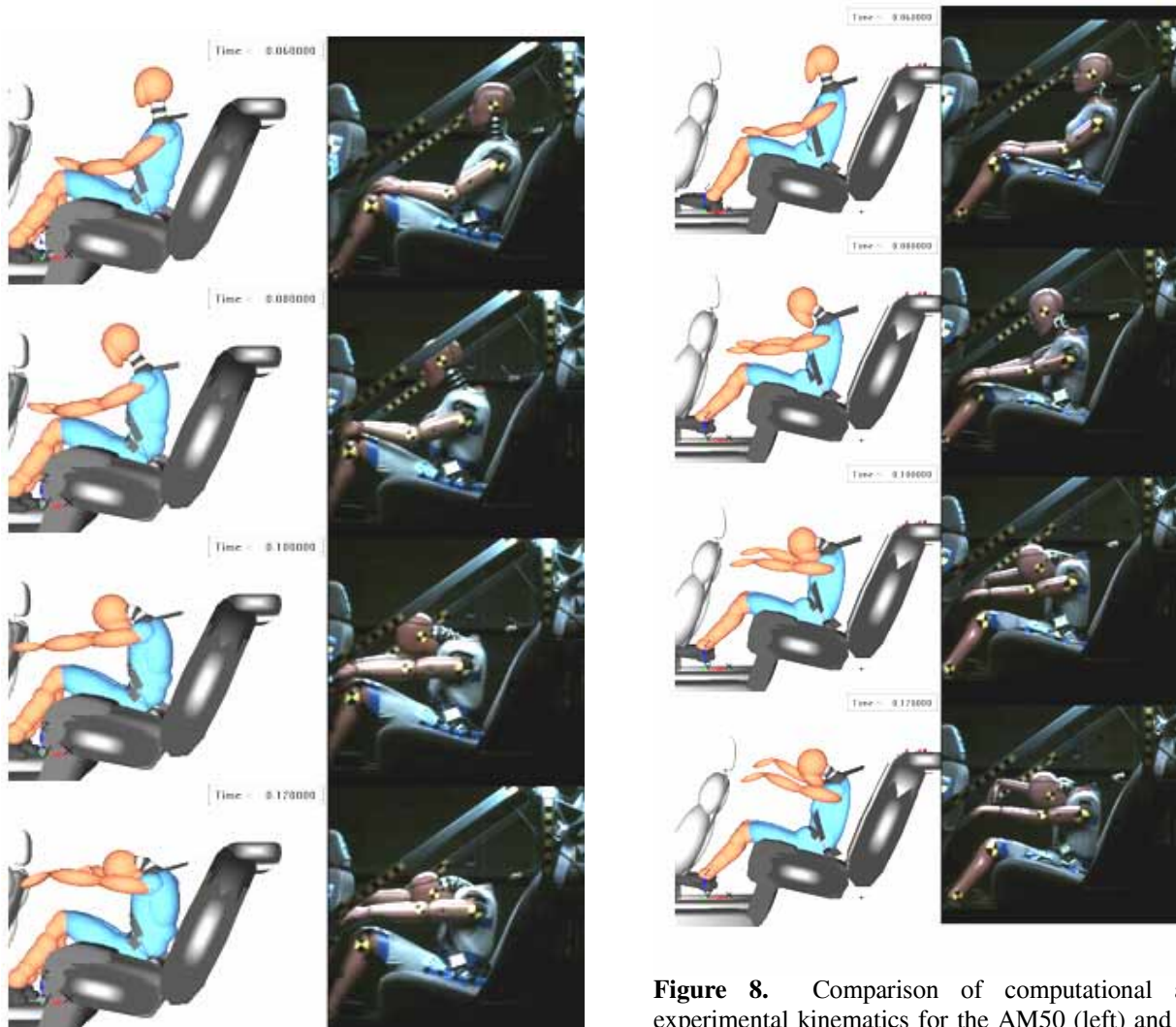


Figure 8. Comparison of computational and experimental kinematics for the AM50 (left) and the AF5 (right).

considered in these simulations require a more conservative approach to establishing an allowable X_h threshold. Though some increase in X_h relative to the baseline is probably tolerable, the initial presentation of these results will consider only those sets of restraint conditions that reduced both X_h and C_{max} relative to the baseline values. These sets of restraint conditions will be referred to as “improved” restraints. At 29 km/h, there were 101 sets of conditions that were “improved”, at 38 km/h there were 69, and at 48 km/h there were 44. There were 42 sets of conditions that were “improved” at all three speeds (Table 3).

Due to the low occupancy rates in the rear seat, it is desirable to minimize the cost of any restraint that is used there, so these “improved” sets of restraint parameters must be evaluated in that light. The most expensive component of a restraint system is the

pretensioner, so “improved” restraints that involve fewer pretensioners would be more economically feasible for implementation in the rear seat. Unfortunately, as expected there were no sets of restraint conditions that reduced both X_h and C_{max} at all speeds without the use of at least one pretensioner. There was also, as expected, a clear tradeoff between belt load limiting and the amount of pretensioning needed to satisfy the definition of “improved.” The “improved” restraint having the lowest load limit (4.5 kN) required two or three pretensioners, each with 75 mm of stroke, in order to qualify as “improved.” Of “improved” systems having a single pretensioner, the lowest load limit was 5.5 kN, and the required pretensioner stroke was 75 mm. The buckle pretensioner was less effective at limiting X_h relative to the retractor pretensioner, but was more effective at reducing C_{max} . Given the distance available prior

to head contact with the front seat back (540 mm), and the importance of thoracic injuries identified in the field data portion of this study, this tradeoff is an important area for additional study. If the buckle

Table 3. Conditions (AM50) that reduced both X_h and C_{max} at all speeds relative to baseline (bold). Systems discussed in the text are in italics.

Load limit (kN)	Preten. arrangement	Preten. stroke (mm)	X_h (mm)*	C_{max} (mm)*
None	None	0	138,178,224	22.7,26.0,29.9
4.5	3	75	<i>56,115,219</i>	<i>18.8,20.7,20.6</i>
4.5	4	75	<i>45,99,195</i>	<i>19.4,21.7,21.1</i>
5	3	50	72,123,221	19.0,21.2,21.5
5	4	50	71,124,221	19.3,21.8,22.7
5	3	75	55,103,191	19.2,21.9,21.5
5	4	75	39,88,170	19.3,23.1,22.9
5.5	3	50	67,114,201	19.4,22.5,23.4
5.5	4	50	62,121,194	18.9,22.8,23.7
5.5	1	75	<i>103,137,219</i>	<i>17.3,18.2,17.7</i>
5.5	2	75	<i>65,111,201</i>	<i>21.2,25.0,25.2</i>
5.5	3	75	51,98,169	19.2,22.5,22.6
5.5	4	75	39,84,150	19.7,23.4,24.0
6	3	25	100,148,224	20.6,24.1,24.7
6	4	25	101,146,222	20.5,24.2,24.7
6	1	50	87,123,205	16.8,19.6,19.4
6	2	50	91,133,219	21.9,25.9,26.6
6	3	50	63,102,177	19.2,22.2,23.9
6	4	50	66,104,177	19.8,21.8,25.0
6	1	75	94,125,203	17.4,17.7,18.5
6	2	75	64,110,184	21.2,25.4,26.7
6	3	75	47,97,148	19.3,22.3,23.1
6	4	75	36,77,135	19.9,23.6,25.5
8	1	25	107,142,197	20.8,23.9,27.8
8	3	25	94,131,187	21.0,24.0,28.6
8	4	25	92,137,183	20.7,24.9,27.8
8	1	50	80,118,158	17.6,20.6,22.6
8	3	50	54,92,138	19.6,22.9,25.7
8	4	50	60,95,143	20.0,22.6,26.8
8	1	75	88,112,160	18.4,18.1,21.3
8	2	75	58,97,148	21.6,25.1,29.4
8	3	75	43,78,136	19.9,21.8,26.3
8	4	75	33,64,121	20.4,23.5,26.9
None	1	25	107,142,197	20.8,23.9,27.8
None	3	25	90,131,171	21.0,24.7,28.5
None	4	25	88,133,176	21.0,24.9,28.0
None	1	50	81,106,152	18.2,20.7,23.0
None	3	50	55,90,149	20.0,23.1,26.5
None	4	50	49,93,147	19.7,22.6,26.4
None	1	75	82,109,150	17.8,18.3,21.5
None	2	75	55,91,141	21.9,25.6,29.3
None	3	75	41,84,116	20.0,23.0,25.8
None	4	75	30,62,113	20.5,23.8,27.2

*The three values listed in the cell correspond to the test speeds 29 km/h (left), 38 km/h (middle), and 48 km/h (right)

pretensioner can indeed provide a substantial reduction in C_{max} , it may be a desirable alternative to the retractor pretensioner. Even though the buckle pretensioner allowed more X_h in these simulations, the X_h generated with either pretensioner is well below a tolerable level.

In order to represent the maximum chest deflection from the simulations in terms of risk of thoracic injury, the AIS 3+ chest injury risk model 6 of Laituri et al. (2005) for AM50 is used. The Laituri injury risk function (Equation 5) using occupant age and the AM50 C_{max} were derived from sled test data with cadaveric subjects and the AM50 at different impact velocities. The AIS 3+ injury risk function was verified against real world thoracic injury risk considering different impact velocities and occupant age and gender.

$$p(AIS\ 3+) = \frac{1}{1 + e^{-(12.597 + 0.05861Age + 1.568C_{max}^{0.4612})}} \quad [5]$$

As mentioned above, no system without a pretensioner was “improved” relative to the baseline. Of systems without a pretensioner, however, there are some systems that may be considered as reasonable alternatives to the baseline since they reduce chest injury risk with a potentially allowable increase in X_h . At 5.5 kN of load limiting with no pretensioning, for example, X_h increased by 80 mm relative to the baseline, but C_{max} decreased from 29.9 mm to 23.5 mm. Using Equation 5 with the C_{max} in Table 3, this results in a risk reduction from 21.9% to 11.3% for a person of age 65. Since the head remains more than 230 mm from the front seat back at its maximum point of excursion, this level of load limiting may be a reasonable option for the rear seat, even without the use of a pretensioner. The tradeoff between X_h and chest injury risk (based on the Laituri model of C_{max}) in 29, 38, and 48 km/h impacts for different types of pretensioning is illustrated in Figure 9. While Table 3 includes only restraints that reduced both chest deflection and head excursion, the plots in Figures 9-11 include all the simulation results (Appendix A). As shown in Figure 9, there is a clear tradeoff between chest risk and head excursion, and this tradeoff exists at all three impact speeds. As the belt force limit is reduced, the chest risk decreases and the head excursion increases. An exponential regression to the AM50 data points reveals a slightly concave-up characteristic to the trend, indicating that the most gain in chest risk reduction is made before the head approaches the excursion limit. As the head approaches 540 mm of excursion, the slope of the tradeoff curve has flattened, and in some cases has actually become positive since the extreme forward torso pitch allowed by those low-force belts allows thoracic loading from the thighs. In contrast, the AF5

tradeoff exhibits a trend that is virtually linear (Figure 10). Presumably, this is due to the smaller head excursion values experienced by that occupant.

DESCRIPTIVE ANALYSIS – AF5

In general, C_{max} and X_h were lower for the AF5 than for the AM50. The baseline restraint condition resulted in AF5 C_{max} of 15.6 mm, 18.5 mm, and 21.6 mm at 29 km/h, 38 km/h, and 48 km/h, respectively. The maximum AF5 X_h at those three speeds was 153 mm, 177 mm, and 201 mm, respectively. None of the simulations resulted in sufficient X_h to allow head contact with the front seat back. As with the AM50 results, there were many sets of restraint parameters that reduced both X_h and C_{max} relative to the baseline (Appendix A). At 29 km/h, there were 115 sets of conditions that were “improved”, at 38 km/h there were 96, and at 48 km/h there were 77. As with the larger dummy, there were no restraint conditions that reduced both X_h and C_{max} at all speeds without a pretensioner.

The AF5 experienced less X_h than the AM50 for the same set of restraint parameters. Thus, the AM50 is the more appropriate model for assessing the minimum acceptable belt load limit. The AF5 results are more useful as an indication of the degree of thoracic benefit that can be realized by a smaller occupant if the belt loads are reduced to a level that retains sufficient head restraint for the AM50. As discussed above, 5.5 kN was the lowest belt load limit for a single-pretensioner system that was “improved” relative to the baseline. This system (5.5 kN, buckle pretensioner with 75-mm stroke) provided a safety benefit to the AF5, as well. Head excursion was reduced at all impact speeds, and C_{max} was reduced to 13.9 mm, 16.6 mm, and 19.8 mm. These gains are modest, however, and argue for a lower load limit even at the expense of some increased X_h for the AM50 – particularly since the AF5 is a better representation of the size of occupants typically in the rear seat. When the same pretensioner was used with the load limit decreased to 3 kN, the AF5 C_{max} dropped to 12.9 mm, 14.7 mm, and 16.8 mm. The tradeoff in AM50 X_h may be tolerable even at this relatively low load limit. At 48 km/h, the AF5 X_h remained below 280 mm, and the AM50 X_h was below 400 mm (i.e., nearly 150 mm clearance remained before the AM50 head contacted the front seat back). The AM50 C_{max} benefit was also substantial at 3 kN with the 75-mm buckle pretensioner, dropping to 13.7, 13.0, and 14.1 mm for the three speeds considered. That load limit is probably not acceptable without a pretensioner,

however, since the AM50 X_h approached 480 mm at 48 km/h (Figure 10, Figure 11).

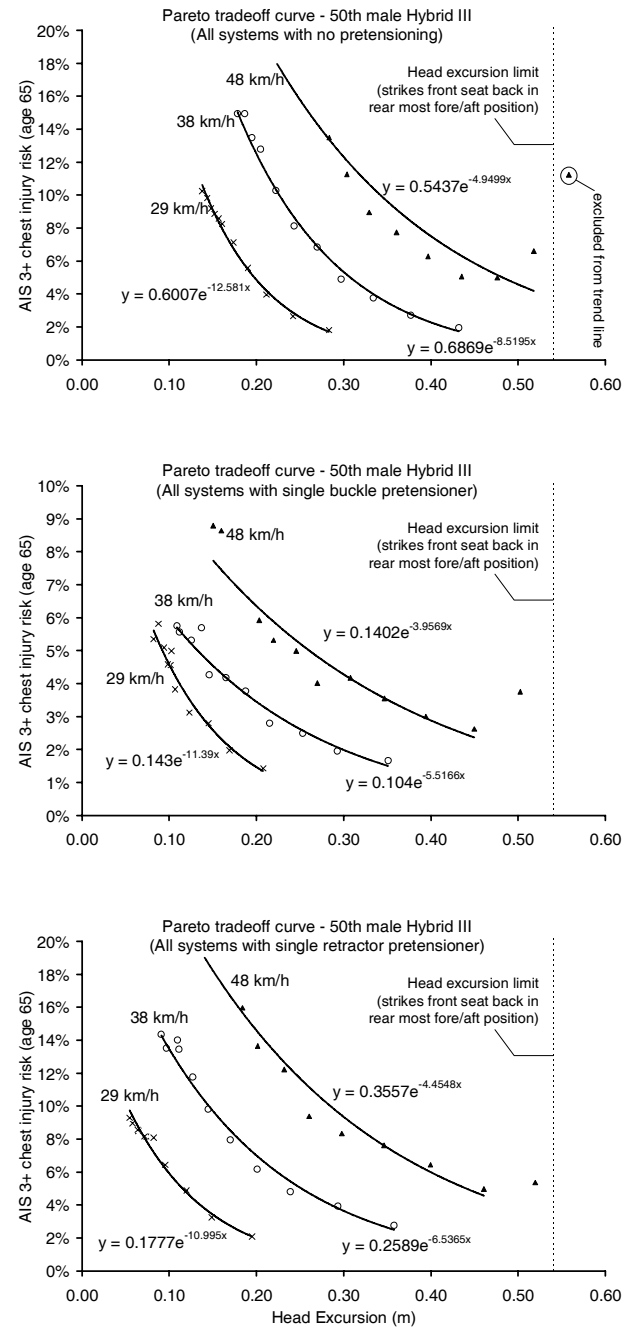


Figure 9. Tradeoff curves for all AM50 simulations involving restraints with no pretensioning (top), a single 75-mm buckle pretensioner (middle), and a single 75-mm retractor pretensioner (bottom). Note change in scale of the ordinate.

DISCUSSION AND CONCLUSIONS

FIELD STUDY

Smith and Cummings (2004) estimated the risk ratio for death and serious injury for rear seat passenger compared to front seat passengers in motor vehicle crashes using the National Automotive Sampling System-Crashworthiness Data System (NASS-CDS) data files. They estimated that the rear seat passenger position may reduce the risk of death in a motor vehicle crash by about 39%. Cummings imputed missing data in this survey sample and included crashes involving vehicles of model years 1948-2001. In general, older vehicle models are involved in more severe crashes than newer models. Thus, the inclusion of very old models in that analysis may have biased the sample towards more severe crashes involving vehicle models with poor crashworthiness compared to newer vehicle models. Later, those authors (Smith and Cummings 2005) performed a matched cohort study using the FARS database, though still with older vehicles included, and found greater rear seat effectiveness estimates than those found either by Kuppa et al. (2005) or in the current study. Limiting vehicle model year to 1991 and newer has the dis-benefit of reducing the sample size, but also increases the number of advanced, front-seat restraint systems considered in the analysis. This difference in model year inclusion criterion is a likely explanation for the lower rear seat effectiveness found here and by Kuppa et al. (2005) compared to the Smith and Cummings papers.

Evans (1991) and others have documented the safety benefit that rear-seat occupants enjoy relative to front-seat occupants. This benefit has been attributed to several characteristics of the rear-seat environment, including the distance from the striking vehicle in a frontal crash, and the relatively pliant structure of the front seat backs. The results of the current field study, however, indicate that this long-standing truism of automobile safety is becoming less certain, and for older adults is no longer true. As the front seat environment has evolved to incorporate more effective restraint systems, it has gotten closer to the safety of the rear seat. While this results in an overall benefit to all occupants, it invites research into how these advanced technologies might be incorporated into the rear seat, especially with the encouraging performance of load limiters in the front seat environment (Foret-Bruno et al. 1978, 1998, 2001, Kent et al. 2001). With a comparable restraint system, it may be possible to increase rear seat effectiveness (relative to the front seat) back to the levels it had in older model vehicles, which would be a further benefit to the overall vehicle fleet. Thus, a

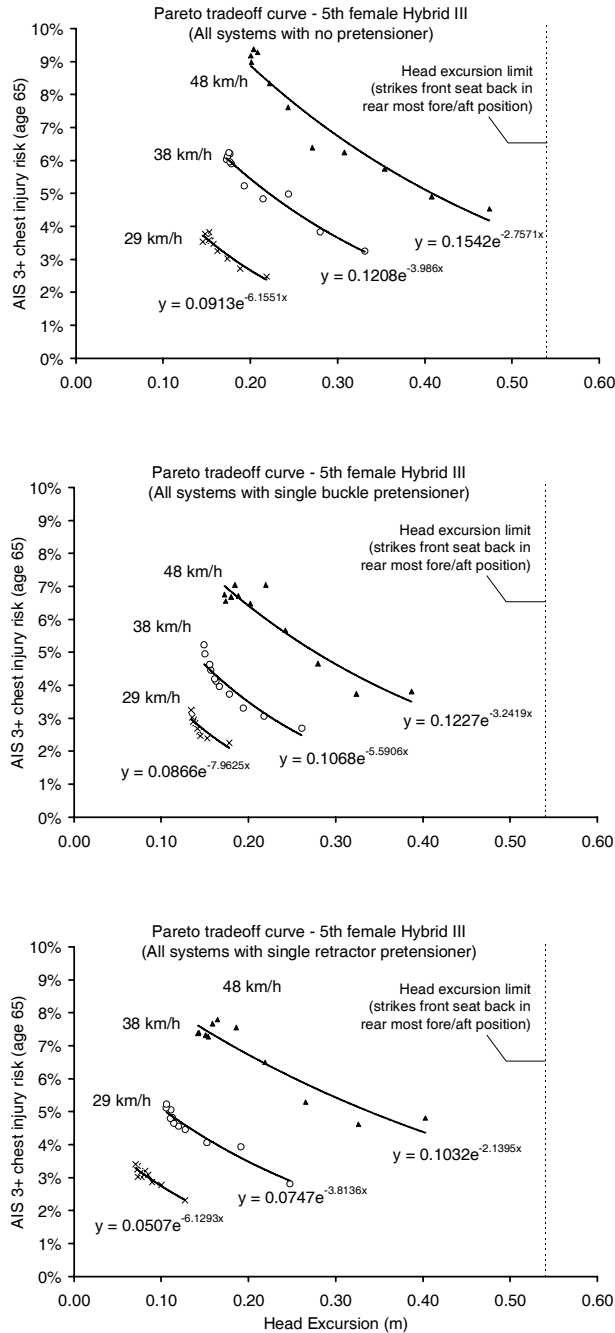


Figure 10. Tradeoff curves for all AF5 simulations involving no pretensioning (top), a single 75-mm buckle pretensioner (middle), and a single 75-mm retractor pretensioner (bottom). Note that the Laituri injury risk curve applied here for the AF5 was developed for the AM50.

reasonable conclusion from this work is that additional research is justified into methods for reducing thoracic injury risk in the rear seat by incorporating restraint concepts currently offered in the front seat. A preliminary computational study illustrated the feasibility of such a strategy.

SIMULATIONS AND RESTRAINT DESIGN FOR THE REAR SEAT

The simulations considered here indicate that a belt load limit as low as 3 kN may sufficiently limit head excursion for the AM50 in a typical sedan at 48 km/h ΔV if a buckle pretensioner with 75-mm of stroke is used. This load limit and pretensioner would substantially reduce chest injury risk for older occupants of both sizes studied, while maintaining the head at least approximately 150 mm from the front seat back in all cases considered here. The results of this study, albeit limited in scope, indicate potential benefits for chest injury reduction with head excursion tradeoffs that are likely acceptable.

This study should not, however, be interpreted as a comprehensive assessment of rear-seat restraint design and performance. Additional work is ongoing in our laboratory to study the response of children in booster seats, and to expand these simulation results by including physical tests of both dummies and human cadavers. The primary goal of this simulation study was to assess the feasibility of load limiting in the rear seat, where an air bag and knee bolsters are not available for load sharing in a frontal collision. This work indicates that the consequences with respect to head excursion are likely not intractable if a load limiting belt is used to reduce chest injury risk in the rear seat. Even without a pretensioner, fairly low belt load limits generated a substantial reduction in chest injury risk for the elderly AM50 without an unacceptable increase in head excursion. If a pretensioner is economically feasible in the rear seat, then the belt load limits, and hence the chest deflection generated by the belt during the crash, are reduced further. Further analysis will examine the feasibility of an optimized belt system in protecting larger occupants as well as children. In the latter case, a study conducted by Van Rooij et al. (2003) demonstrated that the implementation of a pretensioner and a 4 kN force limiter can reduce the injury risk to a 6 year-old occupant without allowing a head excursion in excess of the FMVSS 213 limit.

Of course, prior to implementation of these restraint concepts into the rear seat, additional work is necessary to understand the consequences of occupant mis-positioning, non-frontal collisions, non-planar collisions, and vehicle geometries unlike that considered here. The front seat experience may guide some of that work, but the differences in occupancy rate and occupant types must be considered.

Finally, the limitations of the Hybrid III family of dummies, their associated injury criteria, and their implementation into the MADYMO package must be considered in the interpretation of these results.

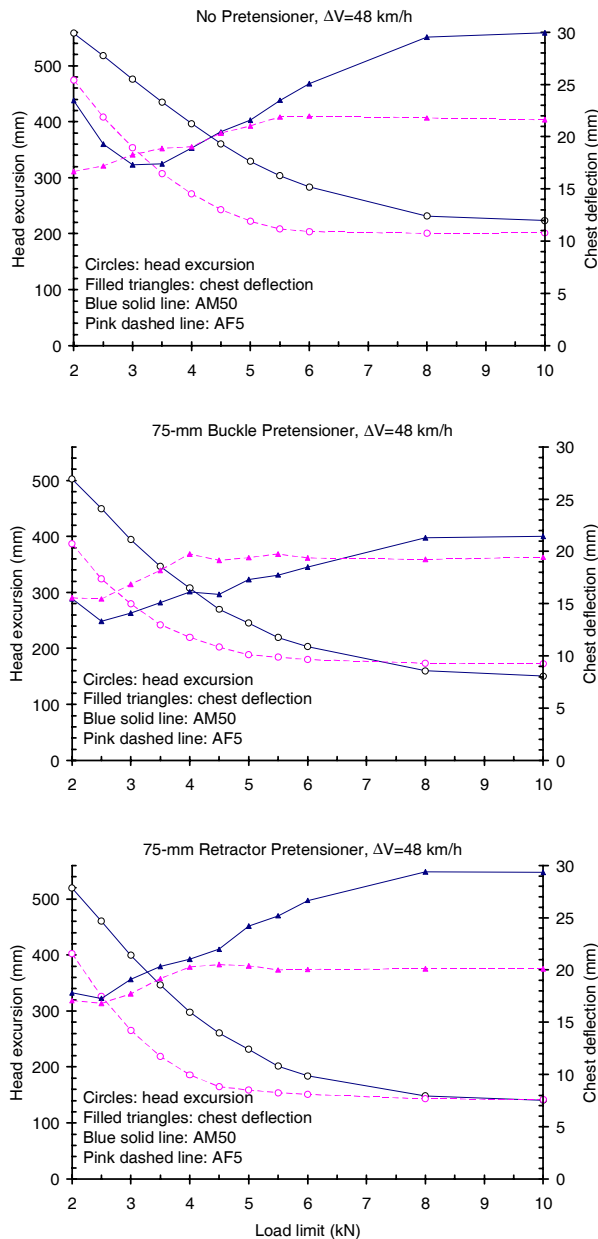


Figure 11. Effect of load limiting at 48 km/h ΔV for systems without pretensioning (top), with a single buckle pretensioner (middle), and with a single retractor pretensioner (bottom).

Significant challenges to the interpretation of these models, especially for use in the refinement of belt load limiting characteristics, have been identified in the literature (e.g., Morgan et al. 1994, Kuppa and Eppinger 1998, Butcher et al. 2001, Petitjean et al. 2002, Kent et al. 2003).

REFERENCES

Butcher, J., Shaw, G., Bass, C., Kent, R., Crandall, J. (2001) Displacement measurements in the Hybrid III chest. Paper No. 2001-01-0118, Society of Automotive Engineers, Warrendale, PA.

Evans, L. (1991) Traffic Safety and the Driver. Van Nostrand Reinhold, New York.

Foret-Bruno, J-Y., Hartemann, F., Thomas, C., Fayon, A., Tarriere, C., Got, C. (1978) Correlation between thoracic lesions and force values measured at the shoulder belt of 92 belted occupants involved in real accidents. Paper 780892, 22nd Stapp Car Crash Conference, Society of Automotive Engineers, Warrendale, PA.

Foret-Bruno, J-Y., Trosseille, X., Le Coz, J-Y., Bendjellal, F., Steyer, C. (1998) Thoracic injury risk in frontal car crashes with occupant restrained with belt load limiter. Proc. 42nd Stapp Car Crash Conference, pp. 331-952., Paper 983166. Society of Automotive Engineers, Warrendale, PA.

Foret-Bruno, J-Y., Trosseille, X., Page, Y., Huere, J-F, Le Coz, J-Y., Bendjellal, F., Diboine, A., Phalempin, T., Villeforceix, D., Baudrit, P., Guillemot, H., Coltat, J-C (2001) Comparison of thoracic injury risk in frontal car crashes for occupants restrained without belt load limiters and those restrained with 6 kN and 4 kN belt load limiters. Stapp Car Crash Journal 45:205-224.

Kent, R. W., Crandall, J. R., Bolton, J. R., Nusholtz, G.S., Prasad, P., Mertz, H. (2001) The Influence of Superficial Soft Tissues and Restraint Condition on Thoracic Skeletal Injury Prediction, Stapp Car Crash Journal, Vol. 45, pp. 183-204.

Kent, R., Patrie, J., Benson, N. (2003) The Hybrid III dummy as a discriminator of injurious and non-injurious restraint loading. Annual Conference of the Association for the Advancement of Automotive Medicine, Des Plaines, IL.

Kuppa, S. and Eppinger, R. (1998) Development of an improved thoracic injury criterion. Paper 983153, Proc. 42nd Stapp Car Crash Conference.

Kuppa, S., Saunders, J., Fessahaie, O. (2005) Rear seat occupant protection in frontal crashes. Paper No. 05-0212, Nineteenth ESV Conference, Washington DC.

Laituri, T., Prasad, P., Sullivan, K., Frankstein, M., Thomas, R. (2005) Derivation and evaluation of a provisional, age-dependent, AIS 3+ thoracic risk curve for belted adults in frontal impacts. Paper 2005-01-0297, Society of Automotive Engineers, Warrendale, PA.

Morgan, R., Eppinger, R., Haffner, M., Yoganandan, N., Pintar, F., Sances, A., Crandall, J., Pilkey, W., Klopp, G., Dallieris, D., Miltner, E., Mattern, R., Kuppa, S., Sharpless, C. (1994) Thoracic trauma assessment formulations for restrained drivers in simulated frontal impacts. Paper number 942206, Proc. 38th Stapp Car Crash Conference, pp. 15-34.

NHTSA, Traffic Safety Facts, 1998-2005. <http://www-nrd.nhtsa.dot.gov/CMSWeb/listpublications.aspx?Id=E&ShowBy=DocType>. Accessed Jan. 18, 2007.

NHTSA, Five Star Crash Test and Rollover Rating, <http://www.nhtsa.dot.gov/ncap/index.cfm>. Accessed Jan. 18, 2007.

Petitjean, A., Lebarbe, M., Potier, P., Trosseille, X., Lassau, J. (2002) Laboratory reconstructions of real world frontal crash configurations using the Hybrid III and THOR dummies and PMHS. Paper Number 2002-22-0002, Stapp Car Crash Journal, 46:27-54.

Smith, K., Cummings, P. (2004) Passenger seating position and the risk of passenger death or injury in traffic crashes. Accident Analysis and Prevention, 36:257-260.

Smith, K., Cummings, P. (2005) Passenger seating position and the risk of passenger death in traffic crashes: A matched cohort study. Injury Prevention, 12:83-86.

Swanson, J., Rockwell, T., Beuse, N., Summers, L., Summers, S., Park, B., (2003) Evaluation of Stiffness Methods from the U.S. New Car Assessment Program, Paper No. 03-0527, Eighteenth ESV Conference, Nagoya, Japan.

van Rooij, L., Sherwood, C., Crandall, J., Orzechowski, K., Eichelberger, M. (2003) The effects of vehicle seat belt parameters on the injury risk for children in booster seats. Paper 2003-01-0500, Society of Automotive Engineers, Warrendale, PA.

Walz, M., 2003. "NCAP Test Improvements with Pretensioners and Load Limiters," NHTSA Report, DOT HS 809-562, Washington, DC.

APPENDIX A. Simulation Results

Load Limit (kN)	Pretension arrangement	Pretension Stroke (mm)	AM50						Improved at all speeds?	AF5						Improved at all speeds?	Improved at all speeds for both AM50 and AF5?
			Xh (mm)			Cmax (mm)				Xh (mm)			Cmax (mm)				
			29 km/h	38 km/h	48 km/h	29 km/h	38 km/h	48 km/h		29 km/h	38 km/h	48 km/h	29 km/h	38 km/h	48 km/h		
None	None	0	138	178	224	22.7	26.0	29.9	NA	153	177	201	15.6	18.5	21.6	NA	NA
2000	1	0	283	432	558	11.3	11.6	23.5		219	331	474	13.0	14.6	16.7		
2000	1	25	245	396	537	11.2	11.5	20.5		170	285	429	11.8	13.5	16.0		
2000	2	25	259	410	548	11.8	12.0	21.6		156	251	393	11.6	13.0	16.0		
2000	3	25	229	383	528	11.3	11.3	20.0		178	261	387	12.5	13.5	15.6		
2000	4	25	221	377	526	10.8	11.4	21.3		191	307	457	12.9	13.7	16.8		
2000	1	50	222	369	519	10.1	10.6	17.6		157	279	431	12.4	13.7	17.5		
2000	2	50	227	385	534	11.7	13.0	19.8		127	248	403	12.6	13.7	17.1		
2000	3	50	186	340	503	11.1	11.6	17.6		156	271	420	12.3	13.3	16.6		
2000	4	50	183	332	496	11.6	12.5	18.9		130	231	369	11.9	13.7	16.3		
2000	1	75	208	351	502	10.1	10.9	15.5		125	222	352	12.6	13.8	15.7		
2000	2	75	195	358	519	12.0	13.6	17.8		148	257	401	12.3	13.5	16.9		
2000	3	75	156	303	476	11.9	11.8	15.4		137	234	367	12.6	14.2	16.7		
2000	4	75	125	283	459	12.8	12.8	15.7		131	234	363	14.1	14.9	17.8		
2500	1	0	242	377	518	13.4	13.5	19.3		189	280	408	13.5	15.6	17.2		
2500	1	25	205	339	490	13.4	13.0	16.7		144	232	356	13.0	13.9	15.7		
2500	2	25	215	353	503	13.7	14.2	17.2		138	202	325	12.5	14.5	16.6		
2500	3	25	189	324	479	13.7	13.0	15.9		153	218	324	12.8	14.2	15.4		
2500	4	25	183	318	476	13.2	13.2	16.4		162	256	385	14.0	15.6	17.6		
2500	1	50	179	308	466	11.9	11.9	13.4		130	224	359	13.9	15.4	17.2		
2500	2	50	184	325	483	14.5	15.0	16.4		100	191	326	13.6	15.8	16.8		
2500	3	50	143	275	444	13.3	13.2	14.3		131	217	346	13.5	14.1	16.0		
2500	4	50	142	274	438	13.3	14.1	15.7		114	179	297	12.1	14.3	17.0		
2500	1	75	169	293	450	11.7	11.7	13.3		101	166	279	13.0	14.5	18.1		
2500	2	75	149	294	461	14.6	15.7	17.3		127	209	331	13.2	14.5	17.2		
2500	3	75	112	237	407	13.9	13.6	14.2		120	189	301	14.3	15.1	17.4		
2500	4	75	87	214	382	15.2	14.8	14.8		101	184	290	15.3	16.1	18.3		
3000	1	0	211	334	476	15.8	15.5	17.3		174	244	354	14.1	17.3	18.3		
3000	1	25	175	292	440	15.1	13.8	15.2		129	195	299	13.8	15.2	16.7		
3000	2	25	183	308	455	16.5	16.1	16.9		131	168	267	13.0	15.1	18.5		
3000	3	25	158	275	430	15.5	14.6	15.8		145	194	280	12.9	14.7	16.8		
3000	4	25	154	274	427	16.1	15.2	15.4		147	218	328	14.6	16.7	18.1		
3000	1	50	148	261	411	13.5	13.3	14.7		118	186	300	14.1	16.8	17.7		
3000	2	50	151	277	431	17.1	17.0	18.0		89	152	266	13.8	15.9	17.7		
3000	3	50	115	229	386	15.6	15.5	16.1		119	181	288	14.1	15.1	17.5		
3000	4	50	113	226	382	15.1	15.6	16.5		107	146	240	12.5	14.9	18.0		
3000	1	75	145	253	394	13.7	13.0	14.1		84	137	224	13.3	15.4	16.7		
3000	2	75	120	239	399	17.2	17.1	19.1		116	173	275	13.7	14.9	18.5		
3000	3	75	83	191	344	16.1	15.4	15.9		106	161	249	13.6	16.3	17.7		
3000	4	75	59	166	318	16.5	16.8	16.7		84	150	239	16.1	16.8	19.4		
3500	1	0	190	297	435	18.1	17.2	17.4		162	215	308	14.6	17.1	18.9		
3500	1	25	154	255	393	17.1	16.1	16.3		115	164	253	14.6	16.1	18.4		
3500	2	25	161	270	412	18.5	18.0	18.7		106	143	220	13.6	16.0	18.5		
3500	3	25	138	240	379	17.3	17.0	17.3		144	178	242	13.3	15.4	18.2		

3500	4	25	133	235	376	17.7	16.9	16.8	132	184	278	14.5	16.1	18.4		
3500	1	50	126	223	358	15.1	14.7	15.6	105	155	250	14.7	16.5	18.5		
3500	2	50	127	235	380	18.7	18.3	19.5	85	128	219	14.3	16.6	19.2		
3500	3	50	92	190	332	17.2	17.1	17.2	102	148	236	14.3	16.5	19.0		
3500	4	50	93	189	331	16.8	17.0	17.4	83	115	192	13.6	16.2	17.5	√	
3500	1	75	123	215	347	14.3	13.7	15.1	85	127	193	13.6	16.0	17.8	√	
3500	2	75	95	201	346	19.1	18.8	20.3	101	144	228	14.0	16.9	18.8		
3500	3	75	70	158	292	17.7	17.5	17.3	85	124	195	13.9	17.1	18.6	√	
3500	4	75	52	135	265	18.3	18.2	18.6	66	122	191	16.9	17.6	18.6		
4000	1	0	174	270	397	19.8	19.5	18.9	158	193	271	15.0	17.6	19.0		
4000	1	25	135	227	352	18.9	18.1	18.0	108	147	219	14.9	17.0	19.1		
4000	2	25	144	238	367	20.0	19.8	19.2	106	135	194	13.9	16.7	18.6	√	
4000	3	25	120	211	338	19.1	18.8	18.3	142	167	220	13.4	15.8	19.8		
4000	4	25	117	206	336	18.9	18.7	18.3	128	167	242	14.7	17.5	18.8		
4000	1	50	107	192	314	15.6	15.8	16.6	100	141	214	14.5	17.4	19.1		
4000	2	50	110	202	336	20.1	19.3	20.6	81	120	186	14.5	16.7	20.3	√	
4000	3	50	80	161	288	18.5	18.6	18.6	95	135	204	14.5	17.2	18.4		
4000	4	50	82	160	283	18.7	19.4	18.2	79	108	169	13.7	16.7	18.2	√	
4000	1	75	107	188	308	15.6	15.5	16.1	82	120	172	13.8	15.8	18.7	√	
4000	2	75	82	170	298	20.8	20.7	21.0	95	133	198	14.2	17.7	18.7	√	
4000	3	75	60	135	251	18.5	19.3	18.8	81	117	168	14.1	16.9	18.4	√	
4000	4	75	47	115	227	18.9	20.3	19.6	67	115	177	17.4	18.4	19.0		
4500	1	0	161	243	361	21.0	20.8	20.5	155	178	243	15.1	18.5	20.3		
4500	1	25	127	203	320	19.7	19.8	19.8	104	141	196	15.3	17.3	18.9	√	
4500	2	25	135	214	332	21.3	21.7	20.8	103	131	171	14.1	16.9	19.3	√	
4500	3	25	117	189	301	20.4	21.0	19.4	139	163	202	13.8	16.1	19.1		
4500	4	25	110	183	298	19.9	20.6	19.3	122	159	216	14.9	18.0	20.2		
4500	1	50	106	170	278	16.6	17.6	17.2	95	135	190	14.9	17.7	19.8	√	
4500	2	50	104	178	296	21.1	21.9	21.4	77	115	165	14.1	16.8	20.5	√	
4500	3	50	75	138	250	18.8	20.2	20.2	90	127	181	14.8	17.6	18.8	√	
4500	4	50	76	138	247	19.1	20.5	20.1	74	102	148	13.8	17.0	18.7	√	
4500	1	75	102	165	270	16.7	16.1	15.9	83	117	158	14.0	16.0	19.6	√	
4500	2	75	74	145	261	20.9	22.3	22.0	92	122	175	14.5	18.0	19.4	√	
4500	3	75	56	115	219	18.8	20.7	20.6	√	78	114	152	13.9	16.7	19.1	√
4500	4	75	45	99	195	19.4	21.7	21.1	√	67	114	163	17.9	18.7	19.9	
5000	1	0	157	222	329	21.3	22.7	21.6	151	177	222	15.3	18.8	21.0		
5000	1	25	120	181	284	20.0	21.1	20.0	100	134	178	15.4	17.4	19.5	√	
5000	2	25	127	192	301	21.7	23.1	23.2	100	126	159	14.3	17.0	19.8	√	
5000	3	25	108	170	272	20.4	22.1	21.3	137	161	189	14.0	16.2	19.4	√	
5000	4	25	105	167	269	20.0	22.3	21.5	120	153	198	15.2	18.2	21.1	√	
5000	1	50	97	151	248	16.9	18.4	17.9	92	134	173	14.9	18.2	20.4	√	
5000	2	50	97	158	264	21.3	23.6	22.7	73	113	159	14.1	17.1	20.4	√	
5000	3	50	71	123	221	19.0	21.2	21.5	√	88	123	167	14.9	17.7	19.4	√
5000	4	50	71	124	221	19.3	21.8	22.7	√	73	99	136	14.1	16.8	19.0	√
5000	1	75	98	146	245	16.7	16.3	17.3	80	116	150	14.2	16.2	19.3	√	
5000	2	75	72	127	232	20.9	23.9	24.2	90	120	161	14.9	17.9	20.4	√	
5000	3	75	55	103	191	19.2	21.9	21.5	√	76	111	141	14.2	16.6	19.5	√
5000	4	75	39	88	170	19.3	23.1	22.9	√	65	112	159	17.9	19.0	20.7	
5500	1	0	152	205	304	21.5	24.6	23.5	146	173	208	15.1	18.6	21.9		
5500	1	25	118	173	256	20.1	22.9	21.4	99	132	169	15.7	17.8	20.1		
5500	2	25	126	181	272	21.7	24.3	23.6	100	122	151	14.4	17.1	19.1	√	
5500	3	25	103	155	249	20.6	23.4	22.9	137	157	185	13.9	16.6	19.8	√	

5500	4	25	103	151	246	20.2	23.6	23.4		119	148	188	15.2	18.4	22.2		
5500	1	50	91	137	226	16.7	19.7	18.8		90	129	165	15.0	18.3	21.0	√	
5500	2	50	90	145	241	21.6	24.6	24.6		76	111	154	14.4	17.0	20.0	√	
5500	3	50	67	114	201	19.4	22.5	23.4	√	86	121	157	15.1	18.0	19.8	√	√
5500	4	50	62	121	194	18.9	22.8	23.7	√	70	96	131	14.3	17.1	19.3	√	√
5500	1	75	103	137	219	17.3	18.2	17.7	√	79	115	150	14.4	16.3	19.4	√	√
5500	2	75	64	111	201	21.2	25.0	25.2	√	87	118	155	14.8	18.4	20.3	√	√
5500	3	75	51	98	169	19.2	22.5	22.6	√	76	107	135	14.4	16.7	19.7	√	√
5500	4	75	39	84	150	19.7	23.4	24.0	√	64	110	153	18.3	19.0	20.6		
6000	1	0	148	195	283	21.8	25.1	25.1		148	174	204	15.5	18.7	22.0		
6000	1	25	119	161	235	20.5	23.8	23.1		97	130	165	15.7	17.9	20.2		
6000	2	25	122	169	254	21.8	25.7	25.6		99	120	149	14.6	17.5	19.5	√	
6000	3	25	100	148	224	20.6	24.1	24.7	√	136	156	180	14.1	16.8	19.4	√	√
6000	4	25	101	146	222	20.5	24.2	24.7	√	117	147	182	15.5	18.3	21.7		
6000	1	50	87	123	205	16.8	19.6	19.4	√	90	125	162	15.1	18.3	21.2	√	√
6000	2	50	91	133	219	21.9	25.9	26.6	√	72	111	151	14.5	17.4	20.0	√	√
6000	3	50	63	102	177	19.2	22.2	23.9	√	84	117	155	15.3	18.0	20.1	√	√
6000	4	50	66	104	177	19.8	21.8	25.0	√	70	94	128	14.5	17.3	19.2	√	√
6000	1	75	94	125	203	17.4	17.7	18.5	√	79	111	145	14.5	16.2	19.4	√	√
6000	2	75	64	110	184	21.2	25.4	26.7	√	87	116	151	15.0	18.3	20.7	√	√
6000	3	75	47	97	148	19.3	22.3	23.1	√	75	105	130	14.4	16.9	19.6	√	√
6000	4	75	36	77	135	19.9	23.6	25.5	√	63	107	149	18.4	19.1	21.1		
8000	1	0	144	187	232	22.3	26.0	29.5		153	175	201	15.2	18.9	21.8		
8000	1	25	107	142	197	20.8	23.9	27.8	√	110	143	171	15.1	18.1	20.1	√	√
8000	2	25	117	156	205	22.3	26.4	29.5		112	127	159	14.5	18.3	19.6	√	
8000	3	25	94	131	187	21.0	24.0	28.6	√	135	150	174	14.5	17.3	19.2	√	√
8000	4	25	92	137	183	20.7	24.9	27.8	√	127	155	187	15.4	18.1	21.2	√	√
8000	1	50	80	118	158	17.6	20.6	22.6	√	96	131	170	14.8	17.9	20.7	√	√
8000	2	50	81	125	175	22.0	26.2	30.2		73	106	143	14.8	17.5	20.1	√	
8000	3	50	54	92	138	19.6	22.9	25.7	√	99	130	163	15.2	17.9	19.4	√	√
8000	4	50	59	95	143	20.0	22.6	26.8	√	90	107	139	13.9	17.4	19.1	√	√
8000	1	75	88	112	160	18.4	18.1	21.3	√	78	107	140	14.8	17.3	19.0	√	√
8000	2	75	58	97	148	21.6	25.1	29.4	√	94	119	157	15.7	18.2	19.9		
8000	3	75	43	78	136	19.9	21.8	26.3	√	96	123	144	15.1	17.3	20.1	√	√
8000	4	75	33	64	121	20.4	23.5	26.9	√	63	102	148	18.8	19.4	21.9		
10000	1	25	103	145	183	21.0	24.6	27.3	√	108	141	167	15.4	18.3	20.3	√	√
10000	2	25	111	151	198	22.5	26.4	29.5		113	127	157	14.3	18.2	20.3	√	
10000	3	25	90	131	171	21.0	24.7	28.5	√	134	149	173	14.6	17.6	19.4	√	√
10000	4	25	88	133	176	21.0	24.9	28.0	√	124	153	185	15.7	18.3	20.9		
10000	1	50	81	106	152	18.2	20.7	23.0	√	95	131	163	15.3	18.0	20.6	√	√
10000	2	50	83	118	166	22.5	26.3	30.4		71	106	142	14.8	17.6	20.1	√	
10000	3	50	55	90	149	20.0	23.1	26.5	√	98	126	162	15.4	18.0	19.7	√	√
10000	4	50	49	93	147	19.7	22.6	26.4	√	92	107	134	14.3	17.5	19.2	√	√
10000	1	75	82	109	150	17.8	18.3	21.5	√	77	108	136	15.2	17.7	19.4	√	√
10000	2	75	55	91	141	21.9	25.6	29.3	√	92	117	148	15.7	18.5	20.5		
10000	3	75	41	83	116	20.0	23.0	25.8	√	94	121	140	15.4	17.5	20.3	√	√
10000	4	75	30	62	113	20.5	23.8	27.2	√	64	105	147	19.0	19.6	21.9		
Totals:									42							66	32

NHTSA's Vision for Human Injury Research

Stephen A. Ridella
Shashi M. Kuppa
Peter G. Martin
Catherine A. McCullough
Rodney W. Rudd
Mark Scarboro
Erik G. Takhounts
National Highway Traffic Safety Administration
United States
Paper Number 07-0043

ABSTRACT

The Human Injury Research Division at NHTSA has a mission to conduct research to advance the scientific knowledge in impact biomechanics that enhances motor vehicle occupant safety and supports NHTSA's mission to save lives, prevent injuries, and reduce economic costs due to road traffic crashes. For over 25 years, NHTSA's research has helped to improve understanding of the mechanisms of human injury and the tolerance of the various regions of the human body to the mechanical forces resulting from a car crash. The crash dummies, injury criteria, and modeling tools developed under this research have enabled the agency to develop regulations and consumer information to make vehicles safer.

This paper will describe how analysis of crash field data and in-depth case analysis has helped to identify vulnerable populations of occupants as well as areas of the human body that require further research. Injury tolerance of the elderly, pediatric biomechanics, head and brain injury, and thoracic and abdominal injuries are examples of the projects that will be described. The use of advanced computer modeling techniques for assessing human injury and enhancements to current and future crash dummies will be discussed. Finally, a framework for carrying out this research plan will be shared with the intent to stimulate future ideas and collaborations.

BACKGROUND

The biomechanics research sponsored and conducted by NHTSA for the last three decades has resulted in significant advances in the knowledge of human impact response and injury tolerance. These advances have led to new crash dummy designs for frontal and side impact, dummy response requirements, associated injury criteria for head, neck, chest, and lower extremities, and the development of computer-based human models. This work has been implemented in Federal motor

vehicle safety standards (FMVSS) to help improve vehicle crash and restraints performance and ultimately to improve safety for all motor vehicle occupants.

This work has not been done alone, but through the relationships developed at many institutions across North America, Europe, Asia, and Australia. NHTSA funding has helped foster and develop a generation of researchers in impact biomechanics who continue to dedicate their careers to understand better the human tolerance to vehicular crash conditions and help NHTSA achieve its mission.

In 2005, NHTSA engaged in discussions with industry and academic researchers and held extensive NHTSA inter-departmental meetings to develop a plan that would set the foundation for future biomechanics research sponsored by NHTSA. This plan is to be a continually evolving plan that considers input from all sources. For example, the IRCOBI (International Research Council on the Biomechanics of Injury, 2006) recently published a document outlining recommended research in impact biomechanics. This kind of input helps the NHTSA plan remain current and relevant. With these inputs in mind, the plan has set strategic objectives to be followed to achieve the plan's success. Those objectives are:

- 1) Conduct detailed analysis of NHTSA Data Systems (NASS, FARS, SCI, and CIREN) to determine injury severity and causation.
- 2) Prioritize and conduct necessary experimental research that identifies and/or improves the understanding of the mechanics of impact trauma in the automotive environment.
- 3) Pursue the development and application of advanced structural and statistical modeling techniques to obtain a better understanding of injury processes and improve the

agency's ability to predict the extent and severity of impact injuries.

- 4) Pursue detailed medical and engineering analysis of selected, real world, automotive crash events to identify causes and consequences of observed trauma and identify and/or monitor emerging field injury issues.
- 5) Develop new and improve existing test devices (dummies, impactors, instrumentation, etc.), to better represent the living crash victim and/or improve the

means by which estimations of expected extent and severity of injury are obtained.

- 6) Promote and conduct necessary design, development, testing, and evaluation efforts to federalize biomechanical test devices to accelerate their introduction into NHTSA's evaluation and regulation activities.
- 7) Maintain a viable database of all NHTSA sponsored biomechanical test results to allow merging of experimental efforts and maximize statistical basis for conclusions derived from analysis of data.

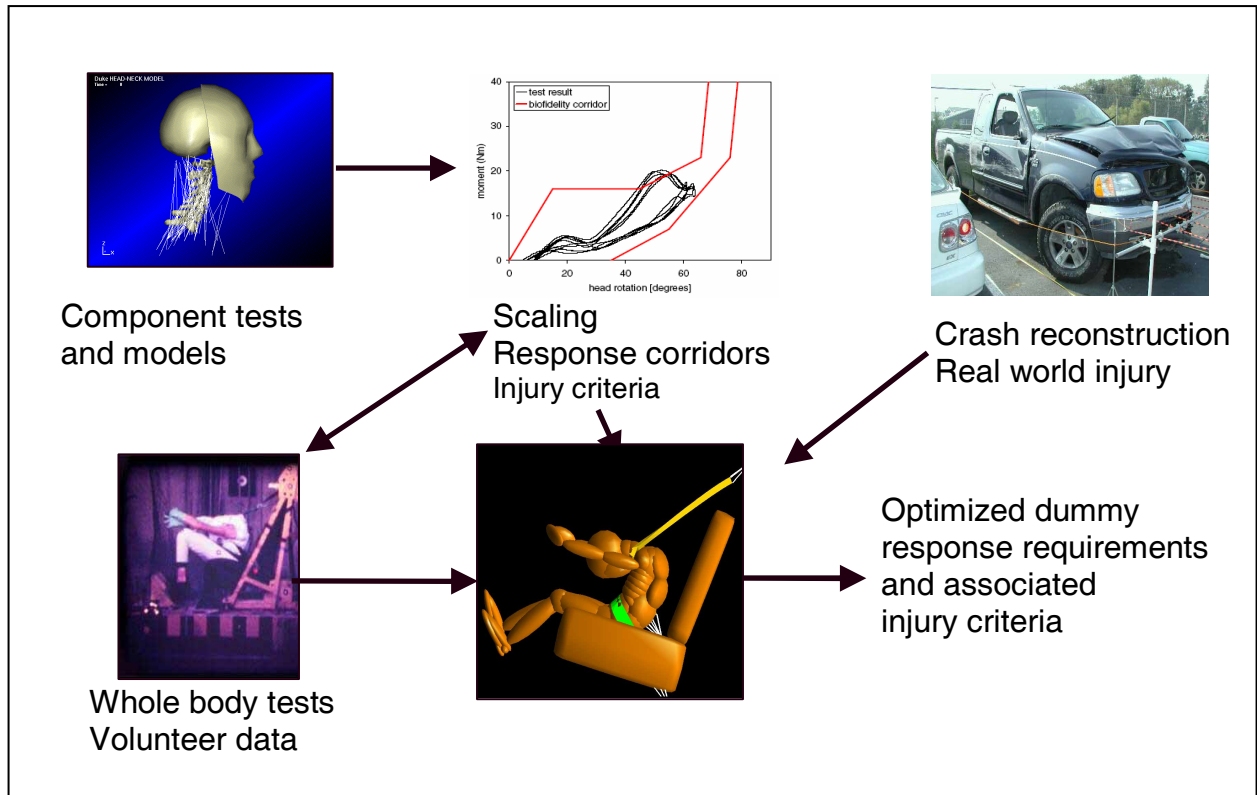


Figure 1: Flow Chart of Principal Methodology for Human Injury Research

Figure 1 shows a schematic as to how the items listed above flow into tangible deliverables that NHTSA and the industry can use to prioritize the safety efforts of vehicles. The following pages describe the initiatives to complete the objectives. Examples of the research and results will be given.

CRASH DATA ANALYSIS

Population-Based Data Analysis

A detailed analysis of NHTSA Data Systems was done to determine injury severity and causation. This analysis queried the National Automotive Sampling

System (NASS) and Fatality Analysis Reporting System (FARS) for the years 1995-2004 covering vehicles with model year 1995-2005. The safety priorities for six different crash modes, nine types of occupants, and eight body regions were considered. The smallest fifteen percent (by height) of the adult population was considered to be represented by the 5th percentile female dummy and the largest fifteen percent of the adult population was considered to be represented by the 95th percentile male dummy. Occupant age 65 years and older were classified as elderly. The safety priority is based on frequency of injury, fatality attributable to a given injury, and disability and cost associated with a particular injury.

Table 1: Distribution of Occupant Involvement in NASS (1995-2004) Crashes (MY 1995-2004).

Occupant	Percent of Total
12 months	1%
3 years	1%
6 years	2%
10 years	4%
5 th Fem	12%
95 th Male	12%
50th Male	57%
Pregnant	<1%
Elderly	11%

Table 2: Distribution of Crash Modes in NASS (1995-2004) Crashes (MY 1995-2004).

Crash Mode	Percent Total
front	50%
side	27%
rear	5%
rollover	10%
pedestrian	3%
motorcycle	5%

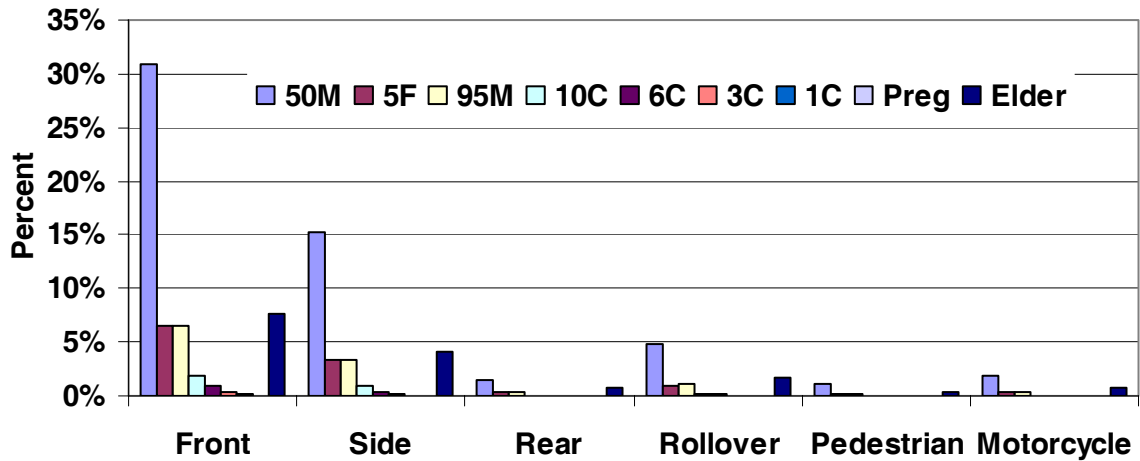


Figure 2: Distribution of Crash Involvement by Occupant Type (NASS 1995-2004, See Table 1 for Occupant Descriptions)

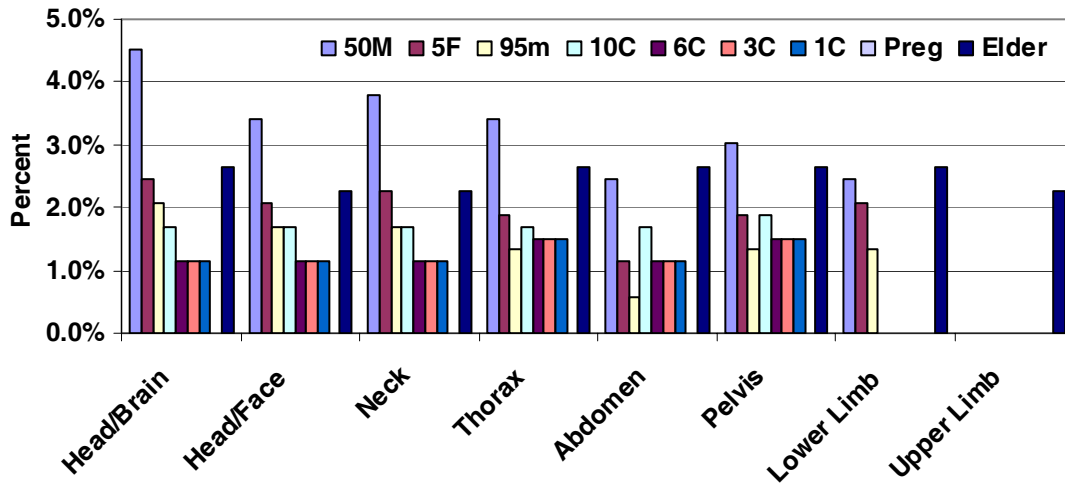


Figure 3: Distribution of Injury Locations by Occupant Type (NASS 1995-2004, all crash modes)

Tables 1 and 2 show the initial results of segregating crash involvement by occupant type and by overall crash mode. The dominant population groups involve the 50th percentile male, large male, small female and elderly. Children (classified by age) comprise a small, but not insignificant, subset of the total occupant population. For crash modes, frontal impact and side impact comprise over three quarters of all crashes in NASS, indicating that a continuing research emphasis is required for these modes. Further analysis of all crash modes by the frequency of involvement by the various occupant groups and the injuries they sustained is shown in Figures 2 and 3. The data indicates that frontal impacts are still a major concern for mid-sized males, and the elderly to a lesser extent, yet side crashes are a major concern also. In terms of injury locations, the various occupant groups show a high representation of head, neck, thorax, and abdominal injury.

More substantial injury analysis for frontal impact assessment was undertaken by Eigen and Martin

(2005). They analyzed the NASS-CDS dataset to include only occupants with an MAIS injury greater than or equal to MAIS 2 (all AIS 1 injuries are disregarded) in vehicles of model year 1998 or later. Also, the dataset included for each case all the traditional descriptive variables (model year 1998 or later, vehicle type, crash type (front, near side, far side, rear, rollover), delta-V, occupant age (12 and older are considered to be adults), seat belt use, seating position, etc. The dataset ultimately resulted in 138,000 weighted NASS occupants and 2,800 weighted fatalities. The injuries were further classified and ranked according to comprehensive descriptions of the injuries as well as the cost and the fatality attributable to an injury (Blincoe, 2002). The result for costs and fatality attributed to an injured body region is shown in Figure 4. This result indicates that the head and chest injuries are responsible for most fatalities while lower leg and head injuries incur the most cost. These results have helped to address the research areas that the NHTSA is pursuing currently.

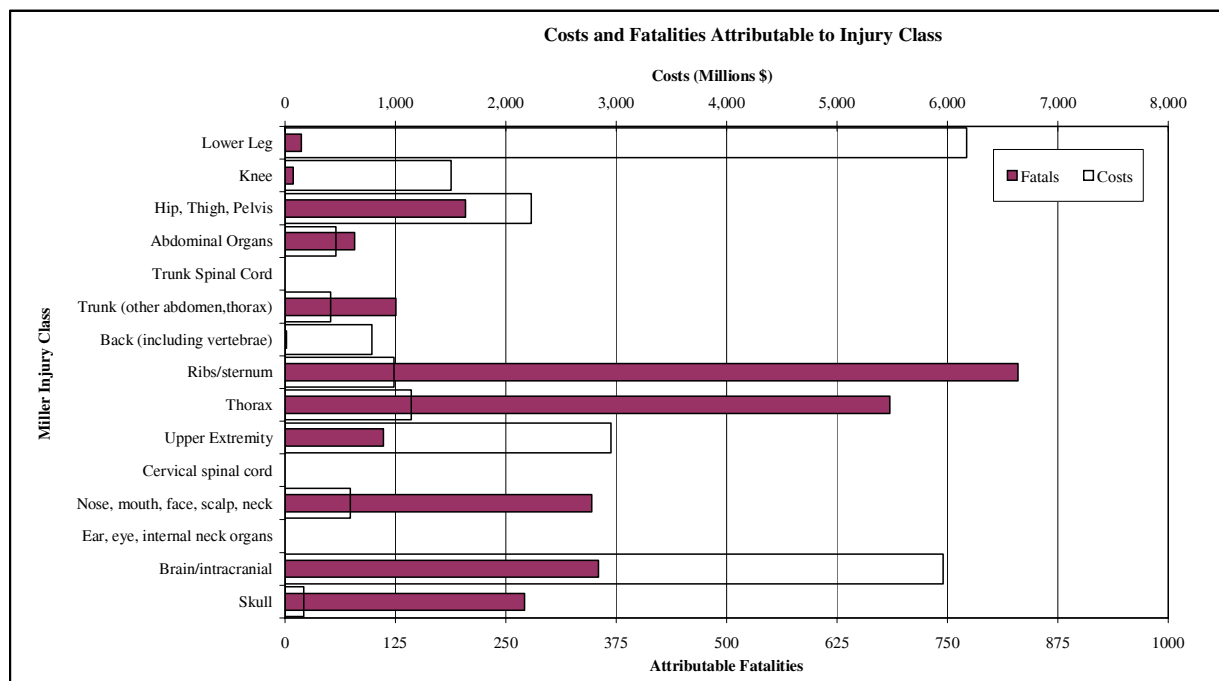


Figure 4: NASS-CDS Analysis of Cost and Fatalities Attributable to Injured Body Regions (see Eigen and Martin, 2005 for additional details)

CIREN Program Enhancements

To gain additional insight into injury causation and mechanisms, the Crash Injury Research and Engineering Network (CIREN) has become integrated into the Human Injury Research Division. For over ten years, CIREN has been a sponsor-led, multi-center collaborative research program that

focuses on in-depth studies of serious motor vehicle crashes. Researchers collect and analyze crash and injury data in order to improve vehicle design and the treatment and rehabilitation of crash victims. One of CIREN's stated goals is to use this information to reduce crash injuries, deaths, disabilities, and associated societal and economic costs.

CIREN began a new chapter in 2005 with new performance-based cooperative agreements for six NHTSA-funded centers spread across the United States joined with two industry-funded centers. The six NHTSA-funded centers are: Children’s Hospital of Philadelphia, Medical College of Wisconsin, University of Maryland-Baltimore, University of Michigan, County of San Diego – Health and Human Services and Harborview Injury Prevention and Research Center (Seattle). The new Toyota-funded center at Wake Forest University School of Medicine in Winston-Salem, North Carolina joins the existing Honda-funded center at Inova Fairfax Hospital in Fairfax, Virginia.

CIREN data is being analyzed at all centers and throughout NHTSA to learn even more about crash injury than ever before. Two new initiative, BioTab and DICOM image collection (described below) will add even more insight.

The Biomechanics Tab or BioTab of the CIREN database provides a means to completely and accurately analyze and document the physical causes of injury based on data obtained from detailed medical records and imaging, in-depth crash investigations, and findings from the medical and biomechanical literature. The BioTab was developed because the terminology and methods currently used to describe and document injury causation from crash investigations are sometimes vague and incomplete. For example, the terms “direct” and “indirect” loading are often used to describe how an injury occurred. However, there are situations where these terms are unclear, e.g., is a femoral shaft fracture from knee-to-knee bolster loading from direct loading of the knee or indirect loading of the femur through the knee? In addition, the term inertial loading is often used to describe how tensile neck injuries occur, however, using this terminology fails to document that neck tension would not have occurred unless the torso was restrained. The BioTab removes these ambiguities by providing a consistent and well-defined manner for coding injuries and recording the biomechanics of injury in crash injury databases. It also allows the identification and documentation of factors that led to a specific AIS 3+ injury such as:

- 1) Whether the injury was caused by another injury (e.g., a rib fracture causes a lung laceration),
- 2) The Source of Energy (SOE) that led to the occupant loading that caused the injury (crash, air bag, etc.),

- 3) The Involved Physical Component (IPC) that caused injury by contacting the occupant and the body region contacted by the IPC, and
- 4) The path by which force was transmitted from the body region contacted, through body components, to the site of injury.

This effort is particularly noteworthy since this will lead to a greater understanding of crash kinematics and injury mechanisms. Users of other NHTSA crash data collection systems have requested to be trained on the use of this coding technique.

Starting in 2006, CIREN centers began collecting 2-D and 3-D DICOM (Digital Imaging and Communications in Medicine) images of all case occupants. DICOM image sets are a standard medical industry method of collecting digital images (e.g., Computed Tomography, CT) of patients. These images may be assembled to allow two and three dimensional views of injured case occupants that will shed further light into the understanding of injury causation and mechanisms. Figure 5 shows an example of a 3-D DICOM reconstruction.

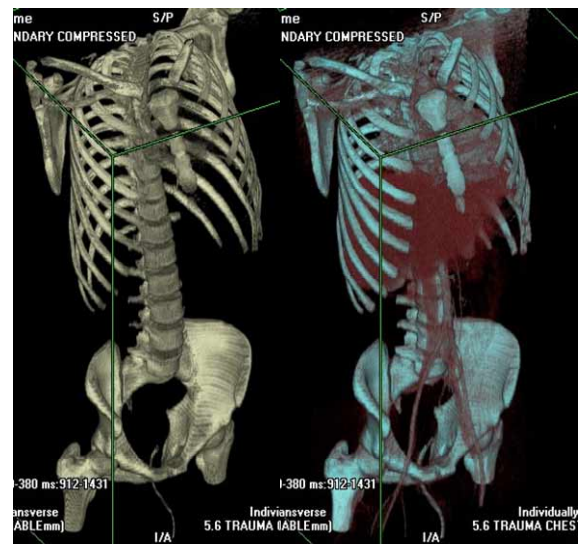


Figure 5: DICOM reconstruction showing bone and organ detail.

With the rich detail of these images, it will be possible to use them to better define human anthropometry in terms of bony geometry, fat and muscle thickness, and organ location. By studying hundreds of such images, NHTSA researchers will be able to understand the human anatomical variability as it relates to injuries suffered in car crashes. The images will be used to create better defined human

finite element models that represent this vast range of human variability in ways that have not yet been attempted. Work is underway to catalog and create standard measures that can be translated into a database for future research. It should be noted that for legal and ethical reasons, all personal data associated with any image collected have been removed.

One example of how CIREN data has been used by NHTSA is represented by the work by Rupp et al (2002). Based on the prevalence of knee-thigh-hip (KTH) injuries and the associated injury causation, Rupp performed research that has led to a proposal for a KTH criteria to assess occupant protection in the NHTSA's New Car Assessment Program (NCAP) (NHTSA,2006). Additional examples of such work are underway for other body regions and that will be described below.

INJURY MECHANISMS AND CRITERIA RESEARCH

To meet objectives 2 and 3 listed in the Background section above, NHTSA engages several institutions to conduct impact trauma research to understand the human body component and system response to these impacts. The crash data from NASS and CIREN indicate the priorities of what body regions should be researched and the research plan is made accordingly. With the data gathered from the research performed by funded institutions, NHTSA uses statistical methods to generate injury risk curves that can be used in the development of potential injury criteria for application to a crash dummy subjected to a similar loading condition. The following are examples of research areas that NHTSA is investigating through its collaborations with research institutions.

Head/Brain Injury

In the analysis of real-world car crashes, head and brain injuries were still a major source of cost and fatality even in later model year vehicles (Figure 4). Researchers place head and brain injuries into three broad categories: those manifested by rotation only (such as diffuse axonal injuries), those manifested by translation with impact (such as skull fractures), and those manifested by a combined rotation/translation.

With that premise, NHTSA is trying to develop a better understanding of the head and brain injury mechanisms. Research is underway to review existing information and to generate needed experimental data to elucidate the mechanics and

detection of skull fracture and closed brain injuries (i.e., diffuse axonal injury, focal injuries, and acute subdural hematomas). Both adult and pediatric brain injury mechanisms will be studied.

NHTSA continues to develop a tool for assessing the potential for brain injury in vehicle crash tests. The SIMon program (Simulated Injury Monitor, Takhounts et al, 2003) was developed to bridge the dummy response to the human response and probability for different brain injuries. SIMon (Figure 6 shows updated model) has been tested in many different areas and is even being used in reconstruction of brain injuries in real vehicle crashes (Hasija et al, 2007). In another funded research project, data is collected from accelerometers embedded in the helmets of football players as they are playing. This data is to be fed into the SIMon program to assess the potential for the SIMon parameters to predict the potential for mild traumatic brain injury that is sometimes suffered by these players.

It is the intent of the brain research to suggest injury criteria and injury threshold levels for brain injury assessment that may be used by NHTSA to further reduce the head injuries seen in the field. In February, 2007, NHTSA hosted a Brain Injury Symposium which gathered over 100 lead brain injury experts to determine short and long term research goals based on the current understanding of the issues.

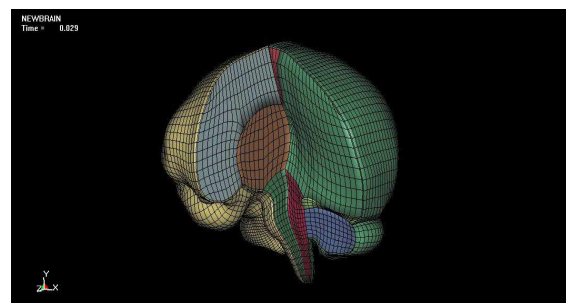


Figure 6: Enhanced SIMon Brain Model

Thoracic Injuries

In spite of the advancement in occupant restraint technology such as force limiting belts, pretensioners, and advanced air bags, thoracic injuries remain a frequent injury in frontal crashes, particularly to the elderly. This research program examines thoracic response and injury criteria for assessing thoracic injury risk in different restraint environments. The research program in this area will include human

cadaver and surrogate testing. Attempts will be made to assess local phenomena correlated with specific injury patterns as opposed to generic thoracic injury predictors. Specifically, injury thresholds (deformation-based or other physical parameters) for various thoracic organs (aorta, liver, spleen, heart and lung) will be assessed. The culmination of this research may provide the information necessary to suggest new impact response requirements (torso and organ level) and improved injury criteria for assessing injury risk in current restraint environments. This research will help improve the ability of frontal crash dummies and other human surrogates to assess the real-world performance of current and future restraint systems.

Particular attention will be paid to thoracic injuries to the elderly occupants in different restraint environments to assess which restraints are more likely to be used (comfort-based) and beneficial (injury-based) to the elderly in frontal crashes. In addition the restraints of rear seats are evaluated using human cadaveric subjects and advanced dummies. The efficacy of improved rear seat restraints is being examined as well.

A new system of evaluating cadaver and dummy thoracic and shoulder response has been developed. Sled tests are being run on a simplified universal buck to facilitate 360 degree visualization of the impact event. The buck will be generic in nature and will be sufficiently simple to serve as a standardized evaluation tool at multiple laboratories. Preliminary dummy and cadaver tests conducted with a standard belt system have confirmed the viability of using a

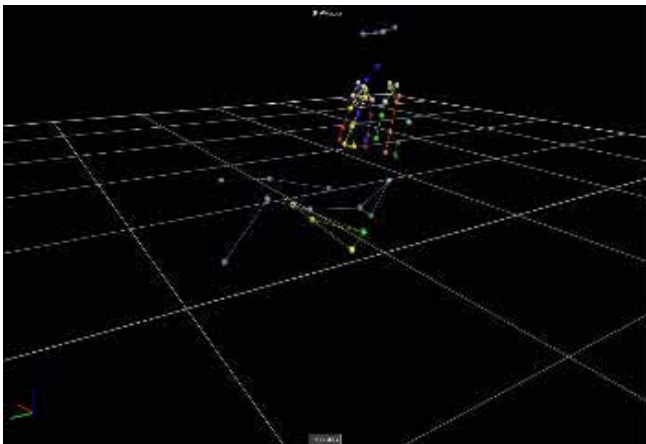


Figure 7: Vicon™ Camera Image of Targets on Dummy (oblique view)

multiple Vicon™ motion-analysis camera system to record thoracic kinematics and deformation (Figure

7). By testing cadaver and dummy surrogates with a variety of standard and force limiting belt conditions, an overall assessment of cadaver and dummy response will be done. This could lead to future improvements in injury criteria and dummy design.

VULNERABLE OCCUPANT INJURY ANALYSIS

Child occupants

A dedicated research effort in understanding child occupant injury patterns and tolerance has been ongoing at NHTSA for many years. The research led to the development of new injury criteria that are now part of FMVSS No. 208 and other standards. A renewed emphasis on child safety is underway as data has showed that motor vehicle crashes are the primary cause of death for children over 4, adolescents and teenagers. In 2005, NHTSA began coordinating meetings between a number of research labs involved in child passenger safety research. These meetings have led NHTSA to fund a number of projects with the intent of creating better understanding of pediatric impact response and in 2006, a more detailed project plan was created. These projects include the following:

- 1) Pediatric neck response and injury tolerance
- 2) Pediatric head injury analysis
- 3) Pediatric spinal kinematics
- 4) Pediatric thoracic response and compliance
- 5) Assessment of pediatric pelvic geometry

The objectives of this combined research are to determine potential child dummy enhancements that could be implemented so that dummy responses better mimic actual child responses. It is also desirable to have injury criteria consistent with tolerance directly measured from pediatric tissue. It may also be possible to support the creation of a child human computer finite element model with the data from these projects. A coordinated effort is needed to better understand this issue.

Elderly Occupants

Real world crash data indicates that elderly vehicle occupants generally have lower impact tolerance than younger occupants (Kent et al, 2003). In addition, the elderly often suffer from pre-existing conditions making them unable to recover as quickly or easily from injuries sustained in a crash. In particular, the data indicates a significantly greater risk of thoracic

injury to the elderly compared to younger occupants while there is no significant difference in injury risk exists between groups for other body regions.

NHTSA is developing an approach to understanding the elderly crash injury response with a program aimed at the following:

- 1) Analysis of CIREN Data
 - a. Perform data analysis from NASS-CDS and CIREN data on elderly occupants to compare injury trends in the two databases.
 - b. Analyze CIREN data regarding injury causation and injury mechanisms for older case occupants compared to younger case occupants.
 - c. Use advanced medical imaging data captured on CIREN subjects to analyze how human body geometry and composition changes with aging and assess its impact on injuries.
- 2) Research Related to Human Injury and Assessment of the Need for an “Elderly” Dummy
 - a. Research on elderly injury tolerance through the testing of human surrogates and different size dummy tests with current and advanced restraint systems.
 - b. Feasibility of developing injury criteria based on age.
 - c. Determination of need for “elderly” crash dummy based on data analysis and available research results.

This research effort will be done both internally at NHTSA research and in collaboration with research institutions that have experience with elderly injury mechanisms and response.

ANTHROPOMETRIC TEST DEVICE RESEARCH

NHTSA has long engaged in the development of anthropometric test devices or crash test dummies. The Federal motor vehicle safety standards stipulate over a dozen crash dummies and dummy components required for testing in a frontal, side, and rear impacts as well as component level tests to evaluate vehicle crashworthiness and occupant protection. These vital tools have helped vehicle manufacturers and suppliers design safer vehicles and restraint systems

for many years. The following discussion describes current crash test dummy research at NHTSA.

WorldSID Evaluation

To assess the potential for incorporating the WorldSID dummy into part 572, CFR 49, NHTSA has been analyzing the biofidelity, repeatability, reproducibility, oblique impact sensitivity, temperature sensitivity and overall performance of the dummy. The NHTSA Vehicle Research and Test Center (VRTC) began testing with the WorldSID 50th Percentile prototype dummy in 2001, using a dummy on loan from the WorldSID Committee. The prototype dummy demonstrated improved biofidelity over all currently existing 50th percentile male side impact dummies, although the pelvis response appeared to need improvement. In August 2004, two production WorldSID dummies on loan from the WorldSID Committee were delivered to VRTC for evaluation testing. VRTC personnel and the WorldSID committee met and agreed to the VRTC evaluation plan. VRTC and the WorldSID committee continue to evaluate and develop the dummy in a cooperative effort.

THOR Advanced Frontal Crash Dummy

Final design drawings for THOR-NT (New Technology) were released to the public in July 2005. The NT version of THOR (Test device for Human Occupant Restraint) incorporated many design changes after the initial release and testing evaluation of THOR Alpha in the late 1990s (Shams et al, 2005). THOR-NT represents the culmination of a project that can trace its beginnings to the advanced dummy projects that NHTSA began in the early 1980's. Since that time, there has been a substantial increase in available anthropometric and biomechanical data that has been incorporated into THOR. THOR is meant to be used to test the emerging advanced restraint systems that are being incorporated into vehicles. With its increased ability to measure neck, chest, abdominal, pelvic, and lower extremity loads, THOR seems well suited to evaluate the capability of these new safety systems.

Since 2005, there have been many industry tests and evaluations of the existing THOR-NT dummies. These data are being analyzed by NHTSA and others to determine if THOR is meeting its design targets. Industry groups in Europe and the U.S. have been meeting regularly to understand the results and to undertake continued testing and analysis of THOR that could lead to an international agreement on a future uses for this frontal impact dummy.

In addition to the 50th percentile male THOR-NT, a 5th percentile female THOR-NT prototype is nearing completion. This dummy will have an improved neck design that mimics the geometry and curvature of the human neck. Currently, the neck design is undergoing prototype testing and will be used in whole dummy out-of-position tests in order to assess its performance capabilities.

Child Dummies

Currently, the Hybrid III 3-year old and 6-year old dummies are used in FMVSS No. 208 out-of-position tests, FMVSS No. 213 frontal sled tests, and have been used for research purposes in the rear seats of NCAP frontal rigid barrier vehicle crash tests. The child dummies are also used in the side impact air bag out-of-position tests. More recently, the Hybrid III 10-year old dummy was proposed by NHTSA to evaluate booster seats as part of Anton's Law.

The Hybrid III type child dummies are scaled versions of the HIII-50M (Hybrid III 50th percentile male dummy) based on scaled biomechanical impact response requirements using previously published scaling methods (Mertz et al, 1997). Regional anthropometry differences and dynamic response differences between children and adults indicate the need for further research. Because of this potential difference, NHTSA is funding a study of child anthropometry to suggest improvements in child dummy design and performance. In addition, work is being carried out to better understand the thoracic, individual rib, and abdominal responses of children in a variety of funded programs. Direct measurement of such properties will lead to more biofidelic dummy designs than could be achieved with scaling methods. This methodology is also being applied to the dummy head and neck properties also.

The TREAD Act requires NHTSA to consider and make recommendation to Congress on the need for and current feasibility of a side impact child dummy and test procedure. The Agency recommended further research primarily because a test procedure and a suitable dummy do not exist. The Q3s child side dummy has been developed in Europe and is being evaluated by VRTC. The intent of the evaluation is to assess the Q3s for biofidelity and usefulness for injury assessment and to work with appropriate national and international organizations to effect needed revisions based on the best available human response data.

COMPUTER MODELING IN INJURY BIOMECHANICS

The impact of computer modeling technology on the safety and crashworthiness of vehicles has been dramatic and continues to grow. The influence of faster computing power and increased storage capacity has allowed the creation of vehicle models and crash dummy models that can be used to develop vehicle crashworthiness and occupant safety.

Dummy modeling

Computer models of current Hybrid III crash dummies have been commercially available for many years. To evaluate dummies under development, such as THOR, a finite element model can be a useful tool to compare responses in different loading conditions and to help identify potential design improvements.

A three-dimensional finite element model was developed to represent the response of the THOR thorax (model named THOR-X). Three dimensional CAD drawings of the THOR hardware were used to construct the geometry of the model. Most of the components were modeled as rigid bodies, with the exception of elastomer (shoulder and neck bumpers, flex joints, jacket and bib), foam material (upper abdomen and mid-sternum), and the steel ribs. The rigid bodies that moved relative to each other were connected with joint elements; a variety of contact definitions were used to define the interaction between rigid bodies and deformable materials. The finite element model outputs the same measurements as the THOR Crux (Compact Rotary Unit) device, that is, deflection units in four locations and one accelerometer located on the mid-sternum of the dummy. The completed finite element model was correlated with the physical THOR by simulating two Kroell impacts; one at 4.3 m/s and the other at 6.7 m/s and comparing model to experimental results. The force deflection curves for impactor force vs. chest deflection derived from the simulation compared well with those obtained from experimental data (Figure 8). It was concluded that the THOR-X finite element model can be used to accurately predict the results of physical tests performed with the THOR.

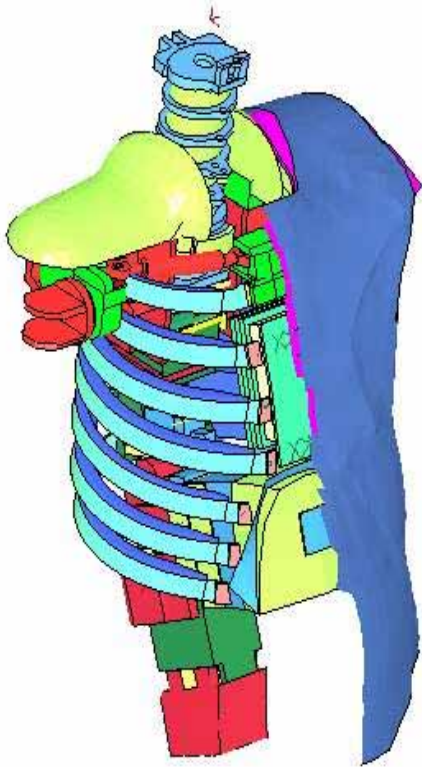


Figure 7: THOR Thorax Finite Element Model (THOR-X)

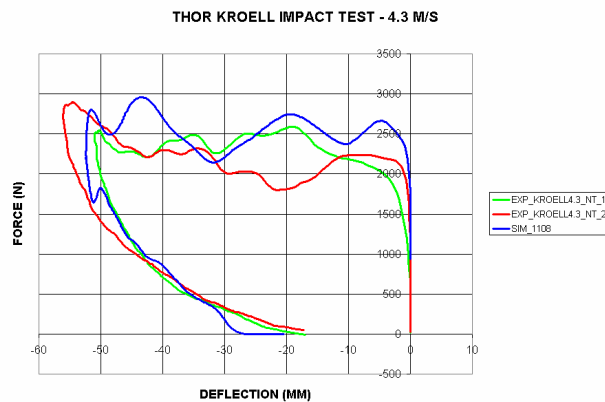


Figure 8: THOR-X Model (blue) Comparison to Weighted Pendulum THOR Dummy Impact Tests (red and green)

Human modeling

NHTSA has been involved in modeling human impact response since the early 1990s. Early versions of human head, brain and chest models were

created and validated (Plank al, 1994 and Bandak et al, 1994). Since that time, significant enhancements in computing power and memory capabilities have allowed the creation of whole human body finite element models. These models are used in the automotive industry to understand the human impact response in a simulated crash environment. The proliferation of such models has led to a call for a set of unified models that can be used by the industry. This endeavor may find the biomechanics research data collected by the Human Injury Research Division useful as it develops its human computer models.

DATA ARCHIVE AND SUMMARY

The value of the research above is the variety of tools and products that are derived from the work. To satisfy objective 7 above, the research data itself is maintained in the NHTSA Biomechanics Database for all interested parties to download and use. NHTSA uses this data to create injury risk curves and criteria. The dummy components, dummies, and computer models are made available to the automotive safety industry for use in the development of safer vehicles. In this way, the mission of NHTSA, to reduce crash related fatalities, injuries, and their associated costs is fulfilled.

The plan for human injury research outlined here is meant to be fluid, not static. Continued acquisition of field crash data and experimental results, discussions with industry, academic, and other interested groups, and influences of government objectives, will help shape future research plans. Publication of results and presentations at all major biomechanics conferences is desired to achieve maximum dissemination of results and feedback on future directions.

REFERENCES

- 1.) Bandak, F.A. and Eppinger, R.H. (1994). A Three-Dimensional Finite Element Analysis of the Human Brain Under Combined Rotational and Translational Accelerations, In : Proceedings of the 38th Stapp Car Crash Conference, pp. 145-163.
- 2.) Blincoe, L. (2002). The Economic Impact of Motor Vehicle Crashes, 2000 (DOT HS 809 446). Washington, DC.
- 3.) Eigen, A.M. and Martin, P.G. (2005). Identification Of Real World Injury Patterns In Aid Of Dummy Development. In: Proceedings of the 19th International Technical Conference on the Enhanced Safety of Vehicles, Paper No. 05-0219, Washington, D.C.

- 4.) Hasija, V., Takhounts, E.G., and Ridella, S.A. (2007). Computational Analysis Of Real World Crashes: A Basis For Accident Reconstruction Methodology. . In: Proceedings of the 20th International Technical Conference on the Enhanced Safety of Vehicles, Lyon, France.
- 5.) International Research Council on the Biomechanics of Injury. (2006). Future Research Directions in Injury Biomechanics and Passive Safety Research.
- 6.) Kent, R.W., Patrie, J., Poteau, F., Matsuoka, F., and Mullen, C. (2003). Development of an Age-Dependent Thoracic Injury Criterion for Frontal Impact Restraint Loading. In: Proceedings the 18th International Technical Conference on the Enhanced Safety of Vehicles, Nagoya, Japan.
- 7.) Mertz, H.J., Prasad, P., and Irwin, A.L. (1997). Injury Risk Curves for Children and Adults in Frontal and Rear Collisions. In: Proceedings of the 41st Stapp Car Crash Conference, pp. 13-30, SAE Paper No. 973318, Warrendale, PA
- 8.) NHTSA. (2006) The New Car Assessment Program; Suggested Approaches for Enhancements. Docket No. NHTSA-2006-26555.
- 9.) Plank GR, Kleinberger M, and Eppinger RH. (1994). Finite element modeling and analysis of thorax/restraint system interaction. In: Proceedings of the 14th International Technical Conference on the Enhanced Safety of Vehicles, Munich, Germany.
- 10.) Rupp, et al., (2002) The Tolerance of the Human Hip to Dynamic Knee Loading,” 46th Stapp Car Crash Conference, 2002.
- 11.) Shams, T., Rangarajan, J., McDonald, J., Wang, C., Patten, G., Spade, C., Pope, P., Haffner, M. (2005). Development of Thor NT: Enhancement of Thor Alpha –The NHTSA Advanced Frontal Dummy. In: Proceedings of the 19th International Technical Conference on the Enhanced Safety of Vehicles, Paper No. 05-0455, Washington, D.C.
- 12.) Takhounts, E.G., Eppinger, R.H., Campbell, J.Q., Tannous, R.E., Power, E. D. and Shook, L.S. (2003). On the Development of the SIMon Finite Element Head Model. Stapp Car Crash Journal, Vol. 47, pp. 107-134.

COMPUTATIONAL ANALYSIS OF REAL WORLD CRASHES: A BASIS FOR ACCIDENT RECONSTRUCTION METHODOLOGY

Vikas Hasija

GESAC, Inc

Erik G. Takhounts

Stephen A. Ridella

NHTSA

United States

Paper Number: 07-0050

ABSTRACT

This paper focuses on an accident reconstruction methodology by estimating the errors introduced into reconstruction analysis as a result of assumptions made due to lack of data availability and other uncertainties. Mathematical models are used to show the sensitivity of their results, i.e., occupant kinematics, injury predictions, etc., to changes in these assumptions. For demonstration purposes, a real world crash involving an occupant with “no brain injury” was selected from NHTSA’s Crash Injury Research and Engineering Network (CIREN) database and reconstruction was carried out using the information available from the crash. The crash pulse for the case was obtained using Human-Vehicle-Environment (HVE) software and then applied to a MADYMO (Mathematical DYnamic MOdel) occupant simulation model of the case vehicle and occupant. Head acceleration output from the model subsequently served as an input into the NHTSA-developed SIMon (Simulated Injury Monitor) finite element (FE) head model and used to compute probabilities of various brain injuries. The results of the SIMon predictions were then compared to the brain injuries reported in CIREN. Sensitivity analysis was carried out at each step with respect to various assumed parameters starting with generation of the collision pulse in HVE and ending with SIMon brain injury predictors. Important parameters required for better injury predictions were also identified, and some observations that may be relevant to the CIREN accident investigation team are made. This paper shows that a “no injury” case can become an “injury” case due to the introduction of variability in reconstruction parameters. This paper thus shows the methodology, including important details to be taken into account as well as the additional information that needs to be collected from the real world crashes for better accident reconstruction analysis.

INTRODUCTION

Computerized accident reconstruction analysis is a tool used to investigate crash sequences and to study occupant kinematics during crashes. Information

obtained on occupant kinematics can then be used to design better and more efficient safety systems for occupant protection. There are several potential parameters influencing a real occupant’s injury risk, but unfortunately many of them are unknown and an accurate accident reconstruction analysis cannot be carried out. As a result, the occupant injuries cannot be predicted correctly. Since assumptions have to be made for these unknown parameters, one set of reconstruction parameters is not sufficient to predict occupant injuries. It becomes imperative to carry out a sensitivity analysis with respect to these assumed parameters to find those critical parameters that affect the injury predictions significantly. These critical parameters need to be controlled better (minimize their range of variation by gathering additional information on these parameters) before injuries are predicted. The predicted injuries can be quite different from the actual injuries if control is not exercised.

In the past, an occupant’s injury evaluation based on reconstruction has been carried out using computational models, but with only one set of reconstruction parameters and without any sensitivity analysis. For example, Franklyn et al [1] presented a paper on accident reconstruction in which they physically reconstructed real world accidents, and the information from these physical tests was used as input to finite element head models for predicting injuries and subsequently compared with actual occupant injuries. During experiments, various errors can affect the data. For example, the crush depth obtained from their physical tests do not match up with the real world crash data, and this discrepancy can certainly affect the crash pulse experienced by the vehicle as well as the accelerations experienced by the Anthropomorphic Test Device (ATD) used in their physical tests, which provides input data for the computational models. Sensitivity analysis was not carried out in the Franklyn study to see how the results, i.e., the injury predictions obtained from the finite element head models, were affected due to these errors. This

analysis is very important when using computational models to predict injuries as the models are only as good in predicting injuries as the input data driving them.

Also, Mardoux et al [2] presented a paper showing the head injury-predicting capability of HIC (Head Injury Criterion), HIP (Head Impact Power), SIMon FE head model and ULP (Louis Pasteur University) FE head model. Input data for the finite element head models was obtained by experimental reconstruction of real-world cases with the Hybrid-III (H-III) dummy head. The experiments have errors associated with them that can lead to errors in the model's injury predictions. Sensitivity analysis of the model or the model's injury prediction was not carried out in this study either. The effect of these uncertainties must be analyzed. Also in this study, von-Mises stress and global strain energy were used as a measure of brain injuries that have not been shown experimentally to be related to brain injuries. Different injury metrics were studied in this paper (and some were shown to be better than others), but it becomes necessary to first control the reconstruction parameters before showing the effectiveness of the injury metrics, as variability in the parameters can lead to quite different injury metrics.

The objective of this paper is to show a reconstruction methodology that involves sensitivity analysis with respect to the assumed parameters and identify the critical parameters using injury assessment quantities such as HIC and SIMon brain injury metrics [3], namely Cumulative Strain Damage Measure (CSDM), a correlate for diffuse axonal injury; Dilatational Damage Measure (DDM), a correlate for contusions; and Relative Motion Damage Measure (RMDM), a correlate for subdural hematoma. The methodology is shown by reconstructing a "no brain injury" real world crash selected from the CIREN database [4] and comparing injury predictions with real world injuries. It shows that due to variability of reconstruction parameters, some injury metrics can switch from "no injury" to "injury." Finally, some observations are made for the CIREN crash investigation team on the additional data that needs to be collected on the field, which can be used for accident reconstruction.

METHODOLOGY

The methodology for reconstructing real world accidents using computer simulations starts with selection of real world case from the CIREN database (Figure 1). The Event Data Recorder (EDR) information listed in CIREN is then searched to find the crash pulse. If no EDR information is available,

the crash details available from the selected case are used in Human-Vehicle-Environment (HVE) software [5] to generate the crash pulse. This is followed by setting up the occupant simulation model in MADYMO [6] using the information available from the selected case such as occupant information, restraints information, etc. The crash pulse obtained from either EDR or HVE is used for driving this occupant simulation model. During the set up, the unknown parameters are identified and assumptions are made for these parameters (Figure 1). Once this model is set up, the baseline run is obtained by matching the occupant-vehicle contacts happening during the simulation with those listed in CIREN. Sensitivity studies are carried out around this baseline run with respect to the assumed parameters. For all these parametric simulations, the CIREN-listed occupant-vehicle contacts are maintained to ascertain the validity of the selected case. The head accelerations obtained as output from the baseline run and all the parametric runs are then used as input into the SIMon finite element head model [7] to predict brain injuries, which are then compared with the actual occupant injuries. HIC and SIMon brain injury metrics obtained are further analyzed to identify the parameters that affect the output considerably and thus need to be controlled better before running the final simulation for injury predictions. The methodology is demonstrated here by reconstructing a "no brain injury" case.

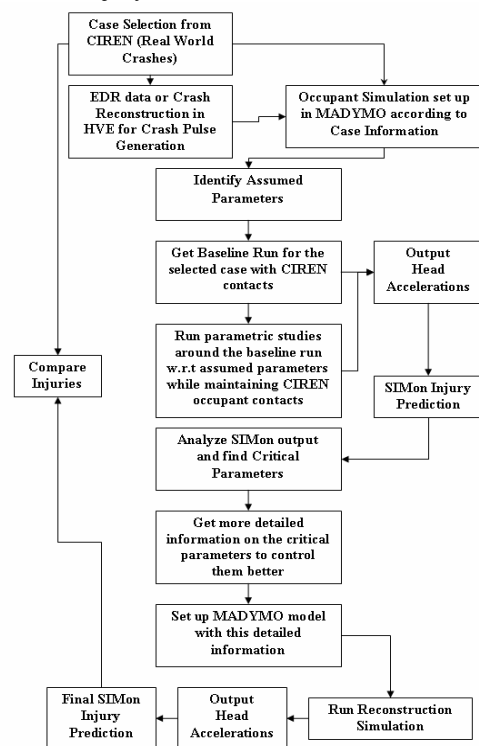


Figure 1. Reconstruction Methodology Diagram.

Case Selection

The case selection matrix was taken from CIREN. Only cases with single event, frontal impact with PDOF of $\pm 10^\circ$, with no rollover and having a status of “COMPLETED” were considered. Cases were selected that provided enough information for reconstruction in HVE (vehicle type, collision partner involved, Collision Deformation Classification (CDC), Principal Direction of Force (PDOF), Crush and DeltaV) and also enough information for occupant simulation in MADYMO (age, height, weight of the occupant, occupant role, restraints used, airbag information, seat performance information, etc). One important criterion for case selection was good occupant-vehicle contacts that could be simulated. All cases with airbag failure, seat performance failure and seatbelt failure were ignored. Cases where the occupant was asleep or in an Out-of-Position (OOP) state were also ignored. Based on these selection criteria, the case that had the most information available for reconstruction was a case of moderate crash severity with the case occupant sustaining “no brain injuries.”

Selected “No Brain Injury” case –Details of the “no brain injury” case that was reconstructed are provided below:

This crash occurred at night with no streetlights while it was raining on a wet roadway surface. The speed limit was posted at 25 mph. Case vehicle one (V1), a 1995 Saturn SL four door sedan, was traveling eastbound on a two lane, two-way roadway that curved right to the south (Figure 2). Vehicle two (V2), a 1988 minivan, was northbound on the same roadway, but was traveling in the opposite lane. As V1 had completed the curve and recognized V2 in the lane, the driver began to apply the brakes and attempted to move right partially on the shoulder. V2 also applied the brakes, leaving lockup evidence prior to striking head-on with V1. Post impact, V1 rotated counterclockwise and was forced rearward into the roadside ditch. This was a moderate severity head-on crash with a delta-V of 34 mph.

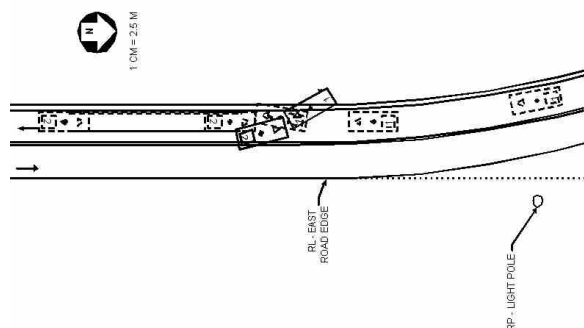


Figure 2. Crash Scene for “no brain injury” case.

In this case, the case occupants were the driver and back center seat passenger in V1. In our study only the driver was considered. The driver (28-year-old female, 173 cm in height and 73 kg in weight) was wearing the lap/shoulder belt and had a frontal airbag deployment. The occupant (driver) did not have any major injuries; all listed injuries were minor skin contusions/lacerations (Table 1).

Table 1.
Occupant Injuries

AIS Code	Description
8906021	Lower Extremity Skin Laceration Minor
4904021	Chest Skin Contusion
7904021	Upper Extremity Skin Contusion
7902021	Upper Extremity Skin Abrasion
2904021	Facial Skin Contusion

The occupant contact points with the vehicle interior (Table 2) were taken from CIREN. During the reconstruction simulations, it was made sure that these contacts were maintained between the occupant and the vehicle interior.

Table 2.
Occupant-Vehicle Contacts

Contact	Component	Body Region
1	Airbag –Driver side	Face
2	Knee Bolster	Knee-Left
3	Steering Column/ Transmission	Knee-Right

Crash Pulse Generation

For the crash pulse (vehicle deceleration pulse during impact), EDR data (if available) should be preferred, but since the EDR data was not available for this case, Human-Vehicle-Environment (HVE) software developed by Engineering Dynamics Corporation (EDC) was used for crash pulse generation. Specifically, Engineering Dynamics Simulation Model of Automobile Collisions (EDSMAC4) module was used for this purpose [5, 8, 9, 10, and 11].

Before using this module for the selected CIREN case, the module’s crash pulse generation capability was evaluated by generating the crash pulse for several tests for which the crash pulse was already known. These were vehicle-vehicle compatibility

tests that were selected from NHTSA's vehicle database [12]. Two different types of vehicle-vehicle impact tests were selected; one full frontal collinear (Figure 3 - Chevy Venture into Honda Accord), and the other 50% offset frontal (Figure 4 - Dodge Grand Caravan into Honda Accord). Vehicle-vehicle impact tests were evaluated so as to be consistent with the selected CIREN case which involves vehicle-vehicle impact.

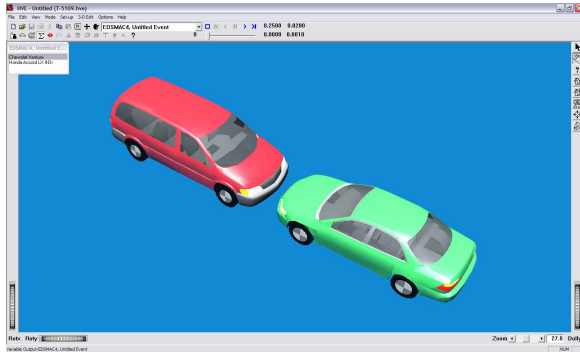


Figure 3. Full frontal case set up.

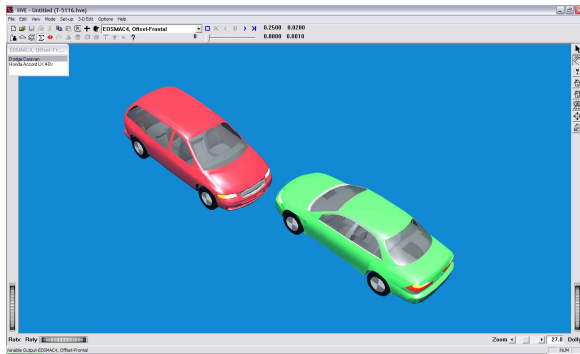


Figure 4. 50% Offset frontal case set up.

For this evaluation study, vehicle models were chosen from the vehicle database and updated with respect to the exterior specifications (overall length, width, wheelbase, front overhang, rear overhang, weight, etc.) as per the test report. The tire model was also updated and was selected from the tire database. Position and velocities were then assigned to the vehicles according to the information in the test report. Delta-V and crush were matched to get the crash pulse.

In HVE, even though only homogeneous and linear stiffness could be defined for any side of the vehicle by specifying parameters A and B (Figure 5), a reasonably good approximation of the crash pulse was obtained (Figures 6 and 7).

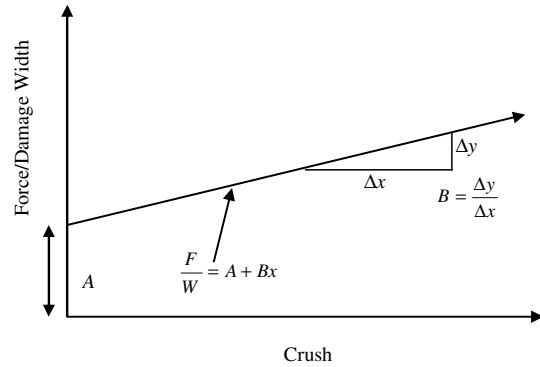
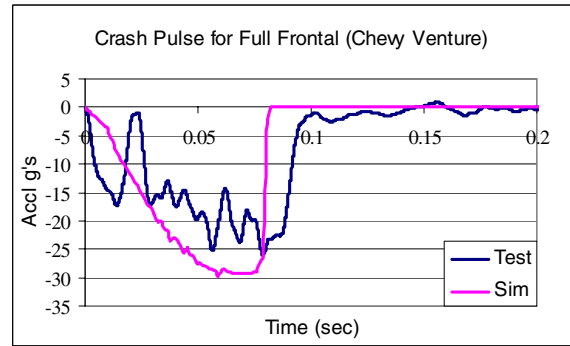
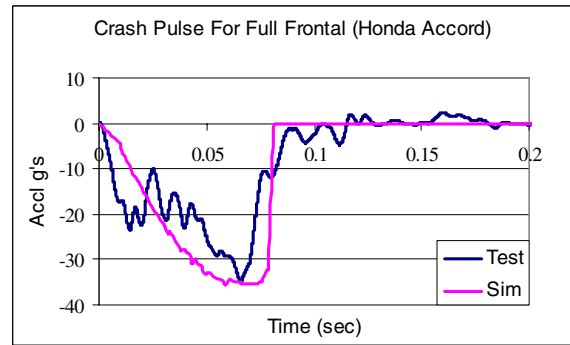


Figure 5. Stiffness used in HVE.

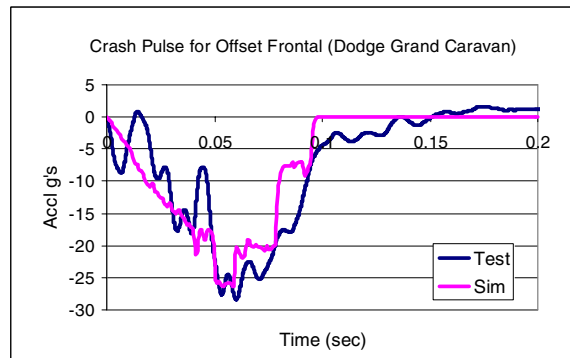


(a)

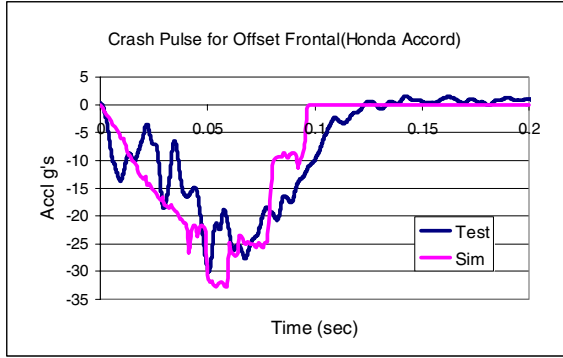


(b)

Figure 6. Crash pulse comparison for full frontal case for (a) Venture and (b) Accord.



(a)



(b)

Figure 7. Crash pulse comparison for offset frontal case for (a) Caravan and (b) Accord.

To generate the crash pulse for the CIREN case, the vehicles involved in the crash were first selected. For the 1995 Saturn SL, which was the case vehicle, a generic passenger car model was used. For the second vehicle (1988 Dodge Caravan) involved in the crash, a generic van model was used. Generic models were used to calculate crush more precisely. Both these vehicle models were then updated with respect to the exterior vehicle specifications: front overhang, rear overhang, overall length and width, wheelbase and weight. The exterior specifications for both vehicles were obtained from the CIREN database. The total weight used was the sum of “Curb weight,” “Weight of the Occupants,” and “Cargo weight.” Since CIREN did not list any information for the occupant in the non-case vehicle (V2), a weight of 150 lbs was assumed for the driver of the non-case vehicle. Vehicle stiffness plays an important role in correct crash pulse generation. Hence, the front, side, rear, top and bottom stiffnesses and the inertias of these generic vehicle models were updated based on the values available from actual vehicle models available in the HVE vehicle database for the case and the non-case vehicle. After these vehicles were set up in the vehicle mode, the crash event was set up in the event mode. The vehicles were positioned (Figure 8) with respect to the global coordinate system according to the heading angles given in CIREN. An estimated initial velocity was then assigned to each vehicle as their velocities were unknown.

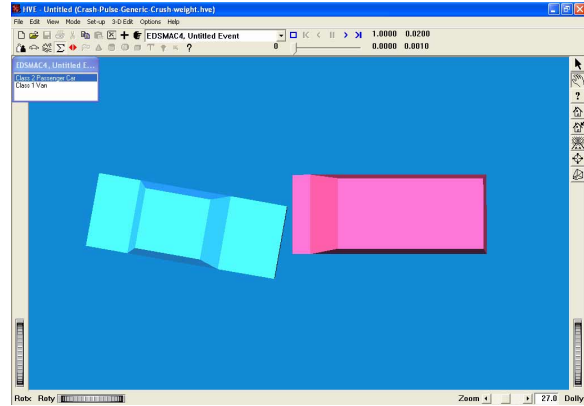


Figure 8. HVE set up for the “no brain injury” case.

To generate a valid crash pulse (Figure 9) for the selected CIREN case, various quantities (i.e., Principal Direction of Force (PDOF), Collision Deformation Classification (CDC), Crush and Delta-V) were matched between CIREN and the HVE simulation by carrying out parametric variations with respect to the impact location, vehicle velocities, inter-vehicle friction, etc. Since CIREN did not report all these quantities for the non-case vehicle, only Delta-V was matched for the non-case vehicle. A good match was obtained for both the case and non-case vehicle (Tables 3 and 4). Post-impact motion obtained for both the case and the non-case vehicle in the HVE simulation was consistent with the information provided in CIREN. The damage photo from CIREN was also compared with the damage profile obtained from HVE (Figure 10). The match seemed to be reasonable coming from an EDSMAC4 module simulation which is a 2D physics program and thus incapable of simulating hood buckling.

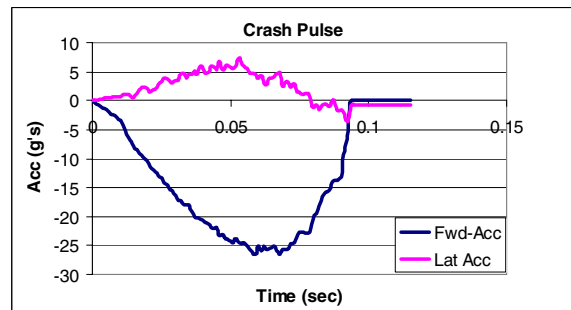


Figure 9. Crash pulse generated using HVE.

Table 3.
Case vehicle match

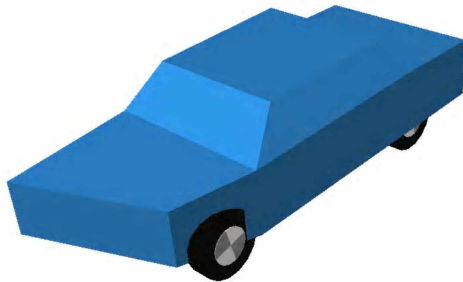
Saturn	CIREN	HVE
DeltaV mph	34	35
Crush, in	31	28.62
CDC	12FYEW4	12FYEW5
PDOF (deg)	350	349.6

Table 4.
Non-case vehicle match

Dodge	CIREN	HVE
DeltaV mph	28	28.9



(a)



(b)

Figure 10. Damage photo from (a) CIREN and (b) HVE.

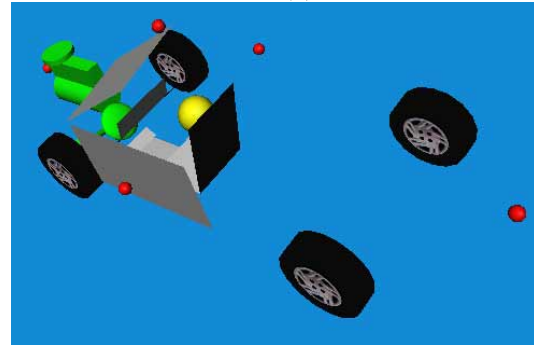
Occupant Simulation

The occupant simulation was carried out using MADYMO, which is a widely used occupant safety analysis tool that can be used to simulate the response of an occupant in a dynamic environment. The occupant size for this “no brain injury” case was close to a 50th percentile size, and hence the H-III 50th ellipsoid model and the 50th percentile human facet model were used as occupant models in MADYMO. The case vehicle interior surfaces were created in MADYMO. The location of these surfaces was obtained from HVE, which had the actual vehicle model of a 1996 Saturn SL available in its vehicle

database. The contact surfaces were first created in HVE (Figure 11), and only the necessary contact surfaces were created based on the contacts listed in CIREN between the occupant and the vehicle interior. This information was then used to create the case vehicle in MADYMO (Figure 12).



(a)



(b)

Figure 11. Contacts Surfaces generated in HVE (a) Full View and (b) No Body View.

The properties for the seat structure, seat back, seat cushion, knee bolster, steering column and the contact characteristics between the occupant model and the vehicle interior were taken from the frontal impact application file [13] available in MADYMO, which has generic but realistic properties. Since the occupant (driver) had an airbag deployment during the crash, a generic airbag model was added to the steering wheel hub. The generic driver airbag model was selected from MADYMO applications [13].

Pre-simulation for positioning the occupant model in the seat was carried out for both the H-III 50th ellipsoid model and the 50th human facet model. Gravity loading was applied for a total time of 1 sec. The joint positions obtained from the last time step were used to update the impact-simulation file to position the dummy correctly in the seat (Figure 12). After this positioning was done, the right foot of the occupant was placed on the brake as mentioned in CIREN case file and the hands were positioned in

driving mode. Since the occupant was wearing the lap/shoulder belt during the event, an FE lap and shoulder belt was created and wrapped around the occupant (Figure 12). The properties for the belts were taken from MADYMO application file to be close to the realistic properties.

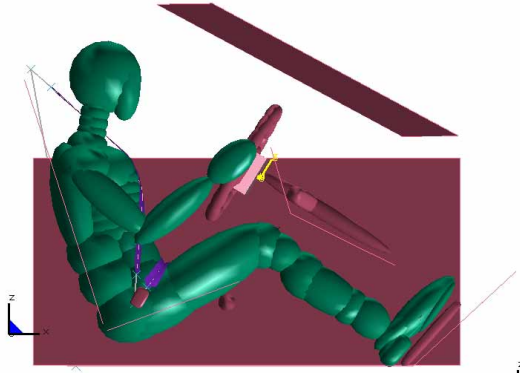


Figure 12. Impact Simulation model for “No Brain Injury” case.

The crash pulse obtained from HVE (Figure 9) was used as a fictitious acceleration field applied on the occupant during the impact simulation. The baseline run was obtained once the occupant-vehicle contacts were matched with those listed in CIREN. Time histories of the head linear accelerations and angular velocities were generated as output to be used for further analysis with SIMon finite element head model. The human facet model took over 15 hours to run as compared to 5 hours for the ellipsoid dummy model on an SGI machine with 1 processor. Because of this time constraint, the human facet model was not used for any parametric studies. The results presented in this paper are thus only from the simulations carried out with the H-III 50th ellipsoid dummy model.

HIC & SIMon Injury Metrics

After the baseline run was obtained in MADYMO, the linear accelerations at the head CG and the angular velocities of the head were obtained in head-body coordinates. These pulses were then input into the NHTSA-developed SIMon finite element head model and the injury metrics were obtained (Table 5), namely CSDM, DDM and RMDM. The HIC values were also calculated (Table 5).

Table 5.
HIC and SIMon Injury Metrics for baseline run

Injury Metrics	Value	Threshold
CSDM (0.15)	0.04628	0.55 *

DDM	0.000185	0.072 *
RMDM	0.8368	1 *
HIC15	424	700
HIC36	564	1000

* Threshold corresponds to 50% probability of injury

The injury metrics CSDM, DDM, RMDM and the HIC values predicted “no brain injury”-below threshold - for the selected case for the baseline run. HIC15, CSDM, DDM and RMDM were further used as assessment quantities to find the critical parameters from the reduced parametric studies carried out with the assumed parameters described in the next section.

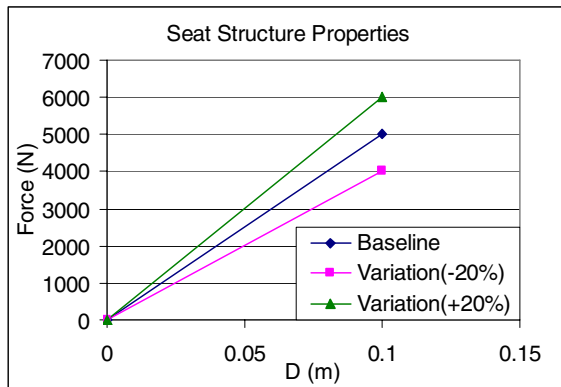
Parametric Studies

Parametric studies were carried out around the baseline run with respect to the assumed parameters to show how the predicted injuries were affected due to changes in these assumed parameters, and to identify the important parameters that need to be controlled better for accurate reconstruction. It was made sure that the CIREN-listed occupant-vehicle contacts were maintained during all these parametric simulations so that the parametric effect could be seen in the valid solution space. Overall, 19 different parameters were studied with an assumed range of variation (Table 6). 9 of these 19 parameters were functions (Figures 9 and 13). Some of the parameter ranges were taken from references [12] and [14].

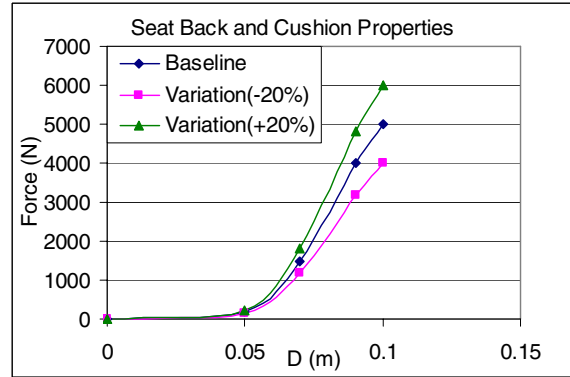
Table 6.
Assumed parameters

	Parameters	Baseline Value	Variations
SEAT	Seat Structure Properties	Figure 13a	± 20%
	Seat Back and Cushion Properties	Figure 13b	± 20%
	Seat Inclination	19	± 5°
	Seat Track Position	Figure 12	56mm ← 22mm →
	Seat Friction	0.3	0.1, 0.6
POSTURE	Seating Posture	Normal	Different positions of left leg
KNEE BOLSTER	Knee Bolster Properties	Figure 13c	± 20%

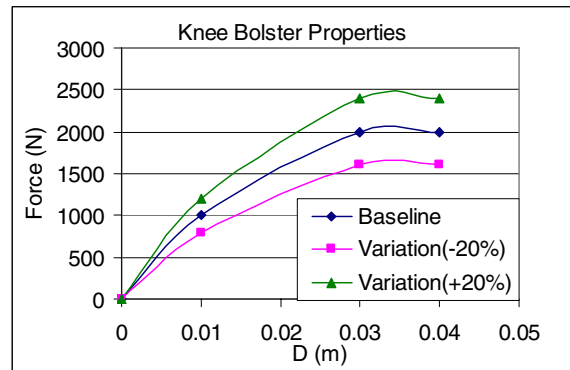
	Knee Bolster Angle	27	$\pm 10^\circ$
BELT SYSTEM	Belt Segment Properties	Figure 13d	$\pm 20\%$
	FE Lap/Shoulder Belt Properties	Figure 13e	$\pm 20\%$
	Belt Friction	0.2	0.1, 0.4
	Retractor Properties (film spool effect)	Figure 13f	$\pm 20\%$
	Retractor Locking Time	1 ms	10ms,20ms
DRIVER AIRBAG	Airbag Firing Time	20ms	25ms,35ms
	Airbag Friction	0.2	0.1, 0.6
	Steering Column Angle (Airbag Deployment Angle)	30	$\pm 5^\circ$
	Airbag Mass Flow Rate	Figure 13g	$\pm 20\%$
CRASH PULSE SCALING FACTORS	Crash Pulse-X component (Fwd Acc)	Figure 9	0.82,1.11
	Crash Pulse-Y component (Lat Acc)	Figure 9	0.5, 1.5



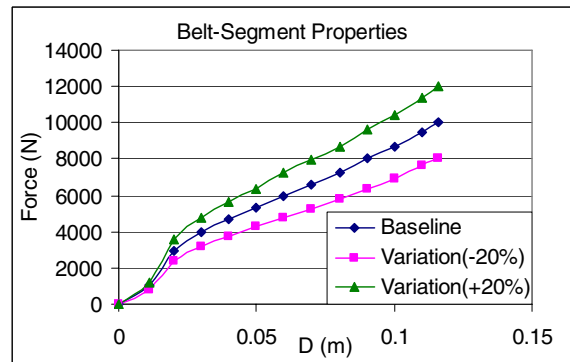
(a)



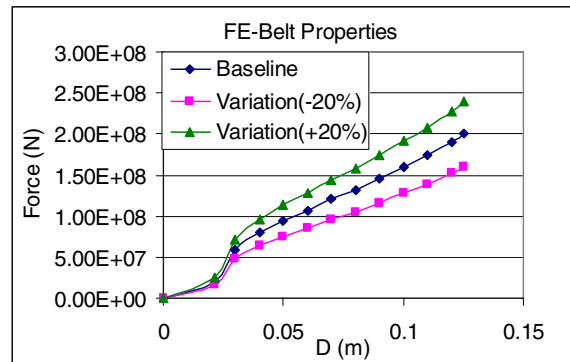
(b)



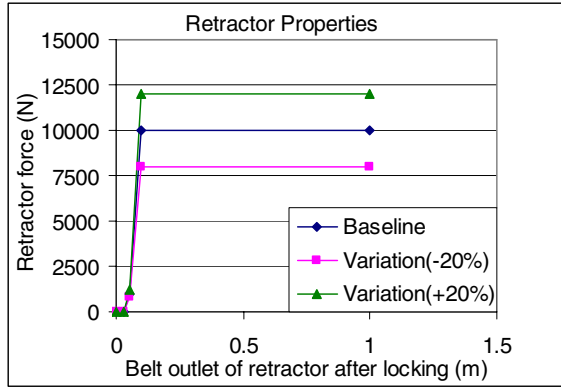
(c)



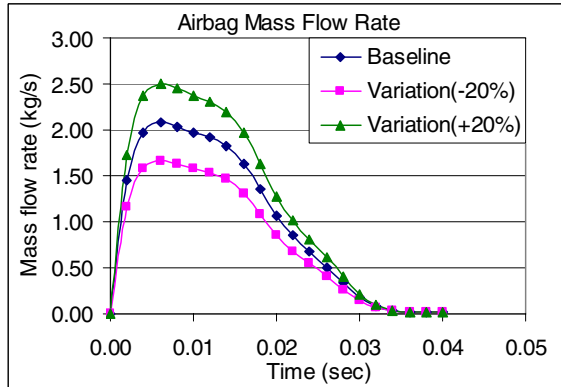
(d)



(e)



(f)



(g)

Figure 13. Plots showing the properties used for different vehicle components.

Even though the knee bolster angle was taken from the HVE vehicle model, it is only an approximate way of obtaining the contact surfaces. Hence, parametric variations were carried out with respect to the knee bolster angle. Also, since the position of the right leg was already known, the position of the left leg was changed to study seating posture effects.

The delta-V reported in CIREN is not exact and an error of ± 5 mph was assumed in the delta-V value (34 mph) reported in CIREN. Based on this assumption, the scaling factors for the X and Y components of the pulse were obtained. The scaling factor range for the X-component was obtained by making sure that the delta-V obtained by integrating the resultant crash pulse stayed within 34 ± 5 mph. Since the Y-component had a much lower magnitude (Figure 9), scaling did not affect delta-V (obtained from the resultant crash pulse) too much. So the scaling factors were selected to produce a change of around $\pm 4g$'s.

Since there were a large number of parameters, it was impossible to use the full parametric matrix. Thus,

reduced parametric studies were carried out where only a subset was performed to demonstrate the effect of variability/uncertainty.

The reduced parametric studies were carried out first by independently changing each parameter while controlling for the others (fixed to the baseline values). 38 MADYMO simulations were run, two variations for each parameter (Table 6), with each simulation having a run time of 5hrs on a SGI system with one processor. Out of these 19 parameters studied, 14 were found to be critical. The critical parameters were identified by using the following methodology:

First the change in each assessment quantity, i.e. HIC15, CSDM, DDM and RMDM, was calculated for each parameter (Equation 1).

$$\Delta_{HIC15i / CSDM i / DDM i / RMDM i} = \text{Max}(\text{run1}, \text{run2}, \text{run3}) - \text{Min}(\text{run1}, \text{run2}, \text{run3}); i=1 \text{ to } 19 \quad (1).$$

Once the change was obtained for each assessment quantity for each parameter, normalization was carried out (Equation 2).

$$\Delta_{normi}^{HIC15} = \frac{\Delta_{HIC15i}}{\text{Max}\Delta_{HIC15}}; i=1 \text{ to } 19 \quad (2).$$

where $\text{Max}\Delta_{HIC15}$ corresponds to the maximum value of Δ_{HIC15} obtained for any parameter.

Similar normalization was carried out for CSDM, DDM and RMDM. This normalization was performed because the scales of HIC, CSDM, DDM and RMDM were quite different. Next, the total effect of each parameter on the output was obtained by summing up the normalized values of each assessment quantity (Equation 3).

$$\text{Total_effect}_i = \Delta_{normi}^{HIC15} + \Delta_{normi}^{CSDM} + \Delta_{normi}^{DDM} + \Delta_{normi}^{RMDM} \quad \text{where, } i=1 \text{ to } 19 \quad (3).$$

Finally the % effect was obtained for each parameter (Equation 4).

$$\% \text{Effect}_i = \frac{\text{Total_Effect}_i}{4}; i=1 \text{ to } 19 \quad (4).$$

From the % effect, the critical parameters were identified. As it was impossible to carry out a full cross-effect study due to large number of parameters, around 12 simulations were run by using some of the critical parameters (identified using independent

parametric analysis) to study the cross-effects. The limited cross-effect study carried out was in the valid solution space, and was sufficient in the context of this paper. Thus, the reduced parametric study consisted of independent parametric analysis plus some cross-effect analysis.

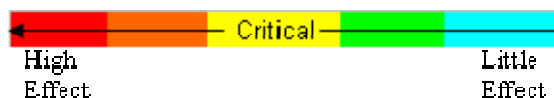
The output from all these occupant simulations was used for driving the SIMon finite element head model to predict brain injuries. 49 FE simulations were run, with each simulation having a run time of around 3hrs on a PC with a Pentium 4 processor. Therefore a total of 100 simulations (51 MADYMO + 49 SIMon) were carried out for this reduced parametric study of the “no brain injury” case.

RESULTS

The results of the first 38 simulations (independent parametric study) were analyzed in terms of the assessment quantities - HIC, CSDM, DDM and RMDM (Table 7) - to show how different parameters affected the output.

Table 7.
Parametric effect (normalized values)

Parameter	HIC 15	CSDM	DDM	RMDM	Total Effect	% effect
Crash Pulse-X component	0.927	1.000	0.343	1.000	3.270	81.76%
Seat Inclination	1.000	0.736	1.000	0.220	2.956	73.91%
Seat Track Position	0.592	0.217	0.564	0.682	2.055	51.39%
Crash Pulse-Y component	0.390	0.495	0.162	0.668	1.716	42.90%
Belt Segment Properties	0.226	0.467	0.475	0.331	1.499	37.48%
Airbag Friction	0.317	0.371	0.204	0.245	1.138	28.44%
Seat Back and Cushion Properties	0.181	0.475	0.060	0.414	1.130	28.25%
Airbag Firing Time	0.160	0.324	0.432	0.150	1.066	26.66%
Seat Friction	0.171	0.532	0.081	0.269	1.053	26.33%
Seating Posture	0.035	0.092	0.565	0.288	0.979	24.48%
Belt Friction	0.240	0.079	0.429	0.171	0.920	23.00%
Steering Column Angle	0.153	0.123	0.174	0.422	0.873	21.82%
Airbag Mass Flow Rate	0.195	0.060	0.295	0.200	0.750	18.76%
Seat Structure	0.042	0.011	0.517	0.039	0.609	15.24%
Knee Bolster Angle	0.031	0.068	0.237	0.232	0.568	14.19%
FE Belt Properties	0.171	0.179	0.019	0.193	0.562	14.05%
Retractor Locking Time	0.049	0.092	0.128	0.176	0.445	11.12%
Knee Bolster Properties	0.035	0.050	0.128	0.149	0.362	9.04%
Retractor Properties	0.000	0.000	0.000	0.000	0.000	0.00%



The assessment quantities for these 38 simulations were also compared with the baseline run (Figures 14 - 17) to show their variation with respect to the assumed parameters.

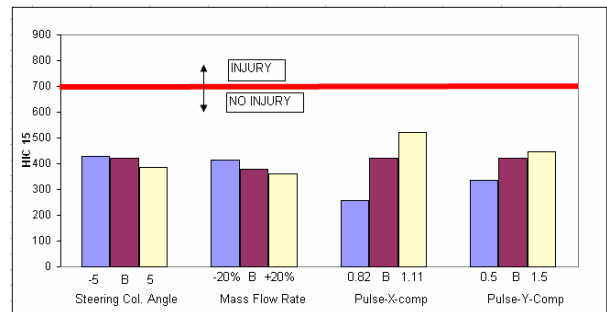
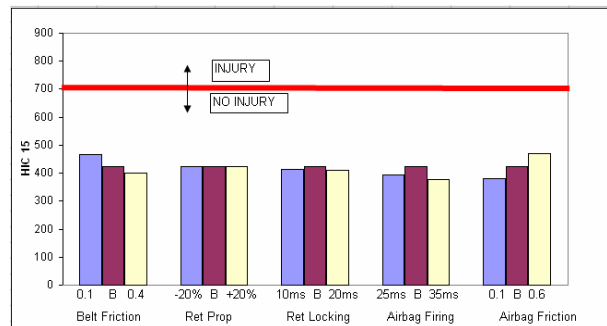
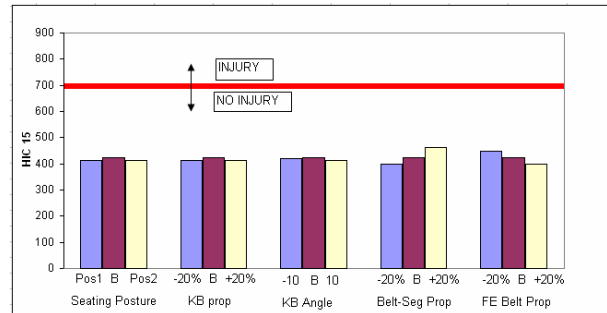
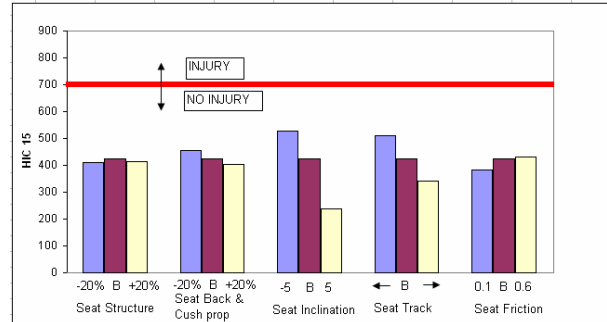


Figure 14. Plots showing the variations in HIC15.

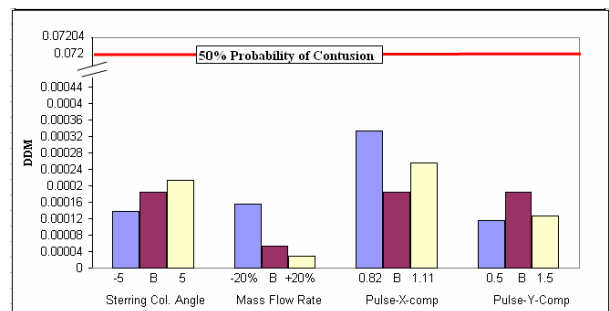
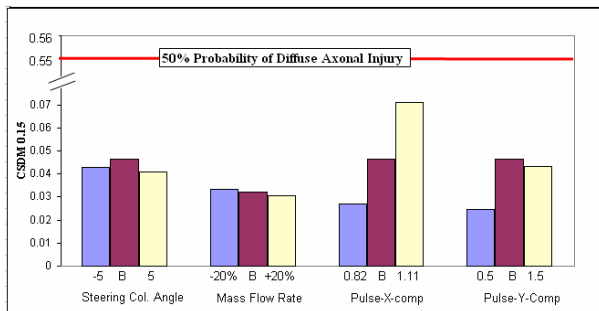
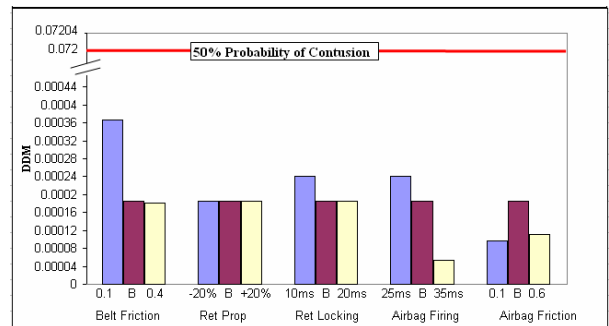
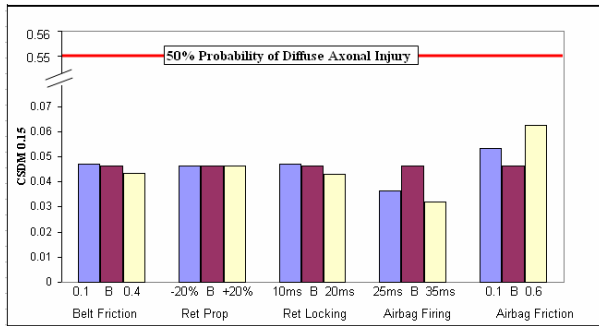
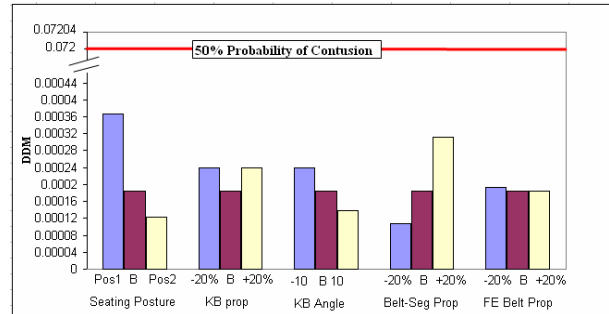
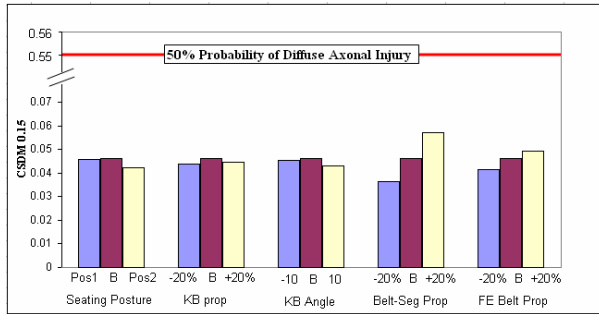
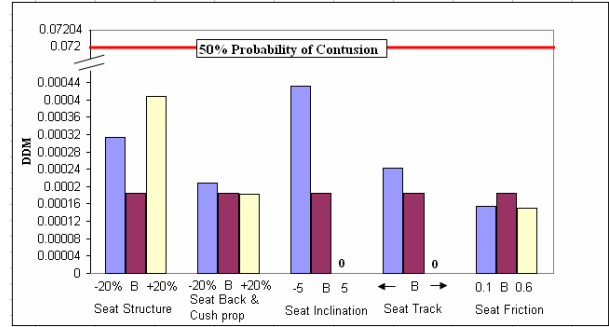
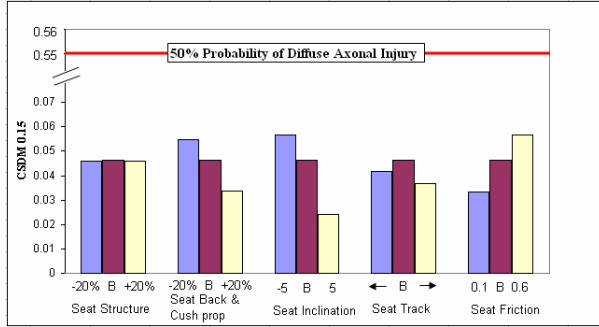


Figure 15. Plots showing the variations in CSDM.

Figure 16. Plots showing the variations in DDM.

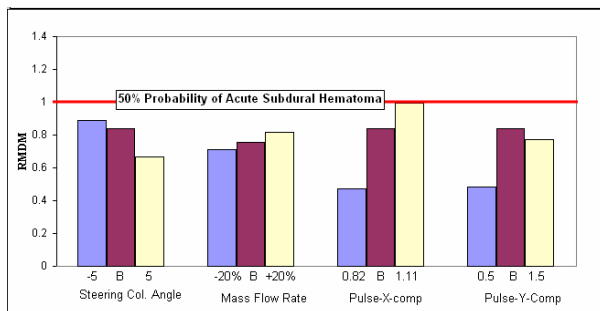
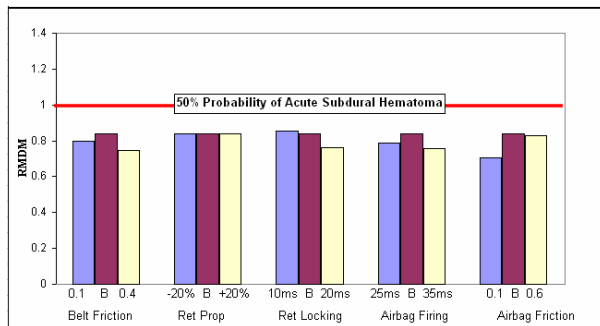
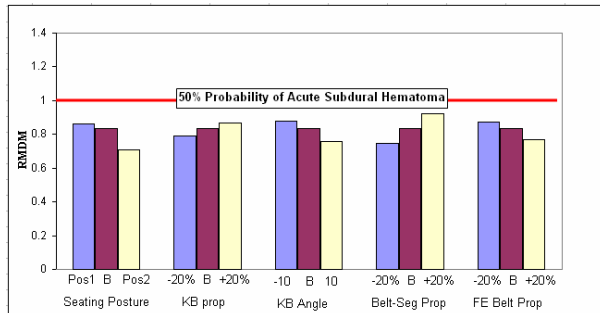
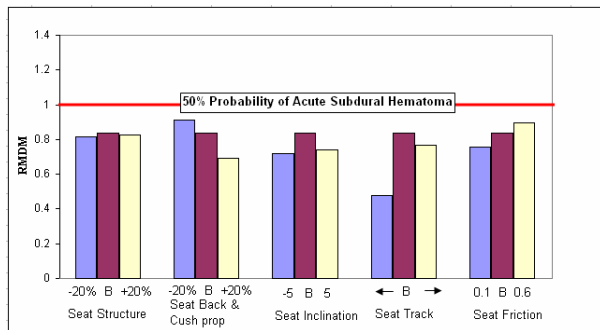


Figure 17. Plots showing the variations in RMDM.

The results (table 7 and figures 14 - 17) showed that the assessment quantities varied more with some parameters and less with other parameters. Hence from this first run we could identify the critical parameters which were: (a) Seat Track position; (b) Seat inclination; (c) Belt Friction; (d) Airbag Friction; (e) Airbag mass flow rate; (f) Airbag firing

time; (g) Crash Pulse; (h) Belt segment properties; (i) Seat back and cushion properties; (j) Seat friction; (k) Seating Posture; (l) Seat Structure properties; and (m) Steering Column Angle (Airbag deployment angle). These critical parameters were the ones that produced 25% or more change in any one of the assessment quantities. This 25% change in assessment quantities corresponded to a % effect of more than 15%.

The highest CSDM, DDM, RMDM and HIC15 obtained from the independent parametric study were 0.0709, 0.000431, 0.9958 and 526 respectively. None of the injury metrics exceeded the threshold, thus predicting “no brain injury.”

Also as part of the reduced parametric study, around 12 simulations were run (Figure 18) using some of these critical parameters while maintaining the range of these parameters and the CIREN contacts to study the cross-effect of parameters.

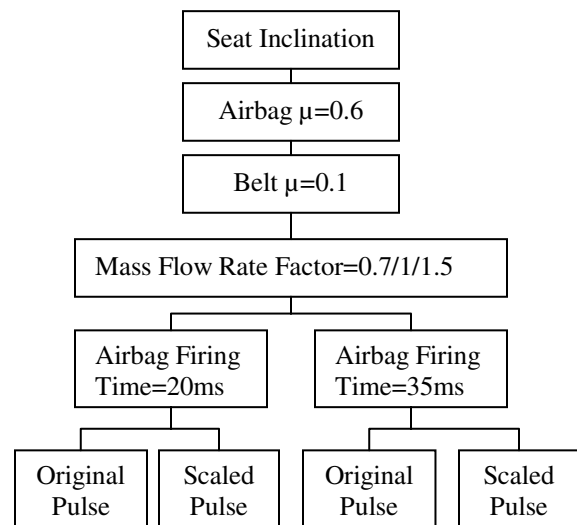


Figure 18. 12 Cross-effect simulations.

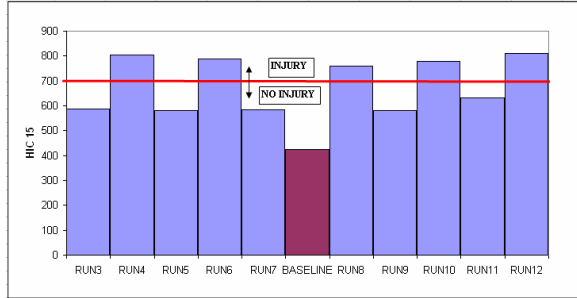
The seat inclination, airbag and belt friction coefficients used above were the ones that produced high HIC value (based on the independent parametric study). These were used in combination along with variations in mass flow rate, airbag firing time and applied pulse to see the effect on the results. Cases that violated CIREN contacts were eliminated (table 8).

Table 8.
Details of the 12 simulations

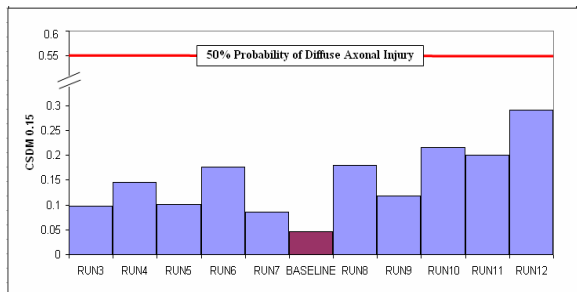
	Seat Inclination	Airbag μ	Belt μ	MFR Factor	Airbag time, ms	Pulse	Validity
RUN1	Incline 1	0.6	0.1	0.7	20	Original	×
RUN2	Incline 1	0.6	0.1	0.7	20	Scaled	×
RUN3	Incline 1	0.6	0.1	0.7	35	Original	✓
RUN4	Incline 1	0.6	0.1	0.7	35	Scaled	✓
RUN5	Incline 1	0.6	0.1	1	20	Original	✓
RUN6	Incline 1	0.6	0.1	1	20	Scaled	✓
RUN7	Incline 1	0.6	0.1	1	35	Original	✓
RUN8	Incline 1	0.6	0.1	1	35	Scaled	✓
RUN9	Incline 1	0.6	0.1	1.5	20	Original	✓
RUN10	Incline 1	0.6	0.1	1.5	20	Scaled	✓
RUN11	Incline 1	0.6	0.1	1.5	35	Original	✓
RUN12	Incline 1	0.6	0.1	1.5	35	Scaled	✓

Two cases (run1 and run2) were eliminated as they produced head-steering wheel contact, which was outside of the valid solution region.

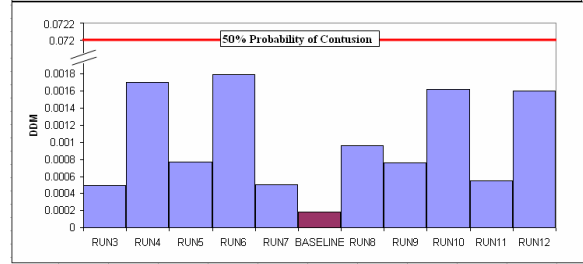
The assessment quantities HIC15, CSDM, DDM and RMDM for the valid runs were compared with the baseline run (Figure 19). The highest CSDM, DDM, RMDM and HIC15 obtained were 0.2901, 0.0018, 1.38 and 812 respectively. Even though CSDM and DDM values did not reach the 50% probability of injury limit, HIC15 and RMDM values exceeded the threshold, and thus predicted “brain injury.”



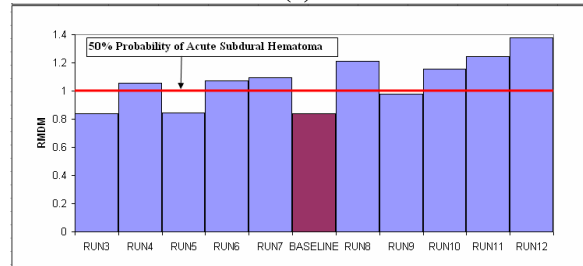
(a)



(b)



(c)



(d)

Figure 19. Plots showing (a) HIC15, (b) CSDM, (c) DDM and (d) RMDM results for the valid cross-effect simulations.

DISCUSSION

This paper shows on one hand the potential of computational tools for reconstructing real world accidents, but on the other hand the difficulty of accurately carrying out the reconstruction as a result of assumptions made due to lack of data availability.

Reconstruction of the “no brain injury” case shows that there are several parameters that have to be assumed in order to obtain a solution. Overall, 19 parameters were assumed for this case. The variability in these parameters can produce quite different results in the valid solution space, as can be seen from the variations in the assessment quantities - HIC, CSDM, DDM and RMDM.

Due to variations in the assessment quantities, one set of reconstruction parameters is not sufficient to evaluate occupant injuries, and it is imperative to identify the critical parameters affecting the results. Parametric analysis can be used to identify the main parameters influencing the occupant response.

The reduced parametric analysis carried out in this paper for the “no brain injury” case shows the process of selecting critical parameters that need to be controlled better. Overall, 14 out of 19 parameters were found to be critical. Lack of parameter control can lead to considerable changes in the injury predictions. The “no brain injury” case reconstructed in this paper went from “no injury” prediction to “injury” prediction due to introduced variability. Out

of four injury assessment quantities, two (HIC and RMDM) switched from “no injury” to “injury.” Although CSDM and DDM did not switch, they did show considerable variation in their values. Depending on the crash scenario, some or all assessment quantities may change from “no injury” to “injury” if control is not exercised.

The results indicated that crash pulse has a considerable affect on the occupant’s injuries. The crash pulse in this study was obtained using HVE, as EDR data was not available. HVE has its own limitations, insofar as the stiffness of the vehicle, which plays an important role in generating the right crash pulse, can only be defined as linear and homogenous for any given side of the vehicle. Additionally, hard spots cannot be defined. As a result the crash pulse obtained from HVE is not precise but approximate. Therefore, EDR data, if available, should be preferred to reduce the variability issues of the crash pulse.

In this study, neither full finite element nor human facet models that better define human geometry and material properties were used for any parametric analysis because of the prohibitive run times. For better reconstruction, human models should be preferred if the run time can be reduced.

All critical parameters substantially affecting reconstruction results were identified using the injury assessment quantities: HIC, CSDM, DDM and RMDM. HIC is based only on the translational accelerations, whereas the SIMon FE model is driven using both translational and angular accelerations. Hence the critical parameters were identified based on changes in both linear and angular components, which were reflected by changes in the injury metrics. Some parameters had more effect on the linear accelerations, and others had more effect on the angular accelerations, thus justifying the use of SIMon injury metrics (CSDM, DDM and RMDM) in addition to HIC for critical parameter identification.

This study only concentrated on identifying critical parameters that affected head injury criteria. These might be different for different body regions and an analysis such as the one presented in this paper can help identify those critical parameters which need to be controlled better before running the final simulation for predicting injuries.

Based on this study some general observations, not limited to the reconstructed case, may be relevant for the CIREN crash investigation team. These are:

1. If possible, CDC, Crush, PDOF and the weight of the occupants for the non-case vehicle should be listed so that a better reconstruction analysis can be carried out to generate the crash pulse.
2. An estimate of the range of variation in the measurement of delta-V, CDC, PDOF and Crush listed in CIREN should be included. Protocols could be developed to eliminate the subjectivity involved in the measurement of CDC, PDOF and Crush.
3. The distances between the seat and vehicle interior surfaces with which the occupant has contacts at different seat track positions obtained from an undamaged, exemplary vehicle should be listed. Protocols could be developed for these measurements.
4. The seat model used in the vehicle should be listed so that the properties can be taken directly from the source. If possible, the seat cushion properties should also be listed.
5. The range of seat back angle (seat inclination) and the value of the seat back angle corresponding to different positions (upright, slightly reclined, etc) obtained from an undamaged, exemplary vehicle could be listed.
6. The seat material could be included to get an idea of the friction coefficient.
7. The knee bolster inclination angle obtained from the undamaged, exemplary vehicle could be listed. If possible, the knee bolster properties (stiffness) could also be mentioned.
8. The belt system model used in the case vehicle should be listed so that the properties can be taken directly from the source, and if possible, the properties (lap/shoulder belt properties, retractor characteristics, etc).
9. The airbag model used should be included so details can be obtained from the source.
10. The range of steering column angle and the value of the angle corresponding to the different positions of the steering column (full up, center, etc., as mentioned in CIREN) obtained from an undamaged, exemplary vehicle could be listed.
11. More details could be mentioned on the seating posture. For example, if the person is asleep, what posture would generate the occupant-vehicle contacts being seen for that case.

The information based on these observations, if made available, may help control the critical parameters and help in a better reconstruction analysis.

Future work may involve, among other things, reconstructing more real world crashes with brain injuries, expanding the parameter matrix, carrying out a more detailed parametric analysis and using human FE or facet models for better occupant simulations.

CONCLUSION

The reconstruction methodology used in this paper and demonstrated by reconstructing a real world crash with “no brain injuries” shows that there are several parameters that have to be assumed during crash reconstruction. The variability in these parameters can change the predicted injury output significantly. The paper indicates the importance of carrying out a sensitivity analysis, identifying the critical parameters and better controlling them before attempting to predict injuries. It was shown that injury predictions for a simulated case can go from “no injury” to “injury” if the analysis is not carried out properly. In essence, sensitivity analysis and parameter control are important steps to improving the injury predictive capabilities of any reconstruction process.

ACKNOWLEDGEMENT

The authors would like to thank Mr. Mark Scarboro of NHTSA and Lauren Shook of GESAC, Inc for their help with CIREN, Mr. Terry Day and Mr. Joe Canova of Engineering Dynamics Corporation and Mr. Wesley Grimes of Collision Engineering Associates, Inc for their Insights on HVE, MADYMO technical support and Aida Barsan-Anelli of ISSI, Inc for their helpful comments on MADYMO.

REFERENCES

- [1] Franklyn, M., Fildes, B., Zhang, L., Yang, K. and Sparke, L. 2005. “Analysis of Finite Element Models for Head Injury Investigation: Reconstruction of Four Real-world Impacts.” Stapp Car Crash Journal, Vol.49, November: 1-32
- [2] Marjoux, D., Baumgartner, D., Deck, C., Willinger, R. 2006. “Head Injury Prediction Capability of the HIC, HIP, SIMon and ULP Criteria” IRCOBI conference, September: 143-157

[3] Takhounts, E.G., Eppinger, R.H., Campbell, J.Q., Tannous, R.E., Power, E.D., Shook, L.S. 2003 “On the Development of SIMon Finite Element Head Model” Stapp Car Crash Journal, Vol. 47, October: 107-133.

[4] Crash Injury Research and Engineering Network (CIREN), National Highway Traffic Safety Administration, Department of Transportation Washington, D.C., United States.

[5] Human-Vehicle-Environment (HVE), Version 5.10, March 2006, Engineering Dynamics Corp.

[6] MADYMO, Version 6.2, 2004, TNO, Delft, The Netherlands.

[7] SIMon Software, Version 3.051, June 2004, National Highway Traffic Safety Administration, Department of Transportation, Washington, D.C, United States.

[8] Day, T.D., 1999, “An Overview of the EDSMAC4 Collision Simulation Model”, SAE 1999-01-0102, Engineering Dynamics Corp.

[9] HVE User’s manual, Version 5, January 2006, Engineering Dynamics Corp.

[10] Validation of Several Reconstruction and Simulation Models in the HVE Scientific Visualization Environment,” SAE 960891, Engineering Dynamics Corp., Beaverton, OR, 1996

[11] Grimes, W., Lee, F.D. 2000 “The Importance of Crash Pulse Data When Analyzing Occupant Kinematics Using Simulations,” HVE white paper

[12] Vehicle Crash Test Reports, Vehicle Database, National Highway Traffic Safety Administration, Department of Transportation, Washington, D.C., United States.

[13] MADYMO Application manual, Version 6.2, 2004, TNO, Delft, The Netherlands.

[14] Bosch, M., Brandse, J., Lemmen, P., Neale, M., Couper, G., Frampton, R. 2005. “Development and evaluation of Smart Restraints: EC PRISM” 5th European MADYMO User Conference, Cambridge, September: 62-71

AN EXPERIMENTAL ANALYSIS OF THE ABDOMINAL PRESSURE OF THE PREGNANT OCCUPANTS DURING AUTOMOTIVE COLLISION USING AF5 PREGNANT DUMMY

Yasuki Motozawa

Honda R&D Co., Ltd. / Department of Legal Medicine, Dokkyo Medical University School of Medicine
Japan

Masahito Hitosugi

Shogo Tokudome

Department of Legal Medicine, Dokkyo Medical University School of Medicine

Japan

Paper Number 07-0094

ABSTRACT

Previously the correlation between the fetal outcome and the injury severity of the pregnant women in automotive collisions were addressed by the authors using the data of the insurance refunds in Japan. The study showed that injury severity scores did not differ significantly between the pregnant occupants with spontaneous abortion and with healthy newborn although the scores were significantly higher in the pregnant occupants whose neonate died. The authors have indicated the prediction of negative fetal outcome with anatomical injury severity of the mothers. Therefore in this study, the abdominal pressure of the pregnant occupant during collisions was focused as a possible predictor of fetal outcome. A series of sled experiment was conducted using the pregnant dummy which represents the anthropometry of the pregnant woman with the gestational age of 30 weeks. The MAMA-2B (Maternal Anthropometric Measurement Apparatus, version 2B) pregnant dummy based on the Hybrid-3 AF5th percentile dummy developed by First Technology Safety Systems Inc. and UMTRI (University of Michigan Transportation Research Institute) was used for the experiments. The values of the pressure during rear impact in a passenger vehicle were measured and compared. The seating posture of the dummy in the experiments was determined by the measurement of pregnant volunteers in an actual passenger vehicle. From the results of the experiments the dominant factor of the change of the abdominal pressure was discussed.

INTRODUCTION

According to Connolly et al., 6–7% of pregnant women suffer some kind of traumatic injuries during pregnancy; approximately two-thirds of such injuries reportedly occur during traffic accidents.(1) Klinich et al., also suggested that 1.3 million women in later terms of pregnancy are involved in traffic accidents in the United States every year, and an estimated 1,500–5,000 abortions or stillbirths occur annually.(2) To reduce traffic accident fatalities, fetal

safety might become one of an important issue in the future.

The authors have already examined the relationship between traffic injuries to pregnant women and the associated fetal outcomes. (3-4) In those reports the circumstances of accidents and the injuries to mothers and fetuses in cases in which claims for payment were made under automobile insurance policies were analyzed. The number of insurance claims made was broken down by what the pregnant women were doing when they were injured, and the results show that the largest number, at 46%, were driving automobiles. However, from the study the difficulty was indicated in the prediction of negative fetal outcome with anatomical injury severity of the mothers. Injury severity scores did not differ significantly between the pregnant occupants with spontaneous abortion and with healthy newborn although the scores were significantly higher in the pregnant occupants whose neonate died. Therefore, clarification of the actual circumstances under which pregnant female drivers are involved in accidents, together with the injury mechanisms during slight impacts as well as high-energy impacts, are needed.

In this study, to investigate the correlation between the injury mechanisms of pregnant female drivers and the associated fetal outcomes, a series of rear impact sled tests were conducted by using a pregnant dummy.

METHOD

The authors of this research contend there is a strong likelihood that fetal death or abortion takes place when pregnant women are involved in traffic accidents in which external force is applied to their abdomens. (3-4) However, so far as it is known, the injury mechanisms for pregnant women and fetuses in traffic accidents have not yet been completely explained.

Needless to say, the greatest difference between pregnant women and non-pregnant women in terms of anthropometry is the forward protrusion of the

abdomen. In collisions, there is forward displacement of the abdomen, resulting in likelihood of contact with interior parts of the automobile. Therefore, ascertaining the driving posture adopted by pregnant women, as well as the differences in their physiques, would be useful in determining the injury mechanisms. Duma et al. assessed pregnant passengers using finite element model simulation to estimate the stress exerted on their abdomens. (4) This study focused on the severe injuries due to frontal collisions with relatively high energy. However, the seating posture applied in the study was based on the measurements in the interior buck of University of Michigan Transportation Research Institute (UMTRI), would be somewhat different from those of actual vehicle. Further more, the authors have been unable to uncover any studies addressing the measurement of the responses of pregnant drivers during slight rear impacts.

Therefore in this study, to investigate the injury mechanisms of pregnant female drivers during rear impacts, a series of rear impact sled tests were conducted by using a pregnant dummy. The responses of impacts and kinematics of the dummy were examined. The seating posture of the dummy in the experiments was determined by the measurement of pregnant volunteers in an actual passenger vehicle. An actual automobile was used to determine the seat adjustment positions used by pregnant female drivers.

Measurement of seating posture

To determine the seat adjustment positions used by pregnant female drivers, the measurement of pregnant volunteers is conducted using an actual passenger vehicle. The gestational age of the pregnant drivers studied in the present research was set at about 30 weeks. An open call for volunteers was issued, and 20 pregnant women who drive a car regularly, were chosen as subjects for the research. The subjects who participated in this research were given full verbal and written explanations of the purpose and method of measurement in advance by a physician, after which the subjects signed their consent in writing. A typical mid-size passenger sedan was used for measurements. The subjects sat in the driver's seat. After receiving an explanation on how to adjust the seat, the subjects themselves adjusted the seat so that the seating posture was close to their normal ones as much as possible. Then the measurements were taken. The results were following.

Basic information: The mean age of the subjects was 30.0 ± 3.0 years, with height of 160.8 ± 6.6 cm, weight

of 60.2 ± 6.0 kg, gestational age of 31.4 ± 1.9 weeks, and an abdominal circumference of 87.1 ± 4.5 cm.

Seat adjustment position: The seat slide position was adjusted to 103 ± 49 mm from the full-forward position, with the reclining angle of $7.1 \pm 3.0^\circ$ from the full-forward position.

Position relative to the steering wheel: The horizontal distance from the lower rim of the steering wheel to the abdomen was 146 ± 56 mm.

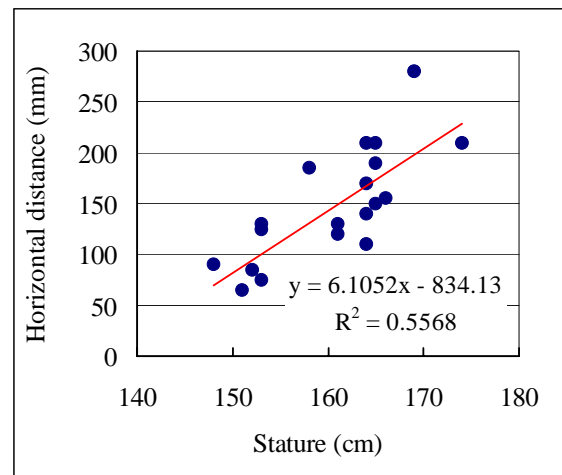


Figure 1. Horizontal distance between the lower rim of the steering wheel and the abdomen as a function of stature

Figure 1 shows the relationship between the horizontal distance from the lower rim of the steering wheel to the abdomen and the height of the subjects. This shows a somewhat strong correlation with the coefficient of 0.72.

Seating posture: The position of the head, the shoulders, and the pelvis were measured relative to the vehicle's reference points. The measurement points on the head, the shoulder and the pelvis were the center of the external acoustic opening, the center of the shoulder joint (the mid-point of the greater and lesser tubercles of the humerus) and the head of the femur, respectively.

Figure 2 shows a graph that represents the positions of the head, pelvis and shoulders of subjects using the horizontal(X) and vertical (Z) coordinates. The shape of the plotted lines in the graph represents a simplified form of the posture of the upper torso for each subject.

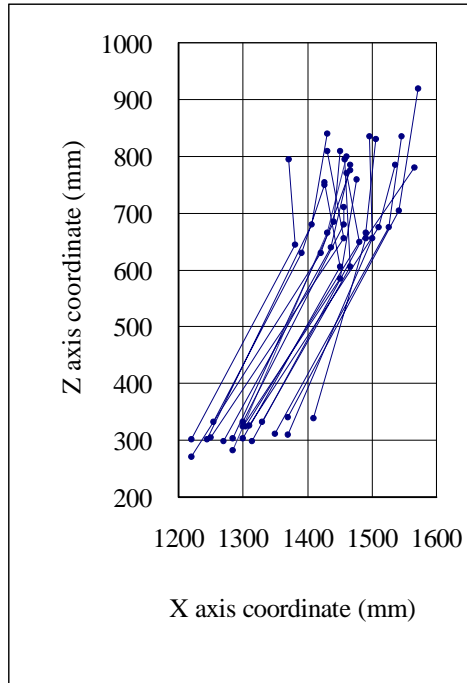


Figure 2. Seating postures represented by the hip, shoulder and head coordinates

Determination of the seating posture of the dummy

From the results of the measurement which shows somewhat strong correlation between the horizontal distance from the lower rim of the steering wheel to the abdomen and the height of the subjects, a verification of the second impact of the pregnant driver using AF5th percentile dummy was deemed appropriate. To determine the seating posture of the dummy from the results, the mean values of the measurements of seven chosen subjects whose anthropometric values are similar to that of AF5th percentile were obtained. The mean age of the chosen subjects was 28.7 ± 2.4 years, with height of 152.6 ± 3.0 cm, weight of 54.7 ± 2.8 kg, gestational age of 30.8 ± 1.0 weeks, and an abdominal circumference of 86.4 ± 4.2 cm. The mean seat slide position was 65 ± 30 mm from the full-forward position, with the reclining angle $7.4 \pm 3.0^\circ$ from the full-forward position (torso angle of 13°). The horizontal distance from the lower rim of the steering wheel to the abdomen was 107 ± 4.2 mm. From the mean values of the chosen subjects, the seating posture of the dummy was determined as the seat slide position of 70mm from the full-forward position with the reclining angle of 8° , taking minimal pitch of seat adjusters into account.

Dummy

The dummy which was used in these experiments is the Maternal Anthropometric Measurement Apparatus, version 2B (MAMA-2B) pregnant dummy developed by First Technology Safety Systems and UMTRI in 2001. Although this is only one pregnant dummy commercially available, development is still on-going at right moment. The latest version which is called as the enhanced MAMA-2B, equipped with a pair of infra-red type chest deflection measurement devices, was used in this study. The history of the development of this dummy was already described in the literatures of Rupp et al. (6) and Ziao. (7) This dummy was developed based on the Hybrid-3 AF5th percentile dummy, by modifying the pelvis and the ribcage, to enable to install the bladder made of silicone rubber representing the uterus of 30 weeks of gestation. The bladder is approximately spherical in shape, approximately 200mm in diameter. Two pressure sensors are installed in the anterior and posterior surfaces of the inside of the bladder respectively. The bladder is filled with the water of 3000ml in use.

Sled pulse

To represent the status in which a pregnant driver encounters slight rear impact in a passenger vehicle, the sled pulse applied in the experiments was the trapezoid waveform, with the delta V of 24kph (mean acceleration of 6.5G), which is defined by the test protocol of Folksam, a representative third party assessment on the rear impacts injuries.

Test setup

Figure 3 shows test setup. The Instron servo sled apparatus was used in the experiments. The seat, the seatbelt, the steering wheel, and the steering column installed in the setup were the same components and in the same relative position as the vehicle used in the measurements of the seating posture. Experiments with seatbelt and without seatbelt were both conducted and compared. The airbag and the pretensioner were not activated in all experiments.

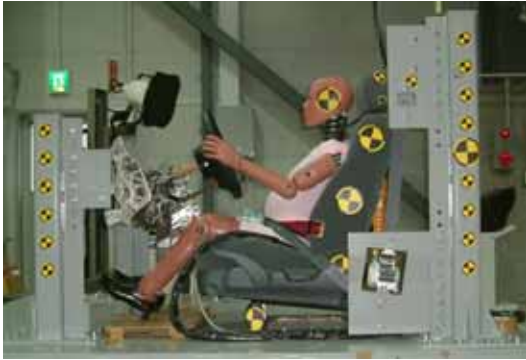
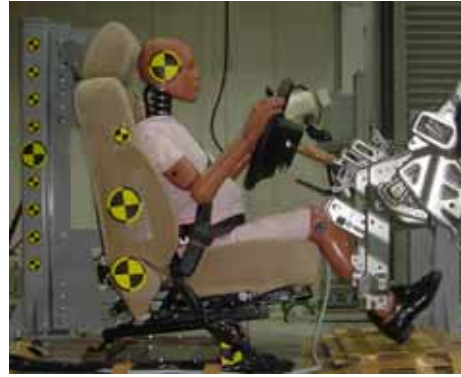


Figure3. Sled setup for the experiments

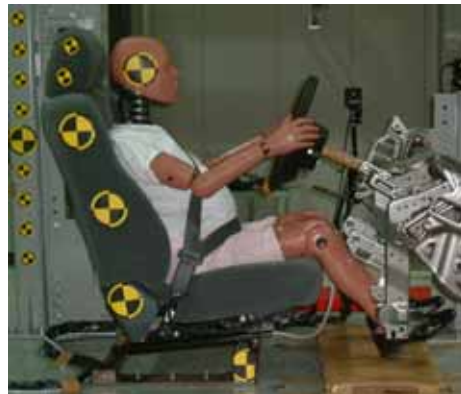
Test matrix

First of all, experiments applying the dummy setting based on the FMVSS frontal impact test protocol were conducted, to compare the kinematics to that of the dummy setting based on the measurement of volunteers. According to the FMVSS protocol for the Hybrid-3 AF5th percentile dummy, seat slide position was determined from the full-forward position or the position at which the lower extremities of the dummy are closest to the dashboard of the testing vehicle unless they do not contact to it. In case of the vehicle used in the volunteer measurements, the position determined by this method is the full-forward position. However, the MAMA-2B could not sit this position due to interference of the abdominal protrusion with the lower rim of the steering wheel. Therefore, the position behind 30 mm from the full-forward position was determined as the dummy setting based on the FMVSS protocol concept (hereafter the MVSS setting).

As noted previously, the dummy setting based on the measurements of volunteers (hereafter the volunteers setting) was determined as the seat slide position of 70mm from the full-forward position with the reclining angle of 8°. The referential horizontal distance from the lower rim of the steering wheel to the abdomen was determined as 100mm. Figure 4 shows both settings. Table 1 shows the matrix of the status of the seatbelt and the dummy settings in the experiments.



MVSS setting



Volunteer setting

Figure 4. Dummy settings

Table 1. Matrix of the experiments

	Dummy setting	Seatbelt setting
Experiment 1	MVSS	Wear
Experiment 2	MVSS	Unwear
Experiment 3	Volunteers	Wear
Experiment 4	Volunteers	Unwear

RESULTS

Figure 5 shows the time histories of the acceleration applied to the sled setup. Figure 6 and 7 shows the time histories of the acceleration of the pelvis of the dummy. Figure 8 shows the time histories of the displacement of the pelvis and the chest of the dummy relative to the sled setup in the horizontal(X) axis. Figure 9 shows the time histories of the pressure of the abdominal bladder of the dummy.

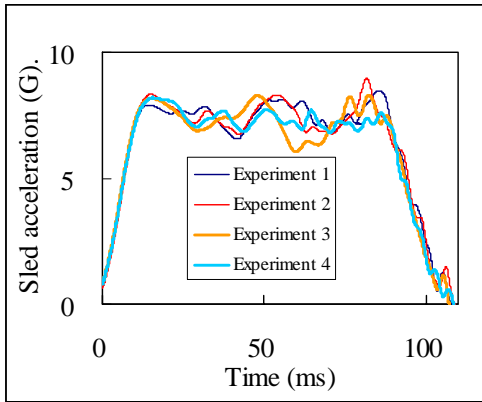


Figure 5. Time histories of the acceleration applied to the sled setup

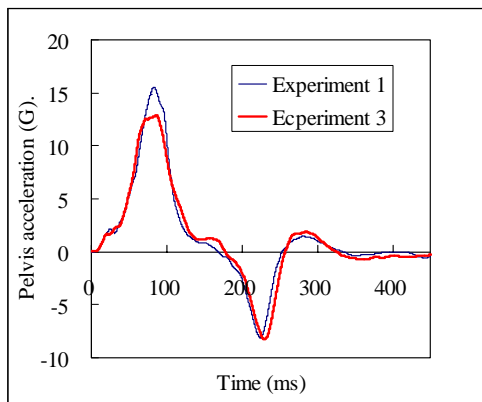


Figure 6. Time histories of the acceleration of the pelvis of the dummy (with seatbelt)

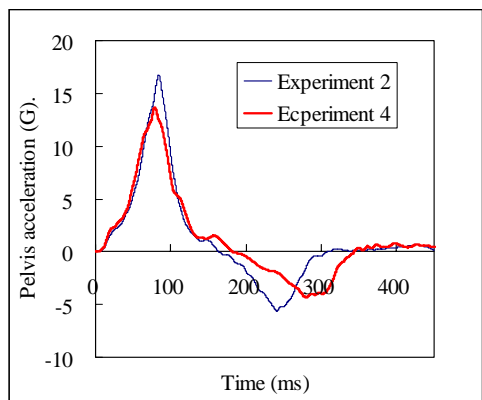


Figure 7. Time histories of the acceleration of the pelvis of the dummy (without seatbelt)

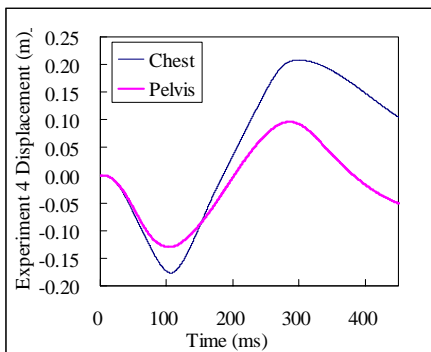
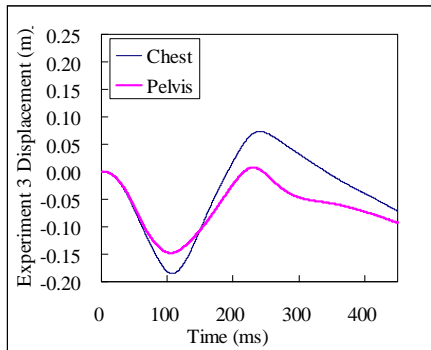
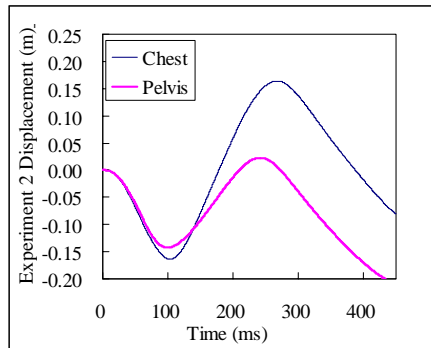
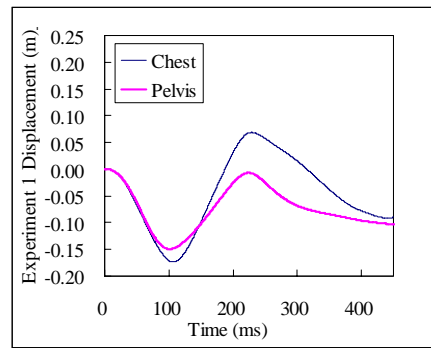


Figure 8. Time histories of the displacement of the pelvis and the chest of the dummy relative to the sled setup

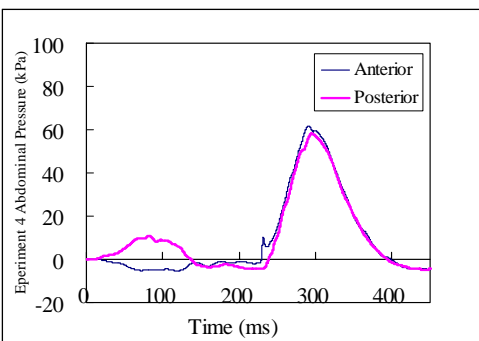
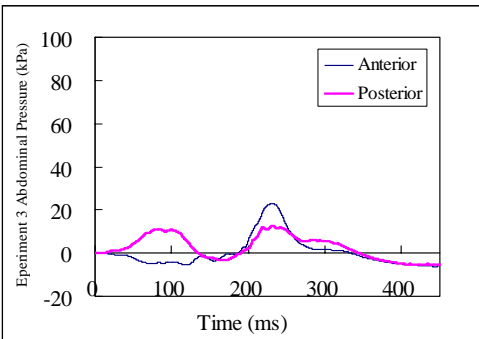
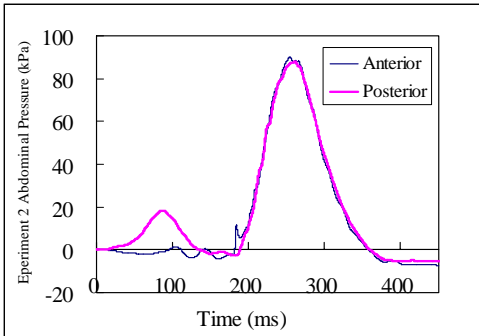
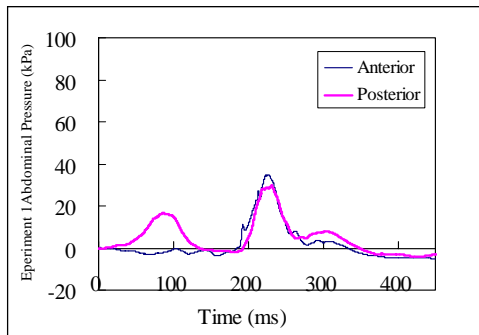


Figure 9. Time histories of the pressure of the abdominal bladder of the dummy

In the experiment 1 (MVSS setting with seatbelt), after the backward movement of approximately 150mm during 100ms from the start of the impact, the dummy commenced moving forward due to rebound. After that, the superior part of abdomen came in contact with the steering wheel at the time of 190ms.

In the experiment 2 (MVSS setting without seatbelt), the backward movement similar to that of the experiment 1 was observed. However, the abdomen came in contact at the time of 180ms, the chest and the head came in contact with the steering wheel at the time of 250ms from the start of the impact.

In the experiment 3 (volunteers setting with seatbelt), the dummy moved forward due to rebound, however, it moved downward in the most forward position of the movement. The contact between the dummy and the steering wheel was not observed finally.

In the experiment 4 (volunteers setting without seatbelt), the abdomen came in contact at the time of 230ms, however, the chest and the head did not come in contact with the steering wheel finally.

DISCUSSION

The results of the measurement showed correlation between the horizontal distance from the steering wheel to the abdomen and the height of the subjects. Furthermore, a verification of the second impact was conducted using AF5th percentile dummy.

As noted previously, the MAMA-2B was developed based on the Hybrid-3 AF5th percentile dummy, which is basically for the measurement apparatus for the injury indices during frontal impact. However, this study focused on the entire kinematics of the pregnant drivers especially the second impact due to rebound. Therefore, the examination using the MAMA-2B was deemed appropriate.

The seat slide position of the MVSS setting is forward in 40mm from that of the volunteers setting. Between the two settings, there was a difference of 100mm in the horizontal distance from the steering wheel to the abdomen and of 8° in the reclining angle. The difference in the contact of the abdomen was observed in the comparison between the experiment 1 and 3. The differences in the kinematics of the upper torso, the contact of the head and the chest were observed in the comparison between the experiment 2 and 4. The results showed that the kinematics and the second impacts were affected by

the seating posture of the dummy; the appropriate setting methodology for the pregnant dummy will be an issue to be discussed.

In the time history of the posterior part of the abdominal pressure, the primary peak value was observed at the time of 100ms from the start of the impact i.e. in the most backward position of the dummy during impact. This response showed good match with the time history of the acceleration of the pelvis. Furthermore, the secondary peak value was observed at the time of 200ms where the dummy came in contact with the steering wheel. The anterior part of the abdominal pressure, on the other hand, indicated slight negative value during backward movement of the dummy. The peak value was observed at the time where the dummy came in contact with the steering wheel as well as the posterior part of the abdominal pressure. From these observations, in the mechanism of the primary peak value, the inertial loading was dominant, and in the mechanism of the secondary peak value, the abdominal compression by the steering wheel and the lumbar spine was dominant. In the experiment, it was also observed that the steering lower rim came in contact to the inferior sternum, i.e. the fundus of the bladder. Previously, Rupp et al. derived the correlation between the peak anterior part of the abdominal pressure and the adverse fetal outcome with actual case analysis and frontal impact experiments using the MAMA-2B. (6) In the study, because only the anterior part of the abdominal pressure was evaluated, the experiments were conducted using rigid seat, consequently the lower steering rim stably compressed the abdomen of the dummy on the umbilicus level. Therefore in this study, we further measured the posterior part of the abdominal pressure to precisely evaluate both direct and inertial loading of the abdomen.

CONCLUSION

Based on the seating posture determined by the measurement of pregnant volunteers in an actual passenger vehicle, a series of rear impact sled tests were conducted by using a pregnant dummy representing 30 weeks of gestation. The responses and its kinematics were examined.

From the results of the measurement showed somewhat strong correlation between the horizontal distance from the lower rim of the steering wheel to the abdomen and the height of the pregnant drivers.

The kinematics and the second impacts were affected by the difference in the seating posture in the experiments both with and without seat belt.

The time history of the anterior part of the abdominal pressure showed a peak value due to the second impact loading, however, the posterior part of the abdominal pressure showed primary peak value due to inertial loading and secondary peak value due to the second impact loading.

REFERENCES

- [1] Connolly AM, et al.1997. "Trauma and Pregnancy." *Am J Perinatol*, Vol. 14, pp.331-336.
- [2] Klinich D, et al. (1999) Challenges in Frontal Crash Protection of Pregnant Drivers based on Anthropometric Considerations," SAE Paper No.1999-01-0711.
- [3] Hitosugi M, et al. 2006. "Traffic Injuries of the pregnant women and fetal or neonatal outcomes." *Forensic Science International*, Vol. 159, pp. 51-54.
- [4] Hitosugi M, et al. 2007. "The Benefits of Seatbelt Use in Pregnant Drivers." *Forensic Science International*, accepted, in press.
- [5] Duma SM, et al. 2005. "A Computational Model of the Pregnant Occupant: Effects of Restraint Usage and Occupant Position of Fatal Injury Risk." 19th ESV Conf., Paper No.05-0367.
- [6] Rupp JD, et al. 2001. "Development and Testing of a Prototype Pregnant Abdomen for the Small-Female Hybrid III ATD." *Stapp Car Crash Journal*, Vol. 45, November: 2001.
- [7] Zhao Y, et al. 2006. "Enhancement and Evaluation of a Small Female Hybrid III Pregnant Dummy." *Proceedings of International IRCOBI Conference 2001*.

DEVELOPMENT OF A GENERALIZED LINEAR SKULL FRACTURE CRITERION

Philemon Chan, Zi Lu and Paul Rigby

L-3/Jaycor

USA

Erik Takhounts

NHTSA

USA

Jiangyue Zhang, Narayan Yoganandan and Frank Pintar

Medical College of Wisconsin

USA

Paper Number 07-0227

ABSTRACT

This work develops a generalized linear skull fracture criterion, the skull fracture correlate, SFC, applicable to impacts by flat targets on the skull in any angle. The SFC is the averaged acceleration over the HIC15 time interval based on data obtained from Hybrid-III headform impact tests. For 15% or less probability of skull fracture the threshold is $SFC < 124$ g, with a 95% confidence band of $96 < SFC < 144$ g. The SFC correlation is established based on logistic regression against an extensive set of post mortem human specimen (PMHS) data. The biomechanical basis of SFC is validated by its good correlation with skull strain calculated using an anthropomorphic finite element model of the skull. This work is an extension and refinement of recent research results including the use of newly obtained PMHS data combined with historical data. Finite element model simulations were performed for all PMHS tests conducted for data comparison and statistical analysis.

INTRODUCTION

At present, in Europe, Japan, Australia, and the United States, a single Hybrid-III based Head Injury Criterion (HIC), is the standard for protection against generalized head injury in a frontal car crash. Current NCAP side impact crash tests use a side impact dummy (Part 572.F) with a Hybrid-III head/neck complex. Recently, biomechanically based multi-component criteria have been developed to separately protect against DAI, SDH, and brain contusions [Takhounts, et al., 2003]. The development of multi-mode injury criteria has the potential to advance the science of head protection.

Previous work by Hodgson and Thomas et al [1971 and 1973] has provided historical skull fracture data for various impact speeds, target compliances, and surface curvatures. In their tests, embalmed whole body Post Mortem Human Specimens (PMHS) were placed on a hinged pallet pivoted at the feet of the specimen, with the head extending over the edge. Known head weights varied between 3.2 and 5.4 kg with an average of 4.7 kg, which is close to the 4.5-kg weight of the 50th percentile male Hybrid-III headform. Impacts against flat targets, cylinders with large radius of curvature, and rubber targets produced primarily linear skull fracture while impact against rigid hemispheres and rigid cylindrical targets with small radius of curvature produced comminuted fracture. Impact speeds varied within $\pm 20\%$ of the theoretical free drop value with a standard deviation of 8%.

Recently, a considerable amount of new skull fracture data have been obtained by the Medical College of Wisconsin (MCW) under the sponsorship of the US National Highway Traffic Safety Administration (NHTSA) using unembalmed free head drops against targets similar to those used by Hodgson and Thomas, including cylindrical and flat targets. Compared to the hinged drop test method of Hodgson and Thomas, free drops of isolated head specimens would provide more accurate specification of impact conditions and allow for higher impact speeds. The softest target used by Hodgson and Thomas was durometer 60 (D60) neoprene. The new tests extended the target compliance to softer materials.

We have developed the linear skull fracture correlate (SFC) risk factor for skull fracture based on biomechanical understanding of the underlying injury

mechanism [Vander Vorst et al, 2003 and 2004]. In the case of the human skull, tensile strain in the compact tables is an indicator of fracture [Wood, 1971]. Skull fracture depends on both the geometry and compliance of the impacting target material and the weight of the head. Together, these factors determine the stress and strain distributions generated in the skull. Fracture occurs when the ultimate strain is exceeded. However, skull strain data at the location of fracture is difficult to measure in an impact test but it can be calculated with a finite element model (FEM) using the PMHS test conditions as input. Furthermore, it is desirable that a risk factor can be computed using data obtained from an anthropomorphic test device (ATD), such as the Hybrid-III headform.

Vander Vorst et al [2003] first developed the biomechanically-based linear skull fracture correlate for frontal impact using PMHS data mostly from Hodgson and Thomas [1971, 1973] and some recent data from the Medical College of Wisconsin for correlation with Hybrid-III headform tests and finite element model simulations. In this early work, FEM simulations were performed using an idealized spherical head model with a uniform skull layer of inner table, diploe and outer table. SFC was established as the averaged headform acceleration over the HIC time interval. The main finding from this first work was that the skull strain calculated from the FEM, the fracture data and SFC all correlated well with one another with well defined confidence bands, hence validating the biofidelity of SFC.

Further work was presented by [Vander Vorst et al, 2004] in expanding the validity of SFC to lateral impact using more newly obtained PMHS data. Different from the earlier work, the work presented in 2004 by Vander Vorst et al used an anthropomorphic FEM of the head with the calculated strain again showing good correlation with PMHS data and SFC. Since then, even more new PMHS data have been obtained that continue to validate the skull fracture data correlations with FEM-calculated strain and SFC. The significance of using the SFC is that it can be computed easily using data obtained from the Hybrid-III headform that can be implemented in standard tests.

The objective of this work is to develop a generalized linear skull fracture criterion for frontal and lateral impacts. The main effort is to refine and bolster the skull strain and SFC correlations with fracture data by pooling all the PMHS data together for analysis.

All frontal drop tests were simulated again using the same anthropomorphic FEM that was used for the lateral impact studies by [Vander Vorst et al, 2004]. The results will lead to skull fracture criteria that are based on the most comprehensive dataset known to date.

METHODS

Frontal impact test cases exhibiting primarily linear skull fracture were extracted from the Hodgson and Thomas [1971 and 1973] data set. Tests against slender rods and hemispheres were excluded since they resulted in depressed comminuted fractures instead of the linear fractures caused by the flat and 5-cm diameter cylindrical targets. Anomalous cases, as reported by Hodgson and Thomas, were also excluded. The analysis of the data from Hodgson and Thomas has been presented in detail previously by Vander Vorst et al [2003].

New lateral impact tests were conducted at the Medical College of Wisconsin using isolated PMHS head specimens. They are hereafter referred to as the MCW tests. A total of thirty-three unembalmed specimens free from HIV and Hepatitis B and C were tested. The intracranial contents were replaced with Sylgard Gel, except for four of the specimens which were left as is. The Institutional Review Board of the Medical College of Wisconsin approved the protocol. Pretest radiographs and computed tomography (CT) images of the specimens were obtained. Lateral impact tests were conducted by dropping the specimens against either flat or cylinder targets at velocities ranging from 2 to 10 m/s. Figure 1 shows a schematic diagram of the test set up. The inferior-superior axis of the specimen was situated at a 10-degree angle with respect to the target, and the anterior-posterior axis was parallel with the target. The orientation of the PMHS head for lateral impacts was such that the same anatomical point, at the temporo-parietal junction, would always be impacted. Because of individual anatomical differences, the skull had to be slightly tilted one way or the other by a few degrees to obtain the orientation. We chose a head alignment angle that is known to produce linear skull fractures that are representative of what occurs in the real world [Yoganandan et al, 1995]

Each specimen was impacted at increasing heights with a single impact at each height, and radiographs were obtained between drops. Impact force histories were recorded using a six-axis load cell. Signals were recorded using a digital data acquisition system (DTS

Technologies, Seal Beach, CA) at a sampling frequency of 12.5 kHz and filtered according to SAE Channel Class 1000 specifications [SAE, 1998]. Testing of a specimen was terminated when fracture was detected or the load cell limit was reached. The specimens underwent CT scanning after the final impact. Again, details of the analysis of the MCW data were previously presented by Vander Vorst et al [2004].

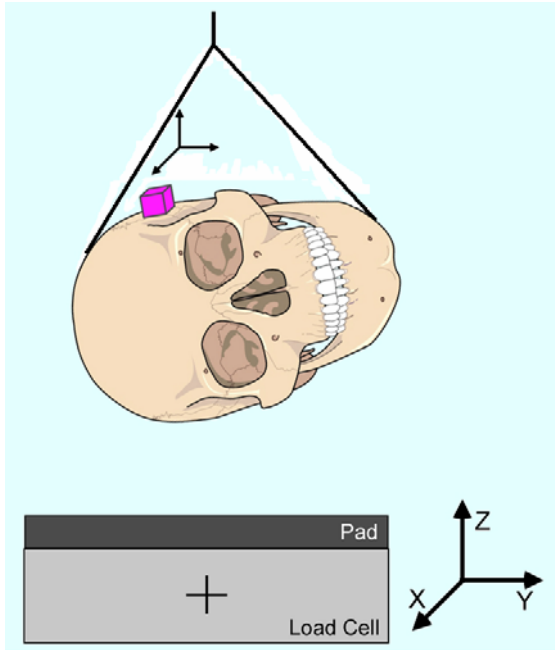


Figure 1. MCW test set up.

Drop tests using a 50th percentile male Hybrid-III headform were conducted corresponding to all PMHS test conditions for calculation of SFC [Vander Vorst et al, 2003 and 2004]. Three repeated drops were made for each impact condition. Repeated tests were checked for consistency and computed risk factors were averaged for statistical analysis. SFC is the averaged acceleration over the HIC time interval ΔT_{HIC}

$$SFC = \frac{\Delta V_{HIC}}{\Delta T_{HIC}} \quad (1)$$

where ΔV_{HIC} is the averaged velocity. For the present work the HIC15 time interval was used but due to the short impact duration (few milliseconds) involved the use of HIC36 time interval would not change the SFC results.

Simulations were carried out for all PMHS tests using the same anthropomorphic FEM presented by

[Vander Vorst et al., 2004]. All frontal drops that were previously simulated using the spherical model were simulated again using the anthropomorphic FEM. All new lateral drop tests performed since 2004 were also simulated. The model was composed of 24,000 elements resolving the outer and inner tables, diploe, brain, scalp, and face. The mass of the baseline model was 4.54 kg. The skull components were modeled using fully integrated thick shells and the brain, scalp, and face were modeled with fully integrated bricks. Since this model was based on CT imaging of a PMHS, the skull shape and thickness are anatomically correct. The thickness of the compact skull tables was set to be 1.3 mm uniformly, as they were too thin to be resolved from the CT scan. The 1.3-mm value was based on measurements of photographic cross-sections from the Visible Man project [National Library of Medicine, 2000]. The properties of the biological materials were taken from the open literature and previously presented [Vander Vorst et al., 2003]. All finite element model simulations were performed using Version 9.70 of LS-Dyna3d software [Livermore Software Technology Corporation, 2003].

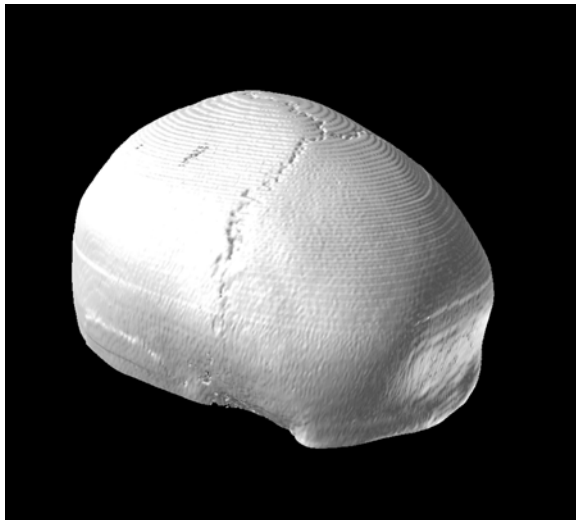
For each PMHS drop test, the SFC calculated from the corresponding Hybrid-III test and the peak skull tensile strain from the inner and outer tables calculated from the finite element model along with the fracture outcomes of the test were placed in a database for statistical analysis. To account for varying head weights, SFC was normalized by the factor $MH/4.54$ kg, where MH is the actual mass of the test specimen in kg [Vander Vorst et al., 2003]. The data were analyzed by logistic regression [Hosmer and Lemeshow, 1989] using the longitudinal, population-averaged model with presumed failures [Zeger and Lian, 1986; Chan et al., 2001]. The data were treated as longitudinal since each specimen proceeded through a test matrix from low to high drop heights with repeated testing. Hence, the specimen responses were not independent between tests. When a specimen fractured at a given drop height, it was presumed to fail at all higher drop heights. All statistical computations were carried out using the STATA software [Stata, 1999].

Statistical analysis was carried out by pooling the PMHS data from the Hodgson and Thomas and MCW tests together. Analysis of the fracture outcomes and FEM results were carried out to evaluate the differences between impacts against cylindrical and flat targets for frontal and lateral drops. As will be presented later, the generalized linear fracture correlations with SFC and skull strain

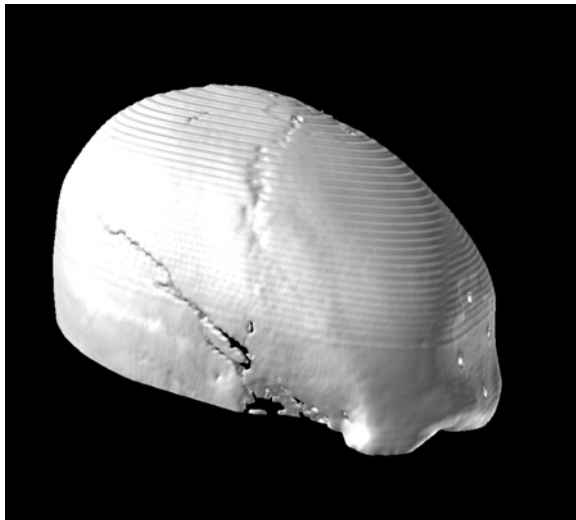
were established by using only the data obtained from the flat target tests.

RESULTS

The Hodgson and Thomas [1971 and 1973] tests contributed all the frontal drop data and some lateral drop data used for the present work. The MCW tests contributed the majority of the lateral drop data. Figure 2 shows an example of the three-dimensional reconstruction of the CT data before and after a test that resulted in fracture as performed by MCW.



(a) Pretest scan



(b) Posttest scan showing fracture

Figure 2. Reconstruction of CT scans.

Frontal vs. Lateral PMHS Skull Fracture

Analysis of the selected outcomes obtained from tests conducted at the same drop height against the same target material suggests that frontal drops are more likely to cause fracture than lateral drops (Figure 3). For the D90 cylindrical target, a 48-in drop height resulted in 100% fracture for frontal impact vs. only 50% for lateral impact, and it needed 72-in drop height for the lateral impact to result in 100% fracture (Figure 3a). For the D90 flat target, the frontal impact resulted in 100% fracture at 36-in drop height while the lateral impact resulted only in 33%, and it also needed 72-in drop height for the lateral impact to result in 100% fracture (Figure 3b). For the drops against the rigid flat target, 100% fracture was observed for the frontal impact at 10-in drop height while only 45% was observed for the lateral impact, and it needed 15-in drop height for the lateral impact to produce 100% fracture (Figure 3c). For the drop outcomes against D90 cylindrical and flat targets shown in Figures 3a and b, respectively, the data for frontal drops are from Hodgson and Thomas while the data for lateral drops are from MCW, while the rigid target data shown in Figure 3c are solely from Hodgson and Thomas.

Based on their own PMHS test results, Hodgson and Thomas had commented that “The head is strongest in respect to fracture in the rear, side and front in that order” [Hodgson and Thomas et al, 1971]. Because of biological variability for PMHS tests, logistic regression was performed to fully determine the difference between the frontal and lateral skull fracture resistance by pooling all the data together with confidence band determined. Statistical correlations of the pooled dataset with FEM results and SFC were established as will be presented.

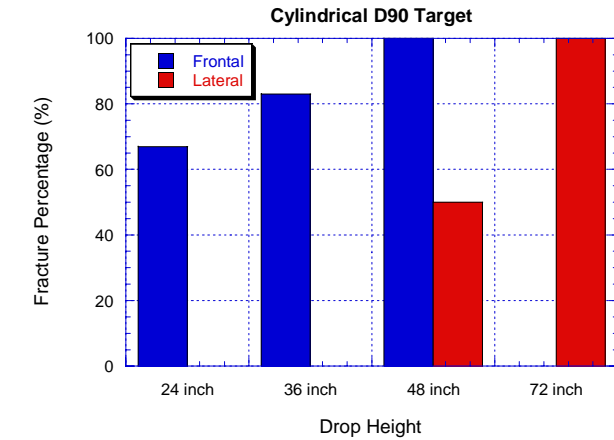
FEM Skull Strain

The pattern of the outer table skull strain calculated from the FEM shows a peak compressive (negative) strain occurring at the impact site with the tensile (positive) strain peaking nearby but away from the impact site as illustrated in Figure 4. This pattern holds true for frontal as well as lateral impacts against cylindrical and flat targets over the full range of target compliance tested. The contact between the head and target creates a large concentrated compression at the contact point (blue) while the skull bending creates large tensile strains in a nearby region (red) as expected from the perspective of bending mechanism (Figures 4a-d).

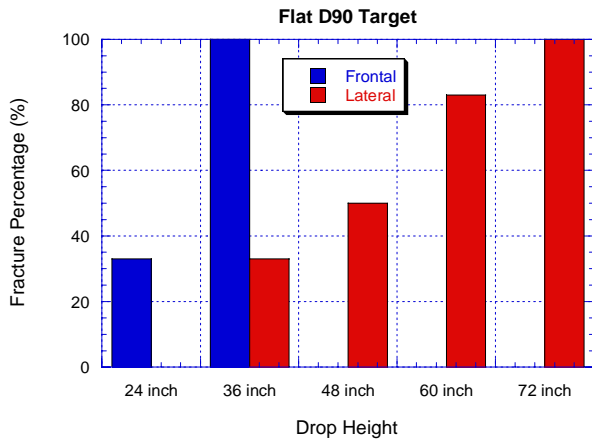
For comparison, the corresponding principal strain patterns in the inner table are shown in Figure 5. Compared to the outer table (Figure 4), the compressive (negative) strains in the inner table are one to two orders of magnitude smaller and they occur around the rim of the inner table (Figure 5). The location of the peak tensile strain in the inner table is not too far from that in the outer table (Figures 4-5). We use the maximum tensile strain from the inner and outer table as indicator for skull fracture and data correlations. For the case shown in Figures 4c and 5c, the location of the peak skull tensile strain (red) in the outer and inner table as calculated from the finite element model occurs in close proximity to the location of the observed fracture (Figure 2b), which is consistent with the skull fracture mechanism proposed by [Wood, 1971].

Skull Fracture Correlations

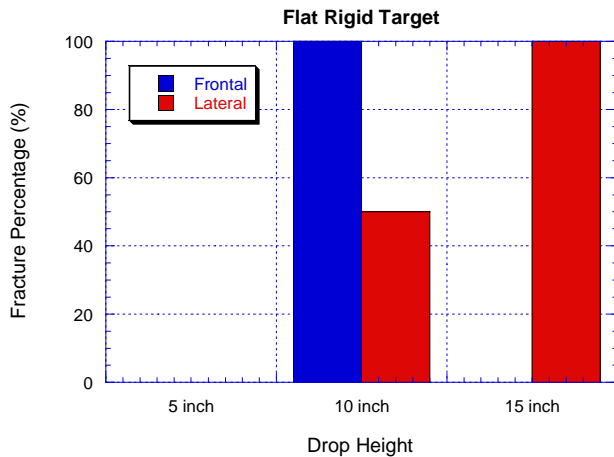
Logistic regression of the combined dataset suggest the frontal drops will have a higher risk of fracture than the lateral drops, and both frontal and lateral correlations have good confidence bands (Figures 6a-b). Based on the mean correlation, a skull strain of 0.2 would result in 52% of fracture for frontal drops but only 13% for lateral drops (Figures 6a-b). This seems to be consistent with the trend of fracture outcomes shown in Figure 3. Nonetheless, a strain-fracture correlation with a fairly good confidence band can be obtained for the combined frontal and lateral drop dataset (Figure 6c). The SFC correlation with fracture data also shows a similar trend as the strain correlation (Figure 7). Figures 7a-b suggest frontal drops would result in a higher probability of fracture than lateral drops. Again, a combined SFC correlation with fracture can still be obtained with a good confidence band (Figure 7c).



(a) D90 neoprene cylindrical target

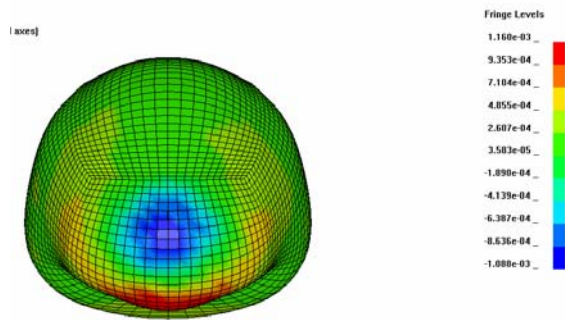


(b) D90 neoprene flat target

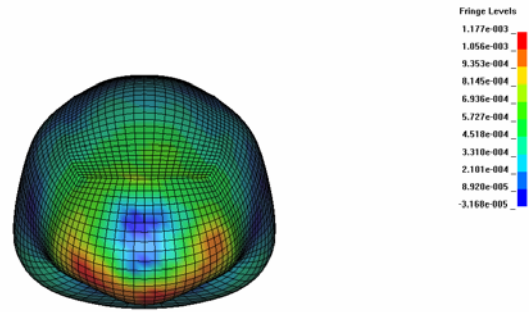


(c) Rigid flat target

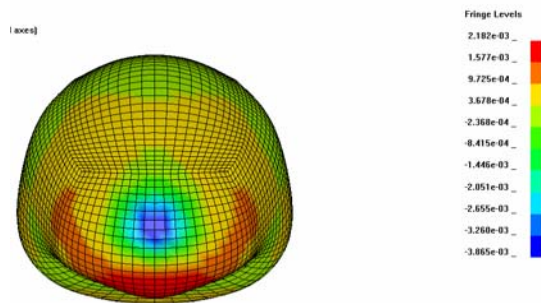
Figure 3 Skull fracture data comparison.



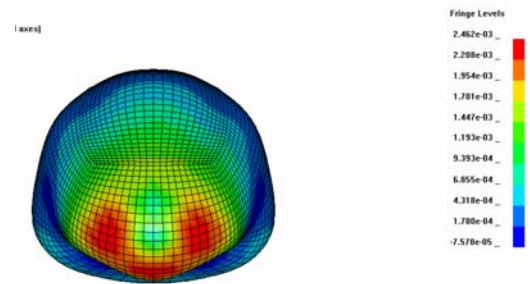
(a) Frontal impact, D40 flat target



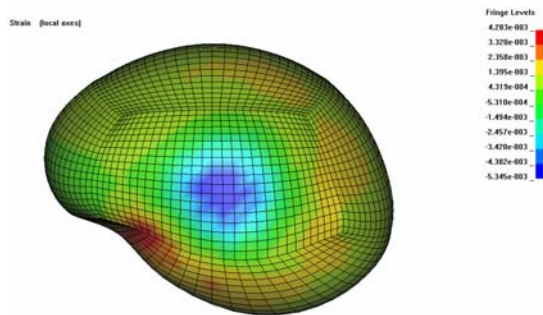
(a) Frontal impact, D40 flat target



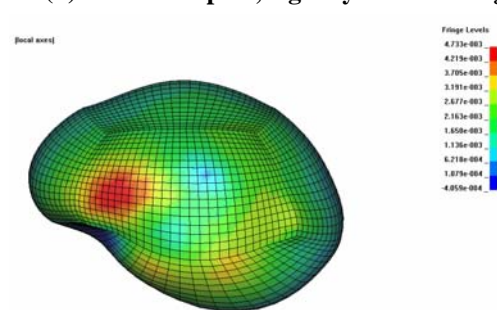
(b) Frontal impact, rigid cylinder target



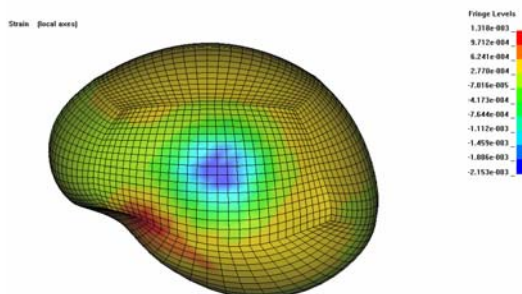
(b) Frontal impact, rigid cylindrical target



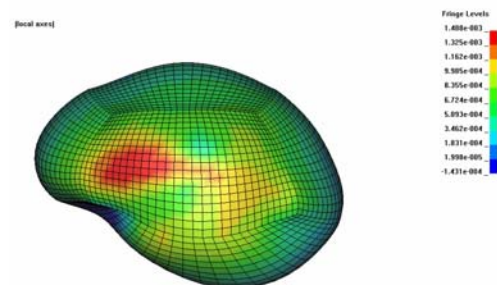
(c) Lateral impact, D90 flat target



(c) Lateral impact, D90 flat target



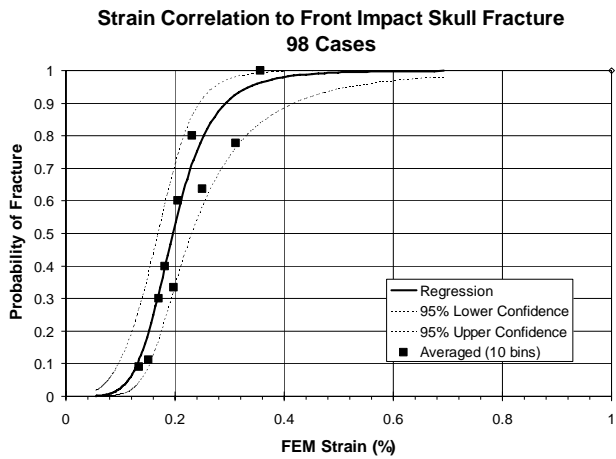
(d) Lateral impact, rigid cylinder target



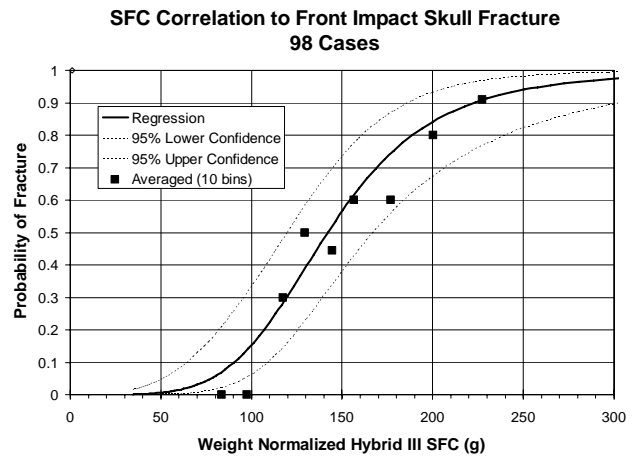
(d) Lateral impact, rigid cylindrical target

Figure 4. Principal strain in outer table.

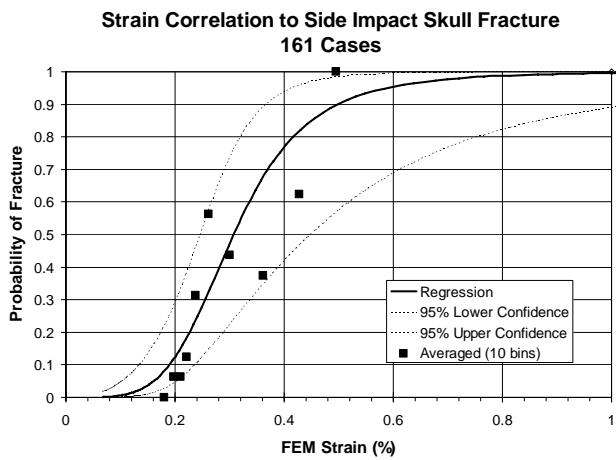
Figure 5. Principal strain in inner table.



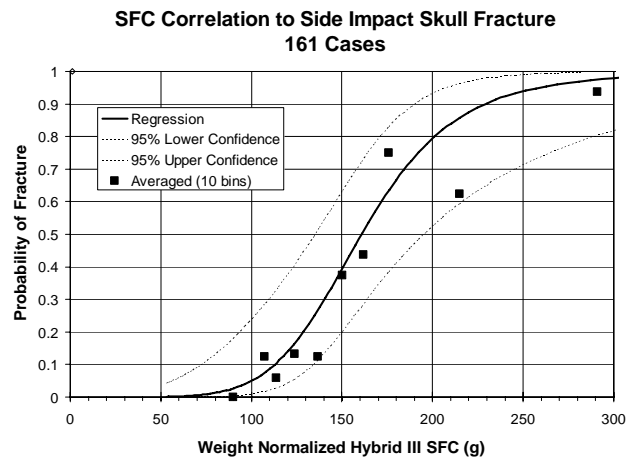
(a) Frontal drop



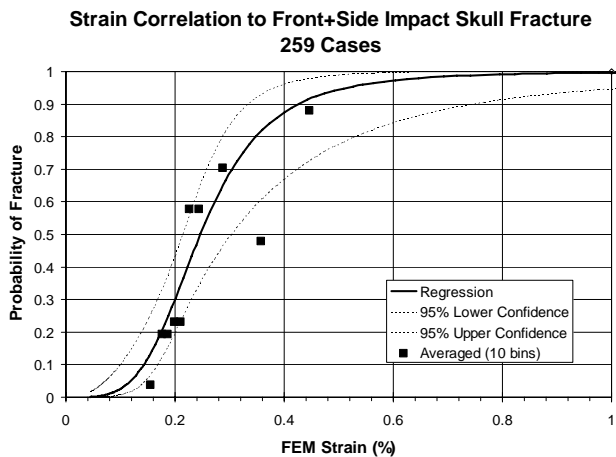
(a) Frontal drop



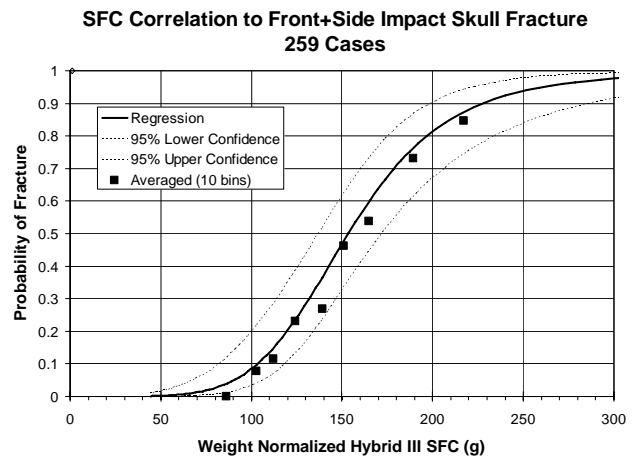
(b) Lateral drop



(b) Lateral drop



(c) Combined frontal and lateral correlation



(c) Combined frontal and lateral correlation

Figure 6. Strain correlation with skull fracture data for all tests.

Figure 7. SFC correlation with skull fracture data for all tests.

The SFC correlation with strain suggests that there is a different fracture trend between the impacts against cylindrical and flat targets. Figure 8 shows that a good linear correlation between SFC and strain is established, especially when only the data for the flat plate target tests are considered. As shown in Figure 8, the data from the cylindrical target tests for both frontal and lateral drops deviate from the linear correlation for the flat target data quite significantly. If only the data for the flat plate targets are used, SFC correlates well with strain with the coefficient of R^2 of 0.95 (Fig. 8).

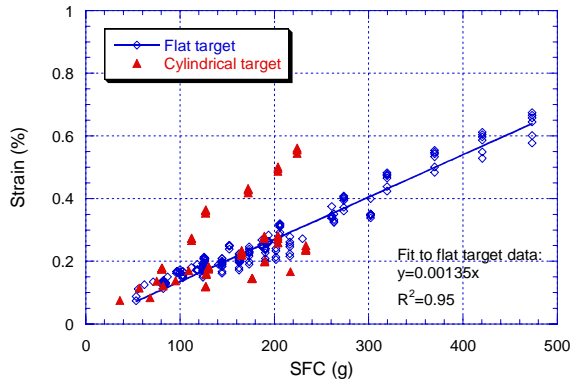


Figure 8. SFC correlation with strain.

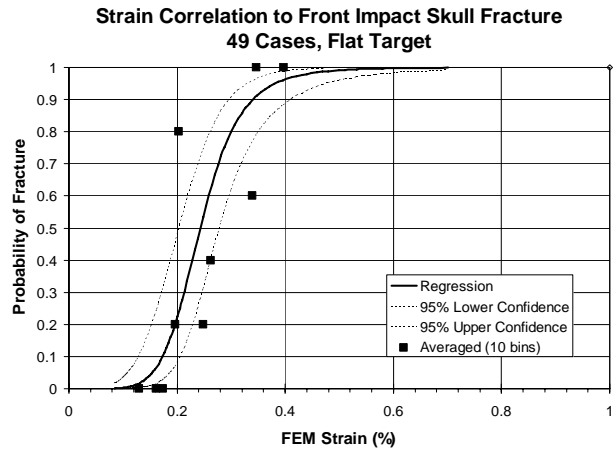
Therefore, to establish a generalized correlation for linear fracture, we only used the flat target test data (Figure 9). Based on the flat target data, Figures 9a-b show that the strain-fracture correlations for the frontal and lateral drops are quite close to each other with the frontal correlation slightly higher than the lateral one, but the confidence band for the lateral correlation is wider. The strain-fracture correlation for the frontal impact is

$$\ln\left(\frac{P}{1-P}\right) = 6.51 * \ln(strain) + 9.21 \quad (2)$$

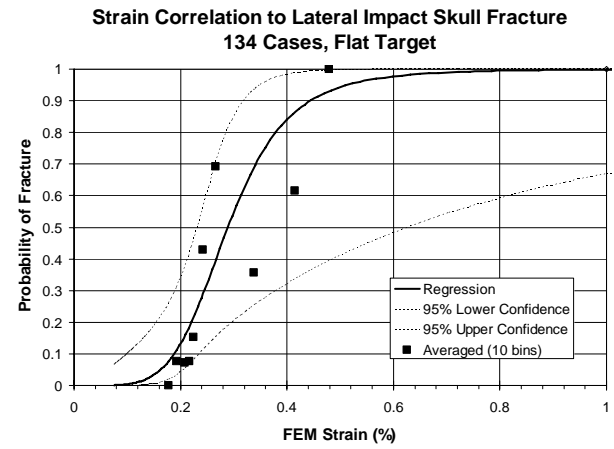
and for lateral impact,

$$\ln\left(\frac{P}{1-P}\right) = 5.12 * \ln(strain) + 6.36 \quad (3)$$

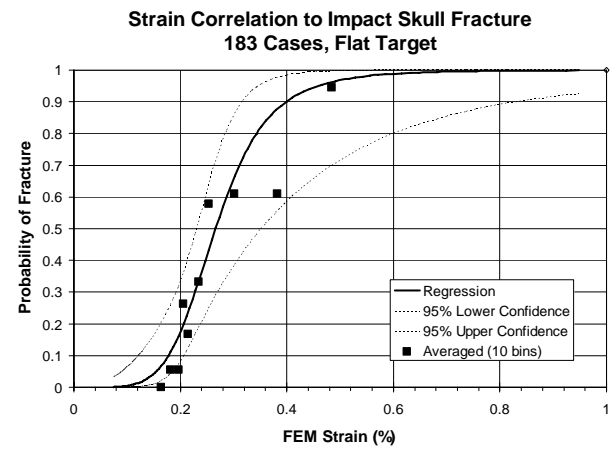
where P is the probability of fracture. The strain of 0.2% corresponds to 22% mean probability of fracture for frontal impact vs. 13% for lateral impact (Eq. 2 vs. 3 and Figure 9a vs. 9b). The difference in



(a) Frontal impact



(b) Lateral impact



(c) Frontal and lateral data combined

Figure 9. Skull strain correlation with fracture data for flat targets.

the strain-fracture correlation between frontal and lateral drops is small in terms of statistics, namely, the frontal correlation falls within the 95% confidence band of the lateral correlation (Figures 9a and b).

A generalized correlation with a good confidence band is obtained by combining the frontal and lateral drop data for the flat targets (Figure 9c). The generalized strain-fracture correlation for both frontal and lateral impacts is

$$\ln\left(\frac{P}{1-P}\right) = 5.43 * \ln(\text{strain}) + 7.19 \quad (4)$$

The strain of 0.2% corresponds to 18% mean probability of fracture.

Using only the flat target data, the SFC correlations with fracture are shown in Figure 10. For frontal impact, the SFC correlation is

$$\ln\left(\frac{P}{1-P}\right) = 8.98 * \ln(SFC) - 45.32 \quad (5)$$

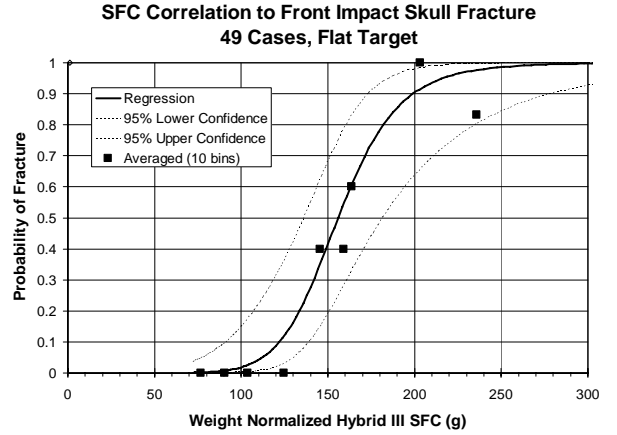
and for lateral impact,

$$\ln\left(\frac{P}{1-P}\right) = 5.76 * \ln(SFC) - 29.59 \quad (6)$$

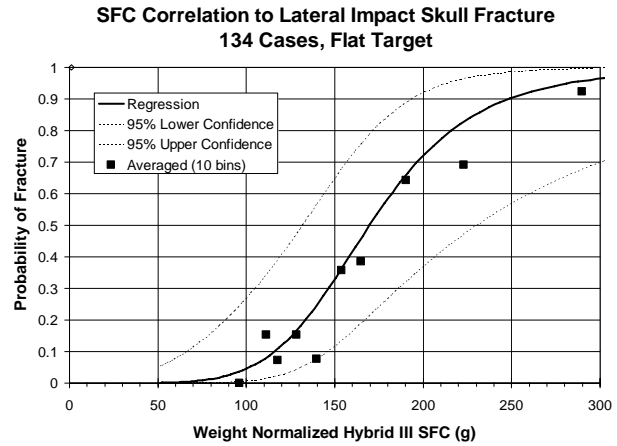
The mean SFC correlations also show frontal impacts giving slightly higher risk of skull fracture (Figure 10a vs. 10b) consistent with the strain-fracture correlations (Figure 9a vs. 9b). SFC of 150 g corresponds to 42% mean probability of fracture for frontal impact vs. 33% for lateral impact (Eq. 5 vs. 6 and Figure 10a vs. 10b).

It should also be noted that the difference in the SFC-fracture correlations between frontal and lateral drops against flat targets is small in terms of statistics as it can be seen that their 95% confidence bands overlap each other (Figures 10a-b). Combining the frontal and lateral data together, a generalized SFC correlation for linear skull fracture becomes

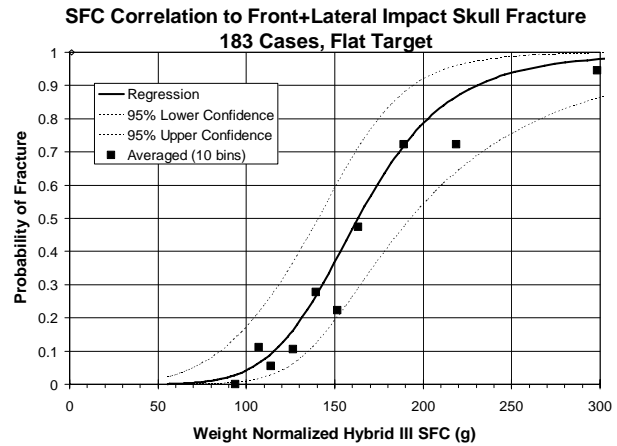
$$\ln\left(\frac{P}{1-P}\right) = 6.39 * \ln(SFC) - 32.53 \quad (7)$$



(a) Frontal impact



(b) Lateral impact



(c) Frontal and lateral data combined

Figure 10. SFC correlation with fracture data for flat targets.

The confidence band of the generalized SFC regression is well behaved (Figure 10c). The SFC of 150 g corresponds to 37% mean probability of fracture. The 15% probability of generalized skull fracture, SFC_{15} , occurs at

$$SFC_{15} = 124\text{g} \quad (8)$$

with a 95% confidence band of (Figure 10c)

$$96 < SFC_{15} < 144\text{g} \quad (9)$$

It should be mentioned that the generalized SFC_{15} of 124g is slightly higher than the previously reported value of 120 g [Vander Vorst et al, 2004], while the new 95% confidence band can be considered comparable to the previous result of $73 < SFC_{15} < 149\text{g}$ for lateral impact and $96 < SFC_{15} < 133\text{g}$ for frontal impact.

DISCUSSION

By pooling the flat target data from frontal and lateral drops together, a generalized SFC is established (Eq. 7), and its biofidelity is validated against peak skull tensile strain calculated using the FEM. This generalized SFC is very close to the separate frontal and lateral impact correlations, with all 95% confidence bands overlapping each other (Figure 10). The use of the generalized SFC should be adequate since in real impact situations, it is impossible to determine or predict the impact angle accurately. The refined generalized SFC threshold for 15% mean probability of fracture is 124 g, which is very close to the previously estimated value of 120 g. The present result is based on correlation with over 30% more PMHS data samples than before.

The main reason why SFC correlates well with skull fracture data is that the effects of target compliance and contact area are well captured by SFC. Details of those findings have been previously presented [Vander Vorst et al, 2003, 2004]. In contrast, previous findings have shown HIC correlates poorly with skull fracture data because the target compliance and contact area effects are not well captured by HIC [Vander Vorst et al, 2003, 2004].

The hard nature of the cylindrical targets used for the PMHS tests may have exaggerated the difference in fracture risk between frontal and lateral drops. Note that the cylindrical targets used for the frontal and lateral drops were of D90 and rigid nature. The full range of target compliance was not used for the tests

with cylindrical targets. More future work is recommended to determine when focal or comminuted fracture begins, or when linear fracture does not apply.

The use of finite element model simulations will play a key role in improving the generalized skull fracture criteria because the injury mechanism can be studied rigorously using the model. Only through its good correlation with the FEM peak skull strain, can we establish the biomechanical basis of SFC. However, the peak skull strain may still not be the best risk factor that can be derived from the FEM simulations. We hypothesize that an improved risk factor that is more fracture mechanics-based than just the peak tensile strain can be developed using the FEM that will truly bring the frontal and lateral fracture correlations together, including the incorporation of the cylindrical target data. It is foreseeable that the generalized skull fracture criterion should be FEM-based. To accomplish that thin-film instrumentation placed on the headform is needed to measure the skull surface pressure distribution as input to the FEM for fracture prediction without the need for modeling the impacting target.

For the present work, the effects of biological variability on the correlations are probably still not fully captured. FEM simulations were not carried out using specimen-specific models, and only the 50th percentile Hybrid-III headform was used to collect data for all the PMHS drop tests. It is known that there is considerable variation in the skull thickness between head specimens, and it will also require much higher computational resolution to resolve these details that are actually very important for fracture predictions. Specimen mass was matched between the test specimen, the FEM, and SFC. Mass scaling may be inadequate for resolving geometrical and structural details. These effects are recognized as part of the limitations of the present work. It will be valuable to construct specimen-specific FEMs for simulation with comparison to the actual fracture data outcome. The FEM used did not involve a fracture material model. The present work is still mostly based on statistical correlation of FEM results with ATD and PMHS test outcomes with limited detailed comparison of simulation results with posttest CT data.

Another limitation of this work is that the generalized criteria developed were validated against flat target impact-induced, linear skull fracture data. Other fracture types, such as focal fractures, were not considered. It is worth mentioning that a fairly large

dataset, perhaps the most extensive to date with over 183 drops, has been used to establish the generalized skull fracture correlations.

CONCLUSION

A generalized injury criterion SFC, the average acceleration over the HIC time interval, is established for the flat target impact-induced, linear skull fracture for crashworthiness assessment. Its biomechanical basis is demonstrated by its good correlation with the skull strain regardless of impact locations or various target compliances. The criterion that the probability of skull fracture is less than 15% is $SFC_{15} < 124$ g.

ACKNOWLEDGMENTS

This research effort was sponsored by the National Highway Traffic Safety Administration, US Department of Transportation through a Joint Cooperative Research Agreement with the US Army Medical Research and Materiel Command under contract W81XWH-06-C-0051.

REFERENCES

Bandak, F.A. and Eppinger, R.H. 1994. "A Three-Dimensional Finite Element Analysis of the Human Brain under Combined Rotational and Translational Accelerations," SAE paper 942215, 38th Stapp Car Crash Proceedings, p. 279

Bandak, F.A. and Vander Vorst, M.J., Stuhmiller, L.M., Mlakar, P.F., Chilton, W.E., and Stuhmiller, J.H. 1995. "An Imaging-Based Computational and Experimental Study of Skull Fracture: Finite Element Model Development," *J. Neurotrauma*, 12(4): 679-688.

Chan, P.C., Ho., K.H., Kan, K.K., and Stuhmiller, J.H. 2001. "Evaluation of Impulse Noise Criteria Using Human Volunteer Data," *Journal of the Acoustical Society of America*, 110(4): 1967-1975.

Hodgson, V.R. and Thomas, L.M. 1971. "Breaking Strength of the Skull vs. Impact Surface Curvature," DOT HS-800 583, Contract No. FH-11-7609, Final Report.

Hodgson, Voigt R. and Thomas, L. Murray. 1973. "Breaking Strength of the Human Skull vs. Impact Surface Curvature," Report DOT HS-801002, National Technical Information Service, Springfield, Virginia.

Hosmer, D. and Lemeshow, S. *Applied Logistic Regression*, John Wiley & Sons, New York; 1989.

Johnson, K.L. (1985), *Contact Mechanics*, Cambridge University Press, London.

Livermore Software Technology Corporation, *LS-Dyna3d Users Manual*, 1998. Livermore, CA, 2003.

S.A.E. "Instrumentation for Impact Test – Part 1- Electronic Instrumentation," *Surface Vehicle Information Report*, Society for Automotive Engineers, Warrendale, Pa, J211-1; 1998.

Stata Users Guide. 1999, Stata Press, College Station, TX, 1999.

Takhounts, E., Eppinger, R., Campbell, J.Q., Tannous, R., Power, E. and Shook, L. 2003. "On the Development of the SIMon Finite Element Head Model," *Stapp Car Crash Journal*, Volume 47.

US Code of Federal Regulations, Title 49 (Transportation), Part 571 (Federal Motor Vehicle Safety Standards); 2003.

Vander Vorst, M., Stuhmiller, J., Ho, K., Yoganandan, N. and Pintar, F. 2003. "Statistically and Biomechanically Based Criterion for Impact-Induced Skull Fracture," 47th Annual Proceedings of the Association for the Advancement of Automotive Medicine, Lisbon, Portugal.

Vander Vorst, M. and Chan, P. C. 2004. "A New Biomechanically-based Criterion for Lateral Skull Fracture," 48th Annual Proceedings of the Association for the Advancement of Automotive Medicine.

Visible Human Project, National Library of Medicine, National Instituted of Health, Bethesda, Maryland, 2000.

Wood, J. L. 1971. "Dynamic Response of Human Cranial Bone," *J. Biomech.* 4: 1-12.

Yoganandan, N, Pintar, F. A., Sances, A Jr, Walsh P. R., Ewing, C. L., Thomas, D. J., Snyder, R. G. 1995. "Biomechanics of Skull Fracture," *J. Neurotrauma*: 12(4) pp.659-668, 1995.

Zeger, S.L. and Liang, K. 1986. "Longitudinal Data Analysis for Discrete and Continuous Outcomes," *Biometrics* 42, 121-130.

UPPER EXTREMITY INJURIES IN ROAD TRAFFIC ACCIDENTS

Wraighte PJ

Manning P

Wallace WA

Institute of Biomechanics

The University of Nottingham

Nottingham, UK

Hynd D

The Transport Research Laboratory, UK

Paper number 07-0239

ABSTRACT

The purpose of this study was to obtain more specific information on upper limb injuries sustained by front seat occupants in car accidents with a view to identifying injuries that are a priority for prevention and further research.

After identification of cases from the Vehicle Safety Research Centre (VSRC) through the Transport Research Laboratory (TRL) the appropriate hospital records and radiographs were reviewed. Data were analysed to identify the frequency and severity of upper limb injuries, the mechanism of injury and the impairment sustained in accordance with the American Medical Association guides [1]. The NHS financial costs of management for the upper limb injury and that for the patient in total were calculated.

Sixty two cases were reviewed (34 male), aged 18-83 years (mean 44 years). There were 20 clavicle fractures, 18 elbow and forearm fractures, 16 shoulder and arm injuries, and 26 wrist and hand injuries.

The median upper limb Abbreviated Injury Score was 2 and the overall Injury Severity Score ranged from 4 to 50 (median 6). In terms of impairment, the upper extremity sensory deficit ranged from 0 to 9% and motor deficit 0 to 22.5% giving up to 5% sensory and 13.5% motor "whole person impairment".

The mean estimated treatment cost for upper limb management was calculated at £2,200 compared with a total injury treatment cost of a mean £11,000 per person.

Limitations of the study include its retrospective nature and possible selection bias.

The study has identified the range and costs (impairment and financial) of upper limb injuries in road traffic accidents. These data will be used by researchers to both improve the current car crash dummies in the upper limb and to allow accurate finite element remodelling. Legislative changes to car requirements for upper limb safety may be brought forward in the longer term.

INTRODUCTION

With the introduction of seat-belt legislation into the UK in 1983 there has been a significant reduction in head and chest injuries but no reduction in lower limb injuries in road traffic accidents [2]. Upper limb injuries in road traffic accidents have been less extensively investigated than is the case with lower limb and visceral injuries and as a result are poorly understood.

There has been an increasing concern that upper limb injuries might be becoming more common but accident analyses have varying conclusions in this area. Upper limb injuries might occur as a result of the acceleration/deceleration forces of the accident resulting in the limb being subjected to injury as a consequence of its momentum or because of the efforts of the occupant to restrain themselves with their upper limbs at the time of the accident. More recently, the possibility has been raised, that the front or side air-bags might also contribute to upper limb injury [3, 4].

The aim of the project was to obtain more specific information on upper extremity injuries sustained by front seat occupants in road traffic accidents, whilst wearing seat-belts and experiencing frontal collisions. The aim was to identify injuries that are a priority for prevention and to help direct further research.

Upper limb injuries have the potential to cause high levels of functional impairment and as a result may have significant unforeseen wider economic costs. This study was designed to specifically evaluate the functional impairment produced as a result of common upper limb RTA injuries.

METHODS

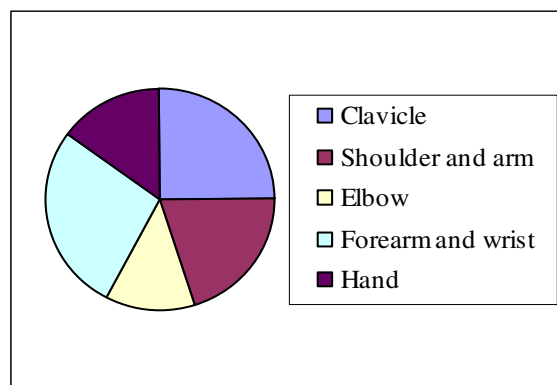
Ethical approval was obtained for this study (Nottingham Research Ethics Committee ref: 04/Q2403/119). Cases were identified through the UK car crash injury data-base by the Vehicle safety research centre (VSRC) in Loughborough and the Transport Research Laboratory (TRL) in Berkshire. Patients were included if they had been recorded on the database as having sustained an upper limb

injury as a seat-belted front seat passenger in a road traffic accident and had further been treated at the Nottingham University Hospitals NHS Trust. Only frontal impact collisions with no rollover were included. Patients sustaining only minor abrasions and contusions were excluded and only AIS 2+ upper extremity injuries were investigated. Hospital records and radiographs were reviewed. These data were analysed to summarise the injuries sustained and to classify them according to their frequency, severity and subsequent impairment using the American Medical Association (AMA) guidelines on the “Evaluation of Permanent Impairment” [1]. The medical researchers comprised two consultant orthopaedic and trauma surgeons and one specialist registrar (senior intern). An initial opinion was formed by consensus between one of the consultants and specialist registrar and in cases where there was a significant difference of opinion a final opinion was given by the senior consultant surgeon. The cost related to upper limb injuries and total cost of care for the injured parties were estimated using standard recognised National Health Service, UK Government, costing methods.

RESULTS

Sixty two appropriate cases (34 male), aged 18-83 years (mean 44 years) identified from the Co-operative Crash Injury Study (CCIS) database were recommended by the TRL team for investigation and these cases were reviewed by the clinicians. Medical records were found for all cases referred by the VSRC with no cases being lost to the study. The location of the upper extremity injuries are shown in Figure 1.

Figure 1. Location of AIS 2+ upper extremity injury in front seat occupants in frontal collisions.



There was a total 20 clavicle fractures of which 19 were sustained by the driver of the vehicle and 18 were right sided. 19 of the 20 occurred in the limb closest to the door (outboard limb). The majority occurred in the region of the middle third of the clavicle (80%) (Table 1).

Table 1. Location of fracture of clavicle in front seat occupants in frontal collisions

Location of fracture of clavicle	Frequency
Medial	1
Middle third	16
Middle/lateral third	1
Lateral	2

The commonest mechanism was identified as three point loading from the seatbelt (Table 2).

Table 2. The suggested mechanisms of AIS 2+ upper extremity injuries in front seat occupants in frontal collisions

Injury location	Type of mechanism	Frequency	Total number
Clavicle	3-point seatbelt loading	15	20
	Lateral compression	3	
	Indirect force	1	
	Airbag to sternum	1	
Shoulder or arm	Whiplash/seatbelt contusion	5	16
	Axial force	3	
	High energy torque force	2	
	Lateral compression	2	
	Flail arm with inertial force	2	
	High energy 3-point bending	1	
	Direct contact A-frame	1	
	Direct trauma/intrusion	7	
Axial load	2		
Indirect torque force arm	1		
Forearm	Pin-point loading	3	8
	Direct contact-Intrusion into driver space	2	
	Direct contact-Steering wheel	1	
	Multiple point contact	1	
	3-point loading ulna	1	
Wrist	Forced hyper-extension	11	14
	Direct impact/intrusion	3	
Hand	Direct impact/intrusion	5	12
	Flail arm	2	
	High torque force finger	1	
	Hyperflexion finger	1	
	Forced extension of thumb	2	
	Forced flexion of extended thumb	1	

Three of the clavicle fractures resulted in a non-union, two of which subsequently required remedial surgery - operative fixation (Figure 2).

Figure 2. One of the clavicle fractures treated with surgical plating after developing a non-union.



A further case with a fracture at the lateral end of the clavicle is currently awaiting operative intervention with an acromio-clavicular joint reconstruction. There were 3 acromio-clavicular dislocations and 1 shoulder dislocation. The forearm sustained significant trauma in this series, involving 8 fracture dislocations of elbow, 4 of which were open injuries. There were 3 open fractures of the forearm, 1 open fracture of the wrist and 1 dislocation of the wrist joint.

The full data and summary is presented in Table 3. The Injury Severity Score (ISS) ranged from 4 to 50 with a median of 6. The Upper Limb Abbreviated Injury Score ranged from 2 to 4 with a median of 2.

Figure 3. A severe fracture of the humerus, radius and ulna just around the elbow required reconstruction with plates and screws.



Upper extremity sensory deficits ranged from 0 to 9% and motor deficits 0 to 22.5% giving up to 5% sensory and 13.5% motor “whole person impairment”.

The mean cost of the medical management of the upper limb injuries in these subjects was £2415 (£5 to £9951). The mean total injury treatment cost of the same group of subjects was £10,883 per person as a consequence of other injuries sustained in the same accident.

Table 3. Severity, financial cost and functional impairment of upper extremity injuries to front seat occupants in frontal crashes

Injury location	Inboard limb	Outboard limb	Total	ISS median (range)	AIS median (range)	Mean Cost of upper limb injury (£)	Mean Cost of other injuries (£)	Mean Total cost (£)	Average Upper limb impairment (%)	Whole person impairment (%)
Clavicle	19	1	20	12 (4-50)	2 (2-4)	2,431	13,545	15,976	1.5	0.9
Shoulder or arm	10	6	16	2 (4-29)	2 (2-4)	1,853	4,877	6,730	2.7	1.6
Elbow	7	3	10	16 (5-29)	3 (2-4)	5,710	14,943	20,653	4.7	3.0
Forearm	5	3	8	16 (4-38)	2.5 (2-3)	4,218	19,489	23,707	0.3	0.3
Wrist	9	5	14	14 (4-24)	2 (2-4)	4,184	9,046	13,230	3.8	2.3
Hand	8	4	12	2 (4-34)	2 (2-3)	1,844	5,330	7,174	1.3	0.8

DISCUSSION

This study highlights the significance of upper limb injuries in road traffic accidents. There was a surprisingly high incidence of clavicle fractures, often the result of three-point seatbelt loading. The number of these injuries, their consequence and the costs of their treatment had not been recognised previously. The medical researchers have raised the possibility that the frequency of these injuries may be increased compared with the past and may relate to advances in car safety and thus resultant morbidity, as opposed to mortality, as more people survive such accidents. Changes in seatbelt design and tensioning may also be a co-factor.

Many clavicle fractures are discharged from primary care prior to healing and therefore impairment may be under-estimated as it is often assumed that they will make a full recovery. A prospective study with adequate follow up is required to establish a more accurate analysis of the degree of impairment sustained.

In these frontal crashes, the outboard limb most frequently sustained AIS 2+ injuries. The outboard limb lies adjacent to the stiff structures of the door, A-pillar and window and is vulnerable to injury from flailing as well as contact from facia/side wall intrusion. 80% of clavicle fractures were attributed to the seatbelt loading from the diagonal section of the seat belt. The shoulder injuries were identified as lateral compression or axial compression sources. Two thirds of the elbow injuries, including the most devastating, were identified as direct point loading, commonly associated with intrusion. There were 8 fracture dislocations/Monteggia fractures of the elbow, including 4 open injuries. This group had a poor functional outcome with an average upper extremity and whole person impairment of 4.8% and 7.8% respectively. The majority (75%) occurred in the outboard limb from direct trauma. The average cost of the upper extremity injuries in these patients was £26,350.

Two thirds of the forearm fractures occurred via 3 point loading, most commonly in the outboard limb, most likely due to flail arm into the side door structure and A-pillar. Wrist injuries were frequently of a hyperextension pattern, most likely from steering wheel or airbag contact.

Hand and wrist injuries have previously been shown to be rare in rollover and side-struck impacts, and relatively common in frontal crashes [5], prompting suggestion that air-bags might significantly contribute to upper limb injury. The majority of hand and wrist injuries in this study of AIS 2+ also occurred in the outboard limb. If these injuries do not result directly from airbag deployment, they may occur as a secondary effect of being forced into the hard side structures.

The cost analysis which was carried out included 1) the length of hospital stay; 2) the cost of medical

investigations; 3) the cost of the treatment carried out including surgery and physiotherapy as well as; 4) the cost of outpatient follow up. The single largest cost was inpatient stay on the Intensive care unit (ITU), High dependency unit or on the ward. As most upper limb injuries do not require ITU care and often only require a minimal inpatient ward stay, the cost to the secondary care unit is thus comparatively small. However the cost to society and to the individual is considerably greater and this has not been fully assessed in this study, although an indication of impairment has been ascertained. It is important to emphasise that a patient with a clavicle fracture is unable to drive and rarely returns to work inside 8 weeks, partly as a consequence of being unable to drive. As 84% of the study population were within the working age range this could have significant effects during the weeks or months required for recovery.

CONCLUSION

The study has demonstrated the significance of upper limb injuries in road traffic accidents both from their functional outcome and their cost. We would recommend further investigation into the high incidence of clavicle fractures and into seatbelt design. A better understanding of the prevalence and implications of these injuries should be obtained via a large prospective, multi-centre study.

RECOMMENDATIONS

The major limitations of this retrospective study are the selection procedure and sample bias and whether the findings are truly representative. To evaluate these further, a prospective study would be required in the form of a multi-centre observational study.

ACKNOWLEDGEMENTS

We are grateful to the Vehicle safety research centre (VSRC), Loughborough and the Transport Research Laboratory (TRL), Berkshire for identification and selection of cases for this study.

REFERENCES

- [1]. Cocchiarella L, Andersson GBJ. Guides to the Evaluation of Permanent Impairment. American Medical Association (5th edition). AMA press 2001. ISBN 1 57947 085 8
- [2]. Manning P, Wallace A. Dynamic response and injury mechanism in the human foot and ankle and an analysis of dummy biofidelity. 16th ESV Conference, Ontario, Canada. May 31st-June 4th 1998.

[3]. Kent R, Viano DC, Crandall J. The field performance of frontal airbags: A review of the literature. *Traffic Injury Prevention*;6(1):1-23. March 2005.

[4]. Jernigan MV, Duma SM. The effects of airbag deployment on severe upper extremity injuries in frontal automobile crashes. *Am J Emerg Med*;21:100-105.

[5]. Frampton RJ, Morris AP, Thomas P, Bodiwala GG. An overview of upper extremity injuries to car occupants in UK vehicle crashes. September 1997. IRCOBI Conference, Hannover.

OCCUPANT DYNAMICS AND INJURIES IN NARROW-OBJECT SIDE IMPACT

Frank A. Pintar

Dennis J. Maiman

Narayan Yoganandan

Medical College of Wisconsin and VA Medical Center

Milwaukee, Wisconsin

United States of America

Paper Number 07-0246

ABSTRACT

Side impact tree/pole crashes can have devastating consequences. A series of 49 CIREN cases of narrow-object side impacts were analyzed. 26 of 49 had serious chest injury and 26 had serious head injury. Of the head trauma patients, 10 had skull fractures, out of which seven were basilar skull fracture. Seventeen of the head trauma patients had some kind of internal bleeding such as subdural or subarachnoid hemorrhage; three were coded as having diffuse axonal injury. Of the chest injuries, 17 occupants had lung contusions and 19 had rib fractures. Of those with rib fractures, 15 of 17 had unilateral rib fractures. Examining crash test data of side pole crashes, it was evident that in tests where the pole caused intrusion at the middle of the occupant's thigh, a high degree of oblique chest loading occurred. The hypothesis was that this oblique chest loading from the door induces unilateral rib fractures, lung contusions, and possible aortic rupture. Additional testing was done in a sled laboratory to induce oblique chest loading to PMHS. A modified side impact sled buck induced oblique loading at 20 and 30 degree angles to the chest. PMHS subjects experienced unilateral rib fracture patterns. Additional dummy tests in this same configuration were also conducted. Chestband data revealed better biofidelity in the WorldSID dummy than the NHTSA-SID for oblique chest loading. These dummies however, are not currently equipped to measure oblique chest deformations. Narrow-object side impacts are realistic crash environments that can induce oblique chest loading. Because the human may be more vulnerable in this type of crash scenario, dummy biofidelity and measurements, as well as a re-examination of side injury criteria may be necessary to design appropriate injury-mitigating safety devices.

INTRODUCTION

Side impact crashes in general have received more attention recently. Despite a lower overall incidence rate, side impact crashes can result in more serious injuries to occupants compared to frontal crashes [NHTSA Traffic Safety Facts, 2005]. Side impact crashes may result from vehicle to vehicle configurations as well as single vehicle crashes. Most single vehicle side crashes result when the driver loses control and collides with a fixed object. Often the fixed object is a tree or pole. Recently the US federal government has proposed a side impact crash into a rigid pole as part of the regulatory test requirements. It has long been presumed that these single vehicle side impacts into narrow objects result in devastating consequences to the occupants on the near side of the crash. There are very few studies however, that have described occupant injury patterns in sufficient detail to assist designers of vehicle safety systems and to assist in the interpretation of dummy response measures. The purpose of the present investigation therefore, was to characterize occupant injury patterns in side pole/tree crashes using detailed real world data and to develop a laboratory sled test to verify occupant injuries and examine dummy biofidelity.

METHODS

The Crash Injury Research and Engineering Network (CIREN) database contains a wealth of detailed information on real world crashes. The CIREN database is populated with a sample of real world crashes from eight centers around the US. To enroll a case occupant in the CIREN database, the injuries sustained by the occupant must be at least AIS=3, or moderate to severe trauma. The case vehicle must also be within eight model years of the crash date.

For the current study, the database was queried for single vehicle side impacts resulting in collision with a tree or pole. The vehicle collision direction was 2-4 or 8-10 o'clock, and only near side occupants were included in the analysis.

To understand occupant responses in narrow object side crashes, the deformation patterns of the vehicles involved in real world crashes were examined. The oblique door deformation pattern to the occupant compartment was simulated in the sled environment by inducing an oblique load wall configuration. A previously established load wall configuration [Pintar et. al. 1997] was modified to include an angled wall configuration for thorax and abdomen plates (Figure 1). Preliminary PMHS and NHTSA-SID dummy tests were run at 6.7 m/s change in velocity (Table 1). The human surrogates were instrumented with head, T1, T12, and sacrum triaxial accelerometer packages. Rib and sternum accelerometers were also mounted. The load wall was instrumented with uniaxial load cells to measure interaction forces. PMHS were examined for injury with a complete autopsy following testing.

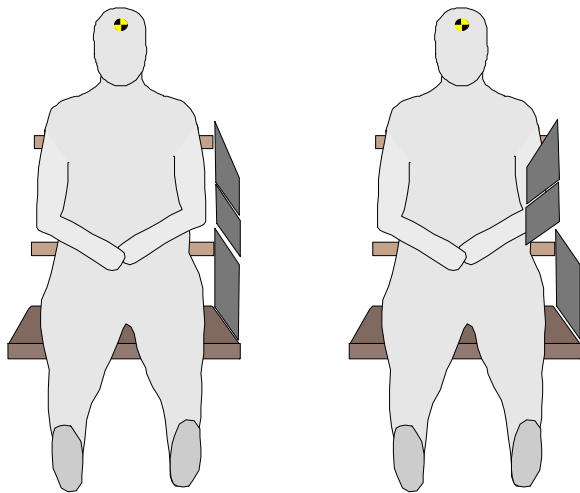


Figure 1. Schematic diagram depicting original flat wall configuration on the left and the modified configuration with angled thoracic and abdominal load plates on the right.

Table 1: Experimental sled tests

Test ID	Configuration	Gender	Age (yrs)	Height (cm)	Weight (kg)
PMHS 102A20	20-deg wall	M	46	186	73
NHTSASID 102A20	20-deg wall	---	---	175	75
WorldSID 112A20	20-deg wall	---	---	175	75
PMHS 103A30	30-deg wall	M	52	179	75
NHTSASID 105A30	30-deg wall	---	---	175	75
WorldSID 108A30	30-deg wall	---	---	175	75

RESULTS

For the CIREN analysis, a total of 49 cases were examined. Of the 49, 25 were male, 24 were female; 15 were in the age range from 10-18 years old, while 34 ranged in age from 19-63. There were 34 drivers and 15 passenger occupants. Out of the total occupants, 38 (78%) were belted. The severity of the crash was rated by delta-V calculations based upon deformations using the WINSMASH software program that is standard for CIREN crash reconstruction analysis. Delta-Vs ranged from 17 to 58 km/h with a preponderance of crashes in the range from 24 – 48 km/h (Figure 2). The majority of the case vehicles (28) were model year 1998 or newer (Figure 3).

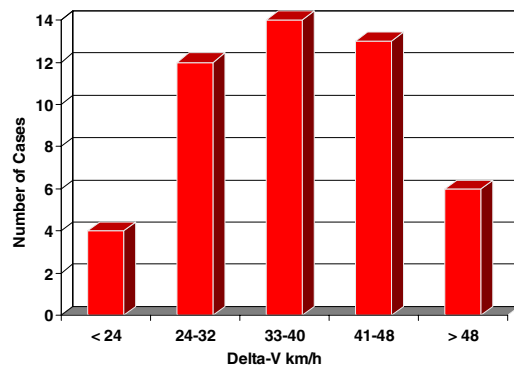


Figure 2. Bar graph representation of the number of CIREN cases analyzed by delta-V range.

Occupant injuries were broadly separated by body region (Figure 4) with at least half sustaining chest and head trauma. Occupants with chest trauma, also had head trauma 73 % of the time. In contrast, pelvis and lower extremity trauma were present in the chest

trauma patients only 35 % and 8 % of the time, respectively. Of the head trauma patients, 10 had skull fractures, out of which seven were basilar skull fracture. Seventeen of the head trauma patients had some kind of internal bleeding such as subdural or subarachnoid hemorrhage; three were coded as having diffuse axonal injury. Of the 26 chest trauma patients, 19 had rib fractures and 17 had lung contusions. Ten of the 17 patients had unilateral lung contusions, and 15 of the 19 patients had unilateral rib fractures. Only four of the 26 occupants with chest trauma had isolated injuries.

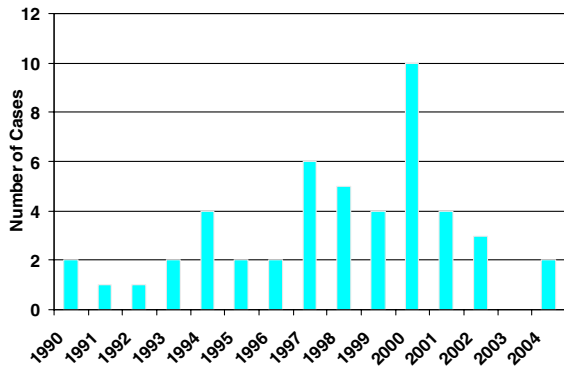


Figure 3. Bar graph representation of the number of CIREN cases analyzed by vehicle model year.

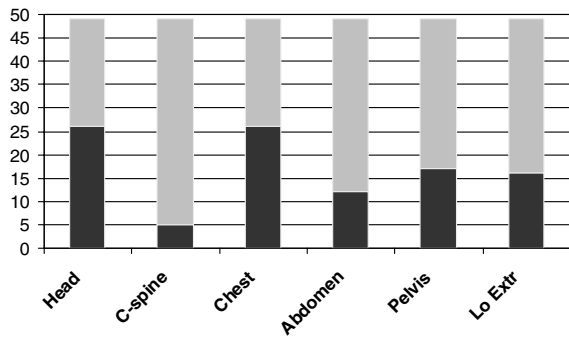


Figure 4. Bar graph representation of the number of CIREN case occupants with trauma by body region. Note that each occupant may sustain multiple trauma.

For the sled studies, a matching test series was done with PMHS, NHTSA-SID, and WorldSID at 20 and 30 degree offset wall conditions. The PMHS that was tested at 20-degrees endured 12 rib fractures that resulted in flail chest. Diaphragm rupture and lung contusion was also present. The PMHS tested at 30 degrees resulted in no skeletal or organ injuries. As an initial assessment of dummy biofidelity, the PMHS load wall responses were scaled to a 50th

percentile male (75 kg) and compared to the dummies. For the 20-degree load wall condition (Figure 5), the thorax and pelvis loads of the WorldSID are comparable in magnitude and time duration to the PMHS. The NHTSA-SID thorax and pelvis forces are greater in magnitude and shorter in duration than the PMHS. For the 30-degree load wall condition (Figure 6) the WorldSID thorax response is comparable in magnitude to the PMHS. Both dummies exert a greater force into the pelvis than the PMHS. For the abdomen forces in either configuration the PMHS loads are greater and the time durations are longer than for the dummies.

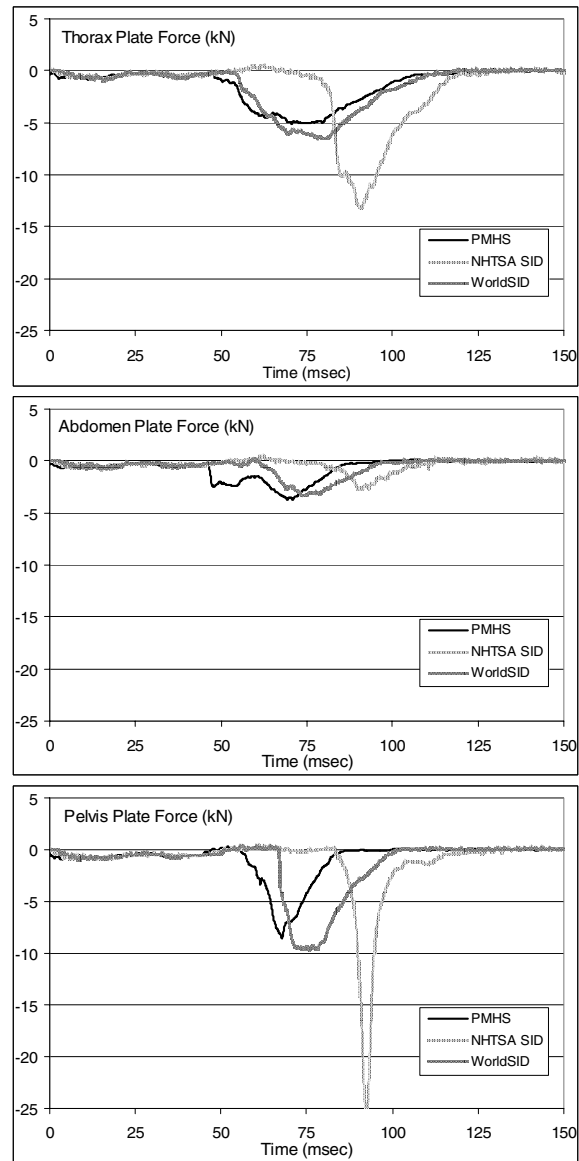


Figure 5. Force response curves from 20 degree oblique load wall sled tests at 6.7 m/s.

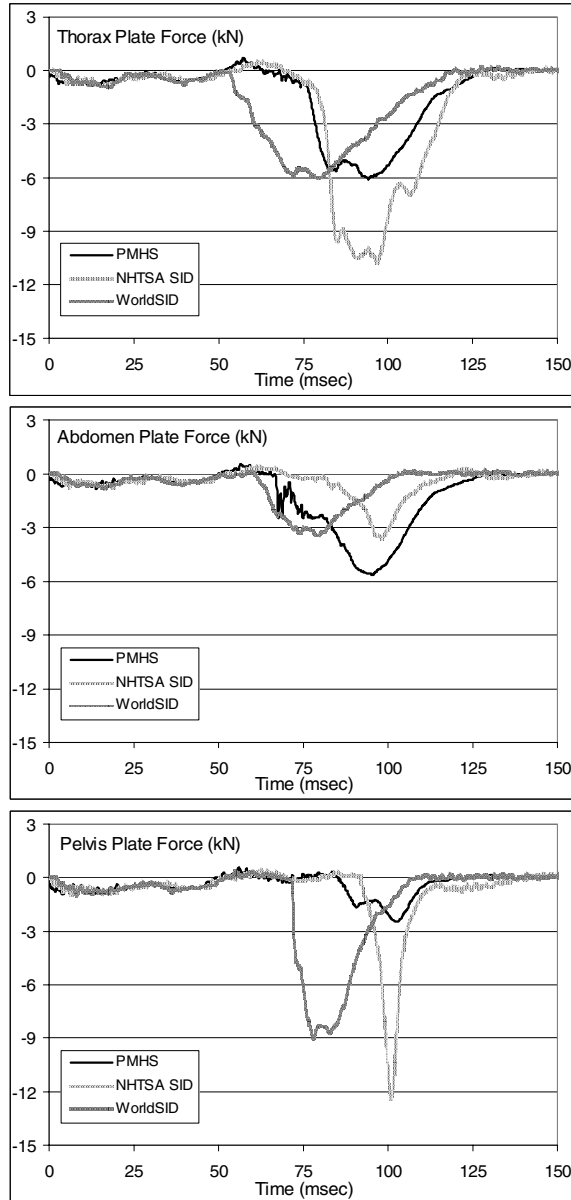


Figure 6. Force response curves from 30 degree oblique load wall sled tests at 6.7 m/s.

DISCUSSION

A side impact into a pole or tree can result in devastating injuries to the near side occupant. A CIREN investigation of 49 cases was undertaken to characterize injury patterns in these types of crashes. The real world data that is collected for CIREN cases results in over 900 data points for each case. The medical images and injury identification documentation is excellent. A prerequisite for inclusion in the CIREN database is that the injuries sustained by the occupant be at least moderate to

severe (AIS = 3). The 49 CIREN cases examined in the current study revealed distinct injury patterns. In more than half the cases, head trauma and chest trauma occurred, most often in combination. It is important to note that in only four of the cases were there side airbags present. None of these four cases resulted in head injuries, however two cases resulted in chest or abdomen trauma. The effectiveness of side airbag technology is, as yet, not fully evaluated [McGwin et.al., 2003; Yoganandan et.al., 2005].

The focus of this presentation was chest trauma due to the difference in mechanism of injury in these narrow object impacts. It was observed from the vehicle deformation photos that the door intrusion into the occupant space resulted in oblique (antero-lateral) chest loading. This was evident by the occupant chest injury patterns; often unilateral rib fractures and unilateral lung contusions resulted on the struck side. An oblique load to the chest results in a different injury mechanism to the rib cage due to difference in arm position and direct exposure of the rib cage to the load with no protection from the shoulder. The internal organs may also receive a more severe load exposure as the lungs and heart are clearly in line with the impact.

To reproduce these injuries in the laboratory, a unique load wall was designed with inclined plates at the thorax and abdomen regions. The pelvis plate was not oriented obliquely due to the practical constraint of inflicting a focal point of loading to the lower legs. It was also noted in the real world that pelvis and lower extremity injuries occurred only about 30 % of the time and in greater isolation when the impact was located forward on the vehicle. The PMHS test at 20 degree oblique wall configuration resulted in a similar injury pattern as seen in the real world occupants: unilateral rib fractures and unilateral lung contusion.

The NHTSA-SID and the WorldSID were tested in the same load wall configurations as the two PMHS. Neither NHTSA-SID nor WorldSID were designed to be biofidelic in oblique side loading conditions. The WorldSID however, seemed to offer greater biofidelity in the pelvis and thorax under oblique loading conditions. A report on a test series that used the WorldSID in a far side impact scenario also concluded that the dummy was valuable for testing outside of its originally intended design [Pintar, et.al., 2006]. The instrumentation to measure chest deflection in both dummies is directly lateral. It is recommended that the dummy chosen for this type of testing be modified to measure deflections in an oblique direction.

CONCLUSIONS

Narrow-object side impacts are realistic crash environments that can induce oblique chest loading. Because the human may be more vulnerable in this type of crash scenario, dummy biofidelity and measurements, as well as a re-examination of side injury criteria may be necessary to design appropriate injury-mitigating safety devices.

This study has also demonstrated that a trend exists between seatbelt geometry and pretension on the level of restraint provided to occupants in far-side impacts. It has also been highlighted that human anthropometry has a major effect on the restraint provided by the seatbelt in far-side impacts.

ACKNOWLEDGEMENTS

This study was supported in part by U.S. Department of Transportation National Highway Traffic Safety Administration DTNH22-05-H-41001 and DTNH22-03-H-07147. It was also supported by the Department of Veterans Affairs Medical Research. The material presented in this manuscript represents the position of the authors and not necessarily that of the associated organizations. The assistance of Dale Halloway, John Humm, Paul Gromowski, and the staff of the VA Neuroscience research laboratories is gratefully acknowledged.

REFERENCES

- NHTSA Traffic Safety Facts-2005. National Center for Statistics and Analysis. National Highway Traffic Safety Administration. US Department of Transportation, Washington DC, 2005.
- McGwin, G., J. Metzger, et al.: Association between side air bags and risk of injury in motor vehicle collisions with near-side impact. *J Trauma* 55(3): 430-436. 2003
- Pintar F, Yoganandan N, Hines M, Maltese M, Mcfadden J, Saul R, Eppinger R, Khaewpong N, Kleinberger M. (1997) "Chestband Analysis of Human Tolerance to Side Impact", Proceedings of 41st Stapp Car Conference, pp. 63-74, November 1997.
- Pintar F, Yoganandan N, Stemper B, Bostrom O, Rouhana S, Smith S, Sparke L, Fildes B, Digges K. (2006) "WorldSID Assessment Of Far Side Impact Countermeasures", Proceedings of the 50th Annual Conference, Association For The Advancement Of Automotive Medicine, October 16-18, 2006.

Yoganandan N, Pintar, FA, Gennarelli TA: Field data on head injuries in side airbag equipped vehicles in lateral impact. AAAM proceedings, pp 171-184. 2005

Elderly Occupant Injury: A Detailed Analysis of Injury Patterns and Quality of Life Indicators

Catherine A. McCullough

Mark Scarboro

National Highway Traffic Safety Administration
United States Department of Transportation
United States of America

Mark Sochor, MD, MS, FACEP

University of Michigan Transportation Research
Center

United States of America

Ramita Sharma

OnPoint

United States of America

Paper Number #07-0277

ABSTRACT

As the population in the United States ages there will be an increase of the exposure of the elderly to motor vehicle collisions. The growing population of elderly (65 years and older) Americans is the fastest growing segment of the population. It is estimated that more than 40 million older adults will be licensed drivers by 2020. [1]

According to the National Highway Traffic Safety Administration (NHTSA), Traffic Safety Facts, in 2005, 191,000 older individuals were injured in traffic crashes accounting for seven percent of all the people injured in traffic crashes during the year. These older individuals made up 15 percent of all traffic fatalities and 14 percent of all vehicle occupant fatalities.

There were over 28 million older licensed drivers in 2004 (2005 data not available) - a 17 percent increase from 1994. In contrast, the total number of licensed drivers increased by only 13 percent from 1994 to 2004. Older drivers made up 15 percent of all licensed drivers in 2004, compared with 14 percent in 1994. [2]

Injuries sustained by these individuals tend to be more life altering and life threatening than the same injuries sustained by younger individuals in similar motor vehicle collisions. This paper will examine the injuries sustained by individuals age 65 and older and compare them with injuries sustained by younger individuals (broken down in three additional age groups) in motor vehicle collisions. The long-term effects on their quality of life will also be analyzed.

This paper will focus on those occupants where a Short Form 36 (SF-36) baseline score and at least one follow-up score (at 9 or more months) is available. We will focus on occupants with an Abbreviated Injury Severity Score (AIS) of 3+ or an Injury Severity Score (ISS) of 8. Relating factors such as crash type, principal direction of force, age and others will be considered. The range of scores in the various levels will be compared and contrasted for the four age groups.

INTRODUCTION

The Crash Injury Research and Engineering Network (CIREN) is a multi-disciplinary collaboration of trauma physicians, engineers, epidemiologists, crash investigators and other social scientists in industry and government researching the "cause and effect" of serious and/or disabling injuries sustained as a result of an automotive collision. CIREN is a network of eight Level 1-trauma centers spanning the United States and investigating approximately 350 crashes per year that result in serious and/or disabling injuries.

CIREN is also the name of a research tool developed, updated, enhanced, and maintained by The Volpe National Transportation Center (Volpe) in Cambridge, Massachusetts, to help researchers collect and review injury data. Variables for CIREN crash reconstruction data are an extension of the National Automotive Sampling System (NASS) Oracle data model. Variables for the medical injury data are based on a variety of sources, including the National Trauma Registry, the Orthopedic Trauma Association, and the Uniform Pre-Hospital EMS Data Elements.

CIREN is the only research program that combines detailed medical data with detailed crash data. Each CIREN Case is one injured occupant in a motor vehicle crash. Multiple CIREN cases can be linked to one NASS case, which is associated with a single crash. There are 3159 cases in the CIREN database (medical side) linked to 2793 NASS cases (crash side).

It is estimated that more than 40 million older adults will be licensed drivers by 2020. It is anticipated as the population ages that these individuals will continue to be at risk unless

countermeasures are developed to mitigate these injuries. This concern has been addressed by congress through the House Committee Appropriation Report that states, "The committee directs NHTSA as part of its CIREN program, to collect data that will measure the impact of crashes on older populations and that would assist in the possible development of a crash test dummy representing the older populations."

This paper will review the injury patterns using the differing body regions (head, neck thorax, pelvis, etc.) of elderly occupants and compare and contrast those of their younger counterparts from CIREN. This paper will also evaluate the initial outcome of injury to the elderly occupant in comparison to the differing age groups (16-30 years old, 31-47 years old, 48-64 years old and 65 and greater years old). Injury for the differing body regions will be calculated for all four age groups. An analysis of elderly occupant SF-36 (quality of life and physical limitations) scores will be compared with the differing age groups.

The CIREN utilizes several unique processes and tools to research automotive crashes and the resulting injuries. One such tool utilized is the Medical Outcomes Study 36 – Item Short Form Survey (SF-36). The SF-36 has become one of the most widely used scoring tools for measuring outcomes after multiple trauma events.

BACKGROUND ON THE SF-36

The Short Form 36 (SF-36) was derived from the work of the Rand Corporation of Santa Monica during the 1970's. Rand's Health Insurance Experiment compared the impact of alternative health insurance systems on health status and utilization. The SF-36 was designed for use in clinical practice and research, health policy evaluations, and general population surveys. The outcome measures developed for the study have been widely used. They were subsequently refined and used in Rand's Medical Outcomes Study (MOS), which focused more narrowly on care for chronic medical and psychiatric conditions. [3]

The form is used in identifying and tracking limitations in physical or social activities because of health problems relating to a medical condition (asthma, diabetes, traumatic injury, etc.). It is a generic measurement and does not target specific ages, sex, or disease. Population and large-group

descriptive studies and clinical trials to date demonstrate that the SF-36 is very useful for descriptive purposes such as documenting differences between sick and well patients and for estimating the relative burden of different medical conditions. [4] The SF-36 measures eight health concepts (See Table 1) [5].

The SF-36 outcome tool has been shown to be less than ideal when testing for outcomes related to brain trauma, especially in the areas of cognitive function. MacKenzie et al. indicated the SF-36 required additional cognitive testing supplements to develop a more accurate outcome indicator for individuals who sustain multiple traumas involving head injury. [6]

Although the SF-36 can be self administered, CIREN uses trained interviewers to administer the questionnaire at the time of the traumatic event to develop a baseline to determine the physical and emotional health status of a person at that time compared to how they were prior to the event. The same 36 questions are asked at 6-months and 12-month post event whenever possible. The SF-36 scores are derived from answers given to those standardized questions. Generally, the lower the score in any given category indicates a decreased ability in that area for the occupant. This data is invaluable in determining overall medical outcomes and societal costs.

The experience to date with the SF-36 has been documented in nearly 4,000 publications. Scales that load highest on the physical component are most responsive to treatments that change physical morbidity, whereas scales loading highest on the mental component respond mostly to drugs and therapies that target mental health. [7]

METHODS

The CIREN database was queried for years 1997 to 2006 to extract all crashes where an SF 36 baseline score and at least one set of follow-up scores (at 9 or more months) post crash are available. Normally, SF-36 is obtained at baseline, 6 and 12 months. However, in this dataset some responses were obtained at 10 or 11 months due to difficulty in contacting the subject for their follow-up. The range of scores in the various levels were compared and contrasted for the four age groups. Typically, elderly has been

Table 1.
SF-36 Health Status Concepts

Health Concept	Description
<u>PF</u> Physical Functioning	The PF score indicates the amount health limits physical activities such as walking, lifting, bending, stair climbing and exercise. A low score indicates limitations in performing all activities. A high score indicates the ability to perform all types of physical activities including vigorous exercise.
<u>RP</u> Role Physical	The RP score indicates the level that physical health interferes with work or other daily activities. A low score indicates that physical health creates problems with daily activities including accomplishing less than wanted, limitations in the kind of activities, or difficulty in performing activities. A high score indicates that physical health has not caused problems with work or daily activities.
<u>BP</u> Bodily Pain	The BP score indicates the intensity of pain and its effect on normal work in and out of the home. A low score indicates very severe and extremely limiting pain. A high score indicates no pain or limitations due to pain.
<u>GH</u> General Health Perceptions	The GH score evaluates health, current and future outlook as well as resistance to illness. A low score indicates individual/personal health perceptions as poor and likely to get worse. A high score indicates individual/personal health perceptions as excellent.
<u>V</u> Vitality	The V score indicates the extent of energy level. A low score indicates you feel tired and worn out all of the time. A high score indicates you have felt full of pep and energy during the past four weeks.
<u>SF</u> Social Functioning	The SF score indicates a level to which physical or emotional problems interfere with daily social activities. A low score indicates extreme and frequent interference. A high score indicates no interference during the past four weeks.
<u>RE</u> Role Emotional	The RE score indicates a level that emotional problems interfere with work or other daily activities. A low score indicates emotional problems interfere with activities including decreased time spent on activities, accomplishing less, and not working as carefully as usual. A high score indicates no interference with activities due to emotional problems.
<u>MH</u> Mental Health	The MH score identifies general mental health including depression, anxiety and behavior. A low score indicates a feeling a nervousness and depression all of the time. A high score indicates you have felt peaceful, happy, and calm during the past four weeks.

* **Physical Functioning, Role Physical, Bodily Pain and General Health scores are combined to obtain the Physical Component Summary.**

** **Vitality, Social Functioning, Role-Emotional and Mental Health are combined to obtain the Mental Component Summary**

defined as 65 years of age and older which we used to constitute the beginning age range for the oldest group (the oldest member in this group was 94). It should be noted that we did not include occupants under the age of 16 since they have their outcomes assessed using the Pediatric Quality of Life tool. With that in mind, the age range for the first age group was set at 16. The difference in years between 16 and 65 was divided into three equal groups with rounding up occurring for the two next older groups and we arrived at the age breakdown for the groups used

in this paper.

Relating crash and injury variables including but not limited to crash type, principal direction of force (PDOF), DeltaV, restraint use, Abbreviated Injury Score (AIS), Injury Severity Score (ISS), Maximum Severity Score (MAIS) along with age and sex were also considered. We focused on injuries AIS 3 or greater or an ISS of 8 or greater. Data was reviewed to help determine the significance of an injury to a specific body region beyond that of “threat to life” measure provided by AIS.

The SF-36 scores are derived from the answers given by the case occupant on 36 standardized questions. The questions inquire about issues ranging from their opinion of General Health now and six months or a year ago; ability to climb stairs, lift groceries, physical limitations at work or daily activities to feelings of depression, pain issues and energy issues. The results are used in calculating scores for eight categories, four physical related and four mental related. The final composite scores are based on a 100 point score. The lower the score in any given SF-36 category indicates a decreased ability in that category for the occupant. The individual scores were then converted into percentages and are presented that way in our tables and graphs. For example: if a subject rated his or her General Health (GH) at baseline (pre traumatic event) = 90 points and 12 months later (post traumatic event) rated his or her GH = 60 points this would represent a 33% drop in GH. For the purposes of this paper, these drops are reported as negative percentages.

RESULTS

There were a total of 469 CIREN occupants (216 male and 253 female) that had completed SF-36 data including baseline and at least one score at 10 months or more at the time of analysis. (See Table 2).

There were some basic similarities and differences in the study group demographics as shown in Table 3. The gender distribution in each group is nearly even with a slight majority going to female in every group. On average, the case occupants were all within 3 cm (1.2 in) of height and 13 kg (28.6 lb) in weight of one another. Their average MAIS scores ranged from

Table 2.
Subject Distribution by Age Group and Gender

Gender	Age Group			
	Group 1 (16-30)	Group 2 (31-47)	Group 3 (48-64)	Group 4 (65+)
Male	88	56	46	26
Female	107	57	62	27
Total	195	113	108	53

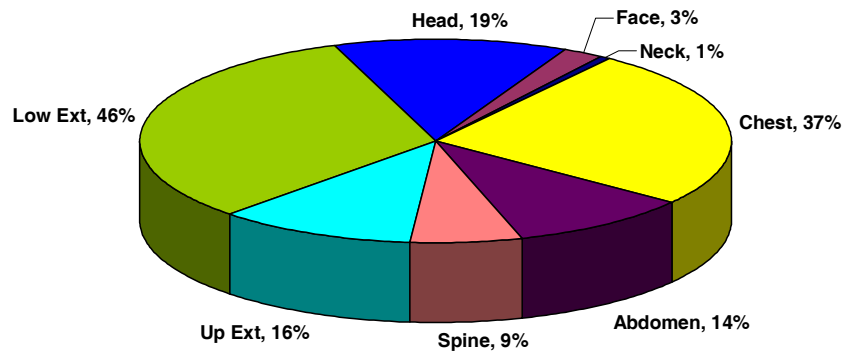
3.1 to 3.3, with the most severe being in the youngest (age 16-30) and the oldest (age 65+) age groups. The ISS score ranged from 17 in three of the groups to 19 in the youngest group. The deltaV's are all at 40 kph (24 mph) with the exception of the older group which averages 35 kph (21 mph). This group on average sustained the same severity of injury or slightly higher as the other groups but at 5 kph (3 mph) lower.

An analysis of the injuries sustained by the study group as a whole revealed that almost half (46%) sustained AIS 3+ lower extremity injuries followed by chest injuries at 37% and head injuries at 19% (See Figure 1). Since this is a count of all AIS3+ injuries, occupants could be counted twice if they sustained injuries in different body regions.

A closer look at these injuries by age (See Figure 2) shows the elderly to have consistent injury for the chest, spine and lower extremities. Head injuries indicate similar distributions with the exception of the 16 to 30 year old group where a spike of twenty-six percent is appreciated. The abdomen injury distribution is similar to the head with the 16 to 30 year old group spiking to nineteen percent. Spinal injury is evenly distributed between all groups. Lastly, the upper extremity injury distribution indicates an opposite trend to those seen in the head and abdomen. The

Table 3.
Study Group Demographics

	Total Group	Group 1 (16-30)	Group 2 (31-47)	Group 3 (48-64)	Group 4 (65+)
Male% / Female%	46 / 54	44 / 56	50 / 50	43 / 57	49 / 51
Mean Age	40	22	40	56	74
Mean MAIS	3.25	3.3	3.12	3.21	3.3
Mean ISS	18	19	17	17	17
Mean delta-V (kph)	40	40	40	40	35
Mean Height (cm)	169	170	169	169	167
Mean Weight (kg)	80	74	84	87	79



*Occupants can be counted multiple times if equal maximum injury severity scores are in different body regions.
(Chart exceeds 100%)

Figure 1. Percent AIS-3+ Injury by Body Region

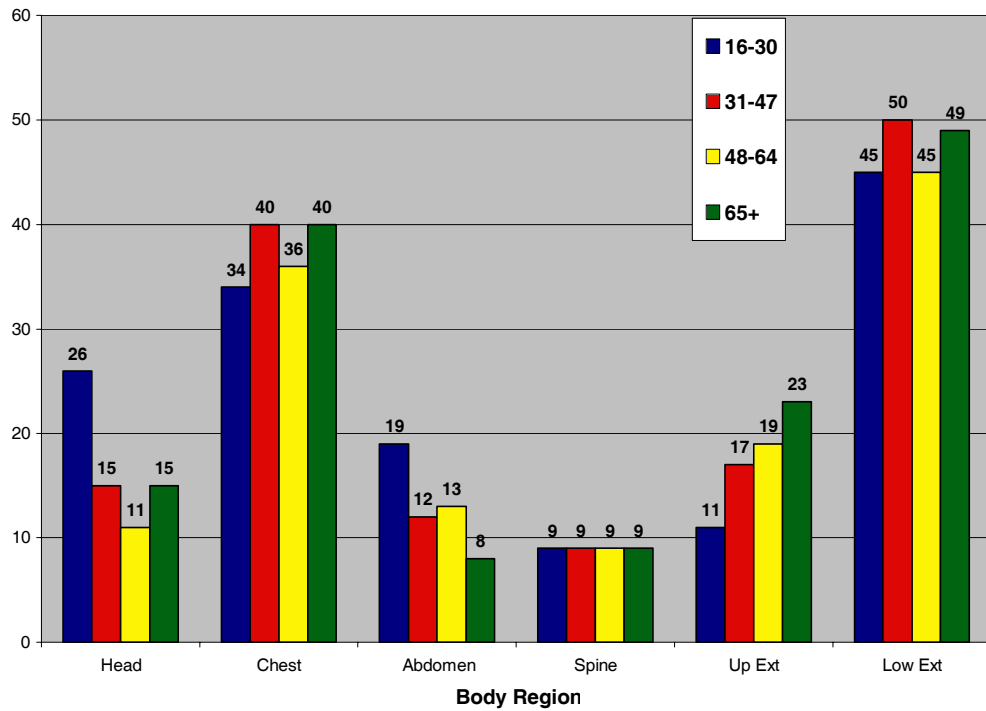


Figure 2. Percent AIS3+ Injury by body Region and Age

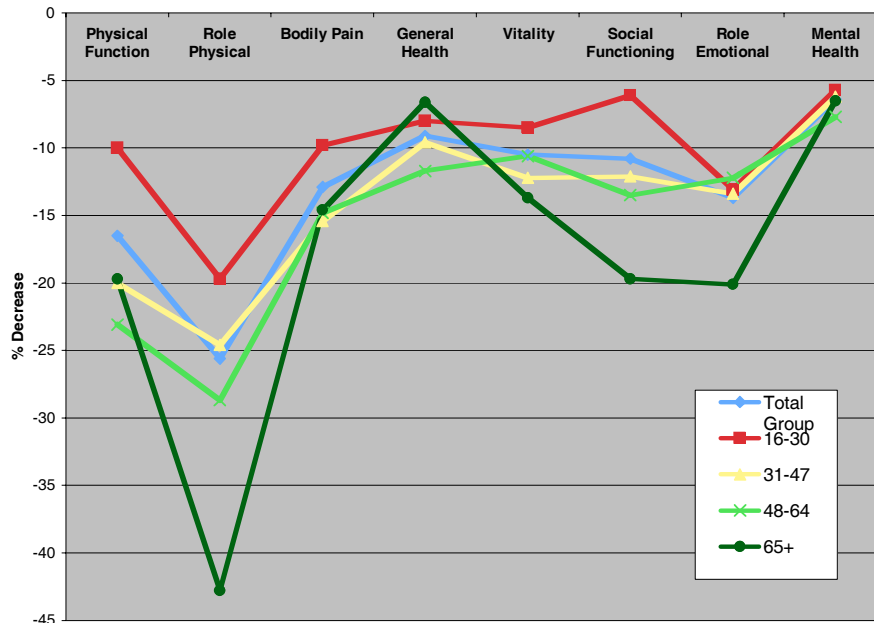


Figure 3. Mean SF-36 Decrease for all age groups individually and as a total composite

spike for the 65+ group was not as dramatic as those seen for the 16 to 30 group in the head and abdomen, but the difference between the 16 to 30 group and the 65+ group results in a twelve percent difference.

The distribution of the study population by occurrence of AIS 3+ injury by body region is shown in Figure 1. A closer analysis of these injuries by body region and age is shown in Figure 2.

The distribution of injury by age shows the elderly (group 4) to have consistent injury patterns to the general population (all Ages) with the exception of head injury and abdominal injury (See Figure 2). In both head and abdominal injury, the elderly have on average 11% less AIS 3+ injuries to these regions.

As previously indicated, SF-36 measures eight health areas (four physical related and four mental) based on the patient’s perception of how well they are doing (or not doing) in those areas at specific points in time after the crash.

For elderly occupants (group 4) Role physical showed the lowest score and was 17.2 % lower than the average score over all age groups and 23.1 % lower than the 16 to 30 year old group. Role Emotional was the next lowest score at -

20.1% followed by Social Functioning and Physical Function both at -19.7%. (See Table 4)

The largest differences between the average scores of the total group and the 65+ group were in Role Physical (-17.2% difference), Role Emotional (-6.4% difference) and Social Functioning (-8.9% difference). All other categories for Group 4 were within 3% of the average score.

Figure 3 shows the relative difference the patients perceived in their physical health (PF, RP, BP and GH) and their Mental Health (V, SF, RE, and MH). Elderly occupants rated Role Physical (RP) as the area where they were affected the most, followed by Social Functioning (SF) and Role Emotional (RE). These are the areas where they perceived they were not doing as well as they were before the traumatic event. Their perception of their decreased Role Physical (42.8%) and Role Emotional (20.1%) is likely to be related to their low Social Functioning (19.7%) role.

Conversely, this same group rated their General Health (GH) higher than other age groups. This indicates that the elderly group had a brighter outlook on their individual health outlook than individuals from the other age groupings. (A low score indicates individual/personal health perceptions as poor and likely to get worse. A

Table 4.
Mean Change in SF-36 Scores at 10-12 Months

Health Concept	Total Group	Group 1	Group 2	Group 3	Group 4
Physical Function	-16.5	-10	-20	-23.1	-19.7
Role Physical	-25.6	-19.7	-24.6	-28.7	-42.8
Bodily Pain	-12.9	-9.8	-15.4	-14.8	-14.6
General Health	-9.1	-8	-9.6	-11.7	-6.6
Vitality	-10.5	-8.5	-12.2	-10.6	-13.7
Social Functioning	-10.8	-6.1	-12.1	-13.5	-19.7
Role Emotional	-13.7	-13.1	-13.4	-12.2	-20.1
Mental Health	-6.4	-5.7	-6.2	-7.7	-6.5

high score indicates individual/personal health perceptions as excellent). There does not seem to be any logical explanation for this and would certainly be a source for further study and analysis. The eldest group assessed their individual change in Mental Health (MH) consistent with the other age groups. (Also refer to Table 4)

An additional analysis was done on each of the AIS group's drop in SF-36 scores, comparing them to the older group and the total group's average. As Figure 4 indicates, there are not significant drops in SF-36 scores in any age group like those in the older group until you reach the MAIS5 level. Granted the AIS5 level scores are much lower in a few categories, but there are many scores at or near the older group (RP, BP, V, SF and MH).

We used SAS 9.1's ANOVA procedure to perform a Dunnett's test on the data, comparing the oldest group (group 4) to each of the other groups in each of the eight health concept areas addressed by the SF-36. This showed significance for Role Physical when comparing the two youngest age groups to the elderly group at a 95% confidence level. Social Functioning between the youngest and oldest age groups at the 95% confidence level was also significant. No significance was identified between the elderly and the other age groups in any of the other health concept areas.

DISCUSSION

As the general driving population ages, they will be involved in more motor vehicle crashes.

Elderly occupants involved in crashes take longer to recover and have higher complication rates than younger patients. This observed vulnerability of older adults because of their lower physiological reserve highlights the importance of "investigating the outcomes of traumatic injuries and identifying risk factors for suboptimal recovery" in elderly patients. [8]

The unprecedented increase in the elderly population in the United States over the next several years will bring with it an increase in the injury burden of the elderly in terms of quality of life and medical costs /outcomes. That is why it is imperative to have a better understanding of the effects of serious injury on the elderly. While medical care in the United States has made great strides in taking care of the trauma population as a whole it is well known that standard treatment approaches do not produce the same outcome for all age groups. Recovery rates for similar injuries have been shown to differ substantially between the young and the elderly. The strongest predictors of long-term functional status of severely injured patients have been shown to be age and co-morbidities. [9]

By studying outcomes with the SF-36, insight is gained into how differing age populations perceive their ability to function post traumatic event. This tool has the potential to allow health care and injury researchers the ability to monitor the effectiveness of differing medical interventions for traumatically injured patients. To date much research has been performed to validate the SF-36 and the injury research community has begun to utilize this tool to give "insight into the distribution and determinants of

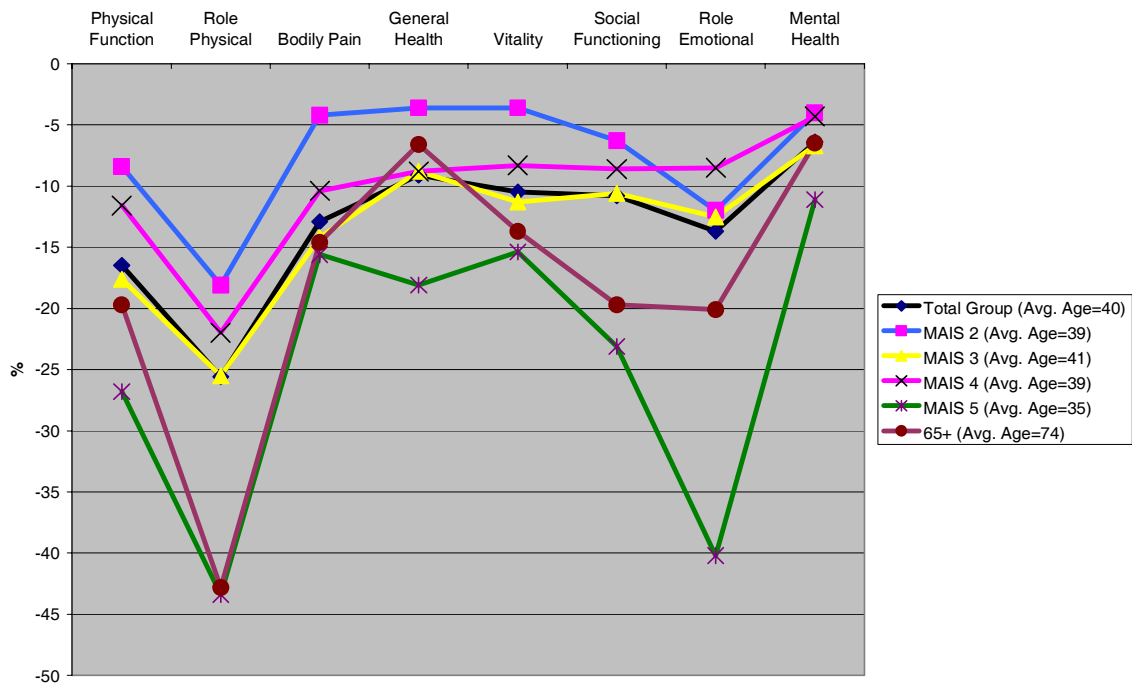


Figure 4. Comparison of Mean SF-36 Decrease - Injury Severity and Older Occupants

both short and long-term disability” and how this tool can be utilized to “prioritize the development of prevention policies and to improve trauma care”. [10]

The CIREN population utilized in this study experienced a high frequency of orthopedic injuries. This type of injury has been studied utilizing the SF-36 and the Sickness Impact Profile work scale and it has been shown that patients with orthopedic injuries have relatively worse functional recovery, and this worsens with time. [11]

The data presented in this paper indicate that not only do elderly occupants have more difficulty with their traumatic injuries affecting their work and daily activities but their mental health is affected as well. The elderly consistently show larger differences in SF-36 scores in the categories of Role Physical, Social Functioning, and Role Emotional. Interestingly, the elderly in this database feel their personal General Health perceptions are not as poor as the other age groupings. It is unknown if this “rose” outlook could keep the elderly from seeking help with any limitations they may have.

The mental scores consisting of V, SF, RE and

ME indicated stronger return to baseline for the 16 to 30 year old group compared to the remaining groups, yet this group indicated the greatest occurrence of head injury. The 65+ year old group was second to the 16 to 30 year old group for maximum head injury and rank below all groups in mean mental scores. Return to baseline for mental scores are better for every group compared to the 65+ group, even by the group who suffered more severe head injuries. Again, this highlights the potential need for differing types of rehabilitation for the elderly as it relates to specific types of injuries. The traditional acute intervention and rehabilitation methods used currently may not be meeting the needs of the elderly population.

Physical scores (PF, RP, BP, GH) indicated some substantial decreases from original baseline functions. Although this would be expected with all study groups indicating lower extremity injury as their most severe injury or one of their most severe injuries 43 to 56 percent of the time the 65+ group with 49 percent lower extremity maximum injury score far below all others in the RP category. This is consistent with the studies that have shown age and co-morbidities play a significant role in the functional recovery from trauma for the elderly patient.

This paper shows in our elderly study group that older occupants injured in crashes on average recover their activities of daily living at a much slower rate than the younger occupants. The younger occupants indicate injury at a higher degree of severity in the same body region or at a higher degree of severity in different body regions (multiple or single) and score closer to original baseline than those sustaining equal or less severe injury.

The distribution of injury by age shows the elderly (group 4) to have consistent injury patterns to the general population (all ages) with the exception of head injury and abdominal injury. In both head and abdominal injury, the elderly have on average 11% less AIS 3+ injuries to these regions. The reasons for this are unclear at this time and warrant further study. This phenomenon may be partially explained by the fact that the elderly were involved in crashes that had a delta V of 5 kph (3 mph) less than the other age groups. However, it is the authors' belief that this small reduction in the amount of kinetic energy is not great enough to explain the difference observed on the SF-36 tool.

Figure 3 shows the relative difference the patients perceived in their physical health (PF, RP, BP and GH) and their Mental Health (V, SF, RE, and MH). Elderly occupants rated Role Physical as the area where they were affected the most. This same age group also rated their personal General health better than the other age groups. This indicates that the elderly seem to have a more optimistic view of their ability to recover from their injuries over the next year than the other age groups.

The other two marked lower categories were in Social Functioning and Role Emotional (See Table 3). It is hypothesized that the scores for these categories could be related to the fact that the elderly subject (as shown by the RP score) struggles with performing daily activities and accomplishes less per day. All of these categories (RP, SF, and RE) ask the subject to comment on how physical and/or emotional problems interfere with work and daily activities. Lack of physical mobility challenges young and old. The old are challenged with many comorbid conditions such as arthritis and Parkinson's and when compounded with their traumatic injury, their locomotion could decrease even more. This

inability to be mobile could also exacerbate their decreased mental SF-36 scores. .

Further study of the injured elderly who do not appear to be recovering as expected may highlight the cases that have developed complications and these cases could be studied in more detail to potentially identify possible interventions that will avoid common complications in these patients. Potential future studies could include follow-up on the subjects who have died prior to the 6 and 12-month follow-up survey.

CONCLUSIONS:

As the NASS is utilized to show general trends in injury from motor vehicle crashes, CIREN gives the injury researcher a unique tool in the SF-36.

Since this is the first motor vehicle crash database of this size to capture SF-36 scores, it has the potential to become a tool to assess which post crash interventions yield the greatest return to normal function for these elderly patients.

REFERENCES

1. Dellinger, Ann M, Langlois, Jean A, Li, Guohua. "Fatal Crashes Among Older Drivers: Decomposition of Rates into Contributing Factors", *American Journal of Epidemiology* 2002; 155(3): 234-241
2. National Highway Traffic Safety Administration. *Traffic Safety Facts 2005 Older Population*, Washington, D.C., United States of America, DOT HS 810 622
3. Rand Corporation and John E. Ware, 1990, "The Short Form 36 Health Survey", *General Status and Quality of Life*"
4. Turner-Bowker, D., P. J. Bartley, et al. (2002). *SF-36® Health Survey & "SF" Bibliography: Third Edition (1988-2000)*. Lincoln, RI, Quality Metric Incorporated.
5. SF-36 Health Survey – Pacific Coast Wellness Center
6. MacKenzie Ellen J, McCarthy ML, Ditunno JF, et al. "Using the SF-36 For Characterizing Outcome After Multiple Trauma Involving Head Injury", *Journal of Trauma*: 527-534.

7. The SF Community – SF36 Health Survey Update” www.sf36.org/tools/sf36.shtm (accessed February 2007)
8. Richmond, T. S., H. J. Thompson, et al. (2006). "A Feasibility Study of Methodological Issues and Short-Term Outcomes in Seriously Injured Older Adults." *American Journal of Critical Care* 15(2): 158-65.
9. Holtslag, H. R., M. W. Post, et al. (2007). "Long-Term Functional Health Status of Severely Injured Patients." *Injury* 38(3): 280-289.
10. Meerding, W. J., C. W. Looman, et al. (2004). "Distribution and Determinants of Health and Work Status in a Comprehensive Population of Injury Patients." *Journal of Trauma* 56(1): 150-161.
11. Michaels, A. J., S. M. Madey, et al. (2001). "Traditional Injury Scoring Underestimates The Relative Consequences Of Orthopedic Injury." *Journal of Trauma* 50(3): 389-395; discussion 396.

USE OF MADYMO'S HUMAN FACET MODEL TO EVALUATE THE RISK OF HEAD INJURY IN IMPACT

Bertrand Fréchède

Andrew McIntosh

The University of New South Wales

Sydney, Australia

Paper Number 07-0300

ABSTRACT

MADYMO® rigid-body models are widely used in the automotive industry for a range of occupant protection related applications. These models have been evaluated at various levels against a range of experimental conditions including blunt impacts. To date the greatest focus for head impacts has been the study of severe impacts. It appears beneficial to broaden the field of validation of these models, and to expand the knowledge of tolerance limits associated with lower severity injury. In this case, mild traumatic brain injury (MTBI).

A simulation protocol was developed using MADYMO's human facet models to reconstruct 27 real-life concussive head impacts from impact sports. The cases were selected from a set that had been studied previously using a video analysis protocol. The contact behaviour of the model was first evaluated against both experimental and numerical results available in the literature. The video impact cases were then reconstructed and simulated, allowing for the assessment of a range of global biomechanical parameters that have been shown to be correlated with injury risk. The reliability of these reconstructions was evaluated by means of a sensitivity analysis of the influence of several independent variables on these dynamic outputs.

The results showed that the use of MADYMO's human facet model was adequate to obtain a representative estimate of head dynamics associated with soft to medium impact severities. They also hinted at the model's limitations to accurately model short impact durations impacts. The following mean peak values for MTBI were obtained from the reconstruction of the real-life impacts: 103 g for the head centre of gravity linear acceleration, 8022 rad/s² for the head angular acceleration and 359 for the HIC.

These values compare well with other studies and should contribute to the identification of the level at which injury first occurs.

INTRODUCTION

The head is exposed to the risk of impact and consequent injury in many areas, eg. transport, recreation, sport and assault.

In automotive accidentology, focus has been drawn so far on mitigating the risks of moderate to severe injuries, this mitigation being a priority in such impacts as pedestrian (Chidester and Isenberg 2001; Otte and Pohlemann 2001), rollover (Otte and Krettek 2005) or lateral impacts (Digges and Dalmotas 2001). Early approaches to understanding the mechanisms of head injury and the tolerance of the head to impact relied on human cadaver or animal experimentation and subsequent medical assessment of the injuries (Ommaya *et al.* 1967; Gennarelli *et al.* 1972; Ono *et al.* 1980). The advent of improved computing and numerical modelling techniques then provided additional methods of study (Ruan *et al.* 1993; Willinger *et al.* 1994; Zhou *et al.* 1995). In particular, mild traumatic brain injury or concussion had not lent itself well to cadaver or animal models, due to the functional nature of the injury and ethical issues; numerical techniques have proven a promising method to investigate this range of energy levels (Zhang *et al.* 2004). As MAIS injury levels have decreased in the last 20 years (Kullgren *et al.* 2002) thanks to improved passive measures, it appears that precise estimates of the risk of injury for contacts with softer parts of a vehicle (eg. dashboard) or other occupants may also benefit from both an improved modelization of the impact and a better knowledge of associated injury levels.

The availability of video of sports head injury events, specific medical information, and numerical methods has provided a new avenue for biomechanical analysis of the mechanisms of mild to moderate severity head injury and related tolerance limits (McIntosh *et al.* 2000; Pellman *et al.* 2003; Zhang *et al.* 2003). Sport provides the opportunity to study impacts that lead to concussion as these events are often filmed and the injured athlete is thoroughly assessed, especially in professional sport.

In this purpose, the MADYMO rigid-body modelling software package was used to simulate real-life concussive cases and to evaluate the dynamics associated with injurious levels. An evaluation of the ability of the model to describe impact dynamics was first performed in order to evaluate the reliability of these simulations and their implications for safety design strategies. Previously recorded real-life concussive head

impacts between football players were then reconstructed using MADYMO.

This paper presents the design of this protocol, including an evaluation of the head contact properties, a parametric study of the main parameters of the impact, and the results of the simulations.

MATERIALS AND METHODS

Background to the modelling

A set of a hundred videos of concussive impacts in both Rugby and Australian Rules Football was analysed and reported previously (McIntosh *et al.* 2000). For each player involved in an impact, anthropometric data (mass, height), conditions of the impact (location of the impact, head orientation, impacting segment) as well as medical assessment of the injury (definition and duration of the symptoms, concussion grade) had been collected. The kinematics of the players were then estimated, based on a 2D analysis of the videos. To refine these first calculations and precisely take into account their out-of-plane components, a 3D numerical analysis was chosen for the study presented here. Depending on the nature and duration of the impacts, an influence of the neck on the head dynamics could be expected (Beusenberg *et al.* 2001). Furthermore, a realistic simulation would depend on accurate modelling of the effective masses involved in the impact, and it was decided to model the whole players. The MADYMO human facet model's behaviour had been previously validated against several sled test as well as blunt test impact configurations (TNO 2005). Due to a more representative geometry, the contact behaviours were expected to be more precise than for the equivalent ellipsoid model. Moreover, its relative simplicity compared to an FE model allowed for easier parametrisation. For these reasons MADYMO's facet models were chosen for these simulations. The following flow-chart (figure 1) describes the methodology of the study, the grey blocks corresponding to the three stages associated to the numerical reconstruction and simulation process.

Definition and evaluation of the model's head contact properties

Management of the contact in numerical impact models is of critical importance and after a preliminary run of the parametric study presented below it appeared that the contact characteristics had a significant influence on the model's head impact responses. Furthermore, and although

MADYMO's human facet model's behaviour had been validated previously (TNO 2005) for various blunt impact locations (thorax, shoulder and pelvis), this was not the case for its head. Therefore it was decided to improve the contact properties based on recent experimental data available in the literature, and to evaluate the resulting behaviour.

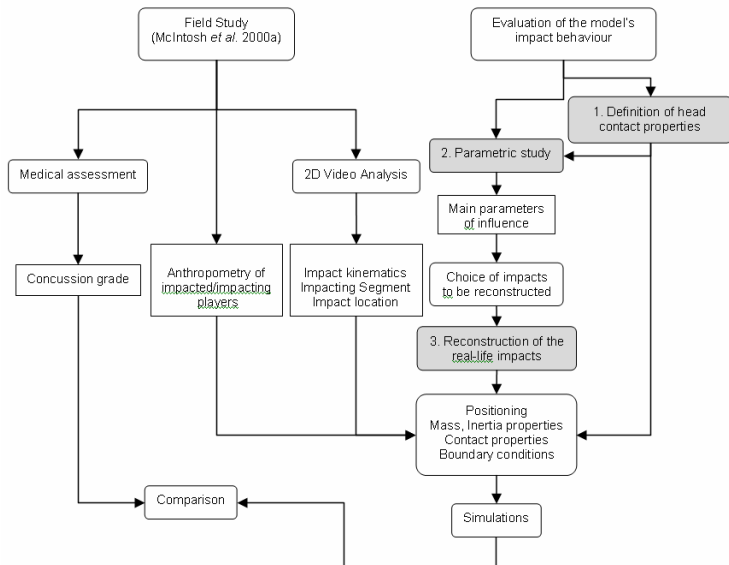


Figure 1. Flow-chart of the study's three stages.

Earlier versions of MADYMO did not allow combining the contact properties of two impacting surfaces. Therefore, combined contact characteristics had to be defined by the user or one of the objects (eg. the head) had to be defined as a rigid body. Versions 6.2 and later now authorize a combined calculation based on the contact properties of each surface and on their respective penetration, which allows for a more accurate modelling of the contact behaviour, especially in the case of two surfaces with similar contact properties. As they included both quasi-static and dynamic test conditions, the results from (Yoganandan *et al.* 1995) were used to refine the contact properties of the head model. In this experimental study, twelve unembalmed cadaveric head segments were rigidly fixed and impacted by a hemispheric rigid anvil at various locations of the head (resp. frontal, occipital, parietal, temporal and vertex impacts) and the force-deflection characteristics were measured. The loading conditions included quasi-static tests at 0.002 m/s and dynamic loadings at 7.5 ± 0.35 m/s. These two conditions (geometry, positioning, loading velocity) were reproduced with MADYMO. A quasi-static stress/penetration characteristic was defined in the model so as to obtain a good fit, respectively between the average quasi-static experimental and simulation force-deflection curves. Damping amplification properties (see appendices) were then

defined to fit the 7.5 m/s dynamic results, allowing for the definition of a complete contact characteristic. Experimental data from (McIntosh *et al.* 1993; Yoganandan *et al.* 2004) as well as FE simulation results from (Neale *et al.* 2004) were used to evaluate this behaviour.

(McIntosh *et al.* 1993) impacted seated human cadavers at head level, respectively in lateral and occipital impacts with a pneumatic impactor. Tests included both unpadding and padded (25.4 mm thick Ensolite®) impact conditions for three different velocities. Boundary conditions were clearly defined for these protocols and pulse durations of impact force and head accelerations were available. These conditions were reproduced with MADYMO and the results, in terms of impact force, head acceleration, and HIC were compared between experiment and simulation.

Published experimental results from (Yoganandan *et al.* 2004) were also used for the specific case of lateral impact. In these drop-test experiments, ten unembalmed cadaveric head specimens were dropped on a 50 mm thick, 40 Durometer material padded anvil, in order to obtain impacts in the temporo-parietal area. Impact velocities were up to 7.7 m/s and results included corridors of the measured force and acceleration responses. The boundary conditions of these tests were reproduced and simulated with MADYMO. The contact behaviour of the padded surface was defined based on Sorbothane® force/deflection characteristics. Force and acceleration results were compared with the experimental corridors.

As the simulation protocol and material properties were clearly described and included several impact conditions, results of Finite Element head drop-test simulations by (Neale *et al.* 2004) were finally used to evaluate the contact options for the head. In these drop-test simulations, a validated FE head model impacted an elastic block whose Young's modulus was chosen with values ranging from 0.63 to 25 MPa in order to control the impact durations (from 20 to 6 ms). The coefficient of friction was 0.3 and impact velocity 4.44 m.s⁻¹. To evaluate the MADYMO head model behaviour, frontal and parietal impacts to the head were modelled, reproducing the above described characteristics and boundary conditions for Young's moduli of respectively 3 MPa and 25 MPa. Results were compared in terms of acceleration of the head's CG, as well as contact forces.

Parametric study

Impacts between players were reconstructed and simulated using numerical rigid-body models in the present study. There are many degrees of freedom in such models, and assumptions regarding the model's geometry and mechanical properties influence the results. Errors may also come from

the case reconstruction process, for example from the transfer of boundary conditions (eg. velocity) assessed on the videos, to the model. Therefore, before reconstructing the real-life impacts, a study of the influence of various independent parameters on the kinematics and the dynamics of the head impact was performed.

A standardized protocol was chosen, where the full body model was positioned in a seated position and its head impacted horizontally by a spherical object. A parametric study was then performed, to assess the influence of the change in six independent variables (see table 1) on the results, when going from a low level (-1) to a high level (1) around a reference level (0) value.

Table 1. Parameters and their low/high levels

Variable	-1 / Low level	1 / High level
Velocity (m/s)	3.6	4.4
Position (cm)	Initial position -4 cm	Initial position + 4 cm
Orientation (degrees)	Perpendicular to sagittal plane	Perpendicular to sagittal plane + 20 deg
Neck stiffness (N.m)	No restraint moment	"aware" condition
Contact stiffness (N/m ²)	MADYMO limb contact stiffness - 20 %	MADYMO limb contact stiffness + 20 %
Friction coefficient	0.2	0.5

This protocol resulted in two matrixes of 64 simulations that were performed for two different changes (forward and backward) in horizontal position for the purpose of the sensitivity analysis. Simulations of the intermediate impact positions (level "0") were also performed as a check for consistency and results distribution.

In the video analysis (McIntosh *et al.* 2000), the minimal closing velocity for concussion was found to be 4.2 m/s. In the same study, the error in evaluating the velocity of the players was estimated to be less than 10 % on this set; as cases with potentially high parallax error had been excluded. Thus a mean velocity of 4 m/s, with a deviation of +/- 10 % was chosen to define the associated high and low level of this parameter in this study.

The reconstruction of the initial position of the players in the real-life impacts was performed by assessing the videos frame-by-frame. For many videos, these frames were blurry and they did not allow a precise assessment of both the location and orientation of the head impact. In order to take into account these potential sources of error, the parametric study included simulations where the centre of impact was varied with regard to an initial

position (see figure 2). As this effect was thought to be maximal on the axial rotation of the head, the positions were chosen on a horizontal plane. For the same reason, the orientation of the blow was varied 20 degrees around an initial lateral impact direction (figure 2).

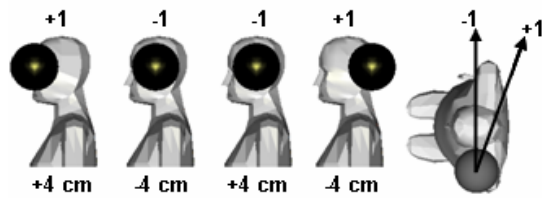


Figure 2. Positions and orientations used for the impactor, with associated low and high levels.

As the neck stiffness, in these cases representative of the player's level of muscular activation and strength, was expected to possibly influence the results, two levels were taken into account in the parametric study. The high level, corresponding to an 'aware' state, was modelled by adding restraint torques at neck level to model muscle contraction. The values, 52 N.m in extension, 30 N.m in flexion, 12 N.m in axial rotation and 31 N.m in lateral bending, were chosen at 80% of the range of maximal isometric neck torques defined in a review by (Portero and Genries 2003), the 80% threshold of maximal voluntary force having been proposed by (Mertz *et al.* 1997) for N_{ij} calculations with aware occupants in frontal impact. No restraint torques were added to the passive properties of each cervical level for the low level.

Finally, contact properties influence the results (Camacho *et al.* 1999); they may depend on the subject and on the location on the body. Therefore, the limb contact characteristics present in MADYMO and used for this analysis were varied within +/- 20% of their mean value to assess this influence. In a review by (Sivamani *et al.* 2003), dynamic friction coefficient for the skin was found to range from 0.2 to 0.7. As a value of 0.34 had been described for the forehead, and as high values induced noise in the calculations, the coefficient was varied between 0.2 and 0.5 in this study.

Simulations were performed on a 200 ms time frame with a time step of 10^{-3} ms, allowing for the description of both the impact and the kinematics shortly thereafter. The dependant variables chosen as output were the Head Impact Power (HIP)- (Newman *et al.* 2000b), Head Impact Criterion (HIC_{15}), 3ms and peak linear (at the head's CG) and angular acceleration of the head.

Reconstruction of the real-life impacts

Following the results of the parametric study, and in order to limit the effects of possible error in the assessment of the impact velocity due to the 2D analysis, 27 cases out of the 100 from the initial database were selected and reconstructed. These

videos were chosen based on their clear description of the event; allowing for both the determination of accurate boundary conditions and the assessment of the reliability of the simulations. In particular, videos were chosen where the closing movement of the players occurred in the plane of the camera, to minimize errors made in the calculation of the initial velocity. In all cases head injuries had been well document and concussion graded according to the following criteria: Grade 1 – no loss of consciousness (LOC); Grade 2 – LOC < 1 min; and, Grade 3 – LOC > 1 min.

The simulations of an impact between two players were performed using the following protocol: first, the models were positioned using HyperMesh® to reproduce the relative position of each player just before the impact (figure 3).



Figure 3. Reconstruction of the relative positions before impact.

The masses and inertias of each model's body segments were calculated based on the known anthropometry of the players and GEBOD (Cheng *et al.* 1994) scaling equations. They were then input into the models. The initial velocities of each human model were the closing velocities previously assessed during the video analysis. The parametric study had concluded that neck stiffness had a low influence on the head behaviour compared to other variables. Furthermore, it was difficult to assess the awareness of the injured players on some of the videos. Therefore, a generic "unaware" state was modelled: joint restraint torques were input into the model so that it could just maintain the standing upright position in a pre-simulation. Finally, the initial position of the model, the initial velocity of each body segment and the stiffness of each joint were tuned in order to obtain a satisfactory match between the kinematic behaviour of the impacting bodies compared to the real event on video. The restraint torques used for the shoulder, elbow, hip, knee, and ankle, were chosen in the range of the values proposed by (Stobbe 1982). The simulation period was 200 ms which incorporated both the impact and immediate post impact kinematics. All simulations were run using HyperMesh v6.0 and MADYMO v6.2.2.

Biomechanical Output Data

In order to compare the results with the existing video analysis data, the Peak Velocity Change (PVC), impulse and impact energy of the head were calculated. For means of comparison with the literature, the impact energy was calculated as the

energy needed to allow the head's peak change in velocity, allowing the definition of an equivalent drop-test impact energy. The impulse was calculated at the same time of peak change. The head's CG linear acceleration, head angular acceleration, HIC₁₅ and HIP were also calculated in order to study the biomechanics of concussion and for comparison with the literature.

RESULTS

Definition and evaluation of the model's head impact properties

An example of simulations of an impact following each protocol (McIntosh *et al.* 1993; Neale *et al.* 2004; Yoganandan *et al.* 2004) is presented in figure 4.

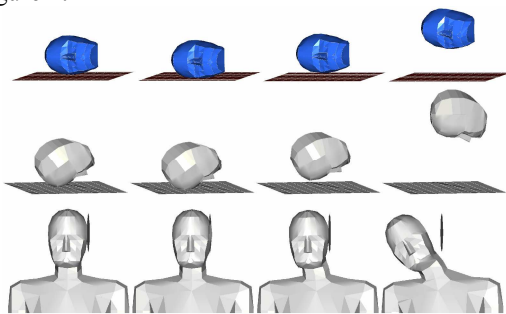


Figure 4. Simulations of Yoganandan *et al.*, Neale *et al.* and McIntosh *et al.* (from top to bottom) impact conditions.

Simulation of Yoganandan's experiments :

Figure 5 presents a comparison between the simulation and experimental results for this series of drop-tests. Experimental results present the average and standard deviation of the 10 tests. Simulations results present outputs for simulations with the min/average/max head weight from the experiment. Both the peak force and acceleration compare well with the experiment for this relatively soft impact.

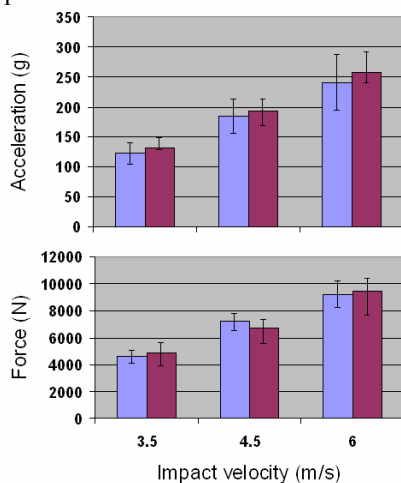


Figure 5. Comparison of experimental (in blue) and simulation (in red) peak force and acceleration.

Simulation of Neale's simulation protocol :

The results are presented in table 2 and table 3. In the 3 MPa frontal and parietal impacts, differences between simulation and experimental results are within 11%. In the 25 MPa impacts, the same trend is observed for the peak force and linear acceleration. However, there are large differences (up to 50 %) between the simulated and experimental peak angular accelerations for both impacts. For the 25 MPa impacts, force pulse durations were significantly higher (up to 25%) in the MADYMO simulation.

Simulation of McIntosh's experiment :

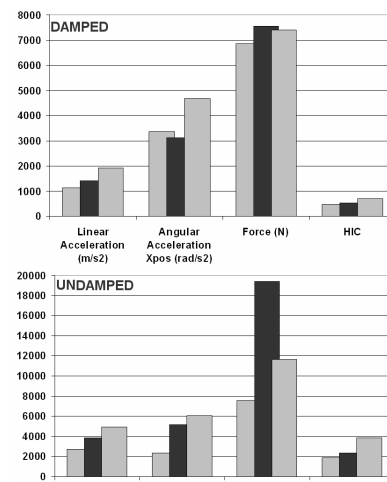


Figure 6. Comparison between simulation and experimental results from (McIntosh *et al.* 1993) for the Aluminium (undamped) and Ensolite (damped) 5.9 m/s parietal impacts.

Figure 6 presents peak values in linear acceleration of the head's CG, Force and HIC for the Aluminium (5 ms) and Ensolite (11 ms) parietal impacts, compared between simulations and experiment. Results are within, or close to the experimental range of values for both impacts. However, for the undamped impact, the peak force output is significantly out of the experimental corridor by 66%.

Parametric study

Table 4 gives a statistical description of the 192 simulations set (including intermediate positions), and Figure 7 shows an example of the distribution of the mean HIC values and peak angular acceleration of the head for the various positions. As none of the outputs were found to be normally distributed, the relative influence of each of the parameter was assessed by representing it as a scatter plot with the means (see figure 7 for an example of the effects). In order to compare the influence of each parameter, changes in the variables between low and high level were normalized by expressing them as a percentage of

Table 2. Comparison between simulations and (Neale *et al.* 2004) for the 12ms and 6ms frontal impacts

FRONTAL IMPACT					
	Acceleration		Force (N)	Duration (ms)	HIC
	Linear (g)	Rotational (rad/s ²)			
E = 3 MPa					
Mean	144	1839	6700	12.5	906
(Neale 2004)	132	1727	6700	12.0	-
E = 25 MPa					
Mean	248	4293	11550	7.5	1536
(Neale 2004)	231	8510	11900	6.0	-

Table 3. Comparison between simulations and (Neale *et al.* 2004) for the 12ms and 6ms parietal impacts

PARIETAL IMPACT					
	Acceleration		Force (N)	Duration (ms)	HIC
	Linear (g)	Rotational (rad/s ²)			
E = 3 MPa					
Mean	151	3372	7026	12.0	1019
(Neale 2004)	140	3774	6800	12.0	-
E = 25 MPa					
Mean	222	5313	10283	7.4	1450
(Neale 2004)	210	7773	11800	6.0	-

Table 4. Descriptive statistics for each parameter, for 192 simulations, including intermediate positions

	HIP (W)	HIC	Linear acceleration (m/s ²)		Angular acceleration (rad/s ²)	
			3ms	Max	3ms	Max
			Mean	9081	287	504
Stdev ¹	2624	124	125	183	711	1994
CV ²	0.29	0.43	0.25	0.23	0.24	0.4
CL Sup. ³	9393	302	519	810	3065	5232
CL Inf. ⁴	8770	272	489	767	2896	4759

⁽¹⁾ Standard deviation

⁽²⁾ Coefficient of variance

^{(3),(4)} 95% Confidence Intervals of the mean, upper and lower limit.

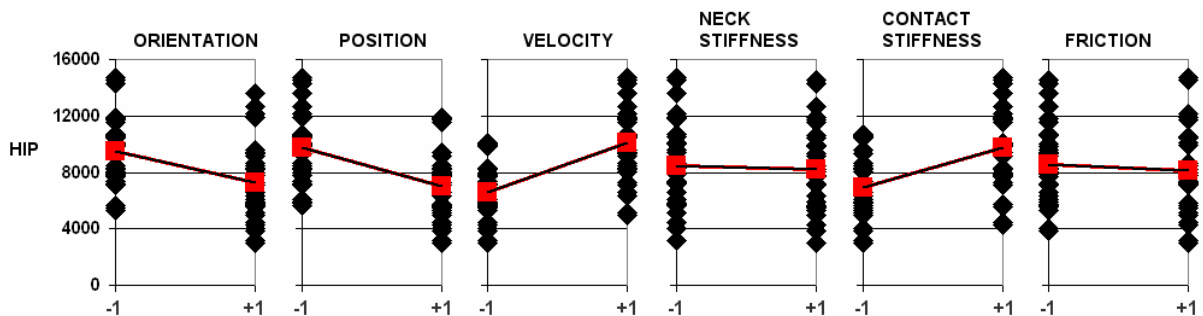


Figure 7. Scatter and mean plot of the influence of each of the six parameters on the HIP values, in the case of the rearward change in position.

the initial (low level) value. These percentages of change were then averaged between the two sets (forward and rearward direction of change), allowing a ranking of each parameter's influence on the output variable (see table 5). From these results, peak angular acceleration of the head is influenced dramatically by changes in position, while changes in velocity affect primarily HIC and HIP values. Changes in contact stiffness of the model also have a significant influence on each variable, although this is not true for the 3ms values (linear and angular acceleration). Friction coefficient, orientation of the impact and neck stiffness have relatively no significant influence. Overall, HIC value and peak angular accelerations of the head are the most influenced by change in the parameters, and 3ms values are the least. Finally, object contact stiffness shows the most influence on variables which depend on durations (HIC and HIP).

In the same way, influence of a combination of two variables, or cross-effects, were then evaluated for combinations of the major influencing parameters. Assuming that cross-effects between two variables would account for the main changes in the model's behaviour, the result show that a cross-effect between velocity and contact stiffness has an important influence both on the HIP and HIC values, while a combination of each of this variable with position influences mainly peak angular acceleration. These effects reached respectively 110%, 141% and 95% of the low level value. The 3ms accelerations, linear and angular are the least influenced, percentages being respectively 40 and 50%.

Real life impacts reconstruction

Figure 8 presents a visual comparison between one of the impacts and its simulation.

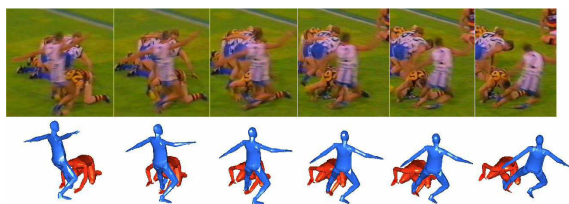


Figure 8. Simulation of an Australian Rules Football impact.

In this case (nb. 4) the player was hit by an opponent's knee while crouching to catch the ball. He was not aware of the incoming impact and suffered no LOC from it, resulting in a Grade 1 concussion classification. Table 6 presents a summary of the mean peak values and range for each biomechanical variable stratified according to each concussion grade and table 7 presents the results of each simulation. There were nine simulations for each grade of concussion. HIC values for concussion ranged from 87 to 994. The

latter HIC was reached for one of the most severe impacts, where peak values of 200 J in impact energy and of 43 kg.m/s impulse were reached. The overall mean values for HIC, peak linear and angular acceleration were 359, 103g, and 8022 rad/s², respectively. Although some of the results demonstrated high standard deviations (respectively 68% and 69% of the mean value for HIC and HIP), a common trend between injury severity and some of the biomechanical parameters can be observed.

DISCUSSION

The initial aim of this study was first to improve the reliability of the case study video analysis performed previously, and to evaluate the dynamics associated with concussive head impacts.

Secondly we also aimed at evaluating the reliability of using a rigid-body software such as MADYMO to estimate these parameters. Although such models are used both in research and in the automotive industry to model pedestrian impacts, an evaluation of the facet model's head behaviour had not been documented before.

A parametric analysis was undertaken, which showed that the rigid-body model's head contact properties influenced the biomechanical parameters used as estimators of the risk of concussion. New contact characteristics were proposed, that allow taking into account the combined behaviours of the two impacting objects, and refine the existing ones by taking into account damping effects. As these contact properties proved to be adequate to model the relatively soft impacts between players, they were used to reconstruct 27 real life concussive impacts in order to obtain an estimate of the biomechanical parameters associated with this first level of injury.

Definition of the model's head contact properties

Results in terms of peak accelerations, peak forces and HIC values compare well with the experiments for the three sets of evaluations. However, significant differences are found for the peak angular accelerations and forces for the short-duration impacts (≤ 6 ms). In the simulation of Neale et al.'s protocol, the differences in angular rotations may be explained by a relative coarseness of the mesh in this version of the model, meaning that small differences in initial positioning between the head models may yield significant differences in their rotational behaviour.

In the same protocol, the peak force results of the simulation for the undamped impact show an important difference (66%) which is accounted mainly by high damping forces. At this stage, it is unclear if this short duration peak is an artefact of the simulation, due for example to the rough mesh, or if the head damping properties have to be

adapted for this kind of very short duration impact. As skull fractures were not modelled, but occurred in each of the undamped experimental impacts, simulations may yield these unrealistic results. Part of the above described inconsistencies may also relate with previous observations by (Neale *et al.* 2004), and may reflect the fact that a rigid-body model may not be accurate enough to model short-duration impacts because of the coupling/decoupling process involved between the brain and skull.

The impact conditions assessed in Yoganandan and al.'s experiments correspond to an impact into a polyurethane material, similar to a dashboard. The combined contact definition yields satisfying results for these impact conditions. Several limitations may be associated with the evaluation process presented here. First, the experimental force-deflection curve used to define the contact properties is an average

of results obtained for several impact locations on the head. It is acknowledged that differences in bone properties and skull thickness will influence the local behaviour of the head, however at this stage our aim was to improve the existing modelling, and to obtain a reasonable estimate of the impact dynamics. The parametric study was intended to allow the definition of possible uncertainties. It is also acknowledged that the impact behaviour will depend from the modelling of the second impact surface (in our case, limb, thorax, abdomen or head of the impacting player). The associated MADYMO bi-linear contact properties had been evaluated previously by means of blunt test simulations based on PMHS experiments, and were used as such. They would however benefit from a refined definition for the purpose of improving the combined contacts approach.

Table 5.
Influence of each parameter (expressed in percentage of change from low to high level), ranked from highest to lowest

(%)	HIP	HIC	Linear acceleration		Angular acceleration		Average effect
			3ms	Max	3ms	Max	
Position	-21.1	-37.9	-37.8	-22	26.5	96.9	40.4
Velocity	51.8	76.9	13.8	25.6	19.8	23.7	35.3
Contact Stiffness	38.6	35.8	1.5	34.8	13.3	21.9	24.3
Orientation	-12.8	-10.5	-5.6	-7.1	-4.4	-16.6	9.5
Friction	-6.3	8.8	8.4	-0.7	-0.2	-5.5	5
Neck Stiffness	-2.4	-1.3	-1.3	-0.7	1.5	-0.90	1.4
Average Effect	22.2	28.5	11.4	15.1	11	27.60	

Table 6.
Mean peak values reached by the biomechanical parameters during the simulations

		Impact energy (J)	Impulse (kg.m/s)	HIP (W)	HIC	Acceleration				PVC ⁽¹⁾ (m/s)	Duration (ms)
						Linear (g)		Angular (rad/s ²)			
						3ms	Max	3ms	Max		
Grade1 ⁽²⁾	Mean	63	24	8830	231	64	86	4380	7240	5.0	21
	Min	25	15	4600	87	47	60	2010	3470	3.2	8
	Max	103	32	14990	471	81	100	9500	14720	6.5	46
Grade2 ⁽²⁾	Mean	82	27	11030	333	72	101	4760	7350	5.7	24
	Min	28	17	5080	111	50	60	2700	3880	3.4	7
	Max	164	40	15550	976	109	183	7100	15130	8.3	54
Grade3 ⁽²⁾	Mean	105	31	21280	513	93	123	5650	9470	6.5	12
	Min	51	22	6800	232	70	84	2950	5100	4.7	7
	Max	200	43	53990	994	122	152	10900	16450	9.3	16
All	Mean	83	27	13715	359	76	103	4930	8020	5.8	19
	Min	25	15	4600	87	47	60	2010	3470	3.2	7
	Max	200	43	53990	994	122	183	10900	16450	9.3	54

⁽¹⁾ Peak Velocity Change

⁽²⁾ Grade 1: no LOC

Grade 2: LOC < 1 min

Grade 3: LOC > 1 min

Table 7. Peak values reached by each biomechanical parameter for each case

Case	Grade	Impact energy (J)	Impulse (kg.m/s)	HIP (W)	HIC	Linear acc. (m/s ²)		Angular acc. (rad/s ²)		PVC (m/s)	Duration (ms)
						(3ms)	(Max)	(3ms)	(Max)		
1	1	78	27	4604	471	799	934	5780	7659	5.8	9.1
2	1	47	21	7788	142	523	710	2610	4070	4.5	14.1
3	1	46	20	8614	87	464	586	7050	9806	4.5	42.0
4	1	59	24	12437	218	653	795	2410	5957	5.0	11.8
5	1	39	20	5536	208	596	980	3085	8526	4.0	8.3
6	1	86	29	6614	294	729	980	2950	3466	5.9	12.4
7	1	25	15	12784	127	520	796	9500	14718	3.2	7.7
8	1	82	29	6101	229	640	906	2010	4379	5.7	42.0
9	1	103	32	14990	301	723	930	4020	6594	6.5	46.0
10	2	78	27	5078	178	542	596	2700	3881	5.8	21.7
11	2	28	17	12963	203	571	963	6345	9301	3.4	7.4
12	2	164	40	14831	250	721	921	4020	5670	8.3	42.0
13	2	93	29	12867	585	983	1338	5150	8285	6.4	9.5
14	2	47	21	6955	111	492	588	5410	6550	4.6	20.7
15	2	106	32	8091	238	674	905	4050	6560	6.6	40.0
16	2	53	23	15549	241	641	1001	3460	4697	4.7	54.0
17	2	62	24	9724	214	651	799	4630	6087	5.2	14.1
18	2	110	33	13233	976	1065	1793	7100	15133	6.7	7.8
19	3	78	28	14074	501	878	1432	6200	13160	5.6	7.0
20	3	120	34	21145	641	1031	1266	4541	7282	7.1	11.3
21	3	99	30	6799	405	900	1136	2950	6366	6.5	14.8
22	3	136	36	30256	684	1078	1300	3400	7738	7.5	12.2
23	3	103	31	19668	422	867	1077	4000	5100	6.5	12.0
24	3	51	22	53993	293	725	1108	10900	16450	4.7	9.8
25	3	77	27	15000	232	687	827	5240	9079	5.8	15.5
26	3	200	43	16258	994	1200	1490	8900	10935	9.3	13.2
27	3	79	27	14358	443	888	1209	4700	9132	5.8	10.7

Parametric study

The results of this study show that errors in evaluating both the exact location and the velocity of the impacting objects may have the strongest influence on the biomechanical parameters used as estimators of the risk of concussion (see table 5). These parameters (HIC, HIP, head linear acceleration and angular acceleration) had been previously shown (Newman *et al.* 2000a; Zhang *et al.* 2004) to be acceptable estimators of the injury risk.

Beusenberg *et al.* (2001) emphasised that the head's behaviour during an impact simulation was dependant on the modelling of the neck with consideration for the rest of the body. This is not the case in this study, and may be explained by the importance of effective masses and compressive loading mechanism of the neck in Beusenberg's simulation protocol; no such loading direction was performed in our real-life scenarios. Also, the range chosen for the low and high level in our parametric study have an influence on the results. They were however chosen carefully to be representative, either of possible errors in the reconstruction of the boundary conditions, or of possible fluctuations in the model's degrees of freedom. Results may also have varied depending on the initial location of the centre of impact. For this reason, the changes in variables were averaged for changes both in the forward and in the rearward direction. Intermediate positions were also simulated in order to check the consistency of the evolution in behaviour.

These results showed that estimating precisely the position and velocity were important for the real-life case study simulations. This suggested restricting the ongoing reconstructions to impacts that were in the plane of the videos and where the

location of the impact could be estimated precisely. Therefore, out of the initial 100 videos available, a set of 27 cases was chosen, where these constraints were met.

Results showed that the model's contact stiffness properties also had an influence on the results, and for this reason the evaluation of the model's head behaviour was undertaken. Following this study, the impact durations of the real-life reconstructions (7-54 ms) were deemed long enough to ensure that the results were not influenced by errors due to short duration impacts reconstructions with MADYMO.

Finally, the low and high levels were chosen to allow a full range of deviation (assuming for example an uncertainty of 20% in estimating the velocity, or of 8 cm in positioning). If we assumed a worst-case scenario with a cross-effect of the two main influencing effects, the boundary of the associated uncertainties would range from +/- 20 % for the 3ms linear and angular acceleration, up to +/- 70 % for the HIC value.

Reconstruction of real-life impacts

Table 8 presents a comparison of the mean peak values reached with the MADYMO simulations with the ones calculated from the video analysis, for the same set of 27 cases and for the whole set of 100 cases. The results show a similar trend between the simulation and the video analysis although mean peak values for the simulations were slightly higher. This difference may be explained by the fact that numerical reconstructions allowed consideration for velocities after impact that were out-of-plane, which could not be evaluated in the previous 2D video analysis.

Table 8.
Compared results for the simulations and previously performed video analysis

SIMULATION			VIDEO ANALYSIS (same 27 cases)			VIDEO ANALYSIS (all 100 cases)		
Impact energy (J)	Impulse (kg.m/s)	PVC (m/s)	Impact energy (J)	Impulse (kg.m/s)	PVC (m/s)	Impact energy (J)	Impulse (kg.m/s)	PVC (m/s)
83	27	5.8	73	24	5.2	67	23	4.8

Numerical studies on head injury biomechanics have been performed previously, and a large number were aimed at describing the mechanisms of injury and therefore used more precise FE models (Ruan *et al.* 1993; Miller *et al.* 1998; Kleiven and Von Holst 2002; Zhang *et al.* 2004). Only a few studies reported on real life accident reconstruction, either using dummy human

surrogates (Newman *et al.* 1999; Pellman *et al.* 2003) or numerical models (Baumgartner *et al.* 2001; O'Riordain *et al.* 2003; Zhang *et al.* 2004). Some of these results are presented and compared with our results in table 11. The results of the present work show that concussion occurs for similar values of HIC, HIP, and accelerations as in similar studies.

Table 9.
Comparison with similar studies

	Impact energy (J)	HIC	HIP (W)	Acceleration		PVC (m/s)	Risk of Concussion
				Linear (g)	Angular (rad/s ²)		
(Newman 2000)		240 485	12790 20880	78 115	6322 9267		50% 95%
(Pellman 2003)	118	381	-	98	6432	7.2	Mean value
(Zhang 2004)		240 369	- -	82 106	5900 7900		50% 95%
This study	83	359	13715	103	8020	5.8	Mean value

These results are encouraging, as they show realistic head dynamics. It is however difficult to assess both the presence and severity of all injury types. Reasons are numerous and relate to the difficulty in taking into account variability both in the injured human and in the impact situations and the range of experimental data acquired. Indeed, the validity, from content to external, of global mechanical parameters and injury criteria to assess injury risk remains a point of argument and controversy (King *et al.* 2003). For example, the HIC is based on the experimental assessment of the presence or absence of fractures and it is a significant extrapolation to use it as a general predictor of concussion or MTBI, as it is now characterised in sport. Nevertheless, some studies have found significant correlations between global criteria and the risk of concussion (Ruan *et al.* 1993; Newman *et al.* 2000a; Zhang *et al.* 2004). They are also simple to calculate, generally highly reliable in impact testing, and may be used effectively for means of comparisons. Some, like the impact energy are a simple approach by which an equivalent impact energy for testing can be determined.

Although no control (no-injury) cases were included in this study, our results are in close agreement with previously (Zhang *et al.* 2004) suggested values for a tolerable reversible brain injury. As Grade 1 MTBI's were associated with mean HIC values of 230, HIP values of 8830 and combined linear and angular acceleration of respectively 86 g and 7240 rad/s², these could be added to the pool of existing tolerance values proposed for this specific injury.

CONCLUSION

Twenty-seven cases of medically verified concussion from rugby union and Australian football were reconstructed using numerical simulation. The simulations were able to refine and add to data obtained from a previously performed video analysis. By modelling real-life concussive head impacts, the results of this study allow us to

precise the knowledge of biomechanical tolerance levels associated to the presence of an injury.

Results from the sensitivity study show that HIC values and peak angular accelerations of the head are significantly influenced by both the degrees of freedom in the model and the boundary conditions of the impact. These conclusions oriented us to restrict drastically the number of reconstructions in the real-life study that followed, and to evaluate the behaviour of the model's head during impact.

In particular, these real-life reconstructions allow presenting the following findings:

- Grade 1 concussions occurred for impacts involving mean energies of 60 J, and impulses of 24 kg.m.s⁻¹. These values confirm previous findings and may contribute to the design of experimental testing procedures.

- Based on our results and similar studies (Pellman *et al.* 2003; Zhang *et al.* 2004), suggested tolerance values for concussion are as follows: 230 for HIC₁₅, 8830 W for HIP, 85 g and 6000 rad/s² for combined peak linear and angular acceleration of the head.

Finally, the evaluation performed in this study is a contribution towards an improvement in the use of head impact models in rigid body simulations. Results from this evaluation suggest that, although the behaviour has to be improved for short impact durations, HIC values, forces and peak linear acceleration of the head's CG obtained by using a rigid-body model with adequate contact characteristics are representative of real-life impacts. As they were not evaluated against experimental results, or presented significant differences with previously published experimental or simulation data, respectively HIP values and angular acceleration of the head should be assessed with caution.

Despite these restrictions, using human rigid-body models in impact present several advantages when the aim is to study the risk of injury associated with real-life accident reconstruction. It is also believed that this approach may be beneficial as an input to more refined simulations more focused at assessing the associated injury mechanisms.

APPENDICES

$$\sigma = \sigma_e + \left[C_d \frac{\dot{\lambda}}{t} \right] \cdot f_d \quad (1)$$

$$\sigma_e = f\left(\frac{\lambda}{t}\right), f_d = f(\sigma_e)$$

σ_e = elastic (quasi-static) stress function

C_d = damping coefficient (0.1333)

f_d = damping amplification function (difference between quasi-static and dynamic functions)

λ = penetration

t = surface thickness (normalized to 1.0 in our case)

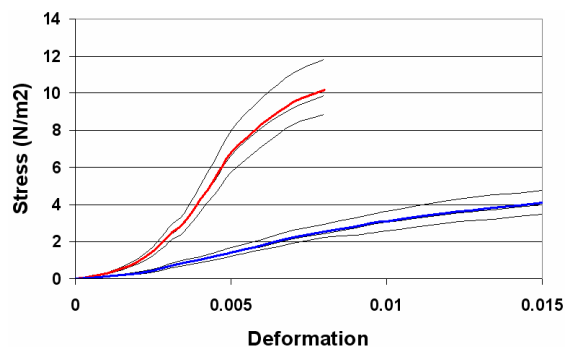


Figure 9. Averaged quasi-static and dynamic (resp. blue and red) stress functions used for MADYMO's head contact properties, based on the response to the occipital, parietal and frontal impacts (corridors in black) described in (Yoganandan *et al.* 1995).

Due to the choice of an averaged normalizing thickness, these characteristics do not represent the stress/penetration characteristics for a human head. However, their use in the previous equations (1) allow for a good fit of the resulting quasi-static and dynamic force-deflection curves obtained with this facet model.

REFERENCES

- [1] Baumgartner D., Willinger R., Shewchenko N. Beusenberg M. 2001. Tolerance limits for mild traumatic brain injury derived from numerical head impact replication. *Proceedings of the IRCOBI Conference*, Isle of Man, UK.
- [2] Beusenberg M., Shewchenko N., Newman J., DeLange R. Cappon H. 2001. Head, neck, and body coupling in reconstructions of helmeted head impacts. *Proceedings of the IRCOBI Conference*, Isle of Man, UK.
- [3] Camacho D., Nightingale R. Myers B., "Surface friction in near-vertex head and neck impact increases risk of injury". *Journal of Biomechanics* 32 (3): 1999, p. 293-301.
- [4] Cheng H., Obergefell L. Rizer A. 1994. Generator of Body (GEBOD) Manual. AL/CF-TR-1994-0051. Wright-Patterson Air Force Base, Ohio, Armstrong Laboratory.
- [5] Chidester A. B. Isenberg R. A. 2001. Final report - the pedestrian crash data study. *Proceedings of the 17th International Conference on the Enhanced Safety of Vehicles*, Amsterdam, The Netherlands, US Department of Transportation National Highway Traffic Safety Administration.
- [6] Digges K. Dalmotas D. 2001. Injuries to restrained occupants in far-side crashes. *Proceedings of the 17th Conference Enhanced Safety of Vehicles*, Amsterdam, The Netherlands, US Department of Transportation National Highway Traffic Safety Administration.
- [7] Gennarelli T., Thibault L. Ommaya A., "Pathophysiologic responses to rotational and translational accelerations of the head". *Proceedings of the 16th Stapp Car Crash Conference Paper 720970*: 1972, p. 296-308.
- [8] King A. I., Yang K. H., Zhang L. Hardy W. 2003. Is head injury caused by linear or angular acceleration? *Proceedings of the IRCOBI Conference*, Lisbon, Portugal.
- [9] Kleiven S. Von Holst H., "Consequences of head size following trauma to the human head". *Journal of Biomechanics* 35: 2002, p. 153-60.
- [10] Kullgren A., Krafft M., Ydenius A., Lie A. Tingvall C. 2002. Developments in car safety with respect to disability - injury distributions for car occupants in cars from the 80's and 90's. *Proceedings of the IRCOBI Conference*, Munich, Germany.
- [11] McIntosh A., Kallieris D. Mattern R., "Head and neck injury resulting from low velocity direct impact". *Proceedings of the 37th Stapp Car Crash Conference Paper 933112*: 1993, p. 43-58.
- [12] McIntosh A. S., McCrory P. Comerford J., "The dynamics of concussive head impacts in rugby and Australian rules football". *Medicine and Science in Sport an Exercise* 32 (12): 2000, p. 1980-84.
- [13] Mertz H. J., Prasad P. Irwin A. L. 1997. Injury risk curves for children and adults in frontal and rear collisions. *41st Stapp Car Crash Conference*.

- [14] Miller R. T., Margulies S. S., Leoni M., Nonaka M., Chen X., Smith D. H. Meaney D. F., "Finite element modeling approaches for predicting injury in an experimental model of severe diffuse axonal injury". *Proceedings of the 42nd Stapp Car Crash Conference* SAE paper 983154: 1998, p. 155-66.
- [15] Neale M., McGrath M., Baumgartner D. Willinger R. 2004. Comparative study between finite element human head and dummy head model responses under impact. *Proceedings of the IRCOBI Conference*, Graz, Austria.
- [16] Newman J., Beusenberg M., Fournier E., Shewchenko N., Withnall C., King A., Yang K., Zang L., McElhaney J., Thibault L. McGinnes G. 1999. A new biomechanical assessment of mild traumatic brain injury: Part 1 - Methodology. *Proceedings of the IRCOBI Conference*, Sitges, Spain.
- [17] Newman J., Barr C., Beusenberg M., Fournier E., Shewchenko N., Welbourne E. Withnall C. 2000a. A new biomechanical assessment of mild traumatic brain injury: Part 2 - Results and conclusions. *Proceedings of the IRCOBI Conference*, Montpellier, France.
- [18] Newman J. A., Barr C., Beusenberg M., Fournier E., Shewchenko N., Welbourne E. Whitnall C., "A new biomechanical head injury assessment function - the maximum power index". *STAPP Car Crash Journal* 44: 2000b, p. 362-94.
- [19] O'Riordain K., Thomas P. M., Phillips J. P. Gilchrist M. D., "Reconstruction of real world head injury accidents resulting from falls using multibody dynamics". *Clinical Biomechanics* 18 (7): 2003, p. 590-600.
- [20] Ommaya A., Yarnell A., Hirsch A. Harries A. 1967. Scaling of experimental data on cerebral concussions in sub-human primates to concussion threshold for man. *Proceedings of the 11th Stapp Car Crash Conference*.
- [21] Ono K., Kikuchi A., Nakamura M., Kobayashi H. Nakamura N., "Human head tolerance to sagittal impact - reliable estimation deduced from experimental head injury using subhuman primates and human cadavers skulls". *Proceedings of the 24th Stapp Car Crash Conference* Paper 801303: 1980, p. 379-89.
- [22] Otte D. Pohlemann T. 2001. Analysis and load assessment of secondary impact to adult pedestrians after car collisions on roads. *Proceedings of the IRCOBI Conference*, Isle of Man.
- [23] Otte D. Krettek C. 2005. Rollover accidents of cars in the german road traffic - an in-depth analysis of injury and deformation pattern by GIDAS. *Proceedings of the 19th Enhanced Safety of Vehicles Conference*, Washington, USA, US Department of Transportation National Highway Traffic Safety Administration.
- [24] Pellman E. J., Viano D. C., Tucker A. M., Casson I. R. Waeckerle J. F., "Concussion in professional football: reconstruction of game impacts and injuries". *Neurosurgery* 53 (4): 2003, p. 799-812; discussion 812-4.
- [25] Portero P. Genries V., "An update of neck muscle strength: from isometric to isokinetic assessment". *Isokinetics and exercise science* 11: 2003, p. 1-8.
- [26] Ruan J. S., Khalil T. B. King A. I. 1993. Finite element modeling of direct head impact. *Proceedings of the 37th Stapp Car Crash Conference*.
- [27] Sivamani R. K., Goodman J., Gitis N. V. Maibach H. I., "Coefficient of friction: tribological studies in man - an overview". *Skin Research and Technology* 9 (3): 2003, p. 227-34.
- [28] Stobbe T. J. 1982. "The development of a practical strength testing program for industry", PhD Dissertation, University of Michigan.
- [29] TNO 2005. MADYMO human models manual version 6.2.2, TNO.
- [30] Willinger R., Taleb L., Viguier P. Kopp C. M., "Rotation-Translation duality in head trauma? Perceptive and objective evidence". *Proceedings of the IRCOBI Conference*: 1994, p. 63-76.
- [31] Yoganandan N., Pintar F., Sances A., Walsh P. R., Ewing C. L., Thomas D. J. Snyder R. G., "Biomechanics of skull fracture". *Journal of Neurotrauma* 12 (4): 1995, p. 659-68.
- [32] Yoganandan N., Zhang J. Pintar F., "Force and acceleration corridor from lateral head impact". *Traffic injury prevention* 5 (4): 2004, p. 368-73.
- [33] Zhang L., Ramesh S., Yang K. H. King A. I. 2003. Effectiveness of the football helmet assessed by finite element modeling and impact testing. *Proceedings of the IRCOBI Conference*, Lisbon, Portugal.
- [34] Zhang L., Yang K. H. King A. I., "A proposed injury threshold for mild traumatic brain

injury". *Journal of Biomechanical Engineering* 126 (2): 2004, p. 226-36.

[35] Zhou C., Khalil T. B. King A. I., "A new model comparing impact responses of the homogeneous and inhomogeneous human brain". *Proceedings of the 39th Stapp Car Crash Conference* Paper 952714: 1995, p. 121-137.

UPPER EXTREMITY INJURY STUDY: RECOMMENDATIONS FOR INJURY PREVENTION PRIORITIES

David Hynd
Jolyon Carroll
Richard Cuerden
TRL Limited
United Kingdom

Paper Number 07-0317

ABSTRACT

A large-scale accident study of injuries in Phases four, five and six of the UK CCIS accident database showed that upper extremity injuries were increasing in frequency in frontal impacts, particularly when an airbag deployed. However, it was difficult to identify injury mechanisms and costs from the information in the database.

Therefore, an in-depth case-by-case study of upper extremity injuries has been undertaken to determine the mechanisms, costs and long-term consequences (disability or impairment) of the injuries, in order to set priorities for injury prevention. The study has been undertaken in three phases:

- A retrospective study of medical notes (74 cases), giving more detail on the specific upper extremity injuries and the mechanisms that could have caused them.
- A prospective study of patients recruited at an Emergency Department (25 cases), with a follow-up of up to six months to assess longer-term consequences of the injury.
- A review of physiotherapy treatment case notes (288 cases), looking at cases that may not have been assessed at a hospital Emergency Department.

Four hospitals and three physiotherapy practices were recruited to this study. Evaluations of short and long-term costs and residual impairment resulting from these injuries have been made. The long-term costs were assessed through surgical costs, cost of other treatment and time off work, whilst impairment was assessed qualitatively by range of motion, pain and functional impairments and quantitatively using the American Medical Association Guides.

This study offers a unique insight into the mechanisms causing and long-term consequences arising from specific upper extremity injuries. From this, priorities for injury prevention are presented. A potential limitation of the study is the extent to which the three samples are representative of the UK population.

INTRODUCTION

An initial analysis of accident data (from Phases four, five and six of the Cooperative Crash Injury Study, CCIS (Mackay, 1985)) considered injury patterns for a variety of crash scenarios (e.g. frontal, side and rear impacts) and occupants, identifying priorities for further research. This stage of the research used the Abbreviated Injury Scale (AIS; AAAM, 1990) to assess injury severity, which is based on the threat to life. No consideration was given to the long-term outcomes or the disabling effects of the injuries seen. The top priorities were identified as MAIS 3+ (MAIS \geq 3) thoracic injuries sustained by front occupants in frontal impacts and AIS 2+ upper extremity injuries sustained by drivers in frontal impacts where an airbag deployed. Upper extremity injuries were not identified as a priority in frontal impacts without airbag deployment. It was not clear from the accident analysis if airbags were contributing, in some way, to upper extremity injury risk. One alternative is that the relative importance of upper extremity injuries in frontal impacts with airbag deployment increases over impacts with no deployment as the airbag is effective at reducing the incidence of injuries to other body regions. Also, airbag equipped vehicles are effective at reducing the risk of fatal head injuries, so it may be that casualties who would have been fatally injured are now surviving accidents and their arm injuries may therefore be more likely to be recorded.

Following this initial analysis, a case study was conducted, which looked at these two priority areas in greater depth and showed that both needed further research. The upper extremity injuries were shown in many cases not to be a direct result of the airbag's deployment and had many locations (on the arm) and many different possible mechanisms.

To determine if similar findings had been found in other studies and to provide direction for further research in this area, accident analyses in the published literature were reviewed. From this review of the published material it seemed that there was general agreement that airbag deployment did not reduce upper extremity injury

risk (Cuereiden *et al.*, 2001, Huere *et al.*, 2001; Morris *et al.*, 2001; Lenard and Welsh, 2001; Siegel *et al.*, 2001; Kirk *et al.*, 2002; Jernigan and Duma, 2003 and Kent *et al.*, 2005). However, this review of previous and current research also identified several limitations of the investigations conducted prior to this study:

- Only hard tissue upper extremity injuries have been considered, not soft tissue injuries with low AIS scores. To overcome this deficiency, there is a need to investigate the frequency and effects of such injuries in terms of treatment and impairment rather than threat to life
- Only drivers' injuries have been investigated, in-depth, within the previous research.
- The CCIS samples accidents where a vehicle, which is less than seven years old, was towed-away. Therefore, the CCIS is biased towards more severe accidents. By investigating all injuries prospectively this bias can be avoided.
- The previous case study indicated that there was often no information about the specific types of injury sustained or their cause or mechanism.

The initial objective of this study was to address the limitations of the research conducted to date. Studies were proposed to investigate hard and soft tissue upper extremity injuries, sustained by drivers and passengers of cars or car-derived motor vehicles, using data from the CCIS and other sources. Particular attention was given to trying to identify mechanisms of injury and specific injury information, such as associated costs and impairments. Based on this information, the final objective was then to determine priorities for future injury prevention. If appropriate, the injuries identified could then be investigated further potentially using PMHS tests and possibly volunteer tests to improve biofidelity requirements for crash test dummies and develop injury criteria for use in regulatory approval tests. The ultimate aim of this work was to encourage effective countermeasures to be designed so as to reduce the incidence of upper limb injury in the future.

The study was conducted in three parts: a retrospective hospital study, a prospective hospital study and a physiotherapy study.

For these studies the upper extremity was defined as the arm and shoulder (where shoulder included the clavicle).

Retrospective Study

From a review of the literature related to vehicle safety, it was observed that little is known about the nature of upper extremity injuries sustained in

frontal crashes in terms of associated impairment or difficulty of treatment and hence as yet, no particular injury has been identified as a priority. It was therefore necessary to select all cases where an upper extremity injury was sustained in a frontal impact.

The in-depth retrospective study required very specific knowledge of: the characteristics of the casualty, the nature and severity of the accident, any contact evidence within the car that could be correlated with the upper extremity injury mechanism, the seating position and seat-belt status of the injured individual and, whether any additional or supplementary restraint devices, such as an airbag, deployed.

The CCIS database was considered as an ideal source of accident information. However, additional information was required concerning the upper limb injuries. Therefore, CCIS cases were revisited and the judgement of medical personnel (mainly registrars and consultants) was sought.

Prospective Study

The prospective study was to provide similar information to the retrospective study but would review casualty information at the time of presentation at the hospital with the potential for a follow-up meeting. This offered the potential to get more specific injury information and a more accurate evaluation of the resulting impairment than from the retrospective study, where impairment was estimated from a review of the patient notes only. Through recruiting patients directly from Accident and Emergency Wards, the prospective study would avoid the stratification bias in the CCIS. However, it was not possible to link cases with the detailed accident and vehicle information, as would be available with CCIS cases. Instead a first-person accident description was obtained from the participant. This offered the additional opportunity to gain information on occupants' perceptions of their accident directly from interviews with the patients.

Physiotherapy Study

It was thought that there may be, proportionally, very few soft tissue injuries to the upper extremities evident in the CCIS data due to the case selection criteria used. It was also of concern that hospital records may indicate the length of stay in hospital associated with a particular injury but may not give any indication of the long-term effects and treatment associated with that injury. This would risk giving an underestimate of the potential whole cost of the injury. Therefore, another source was considered to be necessary to complete the

information on the disabling nature and societal costs associated with upper extremity injuries. For this reason, this third study was set-up to identify:

- Upper extremity injuries sustained as a result of a road traffic accident that resulted (directly or indirectly) in the patient requiring physiotherapy treatment;
- The priorities for prevention amongst those injuries based on: frequency, final level of impairment, duration of temporary impairment and the cost to society in terms of length and intensity of treatment required

METHOD

Retrospective Study

The retrospective study used existing accident information for individual casualties who were known to have sustained a specific upper limb injury and enhanced this with additional information on their injury and, where possible, on the injury mechanism. The study involved a retrospective examination of casualties admitted to selected hospitals during the period from 1998 to 2005. This retrospective investigation included: a review of medical notes and imaging (X-ray) results, and determination of the costs, the functional impairment resulting from the injury and the mechanism necessary to produce that injury.

The additional detailed information on the injuries to the selected casualties was provided by medical researchers, primarily an Emergency Medicine Consultant, Orthopaedic Surgeon and Trauma Surgeon, sub-contracted from the hospitals local to the cases selected. The injury information from the medical researchers was complemented with input from the accident investigation researchers at TRL on the specific accident details. The assessments and conclusions are therefore those made by a collaboration of medical, accident investigation and biomechanics researchers.

The hospitals that contributed to the study were the City Hospital in Nottingham and the Heartlands, Solihull, and Selly Oak Hospitals, located in the Birmingham area. The Loughborough and Birmingham University based accident investigation teams (Ergonomics and Safety Research Institute, ESRI and the Birmingham Automotive Safety Centre, BASC, respectively) also contributed to the study.

To assure that the confidentiality of personal information is retained, use of information, such as names and addresses, is regulated on a legal and ethical level in the UK. This presented a challenge for the retrospective study. To be able to link detailed crash data back to the notes for that patient

at a hospital (to give the detailed injury information), with retention of patient anonymity, two existing crash injury databases had to be used, firstly the Co-operative Crash Injury Study (CCIS) and secondly the STATS19. The STATS19 Database is a source of data concerning national (UK) road accidents (STATS19 ref).

The procedure for linking the upper extremity injury case to the patient's notes was as follows and is shown by the flowchart in Figure 1: After cases of interest were identified from the CCIS database, those cases were linked to the STATS19 record for the accident, based on crash date, time and region. The accident location (which is quite imprecise), date and time were then used to identify hospitals that the injured person was likely to have attended. The hospital records for all road traffic accidents (RTAs) around the date and time of the STATS19 record were extracted and those with appropriate age, gender and arm and shoulder injuries (there may have been more than one case) were selected. The injuries for these occupants were AIS coded by the ESRI or BASC accident investigation teams, in the same way as for the CCIS case. This injury coding was used to confirm that the patient notes were for the same person as was listed in the CCIS database. Although there was no guarantee that the two people were the same using this method, it was chosen because it was expected that the number of false matches would be very low and the anonymity of the patient was assured. To comply with the Data Protection Act and ethical requirements, TRL only received anonymous injury information from the hospitals and has only anonymous accident data in the CCIS database.

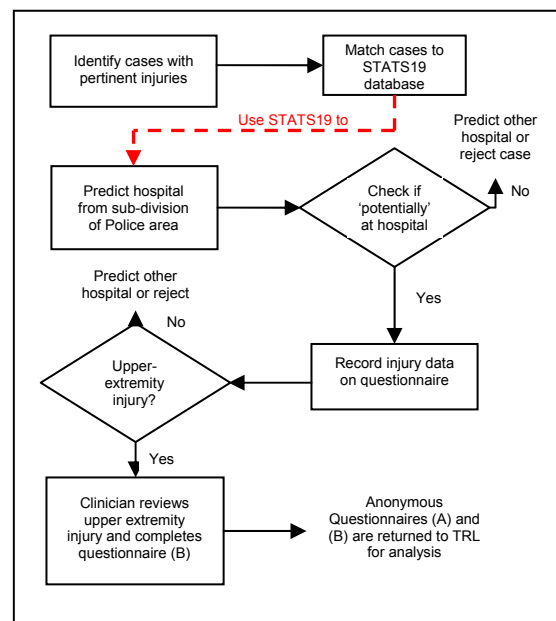


Figure 1. Schematic of the process to identify casualties and investigate their upper extremity injury

Ethical approval in line with the requirements of the UK Department for Health, Central Office for Research Ethics Committees (COREC), was granted at the study and site-specific level.

Front and side impacts were selected for further review. The selection criteria for these groups were:

Frontal impacts;

- Met the injury criteria, one impact only (or the most severe impact with some minor other impacts), no rollover, seat-belted, occupant at least 16 years old, front seat occupant (driver or front seat passenger)

Side impacts;

- Met the injury criteria, one impact (or the most severe impact with some minor other impacts), occupant seated on the struck side, no rollover, occupant at least 16 years old.

These two groups were principally different in that confirmed seat-belt use was not a selection criterion for side impacts. It was thought that confirming the use of a seat-belt in side impacts would be more difficult and less reliable than in frontal impacts and that arm and shoulder injuries would not be influenced by seat-belt use for occupants seated on the struck side.

Based on the inclusion criteria a group of the casualties from Phases five, six and seven of the CCIS were selected that had an upper extremity injury. However, at this stage, it was not known which of these selected casualties would have attended one of the contracted hospitals. To be a 'requested case', those CCIS cases, that met the study inclusion criteria, also had to have occurred in the police regions covered by either the Loughborough (ESRI) or Birmingham (BASC) accident investigation teams. In particular, cases were sought from the police regions that contained the hospitals which had agreed to participate in the study (Nottingham and Birmingham). The accident investigation teams involved in the study then had the responsibility of going to the participating hospitals and trying to identify the selected casualties who had attended there (from the requested cases). Overall, 65 cases were identified from the 227 that were requested (29 %).

It was expected that the main reason why cases were not found was that the casualty attended a hospital that was not participating in the study. In order to try and include more cases, some of the Phase seven CCIS cases were requested from the police region neighbouring the Nottingham hospitals (Leicestershire). This proved to be

successful with nine additional cases being returned. In total 74 cases were analysed.

In order to relate the findings of the retrospective study to implications for UK car occupants, it is important to understand the connection between the cases selected for the retrospective study, the in-depth data available from the CCIS and the national traffic injury statistics. A simple schematic of the relationship between the three sources of retrospective car occupant injury information used in this study is illustrated by Figure 2. It is important to note that there is not a simple one-to-one relationship between the data sources. For matching and scaling purposes detailed consideration has to be given to the sampling strategies and therefore injury severity rates (fatal, serious or slight), types of impact and other factors. However, it is useful to picture the three data sources as detailed in Figure 2, with CCIS being a sample of STATS19 and the retrospective study group being a sample of CCIS.

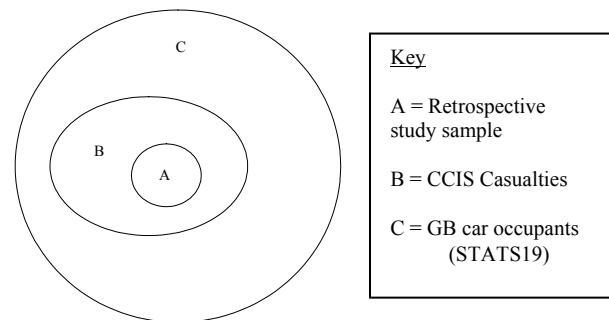


Figure 2. Schematic of the relationship between the available databases.

Prospective Study

The prospective study consisted of information gathered from the casualty on admission to Hospital, the nursing staff in the Accident and Emergency Ward (A&E) and the opinion of the A&E Consultant with respect to the upper extremity injuries. The prospective study was devised to give complementary information to that obtained from the retrospective and physiotherapy studies, thus giving a more complete understanding of upper extremity injury in frontal impacts. In particular the prospective study offered the opportunity to gain more accurate impairment information than from the retrospective study.

The prospective study was undertaken in collaboration with the Queen's Medical Centre (QMC) in Nottingham. The Emergency Department at the QMC is reported as being the busiest in the country, with approximately 120,000

patients attending the department for treatment each year.

The protocol for the prospective study included direct contact with the patient by Hospital staff. This was necessary to obtain accurate, physical assessments of impairment (not estimates) and first-person patient accounts of the accident. The additional contact to gain the information necessary for the study required informed consent to be obtained from the patient, for which a patient information sheet and consent form were developed. Ethical approval in line with the requirements of the UK Department for Health, Central Office for Research Ethics Committees (COREC), was granted at the study and site-specific level.

Each casualty was approached by a member of the A&E staff to gain their permission and willingness to participate in the study. Then basic characteristics of the casualty were taken (such as age, gender, height, weight, etc.), as well as a basic description of the crash circumstances (completed with information supplied by the participant). Detailed information relating to the upper extremity injury, such as severity, estimate of the mechanism of injury and likely outcome was provided by the consultant at the hospital.

Between two and six months after sustaining the injury the participants were contacted, by telephone. This was to find out if they had any on-going impairment, in terms of their ability to work and perform activities associated with daily living, and whether they had received any treatment, since their discharge from hospital. Those subjects with continuing impairment were asked to attend the Hospital for a follow-up assessment by an appropriate clinician.

Participant recruitment and data collection began at the QMC at the end of May 2005. Patients were recruited until the end of 2005, with follow-up appointments (for the assessment of any continuing impairment) being available until the end of February 2006.

The impairment resulting from the upper extremity injuries in the retrospective and prospective studies has been coded using the American Medical Association Guides to the evaluation of permanent impairment (Cocchiarella and Andersson, 2001). This impairment rating system is used widely in the US medico-legal system.

Physiotherapy Study

From the retrospective study it is evident that there are relatively few soft tissue injuries to the upper

extremity in the CCIS database, compared with more severe injuries, due to the selection criteria used in the CCIS. It is also apparent that data in the CCIS taken from hospital records may indicate the length of stay in hospital associated with a particular injury, but in many cases will not give a detailed indication of the long-term effects and treatment associated with that injury. Therefore another source of information regarding the sequelae associated with soft tissue upper extremity injuries from RTAs was required.

This section of the project made use of anonymous information concerning upper extremity injuries supplied by physiotherapists working in connection with hospital outpatients, GP (General Practitioner) doctor's surgeries and private patients. The information from the physiotherapists provided details on the frequency, final level of impairment, duration of temporary impairment and the cost to society (in terms of length and intensity of treatment required) associated with upper extremity injuries from RTAs.

Eight physiotherapy practices across England contributed anonymous injury and impairment information to the study.

As with the retrospective and prospective studies, ethical approval in line with the requirements of the UK Department for Health, Central Office for Research Ethics Committees (COREC), was granted at the study and site-specific level.

RESULTS

Retrospective Study Results

Sample Context: In order to place the retrospective study in context, its sample was compared with the CCIS database. The CCIS database (Phases six and seven) was used for the analysis. This included all completed crashes investigated from June 1998 and released in December 2005 (CCIS Release P7k). This yielded some 6,689 crashes.

Analysis of the Co-operative Crash Injury Study showed that following road traffic collisions, moderate and serious upper extremity injuries are commonly suffered by car occupants. CCIS accidents are investigated according to a stratified sampling procedure which favours cars containing fatal or seriously injured occupants, according to the British Government definitions of fatal, serious and slight. Approximately 34 % and 23 % of the CCIS killed and seriously injured car occupants sustained an upper extremity injury respectively. Only 4 % of the CCIS casualties described by the police as slightly injured sustained an upper

extremity injury that met the criteria of this project. In 2004, there were 1,671 fatal, 14,473 serious and 167,714 slightly injured car occupants in Great Britain. Therefore, it can be estimated that over ten thousand car occupant crash survivors suffered a moderate or serious upper extremity injury in Great Britain in 2004. This estimate highlights the significant magnitude of the upper limb trauma experienced.

Within the CCIS, cases for the retrospective study were selected based on whether an upper extremity injury had been sustained. From these cases, a further selection was requested from regions around the hospitals that had agreed to participate in the study. Finally, the study itself used a selection of these cases that were returned with the available hospital injury and impairment data. Figure 3 and Figure 4 compare the proportions of fatal, serious and slight occupant injury cases as defined by the Police for each of the samples.

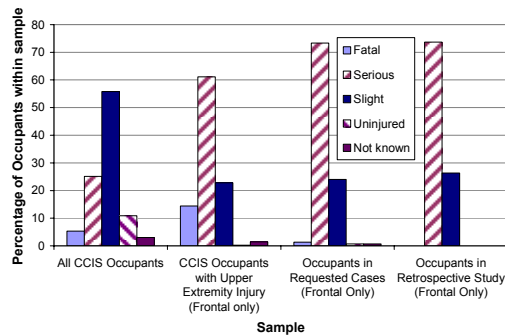


Figure 3. Occupant distribution by police defined injury severity level within each frontal impact sample.

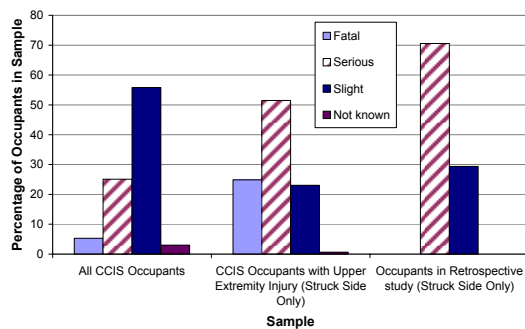


Figure 4. Occupant distribution by police defined injury severity level within each struck-side impact sample.

These figures illustrate that the selection of upper extremity injury cases altered the distribution of fatal, serious and slight injury cases in the sample but that once this initial selection was made, the other samples had similar proportions of serious and slight. The selection process reduced the proportion of fatal cases and effectively removed

all the uninjured cases and a large proportion of the slight injury cases.

Frequency: The sample of in-depth retrospective cases for struck-side impacts was too small to be able to predict confidently the relative importance of the different injuries. This was because some frequently occurring injuries seen in the CCIS were not included in the cases returned to TRL within the retrospective study. However, cost and impairment ranking has been performed with the limited data available to give some priority for the injuries found.

The front impact sample was larger than the side impact sample and the front impact retrospective cases can be said to be generally representative of the upper extremity injury cases in the CCIS population (Figure 3). Therefore it is thought that the relative injury priorities derived from the retrospective study front impact cases are likely to reflect the priorities for front impact cases in the CCIS population.

The largest injury groups in both the sample of the CCIS casualties with an upper extremity injury (meeting the inclusion criteria) and the retrospective study sample are shown in Figure 5.

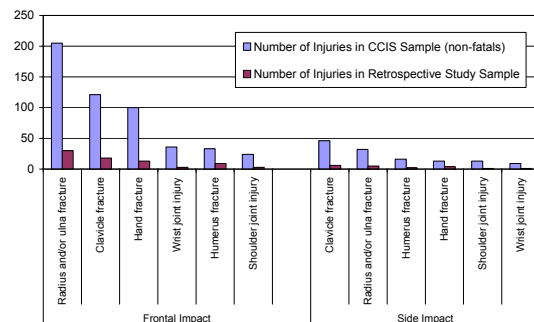


Figure 5. Frequency of the most common injuries in the CCIS sample (non-fatal) and the retrospective study sample.

From this it is clear that the injury priorities, in frequency terms, are:

Frontal impact

- Radius and/or ulna fracture
- Clavicle fracture
- Hand fracture
- Wrist joint injury
- Humerus fracture
- Shoulder joint injury

Side impact

- Clavicle fracture
- Radius and ulna fracture

- Humerus fracture
- Hand fracture and shoulder joint injury
- Wrist joint injury

Costs from the retrospective study cover treatment only. This includes outpatient time and the associated staff time. The costs do not take into account physiotherapy or Accident and Emergency costs. Neither do they account for cost of living or impact on earning potential.

Difficulties in calculating the costs of injuries have been encountered. It was reported by the participating hospitals that it is particularly hard to calculate some staff costs as not all staff time is likely to be funded by the Hospital. For instance Junior Doctors, who do a large part of the work, are not paid by hospitals directly, since their funding would come out of training budgets. In general, the costs quoted in the retrospective study come from hospital managers and are typical costs for treatment types. It is suspected that these are underestimates, but they are the figures provided by the hospital. Whilst there may be underestimates and inaccuracies in the absolute values quoted for costs in this study, it is considered that the relative costs (whole body compared with arm injuries) should be accurate.

In some retrospective cases, the casualty received one upper extremity injury and the cost for this was provided. In other cases, more than one upper extremity injury was sustained and in these cases the medical reviewer did not always separate the injuries to provide individual injury costs. In these cases, the total upper extremity cost was distributed to each individual injury based on the relative mean single injury costs from other cases.

The mean cost of each of the main injury groups identified according to the frequency with which that injury occurs compared with the average cost of all injuries to the same occupants are shown in Figure 6 for frontal impact cases and Figure 7 for struck-side impact cases.

The mean cost for the upper extremity injuries in the retrospective study was £ 2,154, with a median value of £ 835. The minimum cost was £ 0. This was reported in two cases. In one of these cases, the patient had a thumb dislocation which required no treatment. In the other case the three injuries were a left forearm haematoma, a left wrist sprain and a neck strain. It was the opinion of the medical expert that these injuries should be assigned no monetary cost, in terms of primary care at the hospital attended, when considered in the context of the total accident cost.

The most expensive cost for the upper extremity injuries from one patient was £ 9,951. This cost was derived from the treatment for two injuries: a displaced fracture of the left humerus and an open complex Monteggia fracture of the right forearm. A Monteggia fracture is a fracture of the proximal ulna associated with anterior dislocation of the radius (radial head) at the elbow. Despite this large cost from the upper extremity injuries, they still only contributed 19 % of the total injury cost, with a further cost of £ 43,326 arising from other injuries sustained.

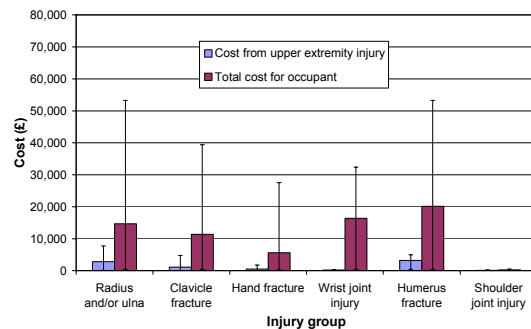


Figure 6. Mean (max and min) cost of upper extremity injury and total injury costs for retrospective study frontal impact cases.

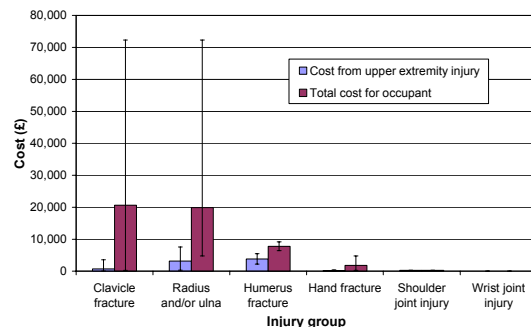


Figure 7. Mean (max and min) cost of upper extremity injury and total injury costs for retrospective study side impact cases.

On average, the costs associated with a single upper extremity injury represent about 20 % of the total injury costs. This is lower than the typical value for lower limb injuries as typical clavicle and wrist fractures do not involve a stay in hospital (which is the largest cost in treatment).

To provide an indication of the injury priority based on cost, the mean cost per injury in each of the main groups was multiplied by the frequency of injury in the whole CCIS upper extremity injury sample (excluding fatalities). It should be noted that the retrospective study contains more complex fractures than the selected upper extremity injuries from the CCIS. Therefore, the mean individual injury cost values for the humerus and radius

and/or ulna groups may be slightly too high for the group on which the frequency is based. However, this slight inaccuracy due to a sample bias is not considered large enough to alter the priorities that have been derived. The priorities for injury groups based on the mean cost multiplied by the frequency of injury in the CCIS database are:

Frontal impact

- Radius and/or ulna fracture
- Clavicle fracture
- Humerus fracture
- Hand fracture
- Wrist joint injury
- Shoulder joint injury

Struck-side impact

- Radius and ulna fracture
- Humerus fracture
- Clavicle fracture
- Shoulder joint injury
- Hand fracture
- Wrist joint injury

Impairment: The American Medical Association Guides to the evaluation of permanent impairment (Cocchiarella and Andersson, 2001) define impairment as “a loss, loss of use, or derangement of any body part, organ or system, or organ function.” As examples of upper extremity impairment, the guide rates amputation of the arm through the humerus (at the top of the arm) as 100 % upper extremity impairment, this is equivalent to 60 % impairment of the whole person. Whereas, an inability to flex the finger at the proximal inter-phalangeal joint, for the little finger, corresponds to 60 % finger impairment, which is 5 % impairment of the upper extremity.

The mean residual impairment for the six most frequent injury groups in frontal impact is shown in Figure 8 for frontal impacts and Figure 9 for side impacts. It should be noted that the number of cases with reported long-term impairment was relatively low, so these figures are likely to have wide error bands.

The mean impairment from an injury in the retrospective study was a 5 % impairment to the upper extremity, which corresponds to about a 3 % whole person impairment.

The maximum impairment at the time of presenting, or on first examination in hospital, was 56 % impairment of the upper extremity and 34 % of the whole person. This impairment was caused by a Monteggia fracture of the right arm. On presentation at the Hospital, the patient reported that they could not move their fingers and had no

flexion, extension, supination or pronation of their elbow. On leaving tertiary care, one year later, this impairment had dropped to 8 % upper extremity and 5 % whole person. At this time, they had decreased forearm rotation and elbow flexion and decreased finger flexion and grip strength. The patient still could not return to their job.

The maximum impairment, on leaving tertiary care, was 23 % of the upper extremity, which was 14 % of the whole person. This patient received several upper extremity injuries including three finger fractures of the left hand, one of which was open and comminuted, as well as a fracture of the right humerus in a supra-condylar position. This impairment level was the combined result of the three left hand fractures. Despite the reduced function of their upper extremities, the patient could return to work as a teacher and was assessed as being able to do other office work and maybe light manual work.

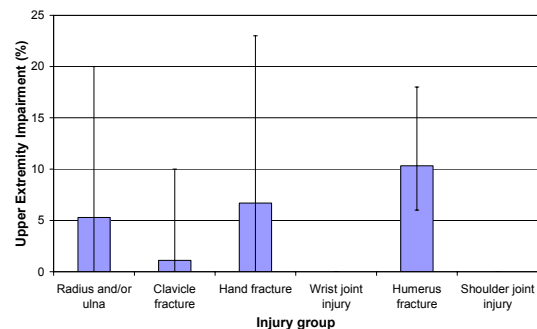


Figure 8. Mean (max and min) residual impairment from upper extremity injury for retrospective study frontal impact cases.

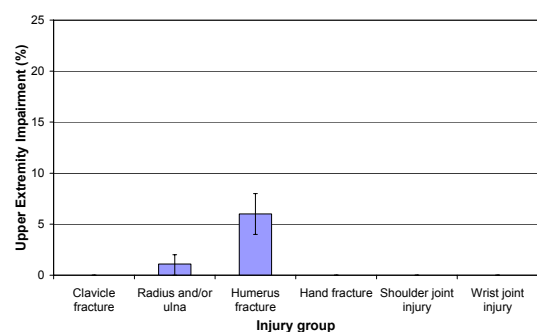


Figure 9. Mean (max and min) residual impairment from upper extremity injury for retrospective study side impact cases.

Humerus fractures accounted for the highest mean functional impairment in both frontal and struck side impacts. In frontal impacts, there were nine humerus fracture injuries. Of these, only two injuries were constrained to the shaft of the humerus. In the other humerus fracture cases, there was some involvement of a joint and this is likely

to have exacerbated the functional impairment caused by the fracture.

The mean impairments were multiplied by the frequency of upper extremity injuries to non-fatal cases in the CCIS sample in order to determine an injury prevention priority ranking based on impairment. The final impairment was not explicitly reported for all cases. In the cases where it was not reported, it was assumed that there was no final impairment.

As discussed in relation to the costs derived above, the retrospective study contains more complex fractures than the selected upper extremity injuries from the CCIS. Therefore, the mean individual injury impairment values for the humerus, and radius and/or ulna groups may be slightly too high for the group on which the frequency is based. This slight inaccuracy due to the sample bias will not have altered the priorities that have been derived.

The priorities for injury groups based on the impairment multiplied by the frequency of injury to non fatal occupants in the CCIS database are:

Frontal impact

- Radius and/or ulna fracture
- Hand fracture
- Humerus fracture
- Clavicle fracture

Struck-side impact

- Humerus fracture
- Radius and ulna fracture

The retrospective study cases were generally representative of the CCIS database and are used to prioritise the specific injuries in terms of frequency, cost and impairment, for the given impact types. However, the potential bias and error margins associated with developing a model to scale the retrospective study findings to a national level were judged to be too large for this to be useful.

Based on the frequency of the main injury groups, the average cost of treatment and the average impairment for each group, an overall priority for injury prevention was determined. For this, equal weighting was given to the cost and impairment priorities. The priorities for upper extremity injury prevention in frontal and side impacts, based on retrospective case data, are:

Frontal impact

- Radius and/or ulna fracture
- Hand, humerus and clavicle fractures

Struck-side impact

- Humerus fracture

- Radius and ulna fracture
- Clavicle fracture

Injury Mechanism: One of the objectives of the retrospective study was to re-examine accident cases in order to get more detailed information on the mechanism of the upper extremity injuries. For fractures, the medical team were able to examine the x-rays and other injury information and from this to estimate the type of loading that would have led to each fracture. For instance, many fracture types are associated with a particular type of loading - spiral fractures from torsional loading, distal fractures of the articular surface of the radius at the wrist due to direct load with the hand fully extended.

For soft-tissue injuries, similar additional information was recorded. For instance, the CCIS case file may note a shoulder sprain, but the detailed medical records enable the clinicians to determine specifically what part of the shoulder was strained and thereby whether the joint was loaded in flexion or extension, etc. This information is useful, in combination with the vehicle information, for determining whether the injury was from bracing (forced extension of the joint) or inertial loading from the arm moving forwards once the shoulder had been restrained by the diagonal seat-belt (flexion of the joint).

Based on an interpretation of the accident information and discussion with the medical staff, where necessary, a mechanism was proposed as the cause for the 106 individual upper extremity injuries from the retrospective study cases. This mechanism consisted of a loading strategy responsible for the injury, as was suggested by the medical personnel, together with potential contacts around the vehicle.

The injury mechanisms for the priority injury groups were investigated in more detail, based on the detailed injury information provided by the medical review, combined with the CCIS accident information.

For upper extremity injuries in general, it was found that there was no one injury mechanism that stood out as a priority for prevention. Instead it appears that the upper extremity injuries investigated in the retrospective study were caused by several different mechanisms and injurious contacts. The wide variety of specific injuries, contact locations and accident configurations in the retrospective study cases make it difficult to suggest a strategy for mitigating these injuries or for replicating them in the laboratory. Where substantial patterns could be determined for a

particular injury group, then they are discussed below.

Frontal Impact - Radius and Ulna Fractures

- Just over half of the 30 radius and ulna fractures were due to direct impact loading with a wide range of contact points (A-pillar, facia top, facia panel, steering wheel, own side door, windscreen and other vehicle).
- Nine of the radius and ulna fracture cases involved extension or hyperextension of the wrist combined with direct contact. This may imply that the hand was in a bracing position or simply holding the steering wheel. All but one of these involved contact with either the facia, facia top or the steering wheel. The contacts and the nature of the injuries imply that reducing the stiffness of the facia and steering wheel may reduce the risk of these injuries, although it may not be practicable to alter the stiffness of the steering wheel in vehicles equipped with a steering wheel airbag, because the steering wheel is a support plane for the deploying airbag.
- Two injuries were probably caused indirectly by the steering wheel airbag. The forearm had probably been parallel to the steering wheel at impact and the airbag had deployed over the forearm, trapping it against the rim and/or spokes of the steering wheel. When the airbag was then loaded by the head and thorax, this load was transferred to the forearm causing it to be fractured at each contact point with the steering wheel. In one case the ulna had been fractured in three places, apparently at the upper rim, spoke and lower rim of the steering wheel (Figure 10). It should be possible to reproduce this injury mechanism in the laboratory, although it may be difficult to get good repeatability with the complex loading environment.

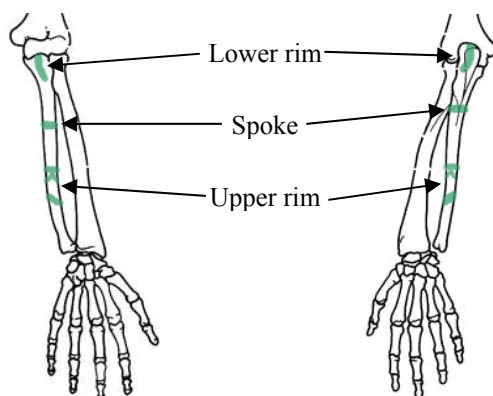


Figure 10. Ulna fracture pattern.

- In two cases involving front seat passengers, one injury was directly attributable to the passenger front airbag or airbag cover and one

possibly involved loading from the airbag or airbag cover. In the first case, the palm had burn marks from the airbag (and a fractured thumb), so direct loading from the airbag or airbag cover seemed most likely. In the second case, the most likely contact was the airbag - the CCIS case recorded this as the contact and on review there was no evidence to suggest any other contact. This loading mechanism is quite well defined and it would be possible to replicate in a laboratory. It may well be important that the arm is straight in order to generate the loads required for the more serious injuries seen in these cases and some replication of the extension moment in bracing may be required.

Frontal Impact - Clavicle Fractures

- 17 out of 18 clavicle fractures were caused by the seat-belt webbing. Additional inertial loading from the arm was considered by the medical review to have been important in 12 of these fractures.
- If this loading was to be recreated in a laboratory, then a whole body dummy or PMHS would be necessary. Given that the inertial loading from the arm was considered to be important in the majority of the clavicle fracture cases, this should be reproduced. The bending moment on the clavicle should be monitored as the parameter most likely to reflect injury risk for the occupant accurately. Alternatively the relationship between belt load and clavicle fracture injury risk should be investigated and established.

Struck Side Impact - Humerus Fractures

- There were two cases of humerus fracture caused in struck side impacts that were linked with an injury mechanism in the retrospective study. Both had high treatment costs and associated impairment. Both injuries were caused by direct loading from the door of the vehicle or perhaps the B-pillar.

Struck Side Impact - Clavicle Fractures

- There were six clavicle fractures in struck side impacts, all due to contact with some part of the vehicle side structure.
- The mechanism of injury was thought to be lateral compression for five of these six cases. PMHS tests to develop an injury criterion and injury risk function for these injuries were recently completed by INRETS as part of the SIBER EC project (Compigne *et al.*, 2003). The WorldSID crash test dummy is instrumented to measure lateral shoulder forces and compression.

For the specific injury priorities identified in this study, only two cases were identified where the airbag was the most likely cause of the injury to a driver. This does not seem to support a hypothesis that airbag deployment increases upper extremity injury risk for drivers in frontal impacts. However, it is possible that this result could be an anomaly due to sampling: it is possible that the previous observations could be due to an increase in the stiffness of steering wheels, necessary to give adequate support to the airbag - many of the priority injuries from this study had the steering wheel as a potential injury causing contact.

A further two cases were identified where the airbag was the most likely cause of the injury to a front seat passenger, one of which involved serious wrist and distal forearm injuries. This is a cause for concern and should be investigated further.

As the incidence of seat-belt caused clavicle fractures was higher than had been expected, the potential for technology to reduce the number of clavicle fractures was investigated. From the seat-belt label information in the CCIS database, it was often possible to determine whether the vehicle had a load-limiter or pre-tensioner fitted in the seating position in which the upper extremity injury occurred. Table 1 shows that the presence of a seat-belt load limiter did not significantly affect the rate of right shoulder AIS2+ injury induced through seat-belt webbing loading suffered by drivers. The CCIS database only started to code load limiter presence accurately and routinely in 2002 and this accounts for the large number of 'not known' entries in Table 1.

Table 1. Load limiter presence versus driver AIS 2+ right shoulder injury

Right shoulder AIS2+ injury	Load limiter present			Total
	No	Yes	Not known	
No	760 26.2%	516 17.8%	1620 55.9%	2896 100.0%
Yes	24 23.3%	21 20.4%	58 56.3%	103 100.0%
Total	784 26.1%	537 17.9%	1678 56.0%	2999 100.0%

For the cases in the retrospective study, no significant difference was found in the probability of clavicle fractures when either a load-limiter or pre-tensioner was fitted in that seating position, compared with the probability of clavicle fracture

without that device. However, it was not known what load limit was used with the load limiters in these cases and this may be significant in determining the likelihood of injury for a particular occupant.

Prospective Study Results

In the Emergency Department (ED) at the QMC, they received 851 drivers or front seat passengers during the period of this study. However, only 75 of these were involved in a (self-reported) front or side impact and had an upper extremity injury. Of the 75 patients who were initially recorded as being eligible, only 25 were recruited and followed through the data collection process. The main reason that eligible patients were not recruited was that they could not be recruited during the time when they received their treatment in the ED, due to medical work pressures on the ED staff. This problem was anticipated when planning the study. Therefore, the protocol and ethical approval for the study included a provision for the study researcher at QMC to follow cases up either later in the day or during the following day, based on 'consent to participate' and contact details taken in the ED. Unfortunately, the pressures on the ED staff meant that in many cases no contact details or unreliable contact details had been taken at the initial contact with the patient.

It was the intention for the prospective study to compliment the retrospective study adding more accurate injury and impairment information through the direct contact with the casualties. However, the unexpected low rate of eligible patients seen in the ED, together with the unexpectedly low recruitment and follow-up rate of only 33% (25 out of 75 eligible cases), meant that the number of complete cases in the prospective study is insufficient to be able to make useful generalisations about the frequency and mechanisms of specific upper extremity injuries. Despite this, the following key results are thought to be of interest.

One of the objectives of the study was to inform future work and it is clear that this type of study would require recruitment over a much longer period of time, or at a larger number of hospitals, to yield significant case numbers. The complexity of, and time required for, the ethical approvals process would suggest that a small increase in the number of participating hospitals (to three or four) combined with an increase in recruitment period (to 12 to 18 months) would provide the most efficient approach for a future study.

One of the anticipated benefits of the prospective study was the opportunity to interview the injured

person in order to understand better the loading conditions that led to their injury. This meant that ‘informed’ consent to participate was required from each patient as part of the ethical approval for the study. However, it should be noted that the relatively high rate of non-recruitment, because not all eligible patients could, or would, consent to participate in the study, will have introduced an uncontrolled bias in the sample.

In addition to the interviews and follow-up assessment, recruited patients were asked to give permission for photographs to be taken of the vehicle. It was not considered ethical for the participant to take the photographs, therefore if the vehicle was at a garage or breakers yard, a disposable camera was provided. Photographs were taken by the garage or breakers yard staff. For the eight sets of photographs that were returned, care had clearly been taken to follow the template that had been given and the photographs were of good quality.

Of the 25 completed cases, 13 occupants (52 %) were male and 12 occupants (48 %) were female. The mean and median ages of the sample were 43 and 34.5 years, respectively, and the distribution of age amongst the male and female participants was similar. Comparison of the height and weight of the prospective study participants with average national (UK) figures showed that the participants were, on average, of relatively normal height and weight. The level of fitness of the participants was described by the QMC staff to be good in 13 cases, average in 10 cases and poor in one case only. Osteoporosis was evident in three of the 25 patients, as a ‘pre-existing condition.’

The principal impact angles for each accident were self reported by the participant relating the impact angle to the hours of a clock. In addition to the impact direction, rollover occurred in six out of the 25 cases (24 %). This is much higher than the national average, with 12 % of car crashes incorporating rollover (average figure for 1999-2003 from STATS19). This is a clear bias in the data set, although the upper extremity injuries in these cases were remarkably slight with only contusions, slight lacerations and abrasions being reported.

The approximate impact velocity for the accident is shown in Figure 11. Both the impact angle and velocity are estimates based on the report of the participant. The approximate nature of these estimates is particularly important for the impact velocity where accurate relative velocities cannot always be established. Indeed the distribution of impact velocities seems highly improbable for the range of injuries seen in this study.

In the few cases, where it was possible to compare the reported impact speed and angle with photographs of the vehicle, it was expected that the reported vehicle speeds would have resulted in greater damage to the vehicle than was evident from the photographs. This supports the observation that the impact velocities, inferred from the reporting of the patient, were higher than would be expected for the injuries recorded in the study.

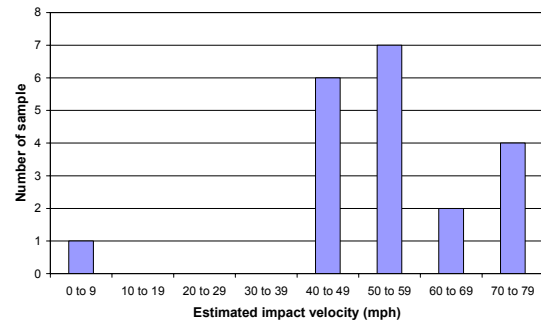


Figure 11. Approximate impact velocity for impacts in the prospective study.

Once the patient had given consent to participate and at a convenient time for the ED staff, the participant was asked for further information on their recollection of the accident. In particular, 13 (54 %) of participants reported that they were aware of the forthcoming impact before it happened. Of the 25 participants, 22 (88 %) said they were wearing a seat-belt. This is similar to the seat-belt wearing rate in a recent national study at 32 different sites around the country, which was determined to be 93 % for car drivers (TRL, 2005).

When asked whether they were braking before the impact, 41 % of the participants reported that they were, and 39 % were bracing in some manner when the impact occurred. 71 % of the participants reported that they made contact with some part of the interior of the vehicle during the impact. Whilst, 13 % said that they were hit by another object (either another object in the vehicle or by an intruding vehicle in a side impact). Two participants reported that they had no recollection of the accident. One of these had a blackout at the wheel. 44 % reported activation of an airbag. In every case, the activated airbag was a frontal airbag.

Frequency: The injury sustained by the occupant was reported to be a fracture in nine of the 25 cases. In three cases, the fracture was comminuted, which would be associated with a score of AIS 3 and in one case the fracture was open and comminuted. The total distribution of injuries is given in Figure 12. These classifications were not exclusive and often the participant would have more than one of these types of injuries. Nine

occupants in the prospective sample had one or more fractures.

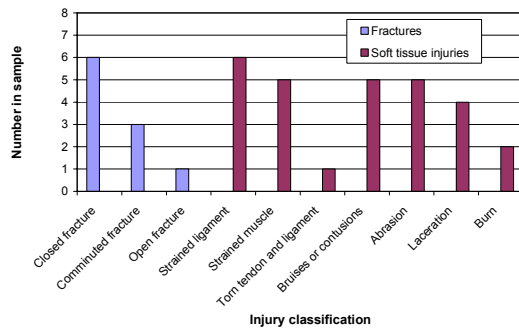


Figure 12. Distribution of reported injury classifications.

Costs were not reported for all injuries but, where reported, the fractures tended to have the highest treatment cost, with an average cost of nearly £2,000. This compares well with the mean cost from the retrospective study for fracture treatment, which was about £1,900. The average cost of the three intra-articular and open fractures from the prospective study was just over £3,500. Of the soft tissue injuries, the mean reported cost was just under £400, with a maximum of £947 for a thumb sprain. These soft tissue treatment values are higher than those from the retrospective study, from which the corresponding costs were £93 and £358.

Impairment: A limitation of the retrospective study was that the value reported for the impairment, which may have been caused by an injury, was the estimation of the medical researcher based on the patient notes. The accuracy of this assessment depends on the experience of the researcher with assessments of recovery following similar injuries. One anticipated benefit of the prospective study was that, by including a follow-up consultation, the longer-term implications of injuries could be determined much more accurately than from retrospective data. The participant would either report no further impairment or their impairment would be assessed directly by the medical team. As a result, it is probably true that the prospective impairment information, as assessed by the medical team, is more accurate than the information gathered in the retrospective study. However, the small number of cases means that only limited conclusions about impairment can be drawn.

Most of the upper extremity injuries from the prospective study resulted in two to three weeks of pain for the patient. The mean time recorded was between three and four weeks. The expected duration of pain for the patients in the study is shown in Figure 13. In two cases, not shown in

Figure 13, pain was expected to continue for three months.

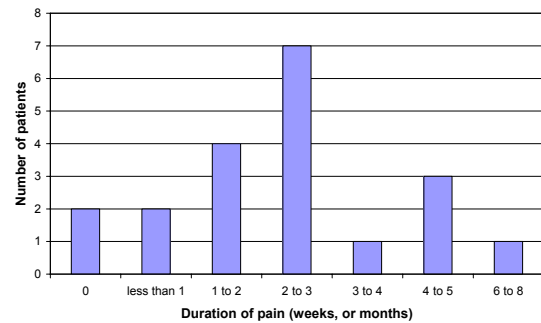


Figure 13. Expected duration of pain for prospective study participants.

At follow-up, (between two and six months after initial presentation), the participants were contacted and asked whether they had any impairment remaining due to their injury. They were also asked about the level of impairment that they had experienced following discharge from the Emergency Department.

From the 25 prospective study cases, only one was lost to follow-up. Six of these patients have also attended a follow-up session with the Emergency Department Consultant.

Of the 24 study participants for whom the follow-up was successful, 13 reported full function from the time of discharge from the hospital.

Whilst some impairment was generally reported following initial discharge from the hospital, six participants reported continuing impairment at the time of follow-up. Two of these participants had received soft tissue injuries to the shoulder. The other four had bone fracture injuries.

Injury Mechanism: In each case, for the prospective study, the medical researcher at the Queen's Medical Centre was asked to comment on the likely mechanism responsible for causing the upper extremity injury.

Steering wheel interaction during the accident was responsible for two of the injuries, although both of these injuries were minor.

An airbag was cited as the cause of two of the injuries. Both of these were airbag friction burns and were expected to have healed within two to three weeks. However, airbag involvement was also suggested to have been potentially significant in a further three cases with more serious injuries (one finger fracture and two wrist fractures).

When developing the protocol for this study it was hypothesised that one benefit of a prospective study would be the opportunity to interview the patient and therefore determine more precisely the contact point within the vehicle and the nature of the loading that caused the injury. The contact was clearly identified for many of the soft tissue injuries for which contact and loading information would be difficult to determine from a retrospective case study. However, for many of the fractures several possible contact sites (such as dashboard, airbag or door) were given. Assuming that the fractures generally occurred in higher severity impacts (which is not clear from the self-reported impact speeds), it is inferred that the patients were not able to recall accurately what had happened during the impact. This implies that in any future studies, it would be most likely that interviews with patients would only be of benefit in determining injury mechanism and contact points in low-severity impacts. The exception to this is bracing, which was reported by nine out of the 25 participants and was unknown for only two participants. If bracing was suspected as being important to an injury mechanism under investigation, a prospective study would clearly be of benefit.

Physiotherapy Study Results

The physiotherapy study is based on retrospective information from physiotherapists on patients who had sustained an upper extremity injury from a road traffic accident. From the three participating physiotherapy practices, TRL received 288 completed case report forms, containing anonymous information on injuries and impairment.

It was intended that the physiotherapy study would compliment the retrospective and prospective study by providing information on injuries that are less threatening to life but that may have longer-term consequences (costs and impairment) associated with them. Unlike the retrospective and prospective studies, the physiotherapy study did not have an exclusion criterion to rule out patients involved in a rear impact. The impact configurations, as determined from the response of the physiotherapists, responsible for causing the injury to the patients are shown in Figure 14. From this figure, it can be observed that the majority of the injuries reported by the physiotherapists were a result of rear impacts.

In the CCIS Phase six and seven sample, rear impacts were responsible for 7.6 % of the injuries to car occupants and 2.7 % of the occupants who received an upper extremity injury, that met the inclusion criteria for the retrospective study. These

percentages are far smaller than the corresponding percentage for the accidents reported in the physiotherapy study, where rear impacts accounted for 60 % of the patients. This suggests that the injuries treated by a physiotherapist (from a practice of the type used in the physiotherapy study) are not well represented in the CCIS and that the CCIS rear impact and low severity sample may well be under reported.

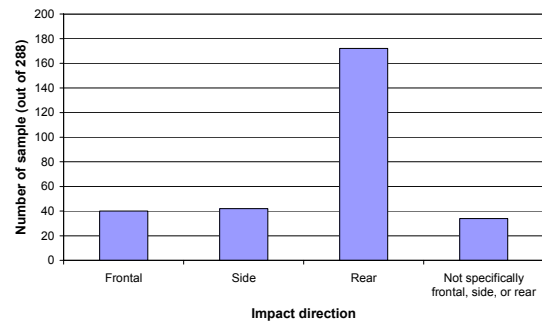


Figure 14. Distribution of impact direction within the physiotherapy study sample cases.

It appears that the cohort of patients treated in the physiotherapy study is not the same as that of the retrospective or prospective studies. The result of the physiotherapy study being based on a different sample of accidents from the retrospective and prospective study is that the results may not be directly comparable. However, the key results are presented below.

Of the physiotherapy study cases returned to TRL, 17 had no age or gender information. Of the remaining 271 out of the 288 patients comprising the physiotherapy study cases, the 31 to 40 year old group is the mean and median age group. This is also the mean and median group for the male and female subsets, although there were proportionally more young adult females than young adult males.

The majority of the vehicle occupants in the sample were drivers (88 %). In the CCIS database, 64 % of occupants were reported as drivers at the time of the accident. This shows that drivers were more prevalent in the physiotherapy study than in CCIS.

As reported by the physiotherapists 95 % of the patients were reported as wearing a seat-belt at the time of the accident. This compares well with the belt wearing rate for car drivers in 2005 of 93 % (TRL, 2005).

Four types of injury were suggested in the questionnaire for the physiotherapists to code their diagnosis of the injury of the patient. The results of the diagnoses are shown in Figure 15. It is clear to see that a joint sprain was the most common injury type, in the sample. A muscle strain or a joint

sprain with associated muscle strain were the next most frequently occurring injuries.

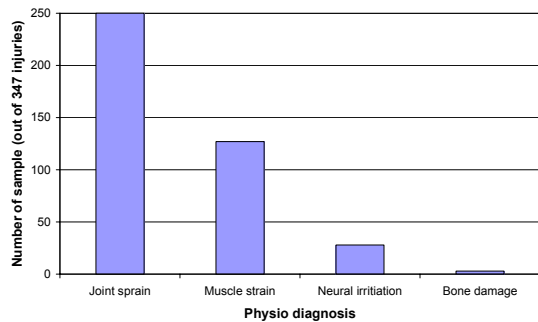


Figure 15. Diagnosis of the physiotherapist, from the four available options.

An injury mechanism was proposed for each case report. This was the opinion of the reporting physiotherapist. Injury trends were difficult to determine for the frontal and side impact scenarios with mechanisms being particular to individual cases.

In rear impacts, it was found that ‘whiplash’ was the most common form of injury mechanism for all of the physiotherapists.

The physiotherapists reported on three impairment criteria (level of function, pain, and range of motion) at three different times in their treatment of the injury (at the time of the accident, at the initial assessment by the physiotherapist, and a final assessment after the course of physiotherapy). The assessments to determine the initial and final levels of impairment were made by the physiotherapist. The ‘time of accident’ impairment level was based on what the patient relayed to the physiotherapist.

The level of function was rated using six levels from ‘full’ function to ‘unable to perform Activities associated with Daily Living (ADLs)’. The ten-item version of the ADLs is reproduced in the AMA Guides to the evaluation of permanent impairment (Cocchiarella and Andersson, 2001).

The results from the level of function assessments are shown in Figure 16. From this figure it can be seen that at the time of the accident, there are more patients with full function than at the initial assessment. It is expected that this relates to injuries where the functional impairment comes on after the accident. For example, a muscle strain that stiffens the following day with increased inflammation or irritation.

Comparing the functional impairment at the initial assessment, with that of the final assessment, it can be seen that the majority of patients appear to have returned to having full function at the time of the

final assessment – their last physiotherapy appointment.

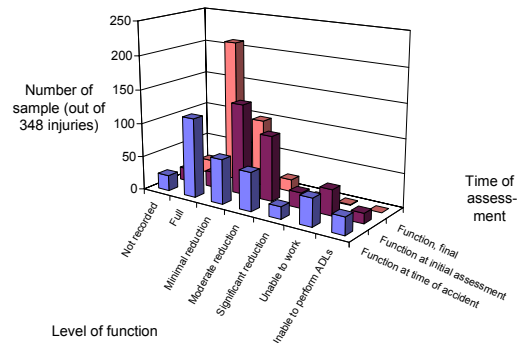


Figure 16. Level of function as assessed by the physiotherapists.

The level of pain for the patient was rated on a scale from 0 to 10. On this scale, 0 corresponded to no pain and 10 to the most pain conceivable. This information was reported by the physiotherapist based on what the patient told them. The pain impairment, as reported by the physiotherapists, is shown in Figure 17.

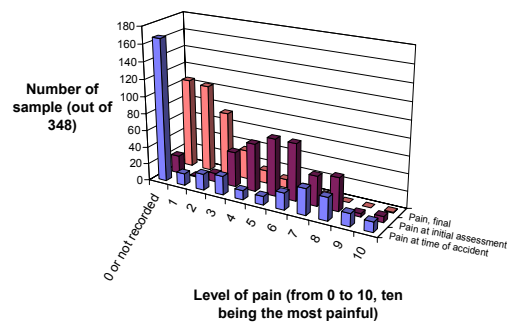


Figure 17. Level of pain reported by the physiotherapists.

At the time of the accident, there are a large number of injuries that had either no pain associated or the level of pain was not recorded. This may be a result of the patient not remembering accurately their pain level at that time or not passing this on to the physiotherapist, or, as with the level of function, the pain could have increased with time after the accident.

The modal levels of pain, as reported by the patient at the time of the initial assessment and at the final assessment by the physiotherapist indicate that the treatment by the physiotherapists was effective in reducing the level of pain impairment for the patient. However, for 243 of the 348 injuries the reported level of pain, at the final assessment by the physiotherapist, was not equal to zero.

As with the functional and pain impairments, the Range Of Motion (ROM) for the patient was assessed at the same times. The reported levels for range of motion are shown in Figure 18. As with both the function and pain, the ROM impairment increased between the time of the accident and the time of the initial assessment by the physiotherapist. Whilst the physiotherapy treatment generally reduces the ROM impairment, two persons were left with significant loss in their ROM at the end of the physiotherapy treatment (final assessment).

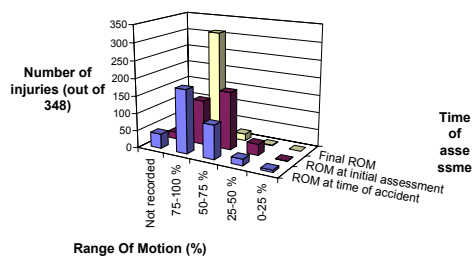


Figure 18. Patient range of motion as assessed by the physiotherapists.

In 43 out of the 288 cases, the physiotherapists were able to report on the time off work that the patient had incurred as a result of the injury, from what the patient had told them. The results of the time spent off work, due to the injuries, are shown in Figure 19. In addition to those cases shown in Figure 19, there was one case where the patient was off work for three months and another two cases where the injury resulted in 18 months off work for the patient.

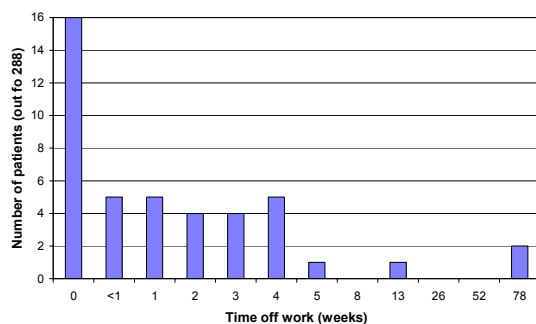


Figure 19. Time the patient spent away from work due to their injuries, as reported by the physiotherapist.

As a time off work figure was reported for such a small proportion of the cases, it is difficult to draw conclusions from this data. However, applying the cost of taking a day off work due to sickness as produced by the Chartered Institute of Personnel and Development (CIPD, 2005) to the mean five weeks off work caused by the injuries in the physiotherapy study sample, then the mean cost due to the injuries is £ 1,810. The median figure of

one week off work would result in a cost of £ 358. This is assuming a five day working week and that the figures from the CIPD are appropriate for the physiotherapy study sample.

These calculations have not included a value for the blank responses from the other 245 questionnaires. It is possible that the physiotherapists were less likely to report time off work if it was 'no time off work'. Therefore, the results may overestimate the mean time resulting from the injuries reviewed by the physiotherapists. The duration of the treatment and the cost for the treatment were also recorded by the physiotherapist. Average values for these data are shown in Table 2, together with the expected duration of the impairment.

From Table 2, it can be seen that the average duration for the physiotherapy treatment was about two months. The maximum treatment duration was 14 months. The modal cost associated with the physiotherapy treatment was £ 100. This relates to four sessions or two hours with the physiotherapist. The maximum cost was £ 1,000.

Table 2. Duration of treatment, treatment cost, and duration of impairment

	Duration of treatment (weeks)	Cost	Duration of impairment (weeks)
Mean	9	£ 184	23
Median	6	£ 150	13
Mode	8	£ 100	8

CONCLUSIONS

Approximately 19 % of all AIS injuries in Phase six and seven of the CCIS database were sustained to the upper extremity. Injuries to the upper extremity comprise 21 % of all AIS 1 injuries and 23 % of all AIS 2 injuries. The analysis of the Co-operative Crash Injury Study showed that, following road traffic collisions, moderate and serious upper extremity injuries are commonly suffered by car occupants. It was estimated that over ten thousand car occupant crash survivors suffered a moderate or serious upper extremity injury in Great Britain in 2004. For 21 % of casualties with known MAIS of 2 to 6, their upper extremity injury was the most severe or equal to the highest AIS code.

It was not possible to develop a robust and accurate cost model to reflect the monetary and impairment implications of the upper limb trauma identified at

a national level. However, the retrospective study cases were generally representative of the CCIS database and were used to prioritise the specific injuries in terms of frequency, cost and impairment, for the given impact types.

Based on the frequency of similar injuries in the CCIS database and the cost and impairment information from the 74 medical and accident review cases in the retrospective study, the priorities for future upper extremity injury prevention are:

In frontal impacts:

- Radius and/or ulna fracture
- Hand, humerus and clavicle fractures

In struck-side impacts:

- Humerus fracture
- Radius and/or ulna fracture
- Clavicle fracture

Soft tissue injury groups were not found to be priorities based on the criteria used in the retrospective study. The prospective and physiotherapy studies did not suggest that soft tissue injuries should be a higher priority than indicated by the retrospective case data.

The injury mechanisms for the priority injury groups were investigated in more detail, based on the detailed injury information provided by the retrospective medical review combined with the CCIS accident information. In many cases, the in-depth medical review was able to provide additional information on the injury that helped to determine the specific mechanism of injury.

For the specific injury priorities identified in this study, only two cases were identified where the airbag was the most likely cause of the injury to a driver. This apparent anomaly could be due to sampling: airbag equipped vehicles are effective at reducing the risk of fatal head injuries, so it may be that casualties who would have been fatally injured are now surviving accidents and their arm injuries may therefore be more likely to be recorded. It could also be due to an increase in the stiffness of steering wheels, necessary to give adequate support to the airbag - many of the priority injuries had the steering wheel as a potential injury causing contact.

A further two cases were identified where the airbag was the most likely cause of the injury to a front seat passenger, one of which involved serious wrist and distal forearm injuries. This is a cause for concern and should be investigated further. Many of the retrospective study injuries, from frontal impacts, for which a medical review was conducted, were caused through some direct loading with the structures in front of the occupant

(e.g. facia, A pillar or steering wheel). The effective stiffness of the parts of the vehicle interior in front of the front seat occupants is regulated according to the Interior Fittings Regulation (ECE, 1993, as amended). This regulation includes a dynamic test simulating contact between the head of an occupant and that part of the interior of the vehicle. It may be possible for this regulation to be upgraded or amended to make contacts between the upper extremities of occupants and the vehicle interior less likely to cause injury.

A large proportion (~90 %) of the drivers or front seat passengers seen at the QMC Emergency Department in the prospective study sustained their injuries as a result of a rear impact or multiple impacts. A 'whiplash' injury mechanism was reported as being responsible for many of the injuries reviewed in the physiotherapy study. As whiplash is often associated with rear impact or multiple impact shunts, it is suggested that rear and multiple impacts are considered a priority for future investigation.

The confidence with which the cost, impairment and injury mechanism conclusions from the retrospective study can be related to the national situation was limited by the number of cases reviewed and how representative those cases were of the national accident statistics. A study in which a larger number of cases was reviewed would allow greater confidence. However, this greater confidence is not expected to change the order of the injury priorities for future prevention. Based on the logistics of setting-up a larger study of this type, it is recommended that this is currently not worthwhile for upper extremity injury.

ACKNOWLEDGEMENTS

The work described in this report was carried out in the Vehicle Engineering Department of TRL Limited. The authors are grateful to the UK Department for Transport, Transport Technology and Standards Division, for supporting this work.

This report uses accident data from the United Kingdom Co-operative Crash Injury Study (CCIS) collected during the period July 1998 to November 2005. Currently, the CCIS is managed by the Transport Research Laboratory (TRL Limited), on behalf of the United Kingdom Department for Transport (DfT) who fund the project along with Autoliv, Ford Motor Company, Nissan Motor Company and Toyota Motor Europe. Previous sponsors of CCIS have included, Daimler Chrysler, LAB, Rover Group Ltd, Visteon, Volvo Car Corporation, Daewoo Motor Company Ltd and Honda R&D Europe (UK) Ltd. Further information on CCIS can be found at <http://www.ukccis.org>.

Contributions to the work reported in this paper came from the Ergonomics and Safety Research Institute, Birmingham Automotive Safety Centre, Nottingham City Hospital (University of Nottingham), Nottingham Queen's Medical Centre, University Hospital Birmingham (Selly Oak Hospital), Heartlands and Solihull Hospital, Brook Lane Physiotherapy Clinic, Connect Physical Health Centres and Pyrford Physiotherapy Clinic.

The authors are grateful for the contributions, at these centres by Jo Barnes; Ali Hassan and Brian Thomas; Philip Wraighte, Paul Manning and Prof. W. Angus Wallace; Philip Miller and Frank Coffey; Keith Porter; Tony Bleetman; Ruth Tayler; Andrew Walton and Michael Harding; and Sally Critien.

REFERENCES

- [1] Mackay G M, Ashton S J, Galer M D and Thomas P D (1985). "The methodology of in-depth studies of car crashes in Britain." SAE technical paper number 850556. pp. 365-390.
- [2] AAAM (1990). "The Abbreviated Injury Scale. 1990 Revision." Des Plaines, Illinois 60018, U.S.A: Association for the Advancement of Automotive Medicine (AAAM).
- [3] Cuerden R, Hill J, Kirk A and Mackay M (2001). "The potential effectiveness of adaptive restraints." Proceedings of the 2001 international IRCOBI conference on the biomechanics of impact, Isle of Man, UK, 10-12 October 2001.
- [4] Huere J-F, Foret-Bruno J-Y, Faverjon G and Le Coz J-Y (2001). "Airbag efficiency in frontal real world accidents." Proceedings of the 17th international technical conference on the Enhanced Safety of Vehicles, Amsterdam The Netherlands, 4-7 June 2001. Washington DC: NHTSA.
- [5] Morris A, Barnes J and Fildes B (2001). "The effectiveness of airbags in Australia as determined by in-depth crash injury research." Proceedings of the 17th international technical conference on the Enhanced Safety of Vehicles, Amsterdam The Netherlands, 4-7 June 2001. Washington DC: NHTSA.
- [6] Lenard J and Welsh R (2001). "A comparison of injury risk and pattern of injury for male and female occupants of modern European passenger cars." Proceedings of the 2001 international IRCOBI conference on the biomechanics of impact. Isle of Man, UK, 10-12 October 2001.
- [7] Siegel J H, Loo G, Dischinger P C, Burgess A R, Wang S C, Schneider L W, Grossman D, Rivara F, Mock C, Natarajan G A, Hutchins K D, Bents F D, McCammon L, Leibovich E and Tenenbaum N (2001). "Factors influencing the patterns of injuries and outcomes in car versus car crashes compared to sport utility, van or pick-up truck versus car crashes: Crash Injury Research Engineering Network study." *Journal of Trauma Injury, Infection and Critical Care* 51 (5) 975-990.
- [8] Kirk A, Frampton R and Thomas P (2002). "An evaluation of airbag benefits/disbenefits in European vehicles – a combined statistical and case study approach." Proceedings of the 2002 international IRCOBI conference on the biomechanics of impact, Munich Germany, 18-20 September 2002.
- [9] Jernigan M V and Duma S M (2003). "The effects of airbag deployment on severe upper extremity injuries in frontal automobile crashes." *American Journal of Emergency Medicine* 21 (2) 100-105.
- [10] Kent R, Viano D C and Crandall J (2005). "The field performance of frontal airbags: a review of the literature." *Traffic Injury Prevention*, 2005 (6) 1-23.
- [11] Department for Transport (2004). Instructions for the completion of road accident reports. STATS 20. Available from the UK DfT internet site: <http://www.dft.gov.uk/pgr/statistics/datatablespublications/accidents/casualtiesgbar/>
- [12] Cocchiarella L and Andersson G B J (2001). "Guides to the evaluation of permanent impairment. Fifth edition." U.S.A: American Medical Association (AMA).
- [13] Compigne S, Caire Y, Quesnel T and Verriest J-P (2003). Lateral and oblique impact loading of the human shoulder 3D acceleration and force-deflection data. Proceedings of the 2003 international IRCOBI conference on the biomechanics of impact, Lisbon Portugal, 25-26 September 2003.
- [14] TRL (2005). "Restraint use by car occupants, 2003-2005." Leaflet LF2096. Crowthorne, United Kingdom: TRL Limited.
- [15] The Chartered Institute of Personnel and Development (2005). "The HR and development website." www.cipd.co.uk. London, United Kingdom: The Chartered Institute of Personnel and Development (CIPD).
- [16] Economic Commission for Europe (1993, as amended). "Uniform provisions concerning the approval of vehicles with regard to their interior fittings." ECE Regulation No. 21, as amended. Geneva: United Nations.

CHARACTERIZATION OF KNEE IMPACTS IN FRONTAL CRASHES

Jonathan D. Rupp^{1,2}, **Carl S. Miller**¹,
Matthew P. Reed^{1,4}, **Nathaniel H. Madura**¹,
Nichole L. Ritchie¹, and **Lawrence W. Schneider**^{1,3}

¹University of Michigan Transportation Research
Institute (UMTRI)

²The University of Michigan, Department of
Emergency Medicine

³The University Michigan, Department of Biomedical
Engineering

⁴ The University Michigan, Department of Industrial
and Operations Engineering

United States
Paper 07-0345

ABSTRACT

Analyses were performed to quantify the conditions under which the knee is loaded in frontal motor-vehicle crashes and to thereby provide insight on the test conditions that should be used in future studies of the tolerance of the knee to loading of its anterior surface. These analyses estimated knee angle and the orientation of the femur relative to the knee bolster during bolster loading, the area of knee over which knee bolster contact loads are distributed, and knee loading rate. The postures of the lower extremities of 18 male and 18 female occupants relative to the knee bolster in three vehicles were used with a 2D kinematic model of the lower extremities to estimate occupant knee angle and the angle between the long axis of the femur and the plane of the knee bolster at initial knee contact and after 100 mm of bolster stroke. At knee contact, the average knee angle was $92^\circ \pm 13^\circ$ (mean \pm sd) and average bolster-to-femur angle was $67^\circ \pm 6^\circ$. After 100 mm of bolster stroke knee angle was reduced to $75^\circ \pm 11^\circ$ and bolster-to-femur angle was $65^\circ \pm 5^\circ$. Bolster-to-knee contact areas produced by a single set of cadaver knees impacting four driver knee bolsters selected for their widely varying force-deflection characteristics resulted in forces being distributed over the majority of the anterior surface of the patella. Analysis of femur force histories in FMVSS 208 and NCAP tests indicated that median femur loading rate was approximately 250 N/ms and 90% of femur loading rates were below 1 kN/ms. These values are only rough estimates of knee loading rates, since contributions of axial and shear forces transmitted through the knee to axial femur force are not quantified in FMVSS 208 and NCAP tests.

INTRODUCTION

A research program is underway at the University of Michigan Transportation Research Institute to develop new injury criteria and injury assessment reference values (IARVs) for the knee-thigh-hip (KTH) complex. A recent focus of this effort is to better understand the injury tolerance of the anterior surface of the flexed knee to knee-bolster loading.

Studies in the biomechanical literature have demonstrated that the stiffness of the surface loading of the knee can have a large effect on knee fracture tolerance. However, none of stiffnesses of the surfaces used to load the knees in these studies have been related to the stiffness of production knee bolsters. Atkinson et al. (1997) analyzed knee-thigh-hip injury patterns produced by knee impacts from tests in which the flexed knees of seated cadavers were dynamically loaded with flat-faced rigid and padded impactors (Patrick et al. 1967, Powell et al. 1975, Melvin et al. 1975, and Stalnaker and Viano 1980) and found that rigid impacts are associated with a greater proportion of knee fractures than padded impacts.

Atkinson et al. also reported on a series of biomechanical tests that further demonstrates that the compliance of the surface impacting the knee can affect knee tolerance. In these tests, pairs of knees from unembalmed cadavers were dynamically loaded in a 90°-flexed posture, such that one knee was impacted with a rigid surface and the contralateral knee was impacted with an energy-absorbing surface. Tests that used a rigid impactor applied a focal load to the knee and produced fractures of the patella or of the patella and femoral condyles at an average force of 5 kN. In contrast, tests that used an energy-absorbing impactor distributed impact forces over the entire anterior surface of the patella and did not produce any injuries, even though peak knee impact forces were approximately 20% higher than those from the corresponding rigid impacts. Despite the strong association between knee tolerance and the manner in which force was distributed over the anterior knee surface, the stiffnesses and knee contact areas produced by the energy-absorbing knee impactors were not compared to those of the surfaces being loaded by driver knees in frontal crashes.

Studies in the biomechanical literature have also hypothesized that knee angle affects knee fracture pattern because changes in knee angle alter the position of the patella on the femoral condyles (Haut

1989, Atkinson et al. 1997). A more flexed knee results in a patella that is located between the femoral condyles, which is thought to be associated with a greater likelihood of split condylar fractures and the surpacondylar fractures that result from split condylar fractures. Conversely, a more extended knee is associated with a patellar position that is above the femoral condyles and is therefore thought to be less likely to split the femoral condyles and more likely to result in fracture of the patella. If these hypotheses are correct, and changes in knee angle are associated with changes in injury pattern, then changes in knee angle may also be associated with differences in knee tolerance.

Another limitation of knee tolerance data in the biomechanical literature is that all of these data were collected in tests in which the knee is loaded by flat surfaces that are perpendicular to the long axis of the femur. In real-world frontal crashes, it is likely that variability in occupant posture, coupled with the initial angle of the knee bolster, results in knee loading that is not perpendicular to the long axis of the femur. If the knee bolster is angled relative to the long axis of the femur, the patella will be forced downward relative to the femoral condyles during knee bolster loading, which may affect knee fracture pattern and knee tolerance.

The current study was performed to provide a foundation for future knee tolerance research by defining the ranges over which test parameters should be varied. Data on occupant posture, position, and vehicle interior geometry were analyzed to estimate the ranges of knee angles and the orientation of the knee bolster relative to the long axis of the femur during bolster loading in frontal crashes. Cadaver knees were impacted by knee bolsters from production vehicles to estimate how load is distributed over the anterior surface of the knee. Loading rates and peak femur forces from FMVSS 208 and NCAP tests were analyzed to provide rough estimates of knee loading rate and peak force applied to the knee in severe full-frontal crashes.

METHODS

Knee and Knee-Bolster-to-Femur Angles

Variations in knee angle and the angle of the knee bolster relative to the long axis of the femur during frontal crashes were estimated using occupant anthropometry, posture, position, and vehicle interior package geometry collected as part of an unpublished previous study at UMTRI in which the seated postures and positions of 18 male and 18 female subjects were recording following normal driving in

three vehicles. These subjects were selected using a stature-based criterion so that tall and short drivers were oversampled relative to the US population, thus allowing a better estimate of the effects of stature on driver posture and position. The three vehicles used in this study were selected because they varied in seat height (H30) and included a midsize sedan (2002 Pontiac Grand Am), a large sedan (2000 Ford Taurus), and a minivan (2001 Dodge Caravan). Figure 2 illustrates the relevant driver lower-extremity posture data that were collected. These data include the locations of the left lateral malleolus, lateral femoral condyle, greater trochanter, and suprapatellar landmark.

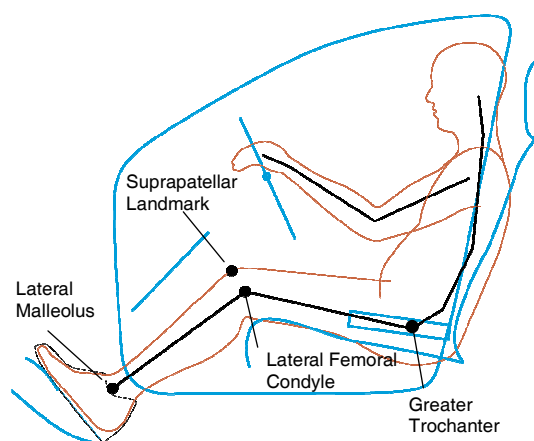


Figure 2. Skeletal landmarks collected in UMTRI studies to define the posture of the driver's lower extremities.

A simple 2D model of the right side of the lower extremities was generated for each occupant in each vehicle package using the points illustrated in Figure 2. This model was used to predict knee angle and bolster-to-femur angle at the time of knee bolster contact by translating the hip forward horizontally while constraining the leg to rotate about an ankle joint (i.e., the lateral malleolus) that was fixed with respect to the vehicle interior until the suprapatellar landmark intersected the plane of the knee bolster. Figure 3 illustrates this posture and defines knee angle and bolster-to-femur angle. These angles were also calculated after 100 mm of knee bolster stroke, which was simulated by moving the knee bolster away from the occupant's knees by 100 mm and repeating the procedure used to determine knee and bolster-to-femur angles at knee bolster contact.

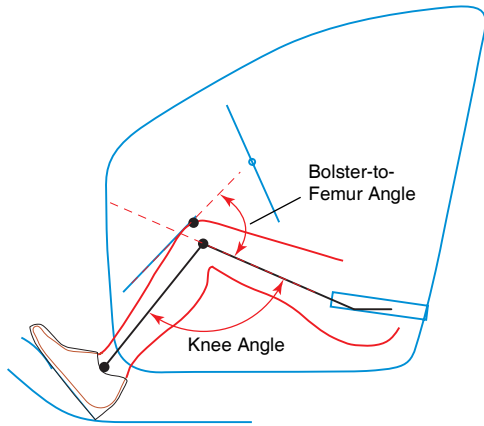


Figure 3. Two-dimensional linkage model of occupant's knee, thigh, leg, and ankle at the time of knee bolster contact illustrating knee and knee-bolster-to-femur angles.

Because the subjects in the driver posture study included a greater proportion of tall men and short women than would be expected in a typical driver population, it was necessary to reweight the predictions of the kinematic model to appropriately estimate the tail percentiles of the expected distributions of model predicted posture variables. The procedure used to do this is similar to the method reported by Flanagan et al. (1998) for analyzing data from stratified samples. In brief, linear regression functions are computed to predict the relationship between stature and posture variables (i.e., knee angle and bolster-to-femur angle) for each gender and each vehicle. If a meaningful relationship between a posture variable and stature exists, the distributions of knee angle and bolster-to-femur angles can be estimated by convolving the single-gender stature distribution by the linear regression model and adding the normally distributed residual variance from the regression. Percentiles of bolster-to-femur angle for each vehicle were calculated by combining the two single-gender normal distributions. If there is not a relationship between a posture variable and stature, tail percentiles can be estimated from the model-predicted distributions of the posture variable.

Knee contact area

Knee specimens from a single midsize male unembalmed cadaver were obtained by sectioning the lower extremities of a single midsize male cadaver slightly distal of the midshaft of the femur. These specimens were impacted by driver-side instrument panel/knee bolster (IP/KB) assemblies from four production vehicles to collect data on the area of the

knee surface loaded by the knee bolster in a frontal crash. Instrument panel/knee bolster assemblies were obtained from the vehicles listed in Table 1. These vehicles were selected because knee bolster force-deflection data from an earlier series of IP/KB tests (available at www-nrd.nhtsa.dot.gov, test numbers 8278-8291) indicate that knee bolsters from these vehicles should have a wide range of force-deflection characteristics and are therefore likely to produce a wide range of knee contact areas. Also, loading rates and peak femur forces from FMVSS 208 tests of the vehicles listed in Table 1 span over 90% of the variance in peak femur force and loading in FMVSS 208 testing, which further suggests that knee contact areas and force-deflection characteristics of these knee bolsters should vary widely.

Table 1. Vehicle Knee Bolsters Tested

Test ID	Make	Model
NKB0612D	Ford	1998 Explorer
NKB0613D	Ford	2000 Focus
NKB0614D	Ford	2003 Escape
NKB0615D	Ford	2001 Taurus

Figure 4 illustrates the test apparatus and Figure 5 provides more detail on the knee mounting hardware and instrumentation. Prior to testing, each IP was cut approximately in half. The driver side of each IP was then rigidly attached to a linearly translating sled using rigid brackets that were connected to structures supporting the IP (most commonly the cross-car beam) and bolted to the sled. Mounting the IP in this manner ensured that the knee bolster and its supporting hardware were intact and thereby ensured that the structural characteristics of the knee bolster were not affected by removal of the passenger side of the IP.

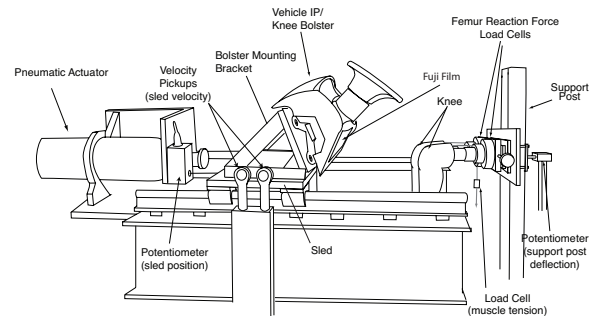


Figure 4. Side view of test apparatus.

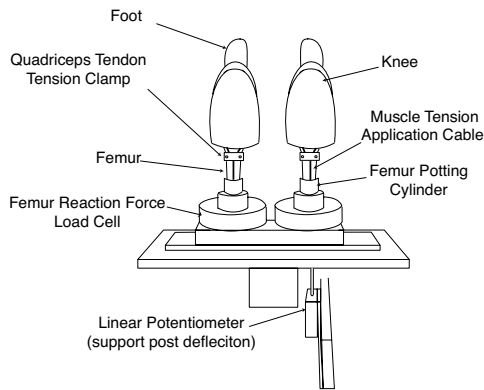


Figure 5. Top view of knee-mounting scheme.

The knee specimens used in these tests were obtained by sectioning the femurs of a single midsize male cadaver at midshaft and potting the truncated ends with room-temperature-curing epoxy. As shown in Figure 5, the potted ends of the femurs were rigidly secured to load cells that were attached to a support post. Both femurs were mounted so that the anterior surfaces of the knees were the same distance forward of the support post. The feet were supported from below by a platform and secured by clamping the ankles to a support positioned immediately behind each heel. For each test, approximately 600 N of tension was applied to each quadriceps tendon along its typical line of action by specialized clamps that were connected to a pneumatic cylinder by means of steel cables that were routed through holes drilled through the potting compound.

All tests were performed with a knee angle of approximately 90° and with the knee bolster oriented to produce a bolster-to-femur angle of approximately 65° , which are the approximate average values for these quantities based on the simulations described in the previous section. For each test, the lateral space between the knees was set to achieve the knee-bolster contact locations observed in FMVSS 208 tests of vehicles that were similar to those from which the knee bolster being tested was obtained.

Contact area was measured by layers of medium (10-50 MPa) and low (2.5-10 MPa) pressure-sensitive Fuji prescale film that were attached to the knee bolster surface. Due to the irregular shapes of the knee bolsters, sheets of prescale film were cut and shaped to follow the contour of the bolster. This also limited the artifacts caused by creases in the film.

To conduct a test, the knee bolster was pneumatically accelerated to a velocity of approximately 1.5 m/s prior to contact with the stationary knee/leg

specimens. This impact velocity and the ~300 kg platform mass were selected to produce an impact energy of 350 J, which was found to produce femur loading rates and peak forces similar to those measured in FMVSS 207 tests of the vehicles listed in Table 1 when KB/IP assemblies from these vehicles were loaded by Hybrid III knees in an earlier series of tests (available at www-nrd.nhtsa.dot.gov, test numbers 8278-8291).

Force applied to each knee was measured by a six-axis load cell positioned behind the potted femur. The force-deflection characteristics of the knee bolster were measured using the average of the left and right femur force histories and the displacement of the platform following knee contact. Average knee-bolster stiffness was calculated by taking the slope of the loading portion of the force-deflection curve between the deflection at which force first exceeded 15% of its maximum value and the deflection at which force last exceeded 85% of peak force. Average knee-bolster loading rate was calculated from the loading portion of the average force history in a similar manner. Each knee bolster was only tested once and the knees of the test specimen were palpated between tests to ensure that gross knee fracture had not occurred.

FMVSS 208 and NCAP Analysis

Femur force histories from FMVSS 208 and NCAP tests conducted between 1998 and 2004 from the NHTSA vehicle database were analyzed to characterize peak femur force and loading rate. A total of 1548 femur force histories from driver and right-front-seat passenger ATDs in 387 frontal impacts were analyzed. Loading rates were calculated by taking the slope of the loading portion of the force histories from the time the force first exceeds 15% of its peak value to the time the force last exceeds 85% of its peak. Table 2 describes the deltaVs, test types, and belt use in these crashes. Eighty of the eighty-nine FMVSS 208 tests were performed using unbelted ATDs and either a 48-kph soft pulse sled test (60/89) or a 40-kph barrier impact (20/89). The remaining nine tests were performed using belted occupants in the same test types. All 298 NCAP tests were performed using a 56-kph barrier impact with belted driver and right-front passenger ATDs.

Table 2. Characteristics of 1998-2004 FMVSS 208 and NCAP Frontal Impacts in the NHTSA Database

Test Category	Test Type	Nominal DeltaV (kph)	Belted/Unbelted	# of Tests
FMVSS 208	Barrier	40	Unbelted	20
			Belted	1
	Barrier	48	Unbelted	1
			Belted	6
Sled	48	Unbelted	60	
NCAP	Barrier	56	Belted	298

RESULTS

Knee and Knee-Bolster-to-Femur Angles

The average knee angles calculated for the 36 driver test subjects are listed in Table 3 for each of the three vehicles. Figures 6 and 7 show that occupant stature has no effect on knee angle at the time of bolster contact or after 100 mm of bolster stroke for all three vehicles. Because knee angle is not related to stature, it is not necessary to account for the effects of the over representation of tall men and short women in the subject population from which posture data were obtained.

Knee angle data were approximately normally distributed. Mean knee angle at contact was $92^{\circ} \pm 13^{\circ}$ (mean \pm sd) across vehicles, which is an average of 29° less than the starting knee angle. After 100 mm of simulated bolster stroke, knee angle was reduced by an average of 17° to a mean of $75^{\circ} \pm 11^{\circ}$, suggesting that most knee bolster loading occurs at knee angles that are less than 90° . The 5th and 95th percentile knee angles are 67° and 116° at bolster contact and 54° and 96° after 100 mm of bolster stroke.

Table 4 lists the knee-bolster-to-femur angles predicted by the simulations. At the time of knee-to-knee-bolster contact, the mean angle between the femur and the knee bolster surface is approximately 65° . This angle changed by an average of only 2° after 100 mm of simulated bolster stroke.

Figures 8 and 9 show a meaningful relationship between stature and bolster-to-femur angle at initial knee contact and after 100 mm of simulated bolster stroke, with short statured occupants having smaller bolster-to-femur angles and taller occupants having bolster-to-femur angles that were closer to 90° . This trend probably occurred because short occupants have shorter legs and therefore start with a smaller bolster-to-femur angle.

After accounting for the effects of the sampling scheme used in the UMTRI study from which posture data were obtained, mean bolster-to-femur angle at knee contact was $65^{\circ} \pm 5^{\circ}$ and the 5th and 95th percentile bolster-to-femur angles were 56° and 74° , respectively. After 100 mm of bolster stroke, bolster-to-femur angle did not change substantially. Mean bolster-to-femur angle was $67^{\circ} \pm 6^{\circ}$ and the 5th and 95th percentile bolster-to-femur angles after 100 mm of bolster stroke were 57° and 77° , respectively.

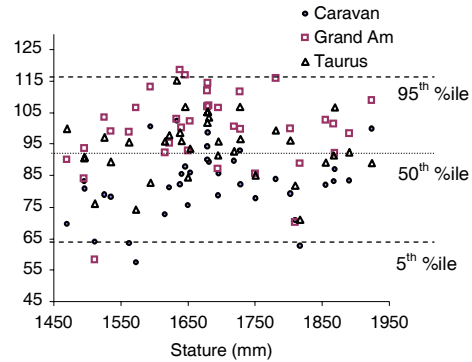


Figure 6. Knee angle at bolster contact versus occupant stature for the Caravan, Grand Am, and Taurus. Percentiles are from the combined data from all vehicles and occupants.

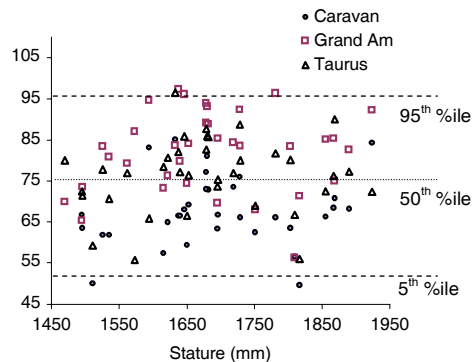


Figure 7. Knee angle after 100 mm of bolster stroke versus occupant stature for the Caravan, Grand Am, and Taurus. Percentiles are from the combined data from all vehicles and occupants.

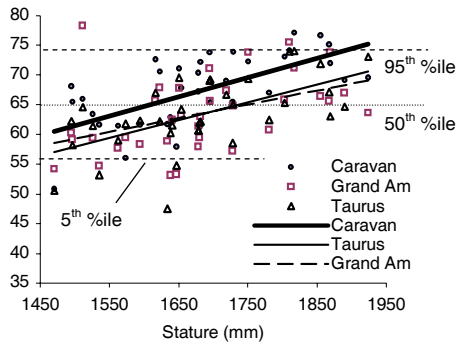


Figure 8. Bolster-to-femur angle at bolster contact to occupant stature for the Caravan, Grand Am and Taurus. Percentiles are from the combined data from all vehicles and occupants.

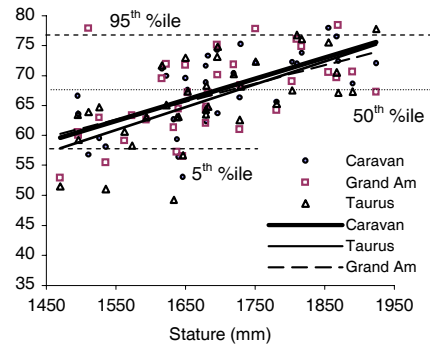


Figure 9. Bolster-to-femur angle after 100 mm of bolster stroke to occupant stature for the Caravan, Grand Am and Taurus. Percentiles are from the combined data from all vehicles and occupants.

Table 3. Mean Calculated Knee Angles

Vehicle	Initial Posture (degrees)	Bolster Contact (degrees)	100 mm of Bolster Stroke (degrees)	Change to Bolster Contact (degrees)	Change at 100 mm of Bolster Stroke (degrees)
Caravan	118	82	68	-36	-15
Grand Am	127	99	81	-27	-18
Taurus	119	94	76	-25	-18
All	121	92	75	-29	-17

Table 4. Mean Calculated Bolster-to-Femur Angles

Vehicle	Initial Posture (degrees)	Bolster Contact (degrees)	100 mm of Bolster Stroke (degrees)	Change to Bolster Contact (degrees)	Change at 100 mm of Bolster Stroke (degrees)
Caravan	63	67	67	4	0
Grand Am	57	63	67	6	3
Taurus	58	63	66	5	3
All	59	65	67	5	2

Knee Contact Area

Autopsy of the cadaver knees following the completion of all tests indicated that loading of the single pair of cadaver knees applied by all four of the knee bolsters did not produce any injuries. Table 5 summarizes results from each test. Peak force measured behind each knee ranged from 2.7 kN to 4.5 kN. Although both knees contacted the knee bolster at the same time in all four tests, peak forces applied to the left and right knees varied, suggesting that the force-deflection characteristics of the left and right sides of the knee bolster differ. The average knee penetration into the knee bolster varied from 79

mm to 94 mm. Knee bolster stiffness varied from 30 to 114 N/mm. In all tests, applied force peaked before maximum platform displacement, indicating bolster stiffness decreases after some amount of bolster deformation.

Figure 10 shows side-view high-speed video images of the left and right sides of the knee bolster at the times of knee contact and peak force for the Explorer, Focus, Escape, and Taurus knee bolsters. Figure 11 shows the contact areas measured by the low-pressure Fuji Film relative to the patella and femoral condyles from the single cadaver knee that was tested. These data provide insight on how the knee

bolsters deformed. The images from tests of the Explorer, Focus and Escape in Figure 10 show the bolster wrapping around the knee. The Fuji films from the corresponding tests show contact areas that are distributed over the entire surface of the patella. The images of the Taurus knee bolster shown in Figure 10 and the contact areas for the Taurus shown in Figure 11 (which only covers part of the patellar surface and one femoral condyle) indicate that the Taurus bolster did not fold around the knees, but instead the forward surface of the bolster displaced rearward as a unit.

Table 5. Cadaver Knee-to-Knee-Bolster Force and Displacement Results

Model	Peak Force, Left / Right (kN)	Penetration into Bolster (mm)	Loading Rate (N/ms)	Bolster Stiffness (N/mm)
Explorer	3.8/4.5	79	200	114
Focus	2.8/4.3	93	47	30
Escape	2.7/3.0	94	200	106
Taurus	3.6/4.2	91	53	38

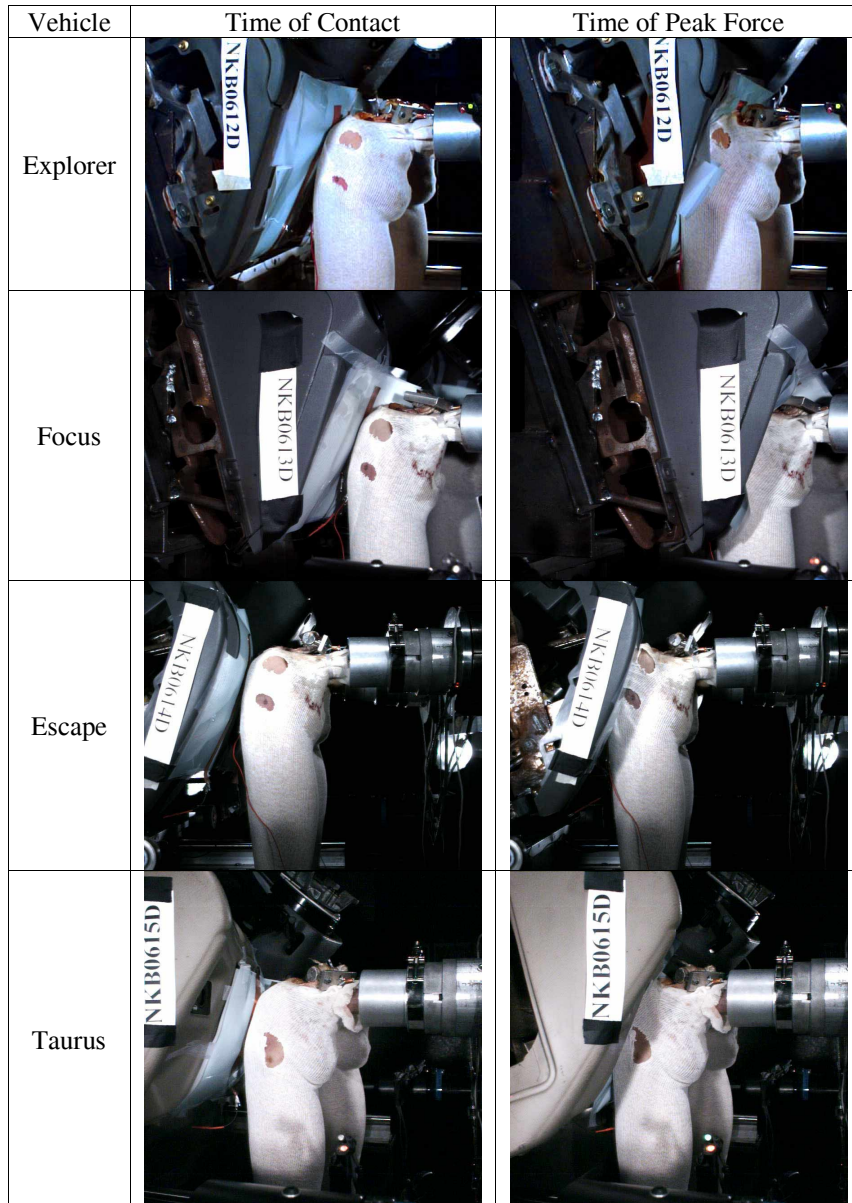


Figure 10. Images from side-view high-speed video showing deformation of KB/IP assemblies.

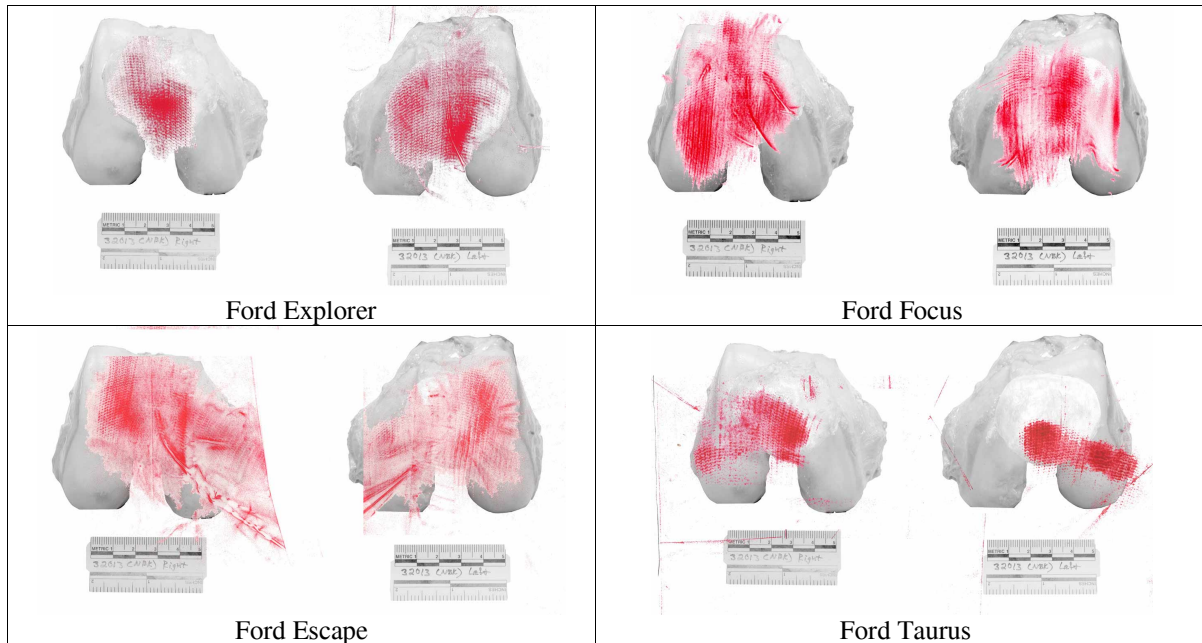


Figure 11. Contact areas recorded during tests of Explorer (upper left), Focus (upper right), Escape (lower left), and Taurus (lower right).

FMVSS 208 and NCAP Analysis

Figure 12 shows the combinations of peak compressive femur force and femur peak loading rate produced in NCAP and FMVSS 208 tests. Table 6 provides quantile values that describe the individual distributions of these parameters. The median peak force for NCAP tests is 3.6 kN and the median peak force for FMVSS 208 tests is 4.8 kN. The median loading rate for both FMVSS 208 and NCAP tests is approximately 250 N/ms and 90% of tests produced loading rates that were less than approximately 1 kN/ms. In general, NCAP tests produced a greater range of peak forces and loading rates than FMVSS 208 tests. This is expected since there are a greater number of NCAP tests and these tests involve a higher deltaV. In addition, these tests involve belted occupants who contact the knee bolster either earlier or later in the crash depending on the pre-impact knee-to-knee bolster spacing, belt restraint characteristics, and the crash pulse.

Although belt use and deltaV varied within the set of FMVSS 208 tests that was analyzed, changes in belt use and deltaV did not produce meaningful changes in loading rates or peak forces because differences between vehicles have a greater effect on these parameters than the differences between types of FMVSS 208 tests.

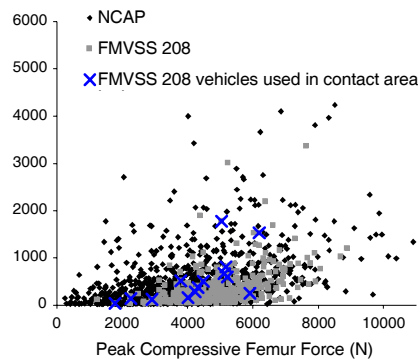


Figure 12. Combinations of peak force and loading rate from FMVSS 208 and NCAP frontal impacts conducted between 1998 and 2004.

Figure 12 also shows the peak forces and femur loading rates for FMVSS 208 tests in which the driver knee bolsters used in the knee contact area testing were loaded (i.e., knee bolsters from the Escape, Explorer, Focus, and Taurus). The ranges of peak force and femur loading rates produced in this subset of force histories were 1.7 kN to 6.2 kN and 40 N/ms to 1800 N/ms, respectively. As shown in Table 5, these ranges incorporate over 90% of the loading rates and peak forces produced in FMVSS 208 tests, suggesting that the knee bolsters used in the knee contact area tests provide a reasonable approximation of the range of knee bolsters in production vehicles.

Table 6. Peak Force and Loading Rate Quantiles for NCAP and FMVSS 208
Femur Force Histories from 1998-2004

Quantile	FMVSS 208 (n = 346)		NCAP (n = 1202)		FMVSS 208 and NCAP (n=1548)	
	Peak Force (N)	Loading Rate (N/ms)	Peak Force (N)	Loading Rate (N/ms)	Peak Force (N)	Loading Rate (N/ms)
100.0%	8897	3364	10910	5567	10910	5567
99.5%	8753	3121	9774	3897	9610	3636
97.5%	7642	1460	7727	2061	7639	1964
90.0%	6478	824	6152	1107	6277	1027
75.0%	5741	468	4856	571	5141	538
50.0%	4793	250	3618	246	3970	249
25.0%	4030	110	2395	92	2709	98
10.0%	3298	69	1416	44	1627	51
2.5%	2251	42	613	26	714	29
0.5%	1184	28	329	21	346	21
0.0%	1023	28	171	20	171	20

DISCUSSION

Three types of analyses were conducted to characterize the knee loading environment in frontal crashes. These include analyses of driver lower-extremity postures relative to knee bolsters during bolster loading, tests to characterize contact areas produced by production driver knee bolsters loading cadaver knees, and analysis of FMVSS 208 and NCAP data to characterize ranges of peak femur forces and loading rates.

Analyses to determine knee angle and bolster-to-femur angle at knee bolster contact and after 100 mm of knee bolster stroke were performed using a 2D kinematic model of the lower extremities that was generated using positions of skeletal surface landmarks relative to vehicle interior components measured from 36 drivers in three vehicles. Because the interior geometries of the entire vehicle population vary more than those of these three vehicles, and because variations in vehicle geometry will change preimpact knee-to-knee bolster spacing and occupant lower extremity posture, which in turn, affect knee angle and bolster-to-femur angle at knee contact, the knee angles and bolster-to-femur predicted by the 2D kinematic model should be considered conservative estimates of the ranges of these parameters for the driver/vehicle population.

In addition, in the simulations with the 2D kinematic model it was assumed that the position of the ankle remains fixed prior to bolster contact. This assumption may not be reasonable for knee-to-knee bolster loading in real crashes, where vehicle deceleration may cause the foot to move forward or

toe pan intrusion may cause the foot to move rearward, thereby making the knee angle either more or less acute.

Tests in which the knees of a single cadaver were loaded by four driver IP/knee bolster assemblies were performed to characterize the area of the anterior surface of the knee that is loaded by knee bolsters. These knee bolsters have widely variable force-deflection characteristics and because FMVSS 208 peak femur forces and femur loading rates further suggest that these results can likely be generalized to knee bolster loading in full-frontal crashes where the occupant's femurs are aligned with the 12 o'clock PDOF. These findings may not be applicable to angled or offset frontal crashes, or cases where occupants have large amounts of leg splay prior to bolster impact because these conditions result in smaller knee-to-knee bolster contact areas (Meyer and Haut, 2004).

The real-world applicability of the data reported in this study is predicated on the assumption that the knees contact the knee bolster in frontal crashes. While this assumption is valid for NCAP and FMVSS 208 crashes with ATDs, and therefore is valid for the using in biomechanical testing aimed at developing injury criteria and IARVs, it may not be valid for crashes angled and offset frontal crashes involving human occupants who will sit differently than ATDs. Because of these differences in occupant posture and crash dynamics, the knees of human occupants may contact surfaces other than the knee bolster (e.g., the steering column). If these surfaces have different geometries and force-deflection

characteristics than knee bolsters, then the contact areas, knee loading rates, knee angles, and bolster-to-femur angles reported in this study may not be applicable to knee-thigh-hip injury causation scenarios in these crash types. To determine the validity of the assumption that most knee-thigh-hip injuries in frontal crashes are caused by knee bolster contact, knee contacts associated with knee-thigh-hip injury in CIREN were analyzed. The results of this analysis are described in detail in the appendix. In brief, the 80% of the KTH injuries sustained by drivers and 64% of the KTH injuries sustained by right-front passengers in frontal crashes were associated with knee bolster contact. This finding indicates that it is appropriate to measure knee tolerance under knee-bolster-like loading conditions.

The analyses of FMVSS 208 and NCAP ATD femur force histories that were performed in this study only provide rough estimates of knee loading rate and peak force applied to the knee in frontal crashes. This is because it is not possible to accurately determine the force applied to the knee (or knee loading rate) in a frontal crash without knowledge of the compressive force on the upper tibia and the shear force at the knee, neither of which are currently measured in FMVSS 208 and NCAP tests. In addition, the acceleration of the distal femur is not measured, making it difficult to account for inertial effects on the decrease in force between the knee and the femur load cell.

The peak femur forces and loading rates measured at by the Hybrid III femur load cell are also difficult to relate to the femur and knee loading rates and peak forces that would be produced by a midsize male human loading the knee bolster. Specifically, the Hybrid III knee-thigh-hip complex is stiffer and has more tightly coupled mass than the cadaver, and presumably the human, knee-thigh-hip complex, Hybrid III knee impact forces and knee and loading rates are likely to be higher than those applied to the human knee (Rupp et al. 2005).

Despite the difficulties in estimating knee loading rate and peak force applied to the human knee using Hybrid III femur load cell data, the knee loading conditions produced in FMVSS 208 and NCAP can be reproduced experimentally, if the contribution of force transmitted through the tibia to femur loading rate is assumed to be negligible. Specifically, an impactor could be designed that produces Hybrid III femur loading rates that are within the range of those produced in FMVSS 208 and NCAP tests.

This study demonstrates that knee bolster loading is distributed over most of the anterior surface of the patella, suggesting that the low fracture forces reported in the literature for rigid knee impacts do not need to be considered when evaluating vehicle knee bolster performance. The findings from this study also indicate that knee angle can vary substantially at the time of knee bolster contact and that knee angle decreases as the knee strokes the knee bolster. If knee angle affects knee injury tolerance, then existing knee tolerance data that have been collected using a ~90° flexed knee do not consider an important factor that affects knee tolerance in frontal crashes.

The findings in this study provide estimates of the ranges of parameters that should be used in future studies of the tolerance of the flexed knee to loading of its anterior surface by a knee-bolster-like surface. These ranges are listed in Table 7. If a worst-case scenario for knee tolerance is simulated, the compliance of the surface loading the knee should be set so that applied forces are distributed over most of the patella. Knee loading rate should be tuned to produce a knee loading condition that results in a loading rate at the Hybrid III femur load cell that is less than approximately 1 kN/ms. To simulate most of the variance in knee angles at bolster contact, knee posture should be varied by approximately ±20° from a value between approximately 90° and 75°. The former value should be chosen if knee angle at contact is simulated, the latter if knee angle after the bolster is fully compressed is simulated. The surface loading the knee in these studies should be angled approximately 65°±9° from the long axis of the femur to simulate most of the variance in the occupant and vehicle population.

Table 7. Ranges of Test Parameters for Future Studies of Knee Tolerance

Parameter	Target Range
Knee contact area	Distributed over the majority of the anterior surface of the patella
Knee angle	110° to 70°, if posture at contact is simulated 95° to 55° if posture after 100 mm of stroke is simulated
Bolster-to-femur angle	65°±9°
Knee loading rate	< ~1kN/ms

CONCLUSIONS

These analyses suggest that:

- Ninety percent of the knee angles at the time of knee bolster contact for the driving population are between 67° and 116°. After 100 mm of bolster stroke, ninety percent of knee angles are between 54° and 96°.
- The average orientation of the long axis of the femur relative to the plane of the knee bolster is approximately 65° and ninety percent of bolster-to-femur angles lie between 56° and 74°. This angle does not meaningfully change after 100 mm of knee bolster stroke.
- Ninety percent of knee-to-knee-bolster loading in FMVSS 208 and NCAP tests produces femur loading rates less than 1 kN/ms.
- Bolster-to-knee loading is distributed over most of the anterior surface of the patella and may be distributed over the entire patella and part of the femoral condyles.

These ranges of knee angle, bolster-to-femur angle, femur loading rate, and knee contact area provide bounds on the parameters that should be used, or produced, in future studies of knee tolerance to loading of the anterior surface of the flexed knee.

ACKNOWLEDGEMENTS

The research described in this paper was sponsored by the National Highway Traffic Safety Administration, U.S. Department of Transportation under contract # DTNH22-05-H-01020. The authors recognize Thomas Jeffreys for his assistance in specimen preparation and testing. The authors would also like to acknowledge the contributions of Charles Bradley, Brian Eby, Stewart Simonett, and James Whitley who assisted in the fabrication of the test apparatus. The assistance of Kathy Klinich in the review of this manuscript is gratefully acknowledged. The advice and guidance provided by Shashi Kuppa is acknowledged and appreciated. The assistance in gathering FMVSS 208 and NCAP femur force histories provided by Felicia McKoy of OnPoint is also gratefully acknowledged.

REFERENCES

Atkinson, P.J., Garcia, J.J., Altiero, N.J., and Haut, R.C. (1997). The influence of impact interface on human knee injury: Implications for instrument panel design and the lower extremity injury criterion. Proceedings of the 41st Stapp Car Crash Conference, Paper No. 973327, pp. 167-180. Society of Automotive Engineers, Warrendale, PA.

Haut, R.H. (1989). Contact pressures in the patellofemoral joint during impact loading on the human flexed knee. *Journal of Biomechanics* 7:272-280.

Flannagan, C., Manary, M.A., Schneider, L.W., and Reed, M.P. (1998). An improved seating accommodation model with application to different user populations. *Journal of Passenger Cars* 107:1189-1197.

Melvin, J.W., Stalnaker, R.L., Alem, N.M., Benson, J.B., and Mohan, D. (1975). Impact response and tolerance of the lower extremities. Proceedings of the Nineteenth Stapp Car Crash Conference. Paper No. 751159, 543-559. Society of Automotive Engineers, Warrendale PA.

Melvin, J.W. and Stalnaker, R.L. (1976). Tolerance and response of the knee-femur-pelvis complex to axial impact. Report No. UM-HSRI-76-33. University of Michigan, Highway Safety Research Institute, Ann Arbor, MI.

Meyer, E.A. and Haut, R.C. (2003). The effect of impact angle on knee tolerance to rigid impacts. *Stapp Car Crash Journal* 47:1-19.

Partick, L.M., Kroell, C.K., and Mertz, H.M. (1966). Forces on the human body in simulated crashes. Proceedings of the Ninth Stapp Car Crash Conference, pp. 237-260. University of Minnesota.

Powell, W.R., Ojala, S.J., Advani S.H., and Martin, R.B. (1975). Cadaver femur responses to longitudinal impacts. Proceedings of the Nineteenth Stapp Car Crash Conference, Paper No. 751160, 561-579. Society of Automotive Engineers, Warrendale PA.

Rupp, J.D., Reed, M.P., Madura, N.H., Kuppa, S., and Schneider L.W. (2003b) Comparison of knee/femur force-deflection response of the Thor, Hybrid III, and human cadaver to dynamic frontal-impact knee loading. Proceedings of the 18th International Conference in the Enhanced Safety of Vehicles. National Highway Traffic Safety Administration, Washington DC.

Stalnaker, R.L., Nusholtz, G.S., and Melvin J.W. (1977). Femur impact study. Final Report No. UM-HSRI-77-25. University of Michigan, Highway Safety Research Institute: Ann Arbor.

**APPENDIX
KNEE CONTACTS IN CIREN**

The CIREN database (1995-2006) was analyzed to identify the vehicle interior components that driver and passenger knees contact in frontal crashes that result in knee, thigh, or hip injury. In this analysis, only frontal crashes with PDOF between 10 o'clock and 2 o'clock were considered. Knee contacts in narrow frontal impacts with corner involvement (FLEE, FREE CDC codes) were excluded from the analysis, since the KTH injuries produced in narrow frontal impacts are often caused by the intruding door loading the thigh and hip, and not by knee contact. In addition, only knee contacts that were assigned a confidence level of certain or probable were used in the analysis.

Figure A1 shows the results of this analysis. Injuries that were associated with contact with the glove box were combined with those coded as the right knee bolster, since the glove box and right knee bolster are equivalent components. In addition, contacts coded "left IP and below" and "right IP and below" were combined with the left and right knee bolster codes, respectively, since the lower IP is typically designed to deform like the knee bolster. Eighty percent of KTH injuries experienced by the driver were attributed to knee bolster contact. A similar trend was observed for KTH injuries to passengers, where 64% of injuries were from knee bolster contacts. However, a greater proportion of passenger KTH injuries were associated with contacts to the center IP and below and the right door, armrest, and door hardware.

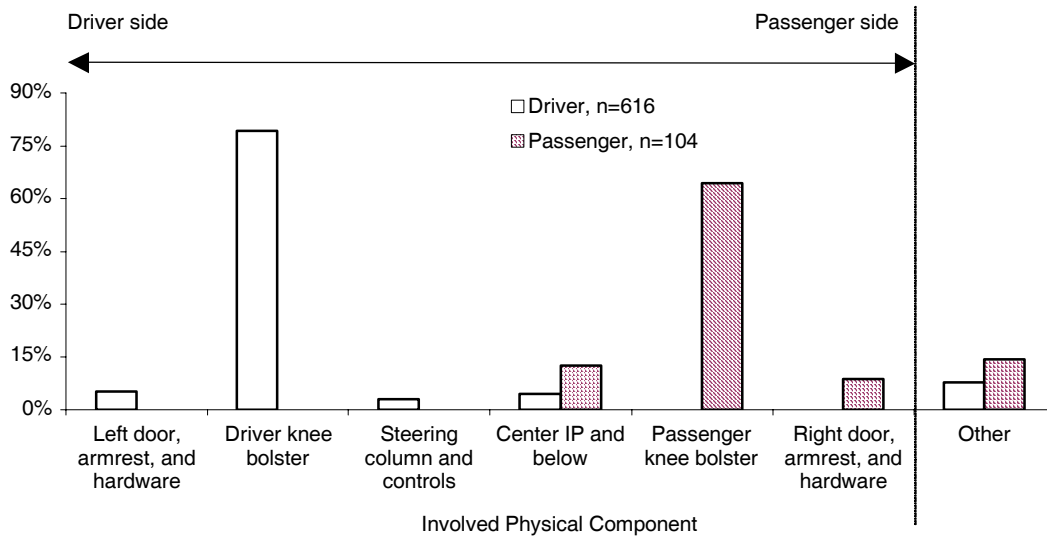


Figure A1. Proportion of driver and passenger AIS 2+ knee-thigh-hip injuries versus involved physical component contacted by the knee in frontal crashes in CIREN (1997-2006).

DEVELOPMENT AND ASSESSMENT OF A SURFACE FORCE ABDOMINAL SENSOR

Heiko Johannsen

Volker Schindler

Technische Universität Berlin

Germany

Paper Number 07-0365

ABSTRACT

Abdominal injuries occur seldom but are often of high severity. Various proposals for the assessment of the abdominal injury risk have been made. Nevertheless only a few dummies are equipped with abdominal sensors.

With support from the European CHILD and APROSYS projects abdominal surface force sensors for Q child dummies and the Hybrid III 50 percentile dummy were developed. The surface matrix force sensors are able to assess the time history of the applied force and the location of the load, which is important as different abdominal regions are meant to require different load limits. The sensors for the Q dummies were used in the CHILD project reconstruction programme. The analysis of 14 accident reconstructions indicates a very good correlation between the applied load assessed by the proposed sensor and the AIS 3+ injury risk. However, the number of cases is still small. Additional reconstruction cases should be able to validate the described results.

INTRODUCTION

Abdominal injuries do not occur very frequently but when they do occur they are often very severe. Although measures against submarining, which was the main cause for abdominal injuries in the past, were established (e.g., seat ramps, belt pretensioners and improved belt geometry), recent accident investigations by LAB (common research institute of Peugeot and Renault) show that there are still abdominal injuries in real world accidents, especially in rear seat occupants [Walfisch, 2002]. Based on the study of US accidents with air bag deployment, Digges et al. [Digges, 1996] proposed the measurement of abdominal injury risk to be a matter of priority. Within the combined work programme of EEVC WG 12 (Crash Dummies) and 18 (Child Safety) the abdomen was defined as an important body region for children using booster seats [Jager, 2005]. However, abdominal injuries were also observed in children using a seat with integral harness.

The current dummies offer various possibilities to measure injury related loads. To assess abdominal injuries, various criteria and possibilities have been proposed. Nevertheless, only a few of them are

used in current adult dummies (e.g., EuroSID, THOR). Furthermore, there are currently no appropriate sensors being used in child dummies to measure abdominal injury related loads, even though children have a considerably higher abdominal injury risk compared to adults.

ANATOMIC BACKGROUND

Abdominal organs are either, thin-walled and hollow (stomach, intestine, urinal bladder etc.) or sponge-like and blood-filled (liver, kidneys, spleen etc.), these are the so-called solid organs. It is important to know that solid organs are located in the upper abdomen, while the hollow ones are generally located in the lower abdomen. However, hollow organs can be found in the upper abdomen as well (e.g., stomach). Hollow and solid organs behave totally different under mechanical loads. Subgroups to be considered in the field of abdominal injuries are children and pregnant women. The latter subject is not discussed in this paper.

There are some differences between adults and children to be considered. One of the main differences is that children's ribs and musculature provide less protection of the organs. For example, the liver is almost completely covered by the ribs in adults, but is only partially covered in children. In addition to this, the abdomen of a child is bigger in relation to height than that of an adult. The function of the organs is the same for children as it is for adults.

ACCIDENT STATISTICS

Based on GDV (association of the German insurance institutes) accident investigations, frontal accidents between 1993 and 2000 with air bag equipped cars Roselt et al. [Roselt, 2002] showed that the abdomen is the second priority for critical injuries (AIS 4/5). In the analysed sample cars with model years up to the year 2000 were analysed. 60% of the sample included models between the years 1996 and 1998, and 80% between 1995 and 1999. This means that more recent models of cars were included in this sample. Figure 1 shows that injury frequency decreases significantly with injury severity for most of the regarded body regions.

However, the abdomen shows more AIS 4 injuries than AIS 3 injuries.

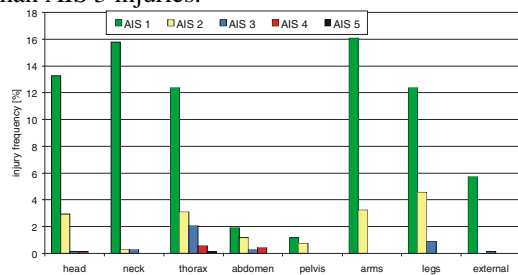


Figure 1. Injury frequency and severity in airbag equipped cars (288 driver) [Roselt, 2002].

The analysis of the AIS 3+ injuries shows that the thorax is most often affected by severe injuries, while legs and abdomen are more or less at an equal level at the second rank. A comparable situation can be observed when the weighted injury frequency (harm) is considered (Figure 2). The abdomen is at an equal level with arms and head, while the thorax is the most affected body region followed by the legs.

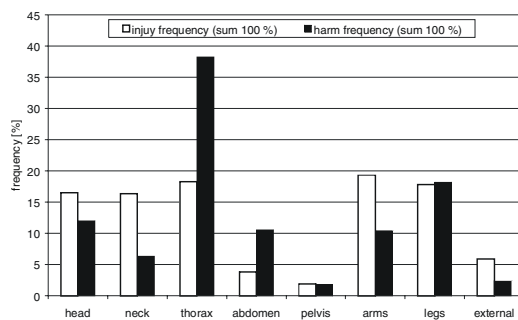


Figure 2. Injury frequency and harm in airbag equipped cars (288 driver) [Roselt, 2002].

Comparison of the drivers and passengers with AIS 3+ injuries shows that the injury severity for passengers is generally lower than for the drivers (Figure 3).

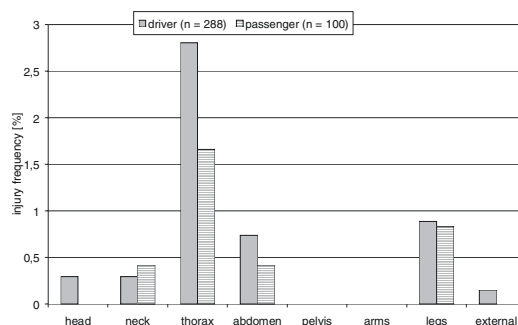


Figure 3. Comparison of AIS 3+ injuries for drivers and passengers [Roselt, 2002].

An earlier study in the UK based on accidents between the years 1984 and 1986 shows that 11% of the occupants sitting on the struck side of the car received abdominal injuries of which 52% were

AIS 3+ rated [Harms, 1987]. The contacts causing abdominal injuries in lateral impacts are doors, door furniture and, in the more severe accidents, intruding objects. In frontal collisions, 20% of the restrained occupants receiving AIS 3+ injuries were hurt at abdomen or lower back. However, it is not possible to divide these injuries into two separate categories; abdominal injuries and lower back injuries. Newer data from the UK and Germany are presented below in the section concerning comparison of airbag-equipped cars with cars without airbag.

To discuss the influence of airbags on the injury distribution amongst body regions, the next chapter compares accidents with and without airbags.

Comparison with/without Airbag

To investigate the differences between airbag equipped and non-airbag equipped cars, Frampton et al. [Frampton, 2000] analysed UK accident data from the year 1992 to 2000 and German accident data from the year 1996 to 1999. The sample included front seat occupants in frontal crashes only. It can be seen, that abdominal injuries occur slightly more often in airbag equipped cars than in those without airbags (Figure 4). Because of the significant reduction of head and spine injuries in the airbag cases, the relative injury outcome of abdominal injuries is now higher for cars equipped with airbags than for those without.

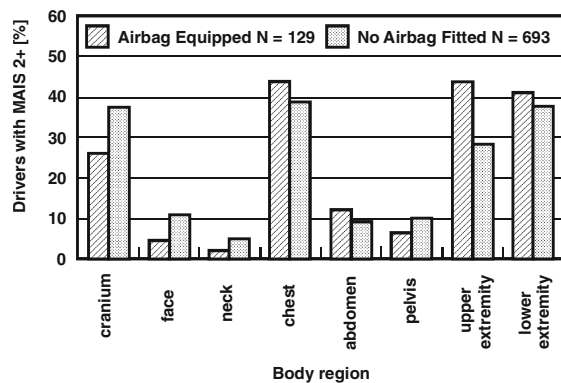


Figure 4. AIS 2+ body region rates for belted drivers with MAIS 2+ (UK) [Frampton, 2000].

Children

Children must be regarded separately because of their biomechanical differences regarding pelvis and abdomen.

Based on GDV data of German accidents during 1990 and 1991 [Langwieder, 1997] it is obvious that children using a CRS properly received the majority of their severe injuries to the head, neck, chest and abdomen (Figure 5).

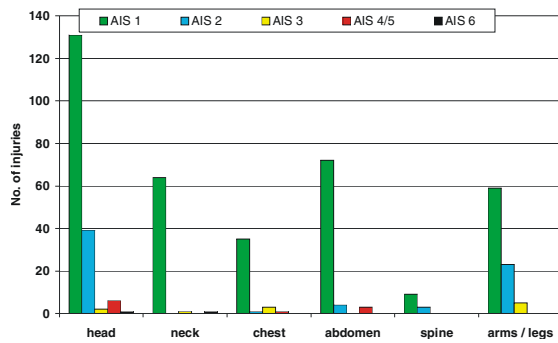


Figure 5. Injuries of 415 children [Langwieder, 1997].

Regarding only those children restrained with a CRS (harness type), there is almost the same distribution of injuries (Figure 6).

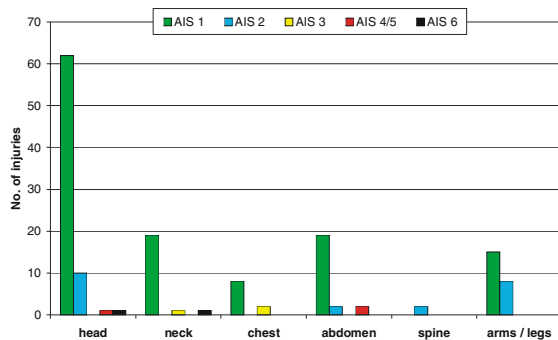


Figure 6. Injuries of 200 children using a CRS [Langwieder, 1997].

Taking into account the “harm” of the different body regions, the abdomen is again shown to be the second ranking region followed by the extremities, neck and chest (see Figure 7).

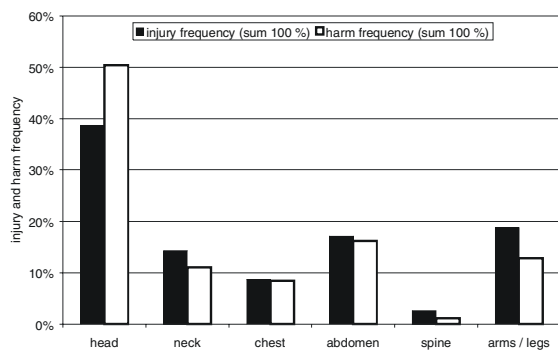


Figure 7. Calculated “harm” for different body regions (415 children) [Langwieder, 1997].

An older study based on the same accident data of the years 1990 and 1991 shows that wearing a 3-point belt or lap belt only was the main problem resulting in abdominal injuries to children [Langwieder, 1994]. However, even children using a CRS suffer abdominal injuries, see Table 1.

Table 1. Number of injuries to different body regions depending on restraint system [Langwieder, 1994]

	Number of injuries AIS 1 – 6		
	CRS	3 point only	Lap only
Head	34	26	4
Neck	13	11	1
Chest	6	6	-
Abdomen	12	17	5
Arms	5	9	1
Legs	5	5	2
T/L Spine	-	2	1
Total	75	76	14

Based on French accidents of the years 1992/1993 and 1995/1996, Trosseille et al. [Trosseille, 1997] came to the conclusion that abdominal injuries occur mainly in older children, with an age above three years, using either boosters or car belt without any CRS.

INJURY PATTERN

Most of the abdominal injuries are located at the skin, the musculature and organs. While the severity of skin and musculature injuries is mostly minor, the severity of organ injuries can be serious. The main injuries to solid organs are crushing or bursting of the organ, laceration and rupture. Hollow organs sustain contusion, haematoma, perforation and laceration, as well as rupture of organs. Besides the risk of bacterial contamination of the abdominal cavity with the intestine content, rupture of organs leads to massive bleeding. The most affected abdominal organs are liver, spleen and kidneys. All of these are solid organs, which have a higher injury risk [Cavanaugh, 1986]. The injuries are caused mainly by contact with lap belt, steering wheel, armrests, etc.

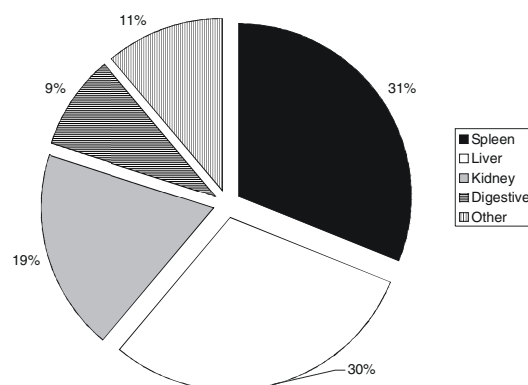


Figure 8. Distribution of the injured abdominal organs for the years 1993 – 1998 [Yoganandan, 2000].

The distribution of injuries amongst the abdominal organs was, for example, investigated by Yoganandan et al. [Yoganandan, 2000], based on NASS

data of front occupants in all accidents except rollover of the years 1993 to 1998. Based on this study, the liver and spleen are the most common abdominal organs involved, followed by the kidneys and the digestive system (Figure 8). The same study shows that abdominal injuries are most common in belt restrained occupants, which is true for frontal, lateral and oblique impacts [Yoganandan, 2000]. The distribution of abdominal injuries for different accident types shows almost an equal share of frontal and lateral impacts (Figure 9).

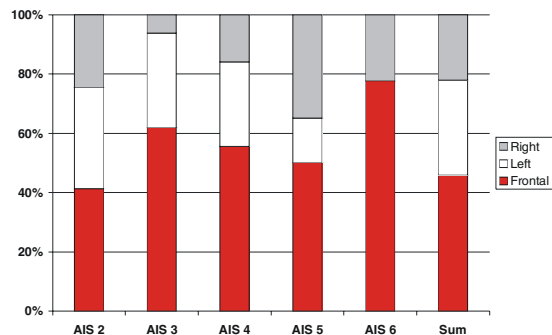


Figure 9. Abdominal injuries dependent on impact direction [Yoganandan, 2000].

In the following part, injury patterns for frontal impacts are described in more detail based mainly on case studies and biomechanical tests. The main causes for abdominal injuries are the belt system for belted occupants and the steering wheel for unbelted occupants. However, because of the increased amount of equipment in cars with airbags, the number of steering wheel induced injuries is decreasing. On the other hand, very little data of abdominal injuries in airbag-equipped cars exists in the literature. Therefore, it is difficult to assess the injury pattern in these cars. According to accident investigations in the UK, abdominal injuries in frontal car accidents between 1984 and 1986 are caused mainly by steering wheel and belt webbing (see Figure 10) [Harms, 1987].

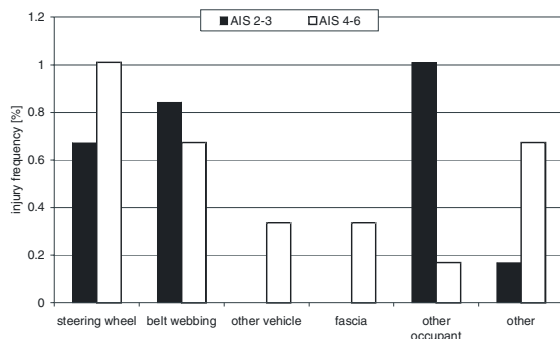


Figure 10. Contact location for abdominal injuries for 594 restrained front occupants [Harms, 1987].

Because of the different loading conditions the belt, steering wheel and airbag induced injuries are described separately.

Belt Induced Injuries

After the introduction of lap belts in cars a new injury pattern was observed. The abdominal injuries induced by the belt were called seat-belt injuries. Under this heading injuries to the abdomen and lumbar spine were summarised. Due to improvements of the belt geometry and the introduction of the automatic three-point belts the situation has changed during the last decades. Abdominal injuries in frontal impacts are mainly caused by the deceleration of the abdominal viscera (here tears, wounds or rupture of the viscera can be observed), flexion of the trunk around the pelvis (which causes pressure injuries by compression between thighs and trunk) and submarining [Leung, 1982].

The most important problem of belt induced abdominal injuries is the phenomenon known as submarining. Submarining describes the situation when the lap belt intrudes the abdomen. There are differences in submarining. In the normal case of submarining, the lap belt rides above the iliac crest during the accident. Another kind of submarining is when the lap belt is positioned above the iliac crest prior to the accident. In submarining cases injuries to liver, spleen, kidney and digestive system are reported [States, 1987]. Although submarining was mainly reported in the more distant past, there are still submarining cases seen in today's accident statistics; e.g., reported by Walfisch [Walfisch, 2002] for rear seat occupants.

However, seatbelt induced injuries seem to be possible without submarining. For example, Witte [Witte, 1968] reported 5 cases of abdominal injuries without submarining. Intestinal injuries seem to be possible because of acceleration of the digestive content against the seatbelt. The acceleration of the digestive content leads to longitudinal ruptures of the intestine, while the acceleration of the intestine itself leads to laceration of the attachments. The risk of submarining is higher for the rear seat because of inclined knees and better-restrained torso. The higher risk for the rear seat was confirmed by an accident analysis in the UK from 1992 to 1995 [Cuerden, 1997].

One serious reported problem is misuse when the shoulder belt is worn under the arm. This is intended to increase comfort but decreases the efficiency of the belt system.

In Heidelberg, in cadaver tests, reported by Schmidt et al. [Schmidt, 1974], abdominal injuries were either caused by the shoulder belt (liver ruptures, spleen ruptures and kidney contusion) or by the lap belt (fat tissue and muscle tissue ruptures, mesentery ruptures and intestinal ruptures).

However, Leung et al. [Leung, 1982] reported cadaver tests in which only a few injuries were caused by the shoulder belt.

Cadaver tests conducted by APR showed 47 out of 70 cases received abdominal injuries [Leung, 1982]. Only 23 of these 47 cases with abdominal injuries were submarining cases. For the non-submarining cases, no intestine, colon or mesentery injuries were reported. Liver injuries were on an equally low level for submarining cases and non-submarining cases. Based on this study, 68% of the abdominal injuries are caused by the lap belt. In a review of the US NASS data from 1988 to 1994 Elhagediab et al. [Elhagediab, 1998] it was found that about 17% of the abdominal injuries were belt induced. These injuries are mainly to the digestive system (Figure 11). In the data set, frontal collisions with un-ejected occupants were investigated.

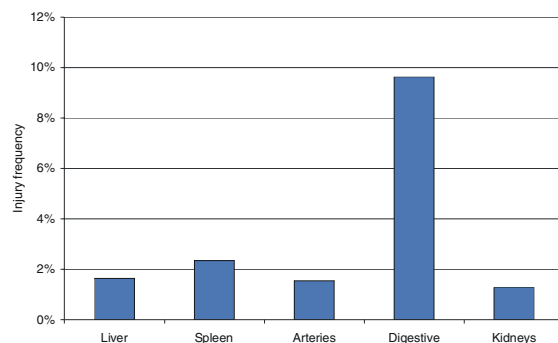


Figure 11. Injury frequency for belt induced injuries [Elhagediab, 1998].

Children need to be regarded separately, because of the lap belt positioning problems and the reduced protection provided for the abdominal organs. Based on French accident data from 1992/1993 and 1995/1996, abdominal injuries to children only occur in older children (age above 3 years) restrained with a booster, or without any CRS, using only the vehicle's belt [Trosseille, 1997]. The affected organs were mainly liver, spleen and intestine. Generally, children restrained by a 3-point belt and booster were injured at the abdomen because of the lap belt position [Walfisch, 2002].

Steering Wheel

Abdominal injuries induced by the steering wheel are mainly a problem for unbelted drivers. This is the reason why there are considerable differences between US and Europe. These differences can be found in accident statistics and is also reflected in research programmes.

Based on the review of the US NASS data from 1988 to 1994 Elhagediab et al. [Elhagediab, 1998] mentioned above, it was found that about 69% of the abdominal injuries are steering wheel induced. These injuries are mainly to the liver (Figure 12).

In the data set, frontal collisions with un-ejected occupants were investigated.

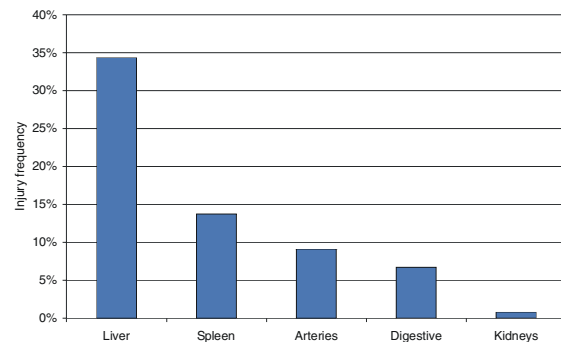


Figure 12. Steering wheel induced injury frequencies [Elhagediab, 1998].

Liver injuries, due to contact with the steering wheel, are mainly laceration of the liver or laceration of the central venous junction between the liver lobes [Lau, 1987].

Airbag

As previously explained, the number of accidents with airbags is too small to assess the injury mechanism in a reliable manner, but trends can be observed.

Augenstein et al. [Augenstein, 1996] investigated frontal accidents with airbag deployment. The most severe injuries occurred in drivers (restrained by 3-point belt, shoulder belt only or without belt) at chest and abdomen. Abdominal injuries were observed in all restraint conditions. They were rated between AIS 2 and AIS 5. Most of the abdominal injuries in this sample were reported for the liver, but spleen, kidneys, pancreas and intestine were also injured. Liver injuries were mainly to the front lobe in severe crashes and to the rear lobe in less severe accidents.

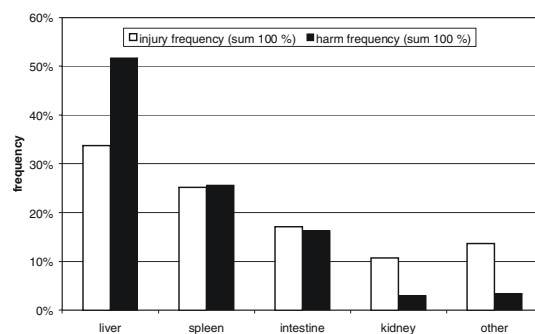


Figure 13. Harm distribution within abdominal region [Augenstein, 1998].

In a later study, Augenstein et al. [Augenstein, 1998] came to the conclusion that about 30% of the injury weighted harm is related to abdominal injuries. Again the liver is the most affected abdominal organ, see Figure 13.

Based on the above-mentioned review of the US NASS data of the years 1988 to 1994, Elhagediab et al. [Elhagediab, 1998] reported that airbag induced abdominal injuries are quite rare and only spleen injuries are associated with the airbag. Dishinger et al. [Dishinger, 1996] came to a different result concerning airbag induced abdominal injuries. Although most abdominal injuries could be reduced by an airbag the number of kidney injuries increased, Figure 14. These findings were again based on data from US accidents collected by the Maryland Hospital in 1993 and 1994. However, accidents with airbag deployment are normally of higher severity than those without (if the car is equipped with an airbag). Accident severity is not considered in this sample.

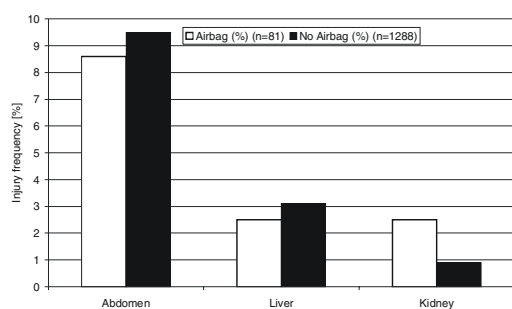


Figure 14. Comparison of selected injuries depending on airbag deployment (belted drivers) [Dishinger, 1996].

Synthesis of Injury Pattern

Most of the analysed data are either old or are coming from the US. Car occupants in the US are often not restrained by belts. For the data outside the US, the restraint system changed over the years – modern cars are equipped with airbags, three point belts with pretensioner and load limiter. Abdominal injuries could be caused by the belt system, steering wheel and airbag. With respect to steering wheel induced injuries, differences between US and European data need to be considered, because the steering wheel impact location is mainly only relevant for unbelted drivers.

Taking into account the injuries caused by the belt system, most of the reported cases are submarining cases. Due to the improvements of the belt system this kind of injury mechanism will decrease with modern cars. However, for rear seat passengers it is still relevant because of the worse belt geometry and lower equipment rates with pretensioner and load limiter. Besides the submarining cases abdominal injuries were reported to be caused by the shoulder belt or the lap belt without submarining. Steering wheel induced abdominal injuries are seldom for belted occupants. Due to improved equipment rates of cars with airbags they are likely to disappear completely.

There are indications that airbags could induce abdominal injuries as well. Due to the low number of airbag-equipped cars included in the accident databases, it is not yet possible to prove this situation.

INJURY CRITERIA

Three mechanisms causing abdominal injuries are possible: blunt trauma, penetration and acceleration. Injuries caused by acceleration are generally ruptures of organs and blood vessels. Bones (e.g., broken ribs) and vehicle parts can cause penetrations. Because of the improvement of the vehicle interior, penetration of abdomen is of less importance.

Impact location, direction and magnitude have a significant influence on injury severity due to mobility, location and natural protection of the abdominal organs.

Most of the abdominal injuries observed after road accidents are caused by blunt trauma. For more detailed answers concerning an appropriate injury criterion a lot of tests with surrogates (e.g., human cadavers, living anaesthetised and cadaver animals) have been conducted. But mostly it remains unclear whether force, intra-organic pressure, compression of abdomen, velocity or a combination of these correlate well with the injury severity. In fact, there is a correlation between force, pressure and compression. The impact speed seems to have an important influence on injury severity. In addition to that, the stiffness of the abdominal organs and, therefore, the stiffness of the abdomen itself is dependant on the impact velocity.

Besides dummy abdominal measurements, other criteria were proposed. For example the EEVC subgroup on Biomechanics came to the conclusion that the risk of injuries to the lower part of the abdomen could be reduced by lap belt positioning criteria. In addition, hard parts of the belt (e.g., the buckle) should not come into contact with the abdominal wall. Upper abdominal injuries were thought to be covered by thorax protection criteria [Halpern-Herla, 1976].

In addition, it could be necessary to have different injury criteria for localised loads (e.g., by belts) and distributed loads (e.g., by airbags) [Elhagediab, 1998].

Within the following chapters the findings explaining a selection of possible injury mechanisms (e.g., compression, force, impact speed) will be described. It is important to consider the test conditions. The pre-test body posture and the preparation of test subjects have an important influence on the abdominal behaviour and the possibilities to detect abdominal injuries. The type of organ (hollow or solid) and impact direction are also important. In addition, the available measurement techniques are of importance.

Compression

Going back in history, compression was the first proposed abdominal injury criterion. From today's point of view it worked well as long as the compression rate was more or less at the same level (e.g., for belted occupants). In the context of abdominal injuries, compression means the relative abdominal deflection for frontal impacts and the relative half width abdominal deflection in lateral impacts.

This chapter summarises findings which do and do not support compression as an appropriate criterion.

In fixed back tests of anaesthetised canine subjects a correlation of intestine compression and the occurrence of abdominal injuries was found by Williams [Williams, 1966].

Experiments with anaesthetised primates and human cadavers showed that abdominal compression was related to injury severity [Stalnacker, 1973].

Miller [Miller, 1989] found a correlation between maximum compression and injury severity in tests with anaesthetised porcine subjects loaded with a safety belt.

In steering wheel tests with anaesthetised swine compression was found to correlate "also" good to injury severity [Miller, 1991]. But in the tests with impact velocities between 1.7 and 12.4 m/s VC_{max} (see below) it was found to correlate better.

A "quite good" correlation of compression to injury severity (correlation factor 0.64) was found in frontal steering wheel impacts to anaesthetised porcine subjects [Lau, 1987]. The viscous criterion was found to correlate better.

Investigation of hepatic injuries with unembalmed human cadavers showed that tolerance levels based on velocity, compression or combination of both seemed to be inappropriate [Nusholtz, 1985]. But it has to be considered that several tests were applied to the same cadaver.

In tests with anaesthetised swine subjects, Lau et al. [Lau, 1988] found that the compression was inappropriate. The probability analysis of liver laceration risk shows a poor result, Figure 15.

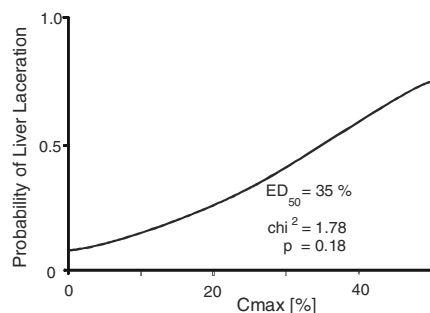


Figure 15. Analysis of liver laceration [Lau, 1988].

Lateral impactor tests to the right side of anaesthetised New Zealand White Rabbits showed better correlation of compression for liver injuries than for kidney injuries [Rouhana, 1986].

In lateral impact tests to exposed human livers and PMHS with different velocities and compressions, deflection was found to be a better parameter than compression. Deflection is measured in cm and not normalised. For the tests with an impactor disc with a diameter of 15 cm, the correlation of deflection to injury severity was $R = 0.85$ [Talantikite, 1993]. Walfisch et al. [Walfisch, 1980] found no obvious relation between compression and injury severity in lateral drop tests of unembalmed human cadavers; this was explained to be caused by the pre-impact body posture. The drop height was 1 and 2 m, which correlates to 4.4 m/s and 6.2 m/s respectively. However, there were no injuries observed for compression below 28% and compression was found to be more easily measured with a dummy. Therefore, a switch which activates at compression above 28%, was proposed for the EuroSID.

The main criticism on compression as an injury criterion is that the abdominal viscera behaves rate sensitive. This means that the abdomen is able to deform without any injury when the blunt loading is applied slowly [Penberthy, 1952]. Crushing of organs is possible with high anteroposterior compression (40 – 60%) and low speeds while fast loading (> 12 m/s) can lead to severe injury with low compression (10 – 20%) [Lau, 1981]. Compression was found to be a good predictor with low impact velocities (< 3 m/s, e.g., for belted occupants) but in sports and for unbelted occupants or belted occupants in high speed accidents compression is not appropriate [Viano, 1988].

Viscous Criterion (VC)

The viscous criterion was initially proposed for thoracic injuries. The product of compression (C) and velocity (V) takes into account the rate sensitive behaviour of the abdominal organs. Dependent on the measurement capabilities of the different authors, either the product of the maximum velocity (normally the initial velocity) and the maximum compression ($V_{max}C_{max}$) or the maximum of the continuously calculated product of compression and velocity were regarded as VC. In some publications, modifications to the pure VC criterion were proposed.

Rouhana et al. [Rouhana, 1984 and Rouhana, 1985] found a good correlation of injury severity and $V_{max}C_{max}$ in lateral impact tests with anaesthetised rabbits. Based on these experiments, the Bounded Abdominal Injury Criterion ($v \cdot C / (1-C)$) was proposed.

Stalnaker et al. [Stalnaker, 1985] confirmed the relevance of $V_{max}C_{max}$ for the prediction of injuries in subhuman primates.

In steering wheel tests with anaesthetised swine, VC_{max} was found to correlate best with injury severity [Miller, 1991]. The impact velocity was varied between 1.7 and 12.4 m/s in these tests. A good correlation of VC_{max} with injury severity was found in frontal steering wheel impacts to anaesthetised porcine subjects [Lau, 1987] (Figure 16). Within these tests, only liver injuries were observed.

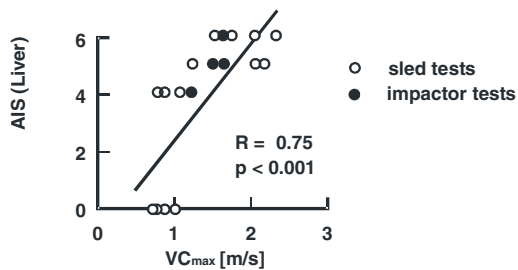


Figure 16. Correlation between abdominal injury severity and VC_{max} [Lau, 1987].

Tests with different velocities and a defined compression of 16% with anaesthetised rabbits showed good correlation of injury severity with $V_{max}C_{max}$ [Lau, 1981]. The test speed varied between 5 and 20 m/s.

Investigation of hepatic injuries with unembalmed human cadavers showed that tolerance levels based on velocity, compression or a combination of both (VC_{max}) seemed to be inappropriate [Nusholtz, 1985]. But it has to be considered that several tests were applied to the same cadaver. Therefore, the allocation of injuries to the impact conditions does not seem to be clear.

In tests with anaesthetised swine subjects, Lau et al. [Lau, 1988] found good correlation of VC_{max} and injury severity in frontal, lateral and oblique impacts.

Comparison of tests with liver laceration and those without showed clear differences between the maximum viscous criteria (VC_{max}) assessed in the tests, Figure 17.

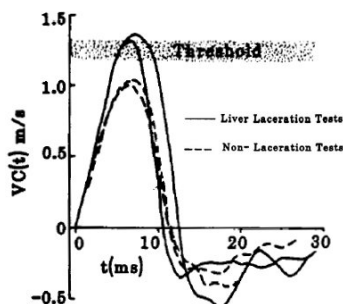


Figure 17. Tests with minor liver laceration versus no injury [Lau, 1988].

In right side lateral impactor tests to anaesthetised New Zealand White Rabbits, Rouhana et al. found good correlation of $V_{max}C_{max}$ with injury severity [Rouhana, 1986].

Lateral pendulum tests with unembalmed human cadavers to chest, abdomen or pelvis showed the best correlation for VC_{max} with abdominal injury severity [Viano, 1989]. The tests were conducted to cadavers in an upright position. It has to be considered that several tests were conducted with one cadaver. Therefore, the allocation of injuries to impact condition seems to be problematic although different body regions were impacted.

Based on frontal steering wheel impact tests with anaesthetised swine Viano et al. [Viano, 1988] proposed VC_{max} as an appropriate injury criterion. Impactor tests with a 15 cm diameter disc impactor to exposed fresh human livers and fresh human cadavers showed a correlation coefficient of VC_{max} with injury severity of 0.71 [Talantikite, 1993]. In the PMHS tests, the impactor hit the side of the body approximately at the COG of the human liver. Comparing the measurement results of VC_{max} and force each showed a correlation coefficient of 0.78.

Force

Most of the published studies are focussing on peak force and do not regard the time history of the load. Force was often found not to be a useful indicator of abdominal injuries because the measurement of abdominal forces was considered to be too complicated [Rouhana, 1987 and Walfisch, 1980].

In impact tests to different anaesthetised primates and porcine subjects, impactor force and duration correlated to injury severity [Trollope, 1973]. The tests were conducted with different impactor properties, of which the impactor size influenced the injury severity (smaller impactor causes higher injury severity). In addition, the subject weight had an important influence.

Stalnaker [Stalnaker, 1973] found a correlation of abdominal injury severity and the logarithm of impact force and time duration squared.

Peak force showed best correlation with AIS 4+ injuries of all biomechanical measurements in rigid lateral pendulum tests to the mid abdomen of cadavers [Viano, 1989].

Miller [Miller, 1989] showed that peak force is well correlated with AIS 3+ injuries and AIS 4+ injuries in belt loading experiments.

In steering wheel tests with anaesthetised swine, force was found to correlate "also" well to injury severity [Miller, 1991]. But in the tests with impact velocities between 1.7 and 12.4 m/s, VC_{max} was found to correlate better.

Comparison of tests with pregnant baboons showed that the belt tension was the only indicator, which differentiates between tests with and without injuries [Snyder, 1966].

Investigation of submarining tests with human cadavers showed that injuries were observed when the belt tension after submarining exceeded a certain limit [Leung, 1982].

In right side lateral impactor tests to anaesthetised New Zealand White Rabbits a correlation of impact force and $V_{max}C_{max}$ to injury severity was found [Rouhana, 1986]. Dependent on the boundary conditions, advantages were found for one or the other. In lateral impact tests to exposed human livers and PMHS with different velocities and compressions, maximum force was found to “strongly correlate” to the impact velocity. For the tests with an impactor disc with a diameter of 15 cm the correlation of maximum force to injury severity was $R = 0.73$ [Talentikite, 1993]. The deflection of the abdomen also correlates with the impact force. However, the correlation of force and velocity is better.

In lateral drop tests of unembalmed human cadavers Walfisch et al. [Walfisch, 1980] found that the normalised force is a reliable indicator for injury severity ($R = 0.98$).

Comparison of Different Criteria

The outcome of the different studies, concerning abdominal injury criteria described above, are summarised in Table 2. Within this table “+” means that the author felt that the criterion is a good predictor of the abdominal injury risk, while “-” stands for the opposite. When a criterion was not investigated the cell is left blank.

Nusholtz et al. [Nusholtz, 1994] compared the different injury criteria in impactor tests with unembalmed, pressurised, sitting, human cadavers.

In these tests, a part of a steering wheel rim contacted with the abdomen at the height of the 2nd lumbar vertebra. The comparison covers compression, deflection, energy loss, velocity, force and spinal acceleration. Most of the different measurements are dependent on each other (within 10% tolerance), except the spinal acceleration. This seems to be the main reason why the review of proposed injury criteria shows a blurred picture with different proposals for the injury criteria, depending on the type of test and the measured quantities in these tests.

One good source for the comparison of different criteria is tests conducted by Hardy et al. [Hardy, 2001]. These tests comprise human cadaver tests using seatbelt impactors, rigid bar impactors and airbag deployment. Compression, impact velocity and impactor force were measured for most of the tests. The main goal of this study was the assessment of force-deflection characteristics of the abdominal region. For the comparison within this study, only subjects that were impacted once were considered. Due to the different injury sensitivity of the different abdominal regions tested in this study, a comparison of different injury criteria based on these tests is not possible. However, a comparison of these tests does allow for analysis to see if the criteria are robust against other load conditions than originally defined for. Because of the available data, the $V_{max}C_{max}$ criterion has to be analysed. Concerning the belt tests, mainly injuries of the rib cage were reported. This includes rib fracture up to rib two. This is the reason why the seat belt tests were not considered within this study.

Table 2.
Summary of different results concerning abdominal injury criteria in frontal impact conditions

Source	Test subject	Test type	C	VC	F	Remark
[Williams, 1966]	Anaesthetised canine	Frontal impactor tests	+			
[Trollope, 1973]	Anaesthetised primates and swine	Frontal impactor tests			+	F and duration
[Lau, 1981]	Anaesthetised rabbits	Frontal impact tests with different V and constant C		+		
[Stalnaker, 1985]	Anaesthetised primates	Frontal impactor tests		+		
[Miller, 1991]	Anaesthetised swine	Frontal steering wheel tests ($1.7 < v < 12.4$ m/s)	“also good”	+	“also good”	
[Lau, 1987]	Anaesthetised swine	Frontal steering wheel impact	“quite good”	+		
[Nusholtz, 1985]	PMHS	Frontal steering wheel impact	-	-		Several tests to one subject
[Viano, 1988]	Anaesthetised swine	Frontal steering wheel impact		+		
[Miller, 1989]	Anaesthetised swine	Frontal belt loading	+		+	
[Lau, 1988]	Anaesthetised swine	Frontal and oblique	-	+		
[Snyder, 1966]	Pregnant anaesthetised baboons	Frontal sled tests			+	Belt force
[Leung, 1982]	PMHS	Frontal sled, submarining			+	Belt force after submarining

The abdominal AIS was coded based on the injury description published by Hardy et al. [Hardy, 2001], the $V_{max}C_{max}$ value was calculated from the impact velocity and maximum compression. It is clear that the abdominal injury severity depends on the location of the load and the Hardy tests were conducted at different abdominal levels (mid abdomen, lower abdomen). Nevertheless, the injury severity of these tests is compared with the measured load, the abdominal compression and the $V_{max}C_{max}$ criterion in Figure 18.

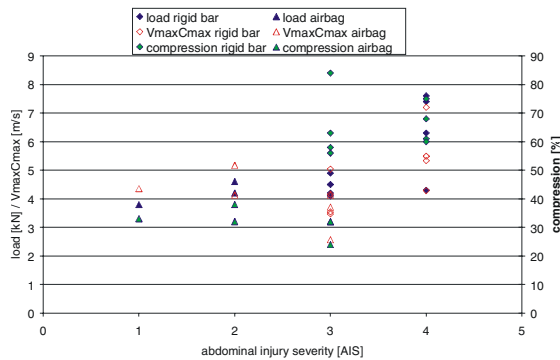


Figure 18. Re-evaluation of Hardy tests (data [Hardy, 2001]).

This comparison shows that in the airbag tests higher VC and lower compression is necessary to cause injuries of a certain level, while the force criterion seems to be independent of the load case. Analysis of the AIS 3+ injury risk of the tests leads to the same conclusion, Figure 19.

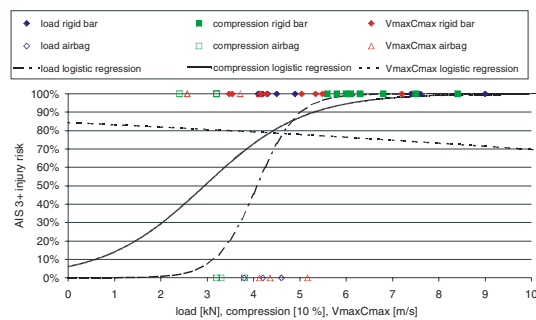


Figure 19. Re-evaluation of AIS3+ injury risk of Hardy tests (data [Hardy, 2001]).

Based on tests of Lau et al. [Lau, 1981], Talantikite et al. [Talantikite, 1993] and Nusholtz et al. [Nusholtz, 1994] it can be noticed that the impact force and VC are more or less linearly dependent on each other.

Another issue to be considered is the application range for which the criterion is applicable. Lau et al. [Lau, 1986] described the compression as valid for compression rates up to 2 m/s and the VC_{max} criterion to be valid in the range between 2 m/s and 30 m/s, see Figure 20.

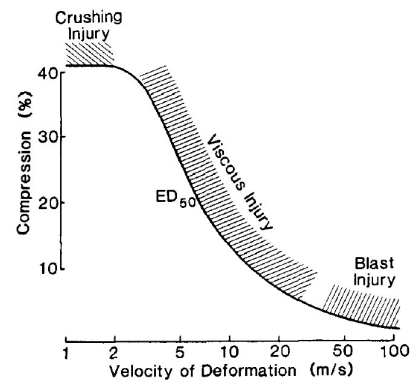


Figure 20. Range of validity for the viscous criterion and compression criterion [Lau, 1986].

While compression rates of 30 m/s and more are unusual in automotive accidents, low compression rates (submarining) are still possible.

From the theoretical point of view, airbag induced loads show a high compression rate combined with a distributed low compression. This combination seems to be problematic for a reliable VC measurement as small measurement mistakes of the compression measurement lead to considerable mistakes when computing the velocity (derivation of the compression).

In conclusion, it can be noticed that all three criteria can be considered as more or less equivalent. However, compression and VC do not seem to be valid for all kinds of load conditions for the abdomen (slow submarining, fast steering wheel and distributed airbag loading). Regarding the surface force, no constraints are known.

SENSOR DEVELOPMENT

The sensor development is based on a detailed state of the art review of proposed and currently realised sensor concepts; see [Johannsen, 2006]. These concepts are assessed based on the following criteria.

Requirements for Abdominal Sensors

The abdominal sensor should be able to cope with the following criteria and properties:

- Measurement of appropriate injury criteria (either contact force or VC)
- Time history measurement
- Detection of location of load
- Ability to assess loads applied by lap and shoulder belt, steering wheel (for adult dummies only) and airbag
- Reliable measurement in the sense of robust sensor and repeatable measurements
- Applicable for existing dummies without major changes to the dummy

- No significant influence on dummy behaviour
- Low purchase and operation costs (easy calibration and long calibration intervals)
- Usable with normal crash equipment (no additional data acquisition system or computing of the signals necessary)

The requirements mentioned above are a maximum design goal. For the first phase of the development, which was focussing on existing technologies, it seemed to be impossible to achieve all requirements. Therefore it was necessary to find a suitable compromise, which should take into account future development possibilities.

Sensor Description

The standard FlexiForce® A102 sensor is a thin (0.1 mm), flexible printed circuit. It is 14 mm wide and 203 mm in length (standard version). The active sensing area is a 9.5 mm diameter circle at the end of the sensor. The sensors are constructed of two layers of substrate, i.e., a polyester film. On each layer, a conductive material (silver) is applied, followed by a layer of pressure-sensitive ink. Adhesive is then used to laminate the two layers of substrate together to form the sensor.

The FlexiForce single element sensor acts as a resistor in an electrical circuit. When the sensor is not loaded, its resistance is approximately 20 MΩ. When a force is applied to the sensor, this resistance decreases. For the use in crashes, it is possible to connect the sensors to a Wheatstone's Bridge by operating the sensor parallel to one of the resistors.

For the use as abdominal sensor, a matrix of a number of single sensors has to be designed taking into account a compromise concerning requirements for maximum distance between the sensors and the number of channels.

Abdominal Sensor for Q-Dummies

This chapter describes the Q-dummy family with emphasis on the abdominal region first and then the final abdominal sensors for the Q3 and Q6, which represent a 3 years old child and a 6 years old child, respectively.

The accident statistics shows that there is no risk for abdominal injuries for children using a rear facing CRS and a very low risk for children using a seat with integral 5-point-harness. Four-point-harness seats, which caused abdominal injuries in the past, are not available any more. Therefore, it is reasonable to limit the sensor development at the first stage to the Q3 and Q6, which represent children, which can be restrained by booster seats.

The sensors were developed within the CHILD project framework. They were used for the CHILD accident reconstruction programme.

Q-Dummy Family - The next generation of European child dummies – the Q family – offers the following dummies: Q0 (newborn), Q1, Q1.5, Q3, Q6 (the numbers are meant to give the age of the child that the dummies represent). The dummies are designed for multidirectional use, which requires abdominal sensors able to cope with at least frontal and lateral impacts. The modular design of the dummies allows using the same philosophy of the abdominal sensors for different dummy sizes.

Except for the Q0, the design of the “extended abdominal region” of all Q-dummies is composed of a rigid thoracic spine, which fixes the rib cage, houses a chest accelerometer and a chest deflection measurement device (capable of measuring either in X or in Y direction). An elastomer lumbar spine is mounted at the lower end of the thoracic spine, which connects the thorax to the pelvis. Between lumbar spine and pelvis a load cell can be installed. In addition, the pelvis houses another accelerometer. An abdominal block made of PU foam and covered with skin simulates the abdomen itself. The dummy is clothed with a wet suit.

Sensor Design - The chosen dummies are usually restrained by the vehicle belt with or without a booster seat or with a CRS with integral belt system. In addition to the belts, abdominal injuries can be caused by parts of the seat – in lateral and oblique impacts – and by the passenger airbag. The minimum width of CRS-belts is 30 mm, the average between 35 and 40 mm. Therefore, the distance between two “neighbour” sensors must be smaller than this width. In addition, it is necessary that the sensors be spaced equally to ensure a good coverage and efficient evaluation of the results.

For both dummies, 20 sensors are arranged in an array across the surface of the abdominal block. The array complies with the requirements mentioned above and the geometry of the abdominal surface.

The dummy design allows placing the sensors directly at the surface of the abdominal block. This allows assessing the loads applied to the “soft” part of the abdominal region. The chest deflection measurement device can assess the loads applied to the “hard” part of the thorax.

The following Figure 21 shows the sensor array for the Q3 dummy. The distance between two sensor centres is 35 mm; because of the diagonal arrangement of the sensors, the vertical and the horizontal distance are below 30 mm each.

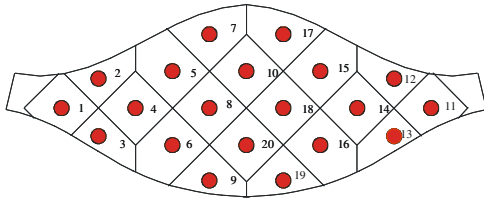


Figure 21. Sensor matrix for the Q3 dummy (front view).

Due to the different shape of the abdominal block for the Q6 the sensor arrangement is slightly different to that of the Q3. Except for four sensors, the distance between two neighbour sensor centres is 30 mm because of the diagonal allocation of the sensors that means a horizontal and a vertical distance of 25 mm.

Abdominal Sensor for the HIII 50th Percentile Dummy

This chapter summarises the Hybrid III design with emphasis on the abdominal region and the relevant load conditions as well as the sensor design for that dummy.

Description of the Hybrid III 50th Percentile Dummy - The Hybrid III dummies are designed for frontal, frontal oblique and frontal off-set collisions. Besides the 50th percentile dummy, a 5th percentile female and a 95th percentile male version of the HIII adult dummies exist.

The dummy is built of a metal skeleton and foam flesh material. It can house various sensors at head, neck, chest, pelvis and legs, consisting of mainly accelerometers and load cells. Regarding the “extended abdominal region” – from chest to pelvis – the dummy has a metal thoracic spine, which houses an accelerometer. Six metal ribs compose the rib cage. A sternum connects the ribs. A chest compression measurement device is fixed between spine and sternum. Soft tissue is simulated by a chest jacket, which offers different thicknesses at different locations of the chest. The thoracic spine is connected to the metal pelvis by a rubber lumbar spine. The pelvis is covered by foam material. An abdominal insert fills the abdominal cavity between chest and pelvis.

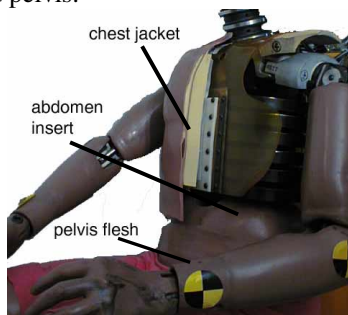


Figure 22. Relevance of the chest jacket for the abdominal response.

Although the chest jacket covers the abdominal region, it does not seem to have any abdominal function, see Figure 22. The jacket is quite thin below the dummy’s rib cage. In the upper region, there is additional foam between jacket and ribs and the jacket itself is thicker. The pelvis flesh also does not seem to perform any abdominal supporting function.

Relevant Load Conditions for the Abdominal Sensor - Abdominal injuries for the adult driver in frontal accidents are induced by lap and shoulder belt, steering wheel and airbag – either separately or by a combination of them. The steering wheel is, of course, not relevant for the front seat passenger; while at the rear seat, lap belt and shoulder belt are the only source of abdominal injuries in frontal accidents today. Frontal accidents include frontal oblique and frontal off-set collisions. Although every new car is equipped with a driver air bag, steering wheel loading is applicable for reconstruction cases with older cars and multiple collision accidents, even with newer cars. While loads applied by steering wheel or belt are local, airbags apply distributed loads to either the entire abdomen or large parts of it. Steering wheels have a diameter of about 380 mm – the rims of steering wheels have a diameter of approximately 30 mm. Standard belts have a width of 45 mm, but one has to take into account that the belt material bends along the longitudinal direction when the belt is tightened.

Sensor Description - Based on the loading cases mentioned above (lap belt, shoulder belt, steering wheel and airbag) the distance between two sensors should not exceed 25 mm in Y and in Z direction. Recognising this distance would prevent missing the load applied by a steering wheel with a rim diameter of 30 mm. As mentioned above, steering wheel loading is not valid for new cars in single collision accidents (as simulated by compulsory crash tests). If this load case is considered not to be necessary, the distance of two sensors should not exceed 35 mm for the belt loading cases. This distance would show enough overlap with the belt width, even when the belt is bent.

The sensors are to be applied at the anterior surface of the abdominal insert. This is the only part that covers the entire abdominal cavity. The chest jacket does not influence the abdominal function and the pelvis flesh does not reach the upper end of the dummy abdomen. For the assessment of the injury risk of the “hard abdomen” covered completely by ribs for the HIII dummy, it is reasonable to measure the rib compression. Although the localised compression measurement for the abdomen is felt to be a disadvantage it should not be a problem for the “hard thorax”. The disadvantages are problems in localised measurement of compression of soft

material, if the load is applied at a different location than the localised measurement device is situated. The following Figure 23 shows the sensor matrix for the Hybrid III 50th dummy in a two-dimensional view. For this dummy, 26 sensors are used; in comparison to 20 sensors for Q3 and Q6 dummy. The horizontal and the vertical distance between two sensors is 22.5 mm.

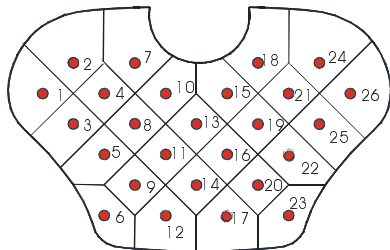


Figure 23. Sensor matrix for HIII 50th percentile.

ASSESSMENT OF THE ABDOMINAL SENSOR

The sensor concept has been assessed by a feasibility study, analysing the sensor behaviour under different load conditions and in the accident reconstruction programme of the EC funded CHILD project.

Amongst other criteria the average surface pressure was analysed regarding the correlation of the abdominal injury severity and the measured load. The probability to sustain an injury of a certain severity level depending on the abdominal average surface pressure was analysed using the logistic regression method. Using this analysis method, one is looking for a clear shift in the injury risk. This clear shift allows the definition of a load limit at the location of the shift.

Figure 24 shows the probability for the AIS 2+, AIS 3+ and AIS 4+ injury risk in relation to the measured abdominal average surface pressure. While this injury criterion seems to be appropriate to predict the AIS 2+ and AIS 3+ injury risk, it is not for the prediction of the AIS 4+ risk.

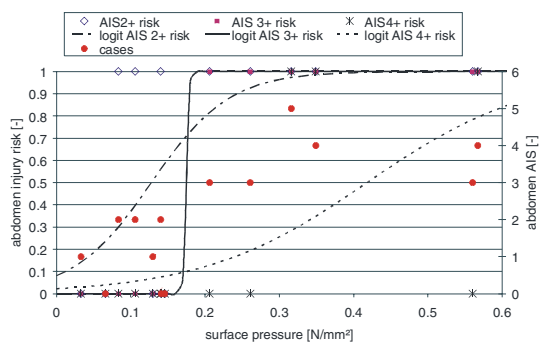


Figure 24. Probability analysis of abdominal injury risk depending on the average surface pressure.

The poor predictability of the AIS 4+ risk is likely to be caused by one of the fourteen analysed cases, where a very high load corresponds to AIS 3 injuries. Going into more detail, it becomes obvious that there is only a little information available in this case. The described intraperitoneal bleeding normally occurs secondary to an organ trauma. It is likely that more information could justify an injury severity coding of AIS 4.

The injury risk curves shown above indicate a load limit for 50% probability of AIS 2+ injuries of 0.13 N/mm² and for 50% probability of AIS 3+ injuries of 0.175 N/mm².

However, the chosen FlexiForce sensor shows considerable disadvantages with respect to reliability. Sensor sensitivity is not stable. The calibration results can differ by 20% between two calibration procedures. The maximum deviation recognised during this study was 74%, which is not acceptable. Accelerometers, for example, show a deviation below 1% within one year.

Additional problems recognised within this study are the considerable amount of channels, the effort for the calibration and the durability of the wiring. Comparing these problems with the sensor reliability shows that they are less severe.

In principle, the number of channels could be significantly reduced by electrical combination of single sensors. In the literature, different load limits for the upper middle and lower part of the abdomen as well as for the left and the right side were discussed. Taking these regions into account the number of channels could be reduced to nine (three rows and three columns). The main effort involved in the calibration of the sensors is their removal from the dummy, and the following reapplication of the sensors to the dummy. It is necessary to perform the calibration when the sensors are mounted at the abdomen, in order to reduce the calibration effort. It is then necessary to analyse the quality of this procedure.

The durability issues are limited to the wiring at the abdominal surface. The compression of the parts of the abdominal insert leads to high tension of the cables. To avoid damage caused by the tension, it is possible to pass the wiring in curves. Another option could be the use of more flexible wiring. In summary, the measurement principle is good, but better sensors need to be developed.

CONCLUSION

In automotive accidents liver, spleen and kidneys are the most affected abdominal organs. All these organs are solid ones. Usually abdominal injuries in frontal accidents are induced by the belt system or the steering wheel. The steering wheel is mainly responsible for injuries of unbelted drivers. Injuries caused by both the lap belt and by the shoulder belt were reported. There are some indications that the

airbag also causes abdominal injuries, but because of the low number of cases analysed in the literature no clear evidence exists. For children, it is the belt system only (either the car belt or the CRS harness).

Based on biomechanical tests, different injury criteria have been proposed. In addition to compression, velocity and force combinations of either of them are in discussion. The most promising injury criteria are the force applied to the abdominal surface and the compression (relative deflection) multiplied by the compression rate (the so-called viscous criterion, VC). The comparison of VC and applied force shows that these two criteria often correlate in a linear way.

Taking into account that abdominal injuries can be caused by steering wheel, lap and shoulder belt, as well as airbags, it is necessary to develop a sensor, which is able to cope with all of these loading cases. Due to high accuracy requirements concerning compression measurement in high speed loading cases with low compression (airbag), the measurement of the surface force offers general advantages. Accuracy of compression measurement is necessary because compression velocity has to be derived from the compression.

The FlexiForce foil sensor was selected as a very promising technology, which can be combined to a sensor matrix. The FlexiForce transducers are flexible pressure sensors with a sensitive area with a diameter of 9.5 mm. They can be used with normal crash equipment and behave sufficiently linearly. In comparison to accelerometers and load cells, they are very cheap. For child dummies of the Q series, namely the Q3 and Q6, 20 of these force sensors cover the entire abdominal insert. In addition to these two dummy sensors, another sensor was developed for the 50th percentile Hybrid III adult dummy using 26 sensors.

Finally, the child dummy sensors were used in a number of detailed accident reconstructions using complete vehicles and fully instrumented dummies within the EC funded CHILD project. The number of cases does not allow a final statistical analysis. However, investigations indicate that the average surface pressure correlates well with injury severity. Additional tests are necessary.

The chosen FlexiForce sensor does not fulfil basic requirements with respect to reliability and repeatability. A considerable change in sensor sensitivity was recognised within a short period of time.

Therefore, it is necessary either to improve the sensors used with respect to their performance or to develop new sensors.

ACKNOWLEDGEMENTS

This paper is an excerpt of a PhD [Johannsen, 2006]. Parts of the research mentioned in this paper were funded by the European Commission within

the CHILD project (5th Frame Work Programme, project no. G3RD-CT-2002-00791) and the APROSYS project (6th Frame Work Programme, project no. FP6-PLT-506503).

BIBLIOGRAPHY

- Augenstein, J.S.; Perdeck, E.B; Murtha, M.; Stratton, J.; Quigley, C.; Zych, G.; Byres, P.; Nunez, D.; Digges, K.; Lombardo, L.; Malliaris, A.: Injuries Sustained by Drivers in Airbag Crashes, 15th ESV Conference, 1996
- Augenstein, J.S.; Perdeck, E.; Williamson, J.; Stratton, J.; Horton, T.; Digges, K.; Malliaris, A.; Lombardo, L.: Injury Pattern among Air Bag Equipped Vehicles, 16th ESV Conference, 1998
- Cavanaugh, J.M.; Nyquist, G.W.; Goldberg, S.J.; King, A.I.: Lower Abdominal Tolerance and Response, 30th Stapp Conference, 1986
- Cuerden, R.W.; Scott, A.W.; Hassan, A.M.; Mackay, M.: The Injury Experience of Adult Rear Seat Car Passengers, IRCOBI, 1997
- Digges, K.; Haffner, M.; Lombardo, L.; Stucki, L.; Malliaris, A.; Augenstein, J.S.; Perdeck E.: Challenges in Injury Measurement Technology For Testing of Driver Air Bag Systems, 15th ESV Conference, 1996
- Dischinger, P.C.; Ho, S.M.; Kerns, T.J.; Brennan, P.: Patterns of Injury in Frontal Collisions with and without Airbags, IRCOBI, 1996
- Elhagediab, A.M.; Rouhana, S.W.: Patterns of Abdominal Injury in Frontal Automotive Crashes, 16th ESV Conference, 1998
- Frampton, R.; Sferco, R.; Welsh, R.; Kirk, A.; Fay, P.: Effectiveness of Airbag Restraints in Frontal Crashes – What European Field Studies Tell Us, IRCOBI, 2000
- Halpern-Herla, M.: Report of a Working Group on Biomechanics (EEVC), 6th ESV Conference, 1976
- Hardy, W.N.; Schneider, L.W.; Rouhana, S.W.: Abdominal Impact Response to Rigid-Bar, Seatbelt and Airbag Loading, 45th Stapp Conference, 2001
- Harms, P.L.; Renouf, M.; Thomas, P.D.; Bradford, M.: Injuries to Restrained Car Occupants; What are the Outstanding Problems?, 11th ESV Conference, 1987
- Jager, K. d.; Ratingen, M. v.; Lesire, P.; Guillemot, H.; Pastor, C.; Schnottale, B.; Tejera, G.; Lepetre, J.-P.: Assessing new Child Dummies and Criteria for Child Occupant Protection in Frontal Impact, 19th ESV Conference, 2005
- Johannsen, H.: The Assessment of Abdominal Injury Risks by Dummy Tests, Fortschritt-Berichte VDI, Reihe 12, No. 631, ISBN 3-18-363112-1, 2006
- Langwieder, K.; Hummel, T.: Biomechanical Risk Factors for Children in Cars and Aggravation by

- Misuse of Restraint System, 14th ESV Conference, 1994
- Langwieder, K.; Stadler, P.; Hummel, T.; Fastemeier, W.; Finkbeiner, F.: Verbesserung des Schutzes von Kindern in Pkw, BASt Report M 73, Bergisch Gladbach, 1997 (in German)
- Lau, V.K.; Viano, D.C.: Influence of Impact Velocity on the Severity of Non Penetrating Hepatic Injury, J-Trauma Vol. 21, Nr. 2, 1981
- Lau, I.V.; Viano, D.C.: The Viscous Criterion – Bases and Applications of an Injury Severity Index for Soft Tissues, 30th Stapp Conference, 1986
- Lau, I.V.; Horsch, J.D.; Viano, D.C.; Andrzejak D.V.: Biomechanics of Liver Injury by Steering Wheel Loading, J-Trauma, No. 3, 1987
- Lau, I.V.; Viano, D.C.: How and When Blunt Injury Occurs – Implication to Frontal and Side Impact Protection, 32nd Stapp Conference, 1988
- Leung, Y. C.; Tarrière, C.; Lestrelin, D.; Got, C.; Guillon, F.; Patel, A.; Hureau, J. : Submarining Injuries of 3 Pt. Belted Occupants in Frontal Collisions – Description, Mechanisms and Protection, 26th Stapp Conference, 1982
- Miller, M.A.: The Biomechanical Response of the Lower Abdomen to Belt Restraint Loading, J-Trauma No. 29, 1989
- Miller, M.A.: Tolerance to Steering Wheel-Induced Lower Abdominal Injury, J-Trauma No. 10, 1991
- Nusholtz, G.S.; Kaiker, P.S.; Huelke, D.F.; Suggitt, B.R.: Thoraco-Abdominal Response to Steering Wheel Impacts, 29th Stapp Conference, 1985
- Nusholtz, G.S.; Kaiker, P.S.: Abdominal Response to Steering Wheel Loading, 14th ESV Conference, 1994
- Penberthy, G.C.: Accute Abdominal Injuries, Surgery Gynecol. Obstet., No. 94, 1952
- Roselt, T.; Langwieder, K.; Hummel, T.; Köster, H.-J.W.: Injury Patterns of Front Seat Occupants in Frontal Car Collisions with Airbags – Effectivity and Optimisation Potential of Airbags, IRCOBI Conference, 2002
- Rouhana, S. W.; Lau, I. V.; Ridella, S. A.: Influence of Velocity and Forced Compression on the Severity of Abdominal Injury in Blunt, Nonpenetrating Lateral Impact, GMR Research Publication N. 4763, 1984
- Rouhana, S.W.; Lau, I.V.; Ridella, S.A.: Influence of Velocity and Forced Compression on the Severity of Abdominal Injury in Blunt, Nonpenetrating Lateral Impact, J-Trauma No. 25, 1985
- Rouhana, S.W.; Ridella, S.A.; Viano, D.C.: The Effects of Limiting Impact Force on Abdominal Injury: A Preliminary Study, 30th Stapp Conference, 1986
- Rouhana, S. W.: Abdominal Injury Prediction in Lateral Impact – An Analysis of the Biofidelity of the Euro-SID Abdomen, 31st Stapp Conference, 1987
- Schmidt, G.; Kallieris, D.; Barz, J.; Mattern, R.: Results of 49 Cadaver Tests Simulating Frontal Collision of Front Seat Passengers, SAE Paper 741182, 1974
- Snyder, R.G.; Snow, C.C.; Crosby, W.M.; Hanson, P.; Fineg, J.; Chandler, R.: Impact Injury to the Pregnant Female and Fetus in Lap Belt Restraints, 10th Stapp Conference, 1966
- Stalnaker, R.L.; Roberts, V.L.; McElhaney J.H.: Side Impact Tolerance to Blunt Trauma, 17th Stapp Conference, 1973
- Stalnaker, R.L.; Ulman, M.S.: Abdominal Trauma – Review, Response and Criteria, 29th Stapp Conference, 1985
- States, J.D.; Huelke, D.M.; Dance, M.; Green, R. N.: Fatal Injuries Caused by Underarm Use of Shoulder Belts, J-Trauma, No. 7, 1987
- Talantikite, Y.; Brun-Cassan, F.; Lecoz, J.-Y.; Tarriere, C.: Abdominal Protection in Side Impact Injury Mechanisms and Protection Criteria, IRCOBI Conference, 1993
- Trollope M. L.; Stalnacker, R. L.; McElhaney J. H.; Frey, C.F.: The mechanism of Injury in Blunt Abdominal Trauma, J-Trauma, Nr. 11, 1973
- Trosseille, X.; Chamouard, F.; Tarriere, C.: Abdominal Injury Risk to Children and its Prevention, IRCOBI Conference, 1997
- Viano, D.C.; Lau, I.V.: A Viscous Tolerance Criterion for Soft Tissue Injury Assessment, J-Biomechanics, Nr. 5, 1988
- Viano, D.C.; Lau, I.V.; Asbury, C.; King, A.I.; Begeman, P.: Biomechanics of the Human Chest, Abdomen and Pelvis in Lateral Impacts, 33rd AAAM, 1989
- Walfisch, G.; Fayon, A.; Tarriere, C.; Rosey, J.P.; Guillon, F.; Got, C.; Patel, A.; Stalnaker, R.L.: Designing of a Dummy's Abdomen for Detecting Injuries in Side Impact Collisions, IRCOBI, 1980
- Walfisch, G.: Fatalities and severe injuries for rear occupants wearing a 3-point seat belt in frontal collisions, EVPSN2 Workshop Cars, 2002
- Wiliams, R. D.; Sargent, F. T.: The Mechanism of Intestinal Injury in Trauma, J-Trauma 3, 1966
- Witte, C.L.: Mesentery and Bowel Injury from Automotive Seat Belts, Annals of Surgery, Vol. 167, No. 4, April 1968
- Yoganandan, N.; Gennarelli, F.A.; Maltese, M.R.: Patterns of Abdominal Injuries in Frontal and Side Impacts, 44th AAAM, 2000

THE MATERIAL PROPERTIES OF HUMAN TIBIA CORTICAL BONE IN TENSION AND COMPRESSION: IMPLICATIONS FOR THE TIBIA INDEX

**Andrew Kemper,
Craig McNally,
Eric Kennedy,
Sarah Manoogian,
Stefan Duma**

Virginia Tech – Wake Forest, Center for Injury Biomechanics
United States
Paper Number 07-0470

ABSTRACT

The risk of sustaining tibia fractures as a result of a frontal crash is commonly assessed by applying measurements taken from anthropometric test devices to the Tibia Index. The Tibia Index is an injury tolerance criterion for combined bending and axial loading experienced at the midshaft of the leg. However, the failure properties of human tibia compact bone have only been determined under static loading. Therefore, the purpose of this study was to develop the tensile and compressive material properties for human tibia cortical bone coupons when subjected to three loading rates: static, quasi-static, and dynamic. This study presents machined cortical bone coupon tests from 6 loading configurations using four male fresh frozen human tibias. A servo-hydraulic Material Testing System (MTS) was used to apply tension and compression loads to failure at approximately 0.05 s^{-1} , 0.5 s^{-1} , and 5.0 s^{-1} to cortical bone coupons oriented along the long axis of the tibia. Although minor, axial tension specimens showed a decrease in the failure strain and an increase the modulus with increasing strain rate. There were no significant trends found for axial compression samples, with respect to the modulus or failure strain. Although the results showed that the average failure stress increased with increasing loading rate for axial tension and compression, the differences were not found to be significant. The average failure stress for the static, quasi-static, and dynamic tests were 150.6 MPa, 159.8 MPa, and 192.3 MPa for axial tension specimens and 177.2 MPa, 208.9 MPa, and 214.1 MPa for axial compression specimens. When the results of the current study are considered in conjunction with the previous work the average compressive strength to tensile strength ratio was found to range from 1.08 to 1.36.

INTRODUCTION

Lower limb injuries resulting from motor vehicle crashes are the second most common site of AIS 2+

injury [27]. In addition, lower limb injuries have been reported to be a frequent cause of permanent disability and impairment [5]. Tibia and fibular shaft fractures account for 5% of AIS ≥ 2 lower extremity injuries and 8% of Life-years lost due to lower extremity injuries for front outboard occupants involved in frontal crashes [19].

The risk of sustaining tibia fractures as a result of a frontal crash is commonly assessed by applying measurements taken from anthropometric test devices to the Tibia Index (TI), developed by Mertz (1993). The Tibia Index, derived from combined stress analysis of a beam, is an injury tolerance criteria for combined bending and axial loading experienced at the midshaft of the leg:

$$TI = \frac{F}{F_c} + \frac{M}{M_c} \quad (1)$$

where F is measured compressive axial force (kN) in the superior-inferior direction, M is measured bending moment (Nm) in the leg, F_c is the critical force values, and M_c is the critical moment value. Mertz (1993) recommend critical force and moment values of 35.9 kN and 225 Nm, respectively. According to Mertz (1993), a TI reading less than 1 indicates that injury is unlikely. In order to protect against tibia plateau fracture, Mertz (1993) proposed a supplemental compressive force limit of 8 kN for the 50th percentile male dummy in addition to the Tibia Index formula.

Several authors have noted that the TI does not properly consider the combined effects of the two types of loading, because the TI assumes that the ultimate tensile strength and compressive strength of bone are equal [15, 26, 29]. Yamada (1970) reported that at static loading rates the ultimate compressive strength is approximately 1.08 times the ultimate tensile strength for human tibia compact, while Burstien and Reilly (1976) reported a slightly higher ratio of 1.25. Welbourne and Shewchenko (1998) illustrated that by arbitrarily increasing the TI injury threshold from 1 to 1.3 expands the injury boundary

to some extent. Currently the European Enhanced Vehicle Safety Committee (EEVC) for Euro NCAP uses the modified TI threshold of 1.3 as a compliance margin with the Hybrid III [19]. However, if maximum allowable force and moment values of 8 kN and 225 Nm are assumed, the TI is 1.223 [29]. Therefore, if the critical force and moment values are not increased by 30% to correspond with the increase in the TI threshold, the critical force and moment limits will always be exceeded before the TI reached 1.3 [29]. In addition, raising the threshold to 1.3 also changes the engineering basis of the TI, because the threshold of 1 is based on a standard engineering failure criterion [15]. Therefore, Funk et al. (2004) proposed a reformulated TI with revised critical values that accounts for effects tibia curvature and the differences in tensile and compressive strength while maintaining a threshold equal to 1. However, the ratio of compressive strength to tensile strength used by Funk et al. (2004) is based on a quasi-static data reported by Yamada (1970) for bone in general and not specifically for tibia cortical bone. Given that the properties of bone are rate dependant, the ability to accurately predict leg injuries could be improved by using a ratio of compressive strength to tensile strength for human tibia compact determined at a loading rate representative of that seen in automotive crashes [8, 21].

Although there have been numerous studies that have reported on the material properties of human tibia cortical bone in tension and compression, the research has been limited to static loading conditions and may not be representative of loading rates seen in automotive crashes. [7, 10, 12, 13, 31]. Therefore, the purpose of this study was to develop the matched tensile and compressive material properties for human tibia cortical bone coupons subjected to three loading rates, and determine the appropriate ratio to apply to the TI.

METHODS

This study presents 20 human tibia cortical bone coupon tests taken from the mid-diaphysis; 11 axial tension, 9 axial compression. The methodology is presented in four parts: experimental configuration,

preparation of cortical bone coupons; testing configuration, detailing the MTS setup and measurement devices; and statistical methodology.

Subject Information

Tibia cortical bone specimens were dissected from two unembalmed fresh frozen male human cadavers. Freezing was used as a means to preserve the specimens because numerous previous studies have indicated that freezing does not significantly affect the material properties of cortical bone when frozen to a temperature of -20° C [14, 16, 17, 20, 25].

For comparison with the standard population, the bone mineral density (BMD) of each cadaver was determined by the Osteogram technique. The left hand of the cadavers was x-rayed, scanned and processed by CompuMed incorporated (Los Angeles, CA). This type of BMD measurement, however, only provides an indication of overall bone strength and does not account for local changes in bone density or composition. Therefore, the BMD obtained through this method is referred to as the “Global BMD”. The global BMD results are reported with respect to the normal population (Table 1). The T-score is used to compare the cadaver’s global BMD with that of the general population, using 30 years of age as the comparison. The Z-score is used to compare the global BMD of the subjects with the average for their age. A T-score of -1 corresponds to one standard deviation below the mean for the general population, meaning the individual is at or above the 63rd percentile for global BMD, or close to normal. T-scores of 2 and 3 correspond to 97th and 99th percentiles, respectively.

Specimen Preparation

In order to conduct material property testing on human cortical bone, the bone coupon must first be machined into a testable geometry. This was done through numerous steps of detailed preparation [18]. First, an oscillating bone saw was used to make two cuts to separate the tibia from the body (Figure 1, (Figure 2A).

Table 1. Osteogram data for cadavers used in tibia cortical bone testing.

Cadaver	Gender	Age	Global BMD	T-Score	Z-Score
Sm39	M	67	105.4	-0.5	0.9
Sm37	M	56	105.3	-0.5	0.3

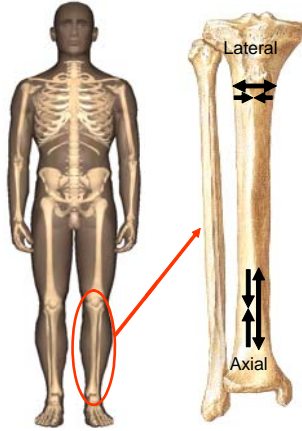


Figure 1. Isolated tibia showing axial and lateral specimen orientations.

The mid-diaphysis of the tibia was cut into sections using a low speed diamond saw with micrometer precision (Figure 2 B). The diamond saw blade was immersed in a saline bath to minimize the heat created from friction and maintain specimen hydration, which has been shown to significantly affect the material properties, specifically plasticity, of cortical bone [6]. Then, the sections cut from the tibia were placed in a bone chuck and two parallel cuts were made along the longitudinal axis to remove a rectangular section of the bone (Figure 2 C). Great care was taken when placing the bone sections in a bone chuck to ensure that the axis of the tibia coincided with the axis of cutting. The rectangular cortical bone specimen was placed in a custom bone chuck, and a third cut was made to remove the cancellous bone from the piece (Figures 2 D and E). This cut also created a flat side that was placed faced down on the milling base. Finally, additional cuts were made to level the uncut side and, if necessary, trim the ends to fit on the milling base. It should be noted that the dimensions of the rectangular cortical bone specimens were cut slightly larger than the final specimen dimension to allow a clamping area for the milling process. Since the tibia is triangularly shaped, this process was repeated in order to obtain rectangular cortical bone specimens from all three sides of the tibia.

The resulting rectangular cortical bone specimen was then milled to the final test specimen dimensions using a small Computer Numerical Control (CNC) machine (MAXNC 10, MAXNC Inc., Chandler, AZ). A rectangular pocket was milled into a plastic milling base to create a surface parallel to the z-axis, or vertical axis, of the mill. The flat side of the rectangular cortical bone specimen was placed on the plastic milling base. This was done to assure that the top face of the cortical bone specimen was milled

parallel to the flat face. Again, great care was taken when placing the cortical bone specimen on the milling base to ensure the axis of interest coincided with the axis of the mill. The milling base was placed in a saline bath to minimize heat and maintain specimen hydration. The mill ran two codes to cut the specimen to the final dimension with micrometer precision. The final test specimen dimensions were based on both previous literature and ASTM standards for tension and compression material testing [3, 4, 9, 10, 24, 21, 30, 32] (Figures 3 and 4). Finally the coupons were evenly sanded with 240, 320, 400, and 600 grit wet sand paper. The finished specimens were kept immersed in a saline solution and refrigerated until tested. Once the specimens were placed on the test setup, they were kept hydrated by spraying a saline solution on them.

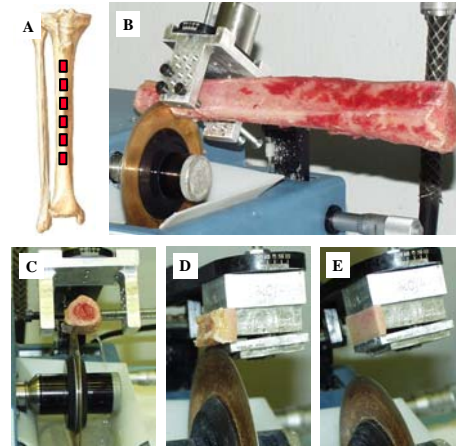


Figure 2. A) Isolate tibia. B) Mid-diaphysis divided into smaller sections. C) Parallel cuts along the long axis of the tibia D) Isolate the cortical bone from the cancellous bone. E) One flat side to place face down on the milling base.

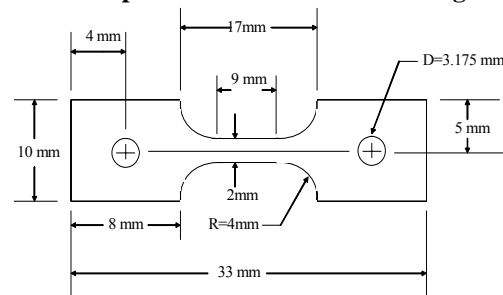


Figure 3. Axial tension specimen dimensions. Note: Specimen thickness = 2mm.

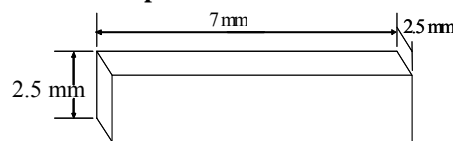


Figure 4. Axial compression specimen dimensions.

Testing Configuration

A high-rate servo-hydraulic Material Testing System (MTS) was used to apply either tension or compression loads to failure at approximately 0.05 s^{-1} , 0.5 s^{-1} , and 5.0 s^{-1} on the cortical bone coupons. For all failure tests, a 2224 N load cell was used to measured load (MTS 661.18E-02, 2224 N, Eden Prairie, MN). Displacement was measured with a laser vibrometer (Polytec, OFV 303, Tustin, CA).

A total of five displacement measurement devices were evaluated for accuracy under both static and dynamic loading conditions. The devices included: a strain gage, potentiometer, extensometer, laser vibrometer, and the MTS internal LVDT. The standard displacement measurement device for static material testing is an extensometer, which provides a direct displacement measurement of the specimen gage length. However, the grips of the extensometer slip during the high rate testing resulting in inaccurate displacement readings. Like the extensometer, a strain gage provides a direct displacement measurement of the specimen gage length. However, tests conducted with a strain gage applied over the specimen gage length showed a large reduction in ultimate stress and strain. This was due to localized specimen drying, required to apply the strain gage, which has been shown to significantly affect the material properties, specifically plasticity, of cortical bone [6]. The

potentiometer is a non-contact displacement measurement device, which does not affect the properties of the material being tested. However, the potentiometer data did not show the same response time as the extensometer for slow rate tests. The MTS internal LVDT was found to have relatively poor resolution. Finally, the laser vibrometer, which has nanometer scale accuracy and a high frequency response of 200 kHz, showed almost the exact response as the extensometer at static and quasi static rates. Unlike the extensometer; however, the laser vibrometer also gives accurate readings during high rate testing.

For dynamic testing, the MTS actuator must travel a finite distance to reach the desired test speed. If the actuator is directly coupled to the test coupon, then a toe region will be seen in the stress vs. strain response. In order to avoid this, the use of a custom lack adapter was employed (Figure 5). A shaft with a male conical end rested inside a hollow tube with a female conical end, which was directly coupled to the MTS actuator. The MTS was programmed lift or lower the slack adapter tube, depending on the testing direction, to allow enough space to reach the desired speed before coming into contact with the slack adapter rod. Once the MTS reached the desired speed and engaged the slack adapter, the piece was loaded at a constant rate to failure. The slack adapter was designed to work in both tension and compression test configurations (Figure 5).

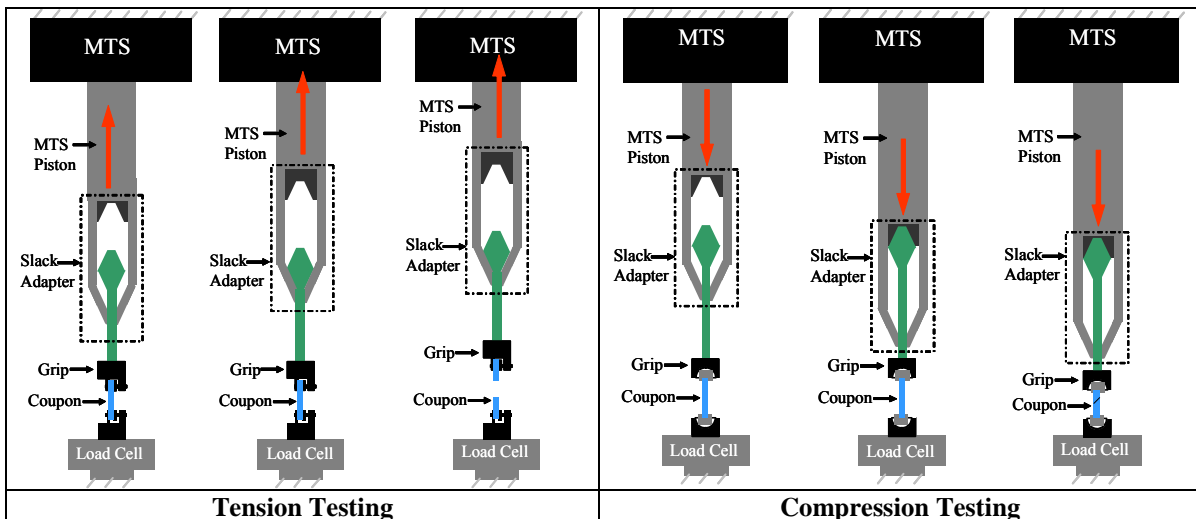


Figure 5. Slack adapter in test configurations.

Alignment of Test Setup

The three main sources of misalignment in a material testing setup were addressed in order to minimize variable bending stresses, which result in a reduction in both strength and ductility. As described earlier, extreme care was taken during the specimen preparation process to maintain symmetric machining along the axis of interest of the test specimens. The conformance of the specimen centerline to the top and bottom grip centerlines was addressed through design and precise machining of the grips. For tension testing, the grips were designed to use both a pin and clamp configuration. The pin ensured proper centerline conformance, and the clamp provided the holding force. To hold the bone coupon in place, the grip screws were tightened, forcing metal plates to clamp both ends of the coupon (Figure 6). For compression testing, proper centerline conformance was ensured by milling a 1 mm deep circular placement groove, concentric with the grip centerline, in the top and bottom loading surfaces

(Figure 7). The diameter of the placement hole was such that the corners of the compression specimen just slightly cleared. In compression testing, it is critical that the two loading faces are parallel. In order to compensate for any angular misalignment of the compression grips or faces of the compression specimen, lubricated rotating hemispheres were placed on the top and bottom grips [4]. The compliance of the lubricant was taken into account by conducting a series of compression tests with no specimen in the grips. The resulting force versus displacement curves were then fitted and used to adjust the displacement data from the actual cortical bone compression tests. In order to align the centerlines of the top and bottom grips, an aluminum specimen with the same dimensions of the cortical bone coupon specimens was instrumented with strain gages on all four sides of the gage length [1]. A dial indicator read the position so the load cell could be adjusted in small increments until the strain gages read within 100 microstrain of one and other, which is less than 1 % of the total loading strain in the tests.

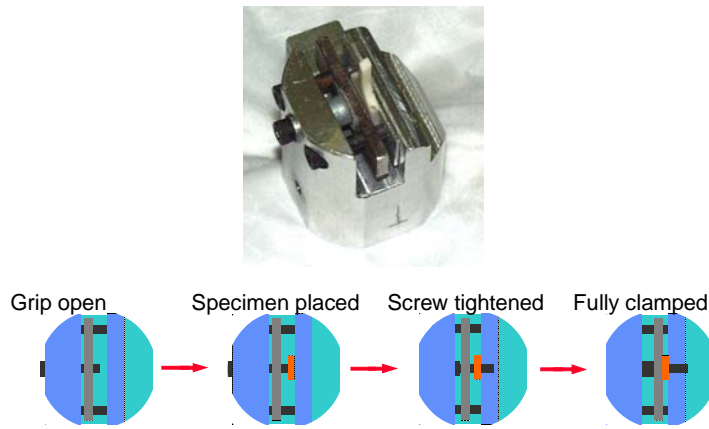


Figure 6. Tension test grips with pin and clamp design.

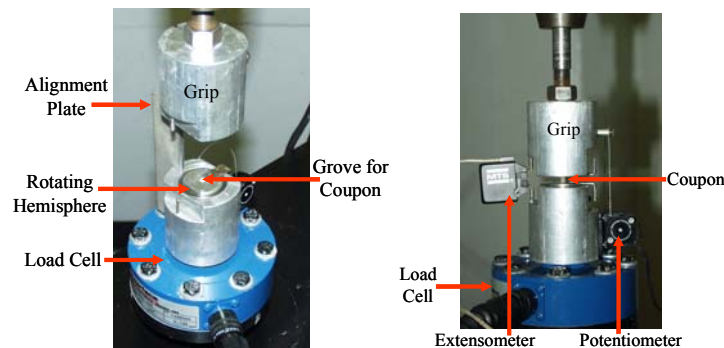


Figure 7. Compression test grips with centering groove to ensure proper centerline conformance.

Data Processing

The load and strain data were collected and filtered at different levels depending on the speed of each test (Table 2). Each filter class changed the peak stress and strain by less than 1%. Stress was calculated by dividing the force measurement by the cross sectional area of the specimen gage length. Strain was determined using the Lagrangian formulation of dividing the change in length by the initial length. The modulus of elasticity was defined as the slope between two points, approximately 30 % and 70 % of the yield point.

Table 2. Sampling frequency and CFC filter for each test series.

Strain Rate	Compression	Tension
0.05 s-1	15kHz/ CFC180	10kHz/ CFC180
0.5 s-1	30kHz/ CFC600	30kHz/ CFC600
5.0 s-1	100kHz/ CFC1000	100kHz/ CFC1000

Statistical Analysis

Statistical analysis was performed on all of the data in order to illustrate significant differences between the values for the 6 different groups of tests. For this analysis, multiple t-tests were performed between each group of data for each value. The

Tukey-Kramer technique was used which adjusts for multiple comparisons. P-values are presented with statistical significance assigned to a p-value of 0.05 or less.

RESULTS

Tension tests were performed on a total of 11 human tibia cortical bone coupons at three stain rates. The tension mechanical properties for each specimen as well as averages by testing group are shown in Table 3. The average failure stress for the static, quasi-static, and dynamic tests were 150.6 MPa, 159.8 MPa, and 192.3 MPa for axial tension. The average failure strain for the static, quasi-static, and dynamic tests were specimens and 23696 microstrain, 19228 microstrain, and 18329 microstrain for axial tension specimens. The stress vs. strain curves for all tension tests are also shown (Figure 8).

Compression tests were performed on a total of 9 human tibia cortical bone coupons at three stain rates. The compression mechanical properties for each specimen as well as averages by testing group are shown in Table 4. The average failure stress for the static, quasi-static, and dynamic tests 177.2 MPa, 208.9 MPa, and 214.1 MPa for axial compression specimens. The average failure strain for the static, quasi-static, and dynamic tests were 16116 microstrain, 19587 microstrain, and 21198 microstrain for axial compression specimens. The stress vs. strain curves for all compression tests are also shown (Figure 9).

Table 3. Axial tension material properties.

Series	Test	Strain Rate (strains/s)	E (GPa)	Ultimate Strain (microstrain)	Ultimate Stress (MPa)
ATF	L1	0.045	19.15	25028	151.3
ATF	L2	0.041	18.89	23392	159.0
ATF	L3	0.044	19.33	24717	151.1
ATF	L4	0.055	16.04	21647	141.1
ATFL Average		0.046	18.35	23696	150.6
ATF	M1	0.656	15.56	20986	152.2
ATF	M2	0.464	19.18	18073	172.9
ATF	M3	0.629	16.35	19918	155.3
ATF	M4	0.586	17.86	17937	158.8
ATFM Average		0.584	17.23	19228	159.8
ATF	H1	5.077	29.88	18966	180.0
ATF	H2	7.336	41.95	21223	230.5
ATF	H3	5.669	30.76	14797	166.5
ATFH Average		6.027	34.19	18329	192.3
ATF Average		2.167	22.27	20607	165.3

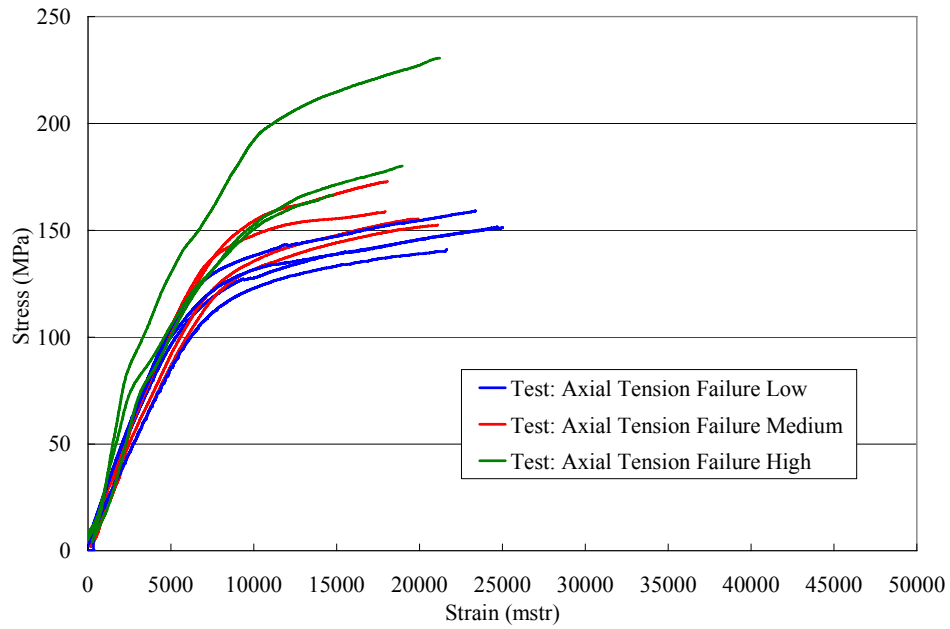


Figure 8. Axial tension static, quasi-static, and dynamic tests.

Table 4. Axial compression material properties.

Series	Test	Strain Rate (strains/s)	E (GPa)	Ultimate Strain (microstrain)	Ultimate Stress (MPa)
ACF	L1	0.043	18.86	15944	197.9
ACF	L2	0.044	13.63	18315	165.6
ACF	L3	0.039	18.23	14089	167.9
ACFL Average		0.042	16.91	16116	177.2
ACF	M1	0.580	16.03	20700	197.7
ACF	M2	0.464	19.58	16568	208.1
ACF	M3	0.453	18.53	21492	220.8
ACFM Average		0.499	18.05	19587	208.9
ACF	H1	4.874	12.82	16137	223.5
ACF	H2	4.591	13.67	22817	195.1
ACF	H3	3.667	13.53	24639	223.6
ACFH Average		4.377	13.34	21198	214.1
ACF Average		1.640	16.10	18967	200.0

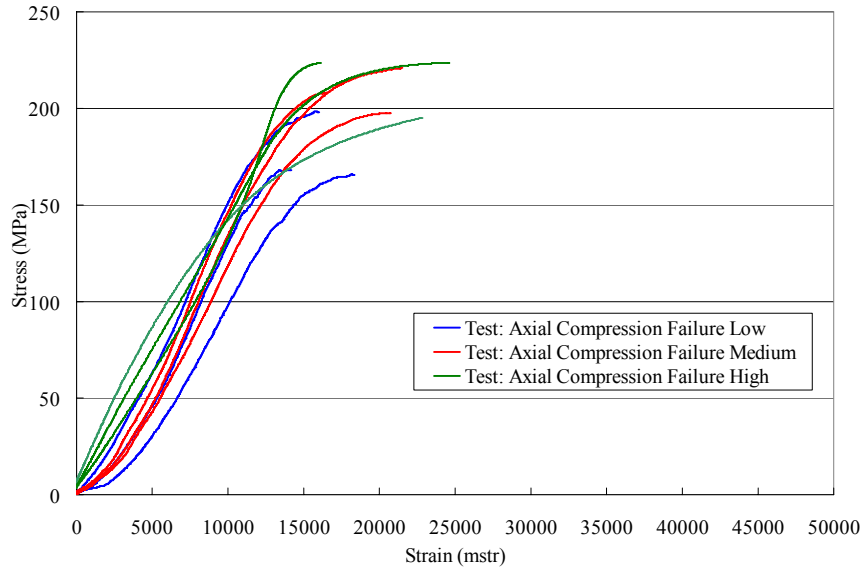


Figure 9. Axial compression static, quasi-static, and dynamic tests.

Statistical Analysis

Statistical analysis was performed on all of the data in order to illustrate significant differences between the values for the 6 different groups of tests. For this analysis, multiple t-tests were performed between each group of data for each value. The Tukey-Kramer technique was used which adjusts for multiple comparisons. P-values are presented with statistical significance assigned to a p-value of

0.05 or less (Tables 5-7). Although minor, axial tension specimens showed a decrease in the failure strain and an increase the modulus with increasing strain rate. There were no significant trends found for axial compression samples, with respect to the modulus or failure strain. Although the results showed that the average failure stress increased with increasing loading rate for axial tension and compression, the differences were not found to be significant.

Table 5. P-values for the elastic modulus (E) for all failure test groups.

	ACFH	ACFL	ACFM	ATFH	ATFL	ATFM
ACFH	*					
ACFL	0.9209	*				
ACFM	0.6789	0.9999	*			
ATFH	0.0001	0.0001	0.0001	*		
ATFL	0.4992	0.9999	0.9999	0.0001	*	
ATFM	0.8139	0.9999	0.9999	0.0001	0.9999	*

Table 6. P-Values for ultimate stress for all failure test groups.

	ACFH	ACFL	ACFM	ATFH	ATFL	ATFM
ACFH	*					
ACFL	0.4564	*				
ACFM	0.9999	0.6706	*			
ATFH	0.9564	0.9973	0.9945	*		
ATFL	0.0065	0.7972	0.0163	0.2062	*	
ATFM	0.0319	0.9861	0.0733	0.5436	0.9999	*

Table 7. P-Values for ultimate strain for all failure test groups.

	ACFH	ACFL	ACFM	ATFH	ATFL	ATFM
ACFH	*					
ACFL	0.8541	*				
ACFM	0.9999	0.9883	*			
ATFH	0.1297	0.9567	0.3464	*		
ATFL	0.9987	0.2661	0.9376	0.0094	*	
ATFM	0.9999	0.9916	0.9999	0.3210	0.8420	*

DISCUSSION

The static tensile material properties of human tibia bone presenting in this study were found to consistent with previously published material property data (Tables 8). The tensile modulus, average ultimate tensile stress, and average ultimate tensile strain data from the current study lie within the values reported by previous authors. The differences in reported material property values could be attributed to a number of variables know to influence the properties of bone: age, bone density, specimen hydration, or gender.

The static compressive material properties of

human tibia bone presenting in this study were also found to consistent with previously published material property data (Table 9). The average compressive ultimate stress data from the current study lie within the values reported by previous authors. Burstein and Reilly(1976) and Evans and Vincentelli (1967) reported higher modulus values, 28.0 GPa and 19.3 GPa respectively, than the current study. However, Evans (1967) reported a lower average ultimate compressive strain value than the current study. Again, differences in reported material property values could be attributed to a number of variables know to influence the properties of bone: age, bone density, specimen hydration, or gender.

Table 8. Comparison of reported human tibia compact bone material properties in axial tension.

Author	Age	Loading Rate	Modulus (GPa)	Ultimate Strain (microstrain)	Ultimate Strength (MPa)
Dempster (1961)	N/R	N/R	N/R	N/R	95.3
Melick (1966)	N/R	N/R	N/R	N/R	138.3
Evans (1967)	33-98	N/R	15.2	16500	97.1
Yamada (1970)	20-39	N/R	18.0	15000	140.3
Burstein (1976)	50-59	0.05 s-1	23.1	31000	164.0
Kemper (2004)	56-67	0.046 s-1	18.4	23696	150.6

Table 9. Comparison of published human tibia compact bone material properties in axial compression.

Author	Age	Loading Rate	Modulus (GPa)	Ultimate strain (microstrain)	Ultimate strength (MPa)
Yamada (1970)	20-39	N/R	N/R	N/R	151.1
Burstein (1976)	50-59	0.05 s ⁻¹	25.1	N/R	183.0
Evans (1974)	26-75	0.045 in/min	19.3	9510	109.0
Kemper (2007)	56-67	0.042 s ⁻¹	16.4	16116	177.2

Although there have been numerous studies that have reported on the material properties of human tibia cortical bone in tension and compression, only two have conducted matched tension and compression testing [7, 31]. The ratio of compressive strength to tensile strength from these studies was compared with the results from the current study (Table 10). In the current study, the ratio of compressive strength to tensile strength ranged static, quasi-static, and dynamic test groups were 1.17, 1.31, and 1.11 respectively. However, given that there were no significant differences found in ultimate stress by loading rate in the current study, all three loading rate groups were used in to determine an average ratio of compressive strength to tensile strength of 1.21. Burstein and Reilly (1976) reported ultimate stress grouped by age. Therefore, a ratio of compressive strength to tensile strength was calculated for each age group, and ranged from 1.15 to 1.36. The average of all the age groups reported by Burstein (1976) was found to be 1.24.

Welbourne and Shewchenko (1998) illustrated that arbitrarily increased the TI injury threshold to 1.3, to account for the differences in compressive strength and tensile strength increases the injury boundary somewhat. However, Welbourne and Shewchenko (1998) also showed that based on the maximum allowable force and moment values proposed by Mertz (1993) the highest TI value is 1.223. Consequently, the modified TI threshold of 1.3 currently used by the European Enhanced Vehicle Safety Committee (EEVC) for Euro NCAP is too high. Funk et al. (2004) used a ratio of 1.2 a reformulated TI formula with revised critical force and moment values, which take both tibia curvature and difference in compressive strength and tensile strength into account, and showed increase the injury prediction over a ratio equal to 1. Although, the ratio of 1.2 was based on static data reported by Yamada (1970) for bone in general, the results of the current study show that 1.2 is a reasonable value for since it lies within the range of ratios for human tibia cortical bone determined at various loading rates.

Table 10. Comparison of tibia compressive strength to tensile strength ratios.

Author	Age	Loading Rate	$\frac{\sigma_{UT}(comp)}{\sigma_{UT}(ten)}$
Yamada (1970)	20-39	N/R	1.08
Burstein (1976)	20-89	0.05 s ⁻¹	1.24 (avg.) [1.15-1.36]
Kemper (2007)	56-67	0.04 to 7.3 s ⁻¹	1.21 (avg.) [1.17-1.31]

CONCLUSIONS

The material properties of human tibia cortical bone were determined from cortical bone coupons obtained from the mid-diaphysis at three different loading rates. The mechanical properties presented in this study were found to be consistent with previously published data at similar loading rates.

Therefore, the specimen preparation and test methods presented in this study are both accurate and precise for determining cortical bone material properties. Although minor, axial tension specimens showed a decrease in the failure strain and an increase the modulus with increasing strain rate. There were no significant trends found for axial compression samples, with respect to the modulus or failure strain.

Although the results showed that the average failure stress increased with increasing loading rate for axial tension and compression, the differences were not found to be significant.

When the results of the current study are considered in conjunction with the previous work the average compressive strength to tensile strength ratio was found to range from 1.08 to 1.36. Although the previously used ratio of 1.2 was based on static, the results of the current study show that it is a reasonable value for since it lies within the range of ratios for human tibia cortical bone determined at various loading rates.

ACKNOWLEDGMENTS

The authors wish to acknowledge Toyota Motor Corporation for providing the funding for this research

REFERENCES

- [1] ASTM Standard E 1012-99, ASTM (2004). "Standard Practice for Verification of Specimen Alignment." American Society of Testing and Materials, Philadelphia, PA.
- [2] ASTM Standard E 8M-01, ASTM (2004). "Standard Test Methods for Tensile Testing of Metallic Materials [Metric]." American Society of Testing and Materials, Philadelphia, PA.
- [3] ASTM Standard D 5026-01, ASTM (2004). "Standard Test Methods for Plastics: Dynamic Mechanical Properties: In Tension." American Society of Testing and Materials, Philadelphia, PA.
- [4] ASTM Standard E 9-89a, ASTM (2004). "Standard Test Methods of Compression Testing of Metallic Materials at Room Temperature." American Society of Testing and Materials, Philadelphia, PA.
- [5] Burgess et al. (1995). "Lower Extremity Injuries in drives od Airbag-Equipped Automobiles- Clinical and Crash Reconstruction Correlations." *J. of Trauma*. 38, 509-516.
- [6] Burstien, A.H., Reilly D.T., and Victor, H.F. (1972). "The Ultimate Properties of Bone Tissue: The Effect of Yielding." *J. Biomechanics*. 5, 35-44.
- [7] BurstienTIEN, A.H., Reilly D.T., and Martens M. (1976). "Aging of bone tissue: Mechanical Properties." *Journal of Bone and Joint Surgery*. 58-A(1),82-86.
- [8] Carter, D.R., and Haynes, W.C. (1976). "The Compressive Behavior of Bone as a Two-Phase Porous Structure." *J. of Bone and Joint Surgery*. 59-A, 954- 962.
- [9] Crowninshield, R., and Pope M. (1974). "The Response of Compact Bone in Tension at Various Strain Rates." *Annals of Biomedical Engineering*. 2, 217-225.
- [10] Dempster, W.T., and Lippicoat R.T. (1952). "Compact Bone as a Non-Isotropic Material." *Amer. J. Anat.* 91, 331-362.
- [11] Dempster, W.T., and Coleman, R.F. (1961). "Tensile Strength of Bone Along and Across the Grain." *J. Appl. Physiol.* 16, 355-360.
- [12] Evans F.G. and Vincentelli R. (1974). "Relations of the Compressive Properties of Human Cortical Bone to Historical Structure and Calcification." *J. Biomechanics*. 7, 1-10.
- [13] Evans, F.G., and Bang, S. (1967). "Differences and Relationships Between the Physical Properties and Microscopic Structure of Human Femoral, Tibial, and Fibular Cortical Bone." *AM. J. ANAT.* 120, 79-88.
- [14] Frankel, V.H. (1960). "The femoral neck. Function. Fracture mechanism. Internal fixation. An experimental study." Almquist and Wiskell, Goteborg, Sweden.
- [15] Funk, J.R., Rudd, R.W., Kerrigan, J.R., and Crandell, J.R. (2004). "The Effect of Tibial Curvature and Fibular Loading on the Tibial Index." *Traffic Injury Prevention*. 5, 164-172.
- [16] Griffon, D.J., Wallace, L.J., and Bechtold, J. (1995). "Biomechal properties of canine corticocancellous bone frozen in normal saline solution." *Am. J. Vet. Res.* 56, 822.
- [17] Hamer, A.J., Strachen, J.R., Black, M.M., Ibbotson, C.J., Stockley, I., and Elson, R.A. (1996). "Biomechanical properties of cortical allograft bone using a new method of bone strength measurement. A comparison of fresh, fresh-frozen and irradiated bone." *J. Bone Joint Surg.* 78B, 363.
- [18] Kemper A, McNally C, Kennedy E, Rath A, Manoogian S, Stitzel J, and Duma S (2005): Material Properties of Human Rib Cortical Bone From Dynamic Tension Coupon Testing. *The Proc. of the*

49th International Stapp Car Crash Conference. 49, 199-230.

[19] Kuppas S, Wang J, Haffner M, Eppinger R. (2001). "Lower Extremity Injuries and Associated Injury Criteria." *Proc. 17th ESV Conf.*, Paper 457, 1-15.

[20] Linde, F., and Sorenson, H.C.F. (1993). "The effect of different storage methods on the mechanical properties of trabecular bone." *J. Biomech.* 26, 1249.

[21] McElhaney, J.H. and Byars, E.F. (1966). "Dynamic Response of Biological Materials." *ASME. Publ.* 65-WA/Huf-9.

[22] Melick, R.A., and Miller, D.R. (1966). "Variations of Tensile Strength of Human Cortical Bone with Age." *Clin. Sci.*, 30, 243.

[23] Mertz HJ. (1993). Anthropometric Test Devices, in *Accidental Injury: Biomechanics and Prevention*. Ed. A. M. Nahum, J. W. Melvin, Springer-Verlag, New York, Chapter 4.

[24] Reilly, D.T., Burstein, A.H. (1975). "The Elastic and Ultimate Properties of Compact Bone Tissue." *J Biomechanics.* 8(6), 393-405.

[25] Sedlin, E.D. (1965) "A rheological model for cortical bone." *Acta Orthop. Scand.* 83, 1.

[26] Tarriere, C. and Viano, D.C. (1995). "Biomechanical Synthesis of New Data on Human Lower Leg Responses and Tolerances in Parallel with Dummies and Injury Criteria." Proceedings of the International Conference on Pelvic and Lower Extremity Injuries, 153- 160. Washington, DC: National Highway Traffic Safety Administration.

[27] Thomas, P. et al. (1995). "Lower Limb Injuries – The Effect of Intrusion, Crash Severity and the Pedals on Injury Risk and Injury Type in Frontal Collisions." Proceeding of the 39th Stapp Car Crash Conference. SAE Paper No. 952728.

[28] Weaver, J.K. (1966). "The microscopic hardness of bone." *J. Bone Joint Surg.* 48-A, 273.

[29] Welbourne ER, Shewchenko N. (1998). "Improved Measurements of Foot and Ankle Injury Risk from the Hybrid III Tibia." *Proc. 16th ESV Conf.*, Paper 98-S7-O-11, 1618-1627.

[30] Wood, J.L. (1971). "Dynamic Response of Human Cranial Bone." *J. Biomechanics.* 4, 1-12.

[31] Yamada H. (1970). "Strength of Biological Materials." Williams and Wilkins Co., Baltimore, Md.

[32] Yeuheui, H.A. and Draughn, R.A. (2000). "Mechanical Testing of Bone and the Bone-Implant Interface." CRC Press LLC, New York.

STIFFNESS PROPERTIES OF HUMAN LUMBAR INTERVERTEBRAL DISCS IN COMPRESSION AND THE INFLUENCE OF STRAIN RATE

**Andrew Kemper,
Craig McNally,
Sarah Manoogian,
Dave McNeely,
Stefan Duma**

Virginia Tech – Wake Forest, Center for Injury Biomechanics
United States
Paper Number 07-0471

ABSTRACT

There have been numerous researchers that have investigated the properties of human intervertebral discs. However, there has been no attempt to characterize the effects of dynamic loading on the compressive stiffness of human lumbar intervertebral discs. Therefore, the purpose of this study was to develop the compressive stiffness properties of lumbar intervertebral discs when subjected to various dynamic compressive loading rates. This was accomplished by performing a total of 33 axial compression tests on 11 human lumbar intervertebral discs dissected from 6 fresh frozen human cadavers, 5 male and 1 female. The adjacent vertebral bodies were fixed to a load cell with a custom aluminum pot and then subjected to three dynamic compressive loading rates using a servo-hydraulic Material Testing System: 6.8, 13.5, and 72.7 strain/ sec. The results show that the compressive stiffness of lumbar intervertebral discs is dependent on the loading rate. There was no significant correlation ($p > 0.05$) between functional spinal unit compressive stiffness and vertebral level at any of the three loading rates. Therefore, a linear relationship between loading rate and vertebral disc compressive stiffness was developed by curve fitting the stiffness data from the current study along with static compressive stiffness data reported by previous studies.

INTRODUCTION

It is estimated that the combined overall cost of vertebral fractures in North America is approximately \$750 million dollars a year [19]. Vertebral fractures can occur as a result of moderate trauma, falls from standing height or less, as well as severe trauma, falls from greater than standing height or motor vehicle accidents [4]. A common fracture seen in motor vehicle accidents is anterior wedge fractures, caused by combined flexion and axial compression [13]. In addition, the increased risk of vertebral fractures with age is directly linked to increased incidence of osteoporosis in individuals over 45 [16].

In order to understand and reduce these injuries, various mathematical and mechanical models of the human spine have been developed. Given that the mechanical response of biological tissues demonstrates some degree of rate dependence, these models must be validated using mechanical properties obtained at the appropriate loading rates in order to accurately simulate spine kinematics and predict injury.

The literature on the biomechanics of the spine has primarily focused on the failure properties of isolated vertebral bodies or functional spinal units (FSU), defined as an intervertebral disc and all or part of the two adjacent vertebral bodies, or the compressive stiffness under static and quasi static different loading conditions [1, 2, 3, 7, 14, 23]. The compressive failure force and stiffness of isolated vertebral bodies have both been shown to increase with increasing of loading rate [9, 10]. Sundararajan et al. [2005] reported that the shear failure force of FSUs increases with increasing of loading rate. There have been a few studies that have investigated the viscoelastic response of functional spinal units in axial compression through static creep or stress relaxation testing [11, 12, 15]. Smeathers and Jones (1988) conducted cyclic axial compression tests on lumbar FSUs at 0.01 Hz, 0.1 Hz, 1.0 Hz, and 10 Hz, and found a moderate increase in compressive stiffness with increasing frequency. However, Smeathers and Jones (1988) used a large preload of 750 N and loaded the specimens to ± 250 N, which resulted in loading rates ranging from only $3.19e^{-6}$ m/s to $2.4e^{-1}$ m/s. Therefore, the purpose of this study was to develop the compressive stiffness properties of individual lumbar intervertebral discs when subjected to various dynamic compressive loading rates.

METHODS

A total of 33 axial compression tests were performed on 11 fresh frozen human lumbar spine intervertebral discs dissected from 6 fresh frozen human cadavers, 5 male and 1 female. The cadavers ranged in age from 18 to 56, with an average age of

42. Freezing was used as a means to preserve the specimens because previous studies have indicated that freezing does not significantly affect the response of FSUs [20].

Functional spinal units (FSU), defined an intervertebral disc and the two adjacent vertebral bodies, were dissected from the cadavers. Prior to specimen preparation, lateral view digital radiographs were taken of each spine in order to identify any pre-existing degenerative changes. The intervertebral discs for each spine were graded by a certified physician on a scale of 1 to 4 based on criteria presented by Gordon *et al.* (1991). Intervertebral levels with a degenerative grade of 3 or 4 were rejected.

For comparison with the standard population, the bone mineral density (BMD) of each cadaver was determined by the Osteogram technique. The left hand of the cadavers was x-rayed, scanned and processed by CompuMed incorporated (Los Angeles, CA). This type of BMD measurement, however, only provides an indication of overall bone strength and does not account for local changes in bone density or composition. Therefore, the BMD obtained through this method is referred to as the “Global BMD”. The global BMD results are reported with respect to the normal population (Table 1). The T-score is used to compare the cadaver’s global BMD with that of the general population, using 30 years of age as the comparison. The Z-score is used to compare the global BMD of the subjects with the average for their age. A T-score of -1 corresponds to one standard deviation below the

mean for the general population, meaning the individual is at or above the 63rd percentile for global BMD, or close to normal. T-scores of 2 and 3 correspond to 97th and 99th percentiles, respectively.

A number of detailed steps were taken in order to ensure the FSUs were rigidly secured while maintaining the proper testing orientation. After the spine was sectioned into the desired FSU, all the soft tissue except the ligaments was removed from the FSU. It should be noted that the posterior elements were left intact because previous researchers found them to have a limited effect on axial compressive stiffness under small deflections [14, 17, 22]. Second, a custom potting cup was filled with a bonding compound (Bondo Corporation, Atlanta, GA), and one half of the proximal vertebral body of the FSU was placed into the bonding compound. Special care was taken to ensure that the mid-plane of the disc was parallel with the potting cup, and that the disc was centered in the potting cup (Figure 1). This potting orientation has been used by numerous previous authors [1, 2, 7, 14, 23]. The potted vertebra was then attached to the test apparatus, and the distal potting cup was filled with the bonding compound. Finally, one half of the distal vertebral body was lowered into the distal potting cup (Figure 1). This procedure prevented any induced flexion or extension moments. After the specimen was lowered into the bonding compound, the bonding compound was allowed to fully cure before testing. The specimen was kept hydrated during the entire potting process by spraying saline directly on the specimen.

Table 1: Test matrix and subject data.

Test ID	IVD Level	Gender	Age	Body Weight	Osteogram		
			(years)	(kg)	Global BMD	t-score	z-score
IVD_1	L2-L3	M	56	81.4	105.3	-0.5	0.3
IVD_2	L2-L3	M	45	73.9	81.4	-2.7	-2.0
IVD_3	L4-L5						
IVD_4	L1-L2	F	46	115.9	93.7	-1.6	-1.6
IVD_5	L3-L4						
IVD_6	L1-L2	M	45	53.0	120.1	0.9	0.9
IVD_7	L3-L4						
IVD_8	L1-L2	M	42	85.9	92.1	-1.7	-1.3
IVD_9	L3-L4						
IVD_10	L2-L3	M	18	100.0	138.3	3.2	3.2
IVD_11	L4-L5						

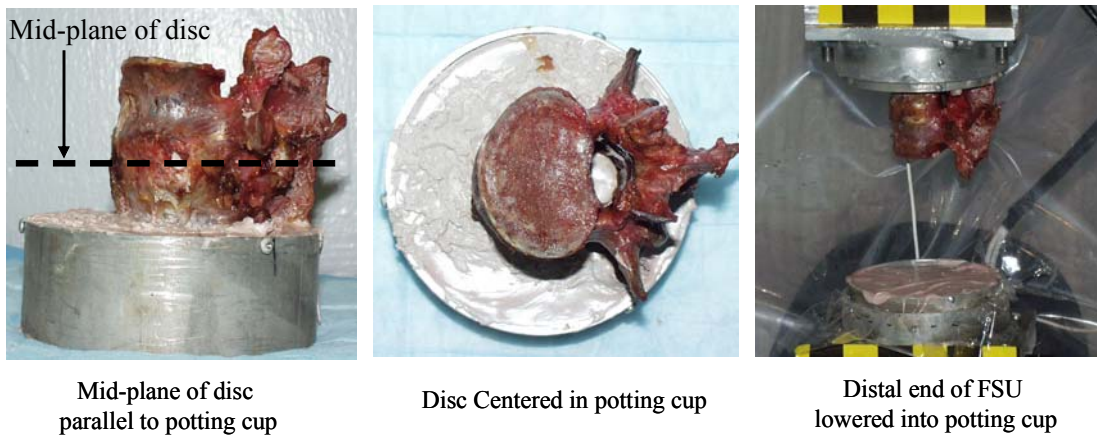


Figure 1: Functional spinal unit potting procedure.

The primary component of the FSU compression test setup was a hydraulic Material Testing System (MTS 810, 22 kN, Eden Prairie, MN) (Figure 2). The MTS actuator deflection was measured using the internal LVDT of the MTS. A five axis load cell (Denton, 1968, 22 kN, Rochester Hills, MI) was used to obtain the reaction force and moment, and a single axis load cell (Denton, 1210AF-5K, 22 kN, Rochester Hills, MI) was used to obtain the impactor force. Additionally, accelerometers (Endevco, 7264B, 2000 g, San Juan Capistrano, CA) were placed on both the reaction and impactor load cell plates.

Each intervertebral disc was subjected to a four part test battery in which the loading rate was increased with each test (Figure 3). First, the intervertebral disc was preconditioned to a displacement of 0.5 mm ($2.5 \text{ mm} \pm 2.5 \text{ mm}$) at a rate of 1 Hz, which is similar to the frequency of normal walking, for 10 cycles. Each intervertebral disc was

then preloaded to 88.96 N and subjected to two dynamic displacement steps, 0.5 mm and 1.0 mm, at rates of 0.1 m/s and 0.2 m/s respectively. For 0.1 m/s and 0.2 m/s loading rates, the data was sampled at 20 KHz and then filtered to CFC 600. Finally, each intervertebral disc was preloaded to 88.96 N and subjected to a dynamic failure test at a rate of 1.0 m/s. For 1.0 m/s loading rate, the data was sampled at 50 KHz and then filtered to CFC 600. However, the failure results are not presented in this paper. After each test, the MTS actuator was returned to the original position of zero strain and the specimen was allowed to relax for 10 minutes. The specimen was kept hydrated during the entire preparation and testing process by spraying saline directly on the specimen. Points used to calculate compressive stiffness and strain rate values were taken at approximately 25% and 50% of the loading curves. Strain was calculated based on the lateral disc height obtained from the digital X-rays.

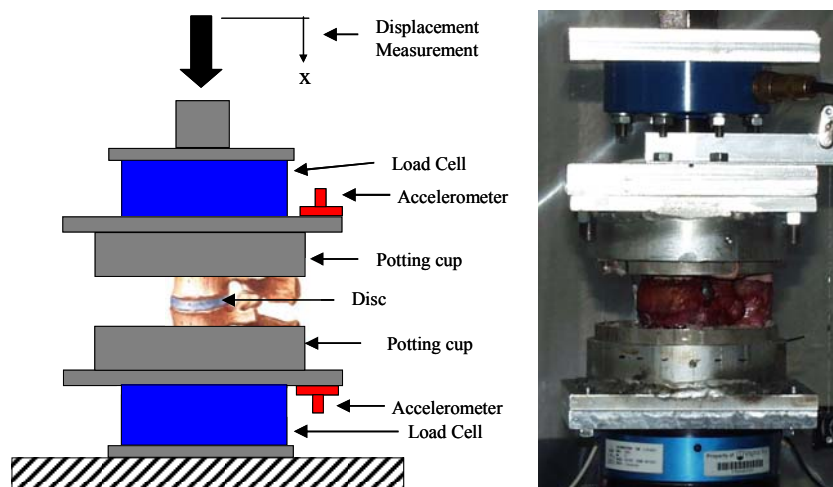


Figure 2: Individual intervertebral disc compression test setup.

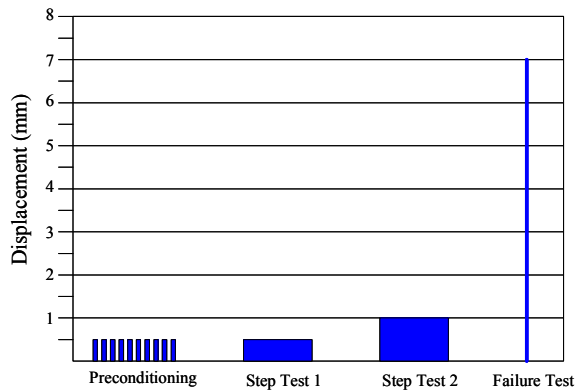


Figure 3. Individual intervertebral disc compression test battery.

RESULTS

The increased loading rate for each test in the three part test battery resulted in increasing compressive stiffness values for each specimen (Figure 4). In order to determine if the differences in vertebral disc compressive stiffness were significantly different with respect to loading rate, two statistical tests were performed. First, a two-tail t-test for the means, assuming unequal variances, was used to determine if there were any significant differences in compressive stiffness by vertebral level. There was no significant correlation ($p > 0.05$) between compressive stiffness and vertebral level at any loading rate (Figure 5). Therefore, all compressive stiffness data was grouped by loading rate. Then, a paired two-tail t-test for the means was used to determine if there were any significant differences in vertebral disc compressive stiffness with respect to loading rate. The statistical analysis showed that the average compressive stiffness at 0.2 m/s was significantly larger than at 0.1 m/s ($p=0.02$). In addition, the average compressive stiffness at 1.0 m/s was significantly larger than at 0.1 m/s and 0.2 m/s ($p < 0.01$).

The 0.1 m/s loading rate resulted in an average compressive stiffness and strain rate of 1835.1 ± 645.6 N/mm and 6.8 ± 1.5 s⁻¹, respectively. The 0.2 m/s loading rate resulted in an average compressive stiffness and strain rate of 2489.5 ± 474.1 N/mm and 13.5 ± 2.0 s⁻¹, respectively. The loading rate for the failure tests, 1.0 m/s, resulted in an average compressive stiffness and strain rate of 6551.1 ± 2017.0 N/mm and 72.7 ± 16.8 s⁻¹, respectively.

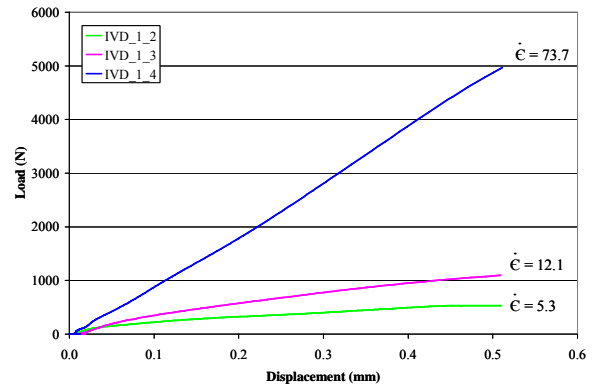


Figure 4. Compressive stiffness by loading rate.
Note: Data cut at 0.51mm for tests shown.

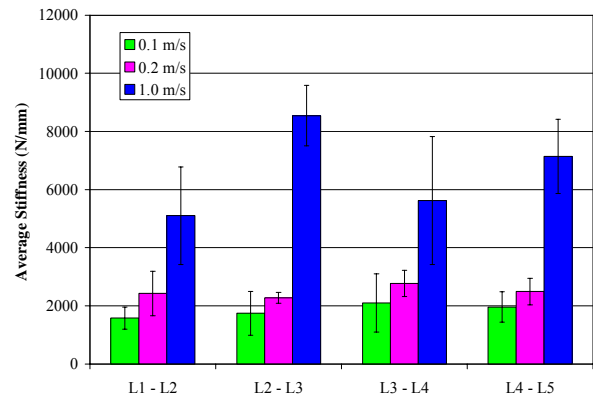


Figure 5. Functional spinal unit compressive stiffness by vertebral level.

DISCUSSION

The results of the current study show that the compressive stiffness of lumbar intervertebral discs is dependent on the loading rate. However, the compressive stiffness at static loading rates was not determined in the current study. Therefore, the data from the current study was combined with static compressive stiffness data from previous studies. Gordon *et al.* (1991) reported an average compressive stiffness after 30 minutes of cyclic loading at 1.5 Hz (approximately 0.14 s⁻¹) to be 2453 ± 654 N/mm. Yoganandan *et al.* (1989) reported an average compressive stiffness for normal and degenerated discs compressed at 2.54 mm/s (approximately 0.22 s⁻¹) to be 2850 ± 293 N/mm and 1642 ± 447 N/mm respectively.

The initial disc heights from the current study were combined with the disc heights reported by Keller *et al.* (1987) to obtain an overall average initial disc height of 11.32 mm. The strain rate for previous studies was then calculated using the overall

average disc height and loading rate. It should be noted that Keller *et al.* (1987) did not report the loading rate. Therefore, the compressive stiffness data reported by Keller *et al.* (1987) could not be included in the curve fitting. Finally, a relationship between loading rate and vertebral disc compressive stiffness was developed by curve fitting the compressive stiffness data from the current study along with the compressive stiffness data reported by Gordon *et al.* (1991) and Yoganandan *et al.* (1989) with a linear relationship (Equation 1 and Figure 6). The R^2 value for the data fit was 0.62.

$$k = 57.328 \varepsilon + 2019.1 \quad (1)$$

This relationship is slightly lower than the linear relationship proposed by Smeathers and Jones (1988). However, Smeathers and Jones (1988) used a much larger preload, which has previously been found to affect the response of intervertebral disc [8, 18].

In order to predict the compressive stiffness of the entire lumbar spine, the compressive stiffness of each lumbar intervertebral disc was assigned the same predicted compressive stiffness value based on Equation 1 and added in series to obtain an effective compressive stiffness, k_{eff} (Equation 2). It should be noted that the vertebral bodies were assumed to be rigid.

$$k_{eff} = \frac{1}{\left[\sum_{i=1}^N \frac{1}{k_N} \right]}; N=5 \quad (2)$$

The predicted effective compressive stiffness for the lumbar spine was then compared to previously published quasi-static and dynamic compression tests performed on isolated cadaver lumbar spines, T12-L5, and the Hybrid II lumbar spine (Figure 7). The comparison shows that the predicted effective compressive stiffness at a loading rate of 0.1 m/s is slightly lower than the average compressive stiffness reported by Demetropoulos *et al.* (1998), but well within the standard deviation. Conversely, the predicted effective compressive stiffness at a loading rate of 1.0 m/s is slightly higher than the average compressive stiffness reported by Duma *et al.* (2006). However, the predicted effective compressive stiffness at a loading rate of 1.0 m/s was well within the standard deviation. Although this method does not take lumbar curvature into account, the relationship between lumbar intervertebral disc compressive stiffness and loading rate presented in the current paper provides reasonable effective compressive stiffness of the whole lumbar spine over a range of loading rates.

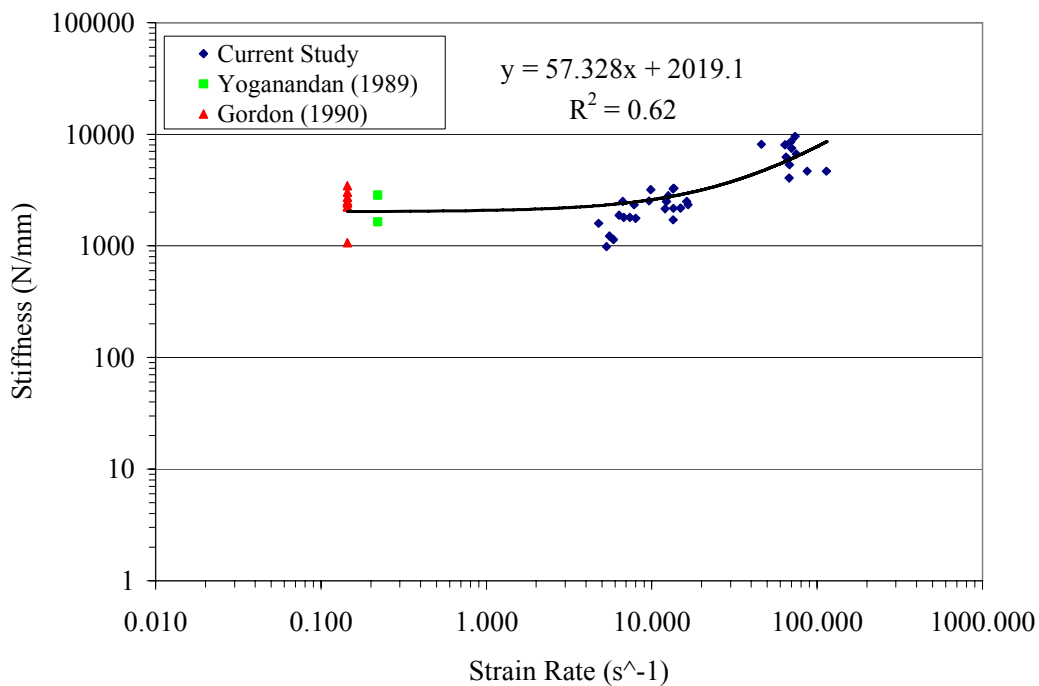


Figure 6. Relationship of intervertebral disc compressive stiffness to strain rate.
(Note: log-log scale)

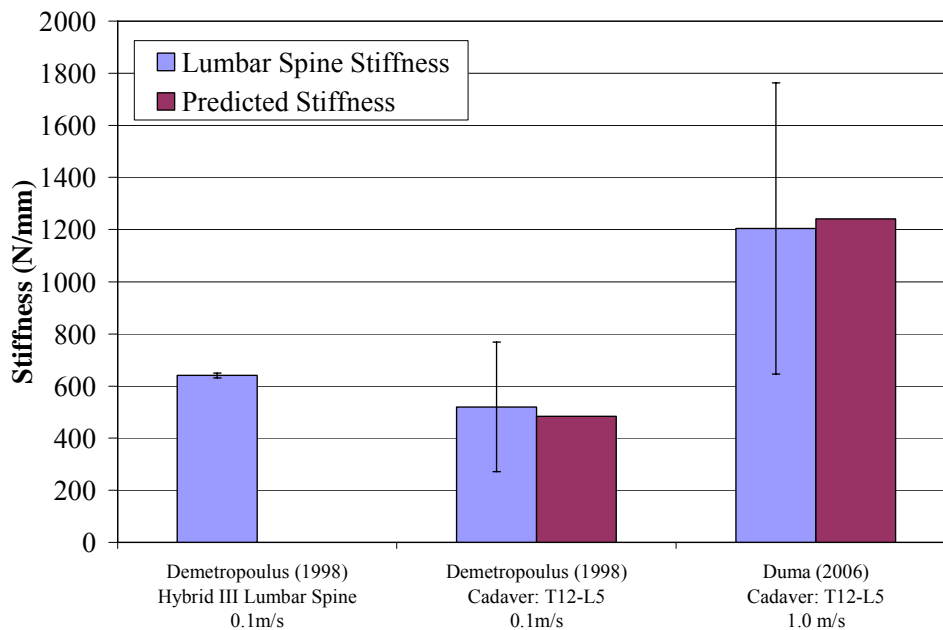


Figure 7. Comparison of predicted values to whole lumbar spine testing.

CONCLUSIONS

The compressive stiffness properties for the individual lumbar intervertebral discs were determined at three dynamic loading rates using a high rate servo-hydraulic material testing machine. The results showed that there was no significant correlation ($p > 0.05$) between compressive stiffness and vertebral level at any loading rate. In addition, the compressive stiffness of lumbar intervertebral discs in axial compression was found to dependent on the loading rate. Therefore, a relationship between loading rate and vertebral disc compressive stiffness was developed by curve fitting the stiffness data from the current study along with static compressive stiffness data reported by previous studies with a linear relationship.

The lumbar FSU research presented in this study will provide useful information for the development and validation of both mathematical and mechanical models of the human lumbar spine. However, in order to fully model the lumbar spine, additional testing will need to be conducted to quantify the effects of loading rate on stiffness in tension, shear, and bending.

ACKNOWLEDGMENTS

The authors wish to acknowledge Toyota Motor Corporation for providing the funding for this research.

REFERENCES

- [1] Adams, M.A. and Hutton, W.C. (1981) "Prolapsed intervertebral disc: A hyper flexion injury". *Spine*, 7(3): 184-191.
- [2] Brickmann, P., Biggemann, M., and Hilweg, D. (1989) "Prediction of the compressive strength of human lumbar vertebrae," *Spine*, 14(6): 606-610.
- [3] Brown, T., Nansen, R.J., and Yorra, A.J. (1957) "Some Mechanical tests on the lumbosacral spine with particular reference to intervertebral discs," *J. Bone and Joint Surg.* 39-A(5):1135-1164. 1957
- [4] Cooper, C., Atkinson, J. O'Fallon, W.M., and Melton, J.L. (1992) "Incidence of clinically diagnosed vertebral fractures in: A population based study in Rochester, Minnesota, 1985-1989," *J. Bone Miner Res*, 2: 221-227.
- [5] Demetropoulos, C.K., Yang, K.H., Grimm, M.J., et al. (1998) "Mechanical Properties of the cadaveric and hybrid II Lumbar spines." *Stapp Car Crash Journal*, 42.SAE 983160
- [6] Duma, S., Kemper, A., McNeely, D., Brolinson, G., and Matsuoka, F. (2006) "Biomechanical Response of the Lumbar Spine in Dynamic Compression." *Biomedical Sciences Instrumentation*. 42: 476-481.
- [7] Gordon, S.J., Yang, K.H., and Mayer, P.J. , et al. (1991) "Mechanism of disk rupture: A Preliminary Report," *Spine*, 16(4): 450-456.

- [8]Hirsch, C. (1966) "The reaction of intervertebral discs to compressive forces." *J. Bone. Joint Surg.* 37A: 1188-1196
- [9]Hutton, W.C., Cyon, B.M., and Scott, J.R. (1979) "The compressive strength of lumbar vertebrae," *J. Anat.*, 129(4): 753-758.
- [10]Kazarian, L. and Graves, G.A. (1977) "Compressive strength characteristics of the human vertebrae centrum," *Spine*, vol. 2(1), pp. 1-14.
- [11]Kazarian, L.E. (1975) "Creep characteristics of human spinal column," *Orthop. Clin. North Am.*, 6:3.
- [12]Keller, T.S., Spengler, D.M., and Huansson, T.H. (1987) "Mechanical behavior of the human lumbar spine. I Creep analysis during static compressive loading," *J. Orthop. Res.* 5: 467-478.
- [13]King, A. (1993) Injury to the Thoracolumbar Spine and Pelvis. *Accidental Injury: Biomechanics and Prevention*, 454-490. New York, Springer Verlag.
- [14]Lin, H.S., Liu, Y.K. and Adams, K.H. (1978) "Mechanical response of the lumbar intervertebral joint under physiological (Complex) Loading," *J. Bone Joint Surg.*, 60A(1): 41-55.
- [15]Markolf, K.L. and Morris, J.M. (1974) "The structural components of the intervertebral disc," *J. Bone Joint Surg.*, 56A: 675-687.
- [16]Melton, L. J., Thamer, N.F., Ray, J.K., *et al* (1997) "Fractures attributed to osteoporosis: Report from the National Osteoporosis Foundation," *J Bone Miner Res*, 12: 16-23.
- [17]Nachemson, A. (1960) "Lumbar intradiscal pressure." *Acta Orthop Scand.* 43(suppl): 1-104.
- [18]Panjabi, M.M., Lic, T., Krag, M.H., White, A.A., *et al.* (1977) "Effects of preload on load displacement curves of the lumbar spine," *Orthop. Clin. North Am.* 88: 181-192.
- [19]Ray, N.F, Chan, J.K., Thamer, M., and Melton, L.J., (1997) "Medical expenditures for the treatment of osteoporosis fractures in the United States in 1995: Report from the National Osteoporosis Foundation," *J Bone Miner Res*, 12:24-35.
- [20]Smeathers, J.E. and Jones, D.N. (1988) "Dynamic compressive properties of human lumbar intervertebral joints: A comparison between fresh and thawed specimens." *J. Biomechanics*, 21: 425-433.
- [21]Sundararajan, S., Priya, P., Rouhana, S., *et al.* (2005) "Characteristics of PMHS lumbar motion segments in lateral shear," *Stapp Car Crash Journal*, 49: 367-379.
- [22]Tencer, A.F., and Mayer, T.G. (1983) "Soft tissue strain and facet face interaction in the lumbar intervertebral joint – Part: Input data and computational technique." *J. Biomech Eng.* 105: 201-209.
- [23]Yoganandan, N., Ray, R., Pintar, F.A., *et al.* (1989) "Stiffness and strain energy criteria to evaluate the threshold of injury to an intervertebral joint," *J. Biomechanics*, 22: 135-142.